Investigation of the mechanism of Epstein-Barr Virus Latent Membrane Protein 1-mediated NF-κB activation.

Dissertation zur Erlangung des akademischen Grades des
Doktors der Naturwissenschaften (Dr. rer. nat.)

eingereicht im Fachbereich Biologie, Chemie, Pharmazie
der Freien Universität Berlin

vorgelegt von

Daniela Böhm
aus Mittweida

Februar 2010

ACKNOWLEDGMENTS

I would like to thank Prof. Ellen D. Cahir McFarland and Prof. Elliott Kieff for giving me the opportunity to complete my thesis in their laboratory. Furthermore, I sincerely thank Ellen D. Cahir McFarland for her great guidance and support throughout my work. In addition, I thank all the members of the Kieff/ Muenger/ Kaye and Wang laboratories at the 8th floor of the Channing lab, especially Mike Calderwood, Ben Gewurz, Aline Habison, Chantal Beauchemin, Kevin Hall, Amy Holthaus, Olga Saturne, Vishal Soni, Thomas Sommermann, Nick Shinners, and Jae Song.

1. INTRODUCTION

1.1 Epstein-Barr Virus

Epstein-Barr virus (EBV), also called *Human herpesvirus 4* (HHV-4), is a virus of the *Herpesviridae* family that infects more than 90% of the human population. However, the majority of carriers remain asymptomatic. It is named after Michael Epstein and Yvonne Barr, who, along with B.G. Achong, discovered the virus in Burkitt's lymphoma cells in 1964 (52,109).

EBV is a member of the *gamma-herpesvirus* subfamily which includes two genera, *Lymphocryptovirus* (LCV) and *Rhadinovirus* (RDV). EBV is the only human LCV (208). Two EBV types circulate in most populations, type 1 and 2 (also named types A and B), which differ largely in nuclear protein genes (82,311,312). Type 1 is dominantly prevalent in developed world populations, whereas type 2 is also prevalent in equatorial Africa and New Guinea (208).

Gamma-herpesviruses replicate in epithelial cells and usually establish long-term latency in lymphocytes which periodically become permissive for virus replication. The virus completes its life cycle by spreading to uninfected lymphocytes or to the epithelium of a nonimmune host (208). The virus persists for life in the serologically immune host (129).

An epidemiologically infrequent characteristic of *gamma-herpesvirus* infection is their oncogenic effects, resulting in lymphomas, carcinomas, or sarcomas (208).

1.1.1 Diseases associated with Epstein-Barr Virus

EBV is the causative agent of infectious mononucleosis (IM), also known as 'glandular fever' or 'Mono' (63,80,193). Infectious mononucleosis arises when a person is first exposed to the virus during or after childhood and adolescence. IM is therefore predominantly found in the developed world, as most children in the developing world are found to be already infected by around 18 months of age. The disease is characterized by debility, fever, sore throat, enlarged lymph nodes, and an increase in white blood cell count (26,111,165).

Other EBV-linked conditions are X-linked lymphoproliferative syndrome (XLP) and virus-associated hemophagocytic syndrome (VAHS). XLP affects young boys and is characterized by extreme sensitivity to EBV (29,291). XLP patients present in childhood with hyperacute IM symptoms, but the disease rapidly leads to liver failure caused by widespread lymphocytic infiltration and hepatic necrosis.

VAHS is characterized by acute fever, lymphadenopathy, hepatosplenemegaly, and widespread hemophagocytosis, often leading to a fatal outcome (373).

Epstein-Barr was the first virus to be identified as an oncovirus. Therefore, EBV-associated diseases include several human lymphoid and epithelial malignancies such as B-cell lymphomas of congenitally immunodeficient children, posttransplant lymphoproliferative disease (PTLD), B-cell lymphomas of patients with acquired immunodeficiency syndrome, smooth muscle cell tumors, Burkitt`s lymphoma (BL), Hodgkin`s lymphoma, T-cell and natural killer (NK) cell lymphomas, and nasopharyngeal carcinoma (NPC) (58,59,93,112,142,225,242,276,367,371) (Tab.1).

In B-cell lymphomas of congenitally immunodeficient children, EBV infection leads to uncontrolled B-lymphoproliferation, rather than hyperactivation of the cellular response, and hemophagocytosis (122).

PTLD are EBV-associated lesions, occurring at high incidence in posttransplant recipients. They are classified into three histologic types: (1) diffuse B-cell hyperplasias without disturbance of normal lymphoid architecture, (2) polymorphic lesions with nuclear atypia, some tumor necrosis, and destruction of underlying lymphoid architecture, and (3) diffuse, large B-cell lymphomas; these are tumors that are monoclonal in origin and typically arise several years after transplant (208).

Smooth muscle cell tumors are leiomyomas or leiomyosarcomas that frequently arise at sites (lung, gastrointestinal tract, or liver) where EBV-infected B cells are known to accumulate in patients who are T-cell compromised (208).

Table 1. Overview of Epstein-Barr Virus (EBV)-Associated Malignancies

Tumor	Subtype	Typical Latent[a] Period	% EBV Association[b]	EBV Antigen Expression[c]	Latency
Burkitts lymphoma	Endemic	3-8 years post-EBV	100	EBNA1	I
	Sporadic	3-8 years post-EBV	15-85		
	AIDS-associated	3-8 years post-HIV	30-40		
Gastric carcinoma	UCNT	>30 years post-EBV	100	EBNA1, LMP2	I/ II
	Adenocarcinoma	>30 years post-EBV	5-15		
Nasopharyngeal carcinoma	Nonkeratinizing	>30 years post-EBV	100	EBNA1, (LMP1), LMP2	I/ II
	Keratinizing	>30 years post-EBV	30-100		
T and NK lymphomas	VAHS-associated	1-2 years post-EBV	100	EBNA1, (LMP1), LMP2	I/II
	Nasal	>30 years post-EBV	100		
Hodgkin's lymphoma	Mixed cell,	>10 years post-EBV	60-80	EBNA1, LMP1, LMP2	II
	Nodular scleosing	>10 years post-EBV	20-40		
Post-transplant lymphoproliferative disease & simil.lesions	Immunodeficiency	<3 months post-EBV	100	EBNA1, 2, 3A, 3B, 3C, EBNA-LP, LMP1, LMP2	III
	Posttransplant	<1 year posttransplant	>90		
	AIDS-associated	>8 years post-HIV	>80		
Leiomyosarcoma	Immunodeficiency	?<3 years post-EBV	?100	?	?
	Posttransplant	?<3 years post-EBV	?100		
	AIDS-associated	?<3 y. post-EBV/ HIV	?100		

(adapted from Rickinson AB, Kieff E., 2007. Epstein-Barr virus; in Fields Virology pp2684)
AIDS, acquired immunodeficiency syndrome; UCNT, undifferentiated carcinomas of the nasopharyngeal type; VAHS, virus-associated hemophagocytic syndrome; EBNA, Epstein-Barr nuclear antigen; LMP, latent membrane protein.
[a] Typical latent period between EBV infection and tumor development or, where appropriate, between onset of T cell-impairment (transplant of HIV infection) and tumor development. Note that leiomyosarcoma is a tumor typically seen in infants who are congenially immunodeficient or who were transplant recipients or became HIV-infected early in infancy.
[b] Percentage of tumors that are EBV genome-positive. Note that, for some tumors (sporadic BL, keratinizing NPC), the strength of the EBV association varies with geographic location, hence the wide percent range.
[c] Antigen expression is identified by monoclonal antibody staining or is inferred from analysis of latent gene transcripts. Where variability is seen between tumors in terms of antigen status, the antigen is shown in brackets.

Burkitt's lymphoma is a type of Non-Hodgkin's lymphoma (52). It is the most common cancer of childhood in equatorial Africa with a male-to-female ratio of 3:1. It is co-existent with the presence of malaria. Malaria infection causes reduced immune surveillance of EBV immortalized B cells, allowing their proliferation and resulting in the formation of Burkitt's lymphoma. It commonly affects the jaw bone, the orbit of the eye, or the ovaries, forming a huge tumor mass (240).

Hodgkin`s lymphoma (HL) is an unusual tumor with a malignant population of mononuclear Hodgkin's and multinuclear Reed-Sternberg (H-RS) cells. It is seen worldwide (137,154).

Besides B-cell lymphomas, EBV-positive T-cell and natural killer cell lymphomas, derived from α/β T cells, γ/δ T cells and NK cells, have been described (187,335). They are most prevalent in Japan and other countries in Southeast Asia. One example is nasal lymphoma of T or NK cells, which is found in the nasal cavity and causes progressive erosion of bone tissue (335).

EBV is also associated with a carcinoma of nasopharyngeal epithelium (NPC). It is a cancer found in the upper respiratory tract, most commonly in the nasopharynx (297). NPC is common in Southeast Asia, among Inuit people and in some populations in northern and eastern Africa, due to both genetic and environmental factors. Its incidence is high in people of Chinese ancestry (genetic), but is also linked to environmental factors and the Chinese diet of high amounts of smoked fish, which contains nitrosamines, well known carcinogens (16).

1.1.2 Virus Structure and Genome

Epstein-Barr virions consist of a toroid-shaped protein core that is wrapped with linear, double stranded DNA; an icosahedral capsid, approximately 100-110 nm in diameter, containing 162 capsomeres with a hole running down the long axis; protein tegument between the nucleocapsid and envelope; and an outer envelope containing viral glycoprotein spikes on its surface (96,97,110,191).
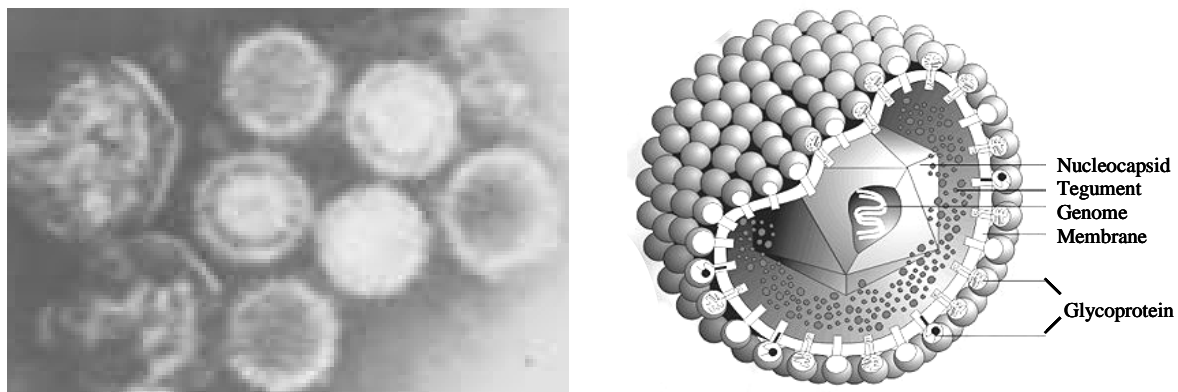
Figure 1. Epstein-Barr-virus (392,296)

The Epstein-Barr viral genome is a linear, double-stranded, 184kbp DNA composed of 60 mole percent guanine or cytosine (25,207,290). The genome is characterized by a number of different repetitions. The termini consist of tandem repeats (TR) of approximately 540bp (135). Six to twelve large internal repeats (IR1) of about 3,1kbp join a short and a long unique region (US and UL) (69). Several different other repeats are interspersed in the genome. Two clusters of small tandem repeats of 125bp and 102bp show partial homology and have the same orientation on the genome. Each cluster is flanked by a highly conserved region of about 1kbp. These left and right duplicated regions, which are denoted DL and DR respectively, are located about 100kbp apart from each other in the viral genome (83). DL and DR include the origins for initiation of viral DNA replication in lytic infection (148,305).

The EBV genome encodes about 100 viral proteins. The majority of them encode for proteins that are involved in nucleotide metabolism, that replicate and process viral DNA, and that comprise the structural components of the virion, capsid, tegument, and envelope. Furthermore, the genome encodes for a number of latency associated

RNAs and proteins (see 1.1.3 EBV infection of cells), an IL10 and a Bcl-2 homologue (261,279), distinctive micro RNAs (miRNA) (56,281,282) and a glycoprotein that binds to the B-lymphocyte surface protein, CD21 (269,349,350).

When EBV infects a cell, the genome becomes an episome. Therefore, the virus has cis-acting DNA sequences (*oriP*) and trans-acting nuclear proteins that are necessary for persistence of the genome as episome in dividing cells (27,30,402). Although EBV DNA usually persists in cells as an episome, EBV DNA can also integrate into chromosomal DNA or persist as integrated and episomal DNA (88,141,173,223,248).

1.1.3 EBV Infection of Cells

EBV is spread by the oral route. The identity of the primary target of orally transmitted EBV is still in doubt. Several studies prefer the epithelium as primary site for EBV replication (120,327,161), while others propose B-lymphocytes (114). However, the observation, that patients with B-cell-deficient, X-linked agammaglobulinemia show no evidence of EBV infection in the throat, implies that acquisition of EBV by the naïve host depends on initial B-cell infection (114). The current model for primary EBV infection, *in vivo*, is that orally transmitted virus establishes replicative foci within the oropharynx, possibly involving epithelial and/ or B-cells. At the same time the virus begins to colonize the B-cell system where it forms a latent infection.

Latent EBV infection involves the expression of three to eleven genes that determine three different types of latency (types I, II, or III) (Fig. 2) (208,298). Two types of nonpolyadenylated RNA (Epstein-Barr early regions (EBERs)), six nuclear proteins (Epstein-Barr nuclear antigen (EBNAs 1, 2, 3A, 3B 3C) and Epstein-Barr leader protein (EBNA-LP)), and two integral membrane proteins (latent membrane protein (LMP)) are expressed in these latently infected B lymphocytes. Other viral genes are also expressed in latency, including complementary-strand Bam A rightward transcripts (BARTs), which appear to encode at least two differentially spliced forms of the BARF0 peptide. Although not critical for transformation, BARF0 peptides may regulate cellular and/ or viral gene expression (208,298).
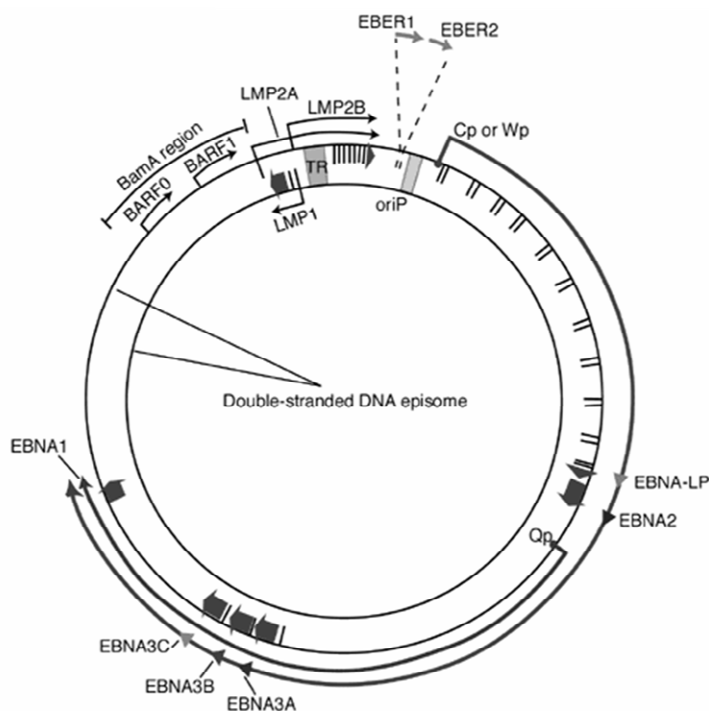
Figure 2. EBV latent genes.
Adapted from: Kieff E. Rickinson AB. 2007. Epstein-Barr virus and its replication. In: Fields virology. pp2603-2700.

In the oropharynx infected B cells express the full spectrum of latent proteins (latency III) (Fig.3a). The virus can thereby drive the activation and proliferation of these B cells, which then migrate to lymphoid follicles and form germinal centers. Concomitantly, expression of EBNA2, EBNA3s and LP are downregulated, leaving EBNA1, EBERs, BARTs and the LMPs expressed (latency II) (Fig.3a). Expression of the LMPs provides signals that allow the B cells to survive the germinal centre reaction and to form resting memory B cells. These resting memory B cells exit to the periphery (Fig.3b). At this point, expression of other EBV proteins is downregulated, thereby allowing the virus to persist within the B cells but to evade a host immune response (Fig.3b). Expression of EBNA1, EBERs and BARTs within dividing B cells allows the virus genome to be distributed to each of the daughter B cells (latency I). The entire genome persists in the proliferating lymphocytes as covalently closed circular episomal DNA (115,208). Circularization is a hallmark of latent infection because it ensures that the viral DNA will be replicated along with the cellular DNA.

As B cells recirculate to the oropharynx, a switch to the EBV lytic cycle might occur, possibly triggered by maturation of B cells into plasma cells, allowing for virus replication, shedding into saliva and transmission both to new hosts and to previously uninfected B cells within the same host (Fig.3c) (208,298,354,355).

Figure 3. **A model for Epstein-Barr virus (EBV) infection and persistence.**
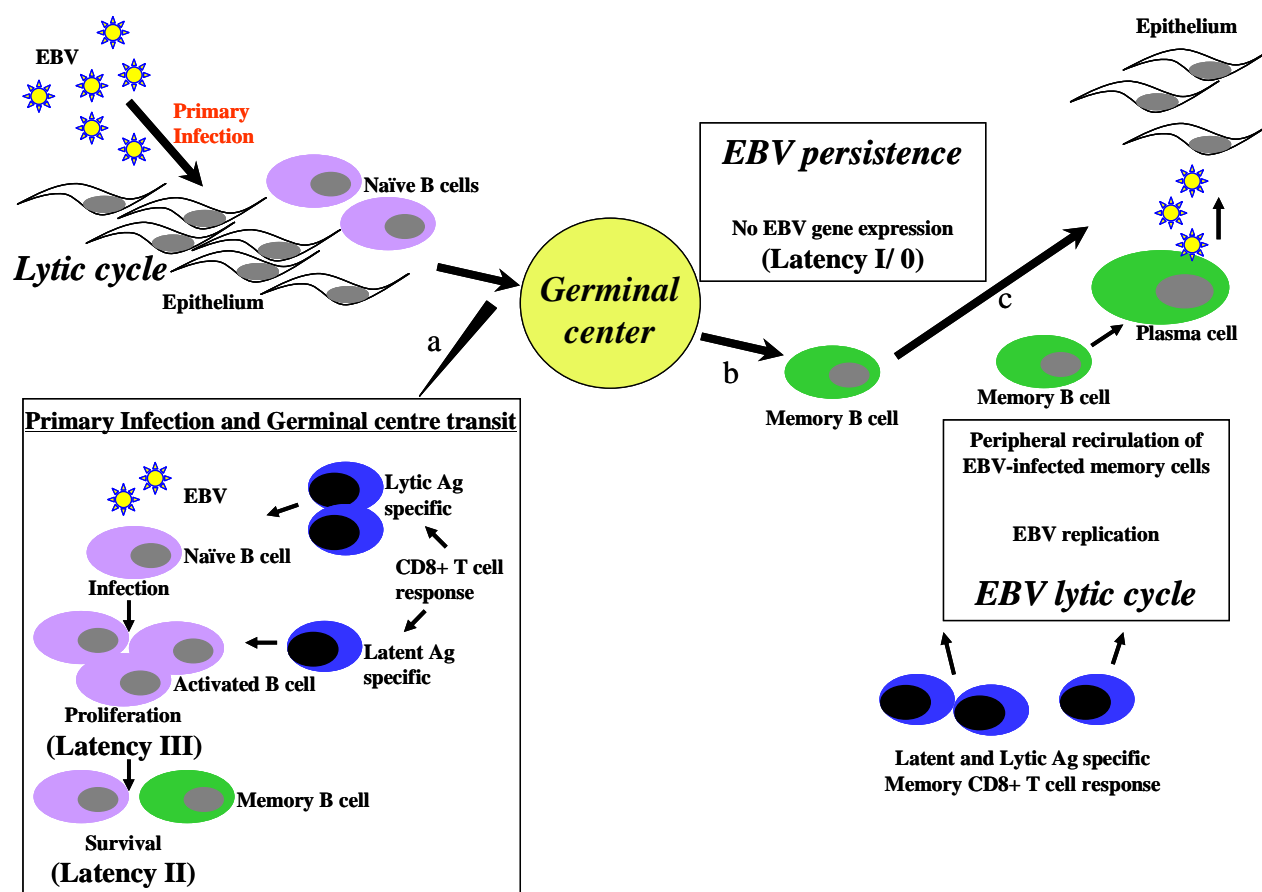Modified from: Kieff E. Rickinson AB. 2007. Epstein-Barr virus and its replication. In: Fields virology. pp2603-2700.
And: David A. Thorley-Lawson. A Hypothetical model of EBV persistence. From: Epstein-Barr virus: exploiting the immune system, Nature Reviews Immunology 1, 75-82 (2001)

Type I latency is associated with Burkitt's lymphoma, type II latency has been recognized in non-B cell tumors, such as nasopharyngeal carcinomas, T cell tumors, and Hodgkin's disease, and latency III has been identified in some Burkitt's lymphoma cell lines and EBV transformed lymphoblastoid cell lines (Tab.1)(208).

In vitro, EBV infects only primary human B-cells with efficiency (157,159,286,287,342). The virus can also establish latent infection in other cell types, including T lymphocytes, natural killer (NK) cells, and primary epithelial cells, although the efficiency is very low (194,381,404).

Infection of primary human B lymphocytes with EBV, *in vitro,* leads to nonpermissivity for virus replication and conversion of the infected cells to lymphoblasts capable of proliferation into lymphoblastoid cell lines (LCL) (159,287). The infection of primary B cells, *in vitro*, also results in the cells becoming latently infected, and immortalization of 3-10% of the cells (157,342).

In vitro, B lymphocyte infection is initiated by the EBV envelope glycoprotein gp350/220, which binds to CD21 (118,268). CD21 is found on mature B lymphocytes as well as follicular dendritic cells. It functions as the receptor for the complement protein C3d, as well as forming the B cell co-receptor when associated with CD19 and CD81 (189). Engagement of CD21 likely activates a signaling pathway similar to B-cell receptor (BCR) tyrosine kinase signal transduction, involving CD19, src kinases, and syk (246,247,349).

EBV enters B cells though the endocytic pathway and fuses with the endosome membrane at low pH (258,267), whereas epithelial cells appear to be infected at the cell surface (258).

EBV encoded BMRF2 is implicated as a mediator of epithelial cell infection (363). However, the exact mechanism of epithelial cell infection is still unclear. Yoshiyama *et al.* have shown a CD21 independent route of entry (406), while Sixbey *et al.* have demonstrated that epithelial cells expressing IgA antibody receptor can internalize EBV bound to polymeric IgA (326). Beyond that, HLA antigen class II has been described as second EBV entry receptor on B lymphocytes and epithelial cells (227). Infection occurs with reduced efficiency and is mediated by the EBV encoded protein gp42 (263).

In B-lymphocyte infection, *in vitro*, after EBV is endocytosed, the EBV envelope fuses with an endocytic vesicle membrane, and capsids are released into the cytoplasm (267). Then the capsids are likely to be transported on microtubules to nuclear pores using dynein and dinactin motors (98,191). In the nucleus the EBV DNA circularization occurs within 8-12 hours (8,172). Host cell RNA polymerase II transcribes viral mRNA. At 12-16 hours after infection, EBNA-LP and EBNA-2 mRNA are the first transcripts (8). EBNA-2 upregulates specific EBV and cell promoters and EBNA-LP potentiates EBNA-2 effects (3,151,362,378). By 72 hours, EBNA-1, EBNA-2, EBNA-3A, EBNA-3B, EBNA-3C, EBNA-LP, LMP1, LMP2, EBERs, and BARTs are expressed (208). These genes products maintain latent infection and cause the previously resting B lymphocytes to enter cycle and continuously proliferate as LCL.

To study EBV infection*, in vitro,* latently infected B cells can be induced to replicate EBV by cross-linking surface immunoglobulin, treatment with phorbol ester and calcium ionophore, or conditional BZLF1 (an EBV immediate early gene) expression (64). Following induction, cells that have become permissive for virus replication undergo cytopathic changes, including margination of nuclear chromatin (199), inhibition of host macromolecular synthesis (130), replication of viral DNA at the center of the nucleus, assembly of nucleocapsids at the nuclear periphery, nucleation of nucleocapsids, initial virus envelopment by budding through the inner nuclear membrane, and final envelopment at cytoplasmic membranes (138,278,314). Virus gene expression follows a temporal and sequential order: (1) immediate early genes, (2) early genes, and (3) late genes (113,345,408).

1.2 EBV Latent Membrane Protein-1 (LMP1)

Epstein-Barr virus latent infection membrane protein 1 (LMP1) is expressed in EBV latency III infected human B lymphocytes that have been converted into lymphoblastoid cell lines (LCL), *in vitro*, in latency III primary EBV infection of human B lymphoblasts, *in vivo*, in latency III post-transplant lymphoproliferative disease, in EBV associated Hodgkin's Disease, and in many nasopharyngeal cancers. It is one of five latent genes shown to be essential for EBV-induced transformation of B lymphocytes, for LCL establishment and continued proliferation (203,211,250). LMP1 has the potential to transform *in vitro* immortalized rodent fibroblasts to anchorage, contact, and serum-independent growth (376,377). Moreover, LMP1 expression in human B lymphoblasts alters cell growth, and transgenic expression in murine B cells causes hyperplasia and lymphoma (218,387).

The LMP1 gene consists of 3 exons and 2 introns (40). Three promoters can regulate LMP1 gene transcription. In initial latency III lymphocyte infection, LMP1 transcription is turned on by EBNA2 (379) and EBNA-LP (151). In latency II infected NPC cells, LMP1 transcription originates from a STAT regulated upstream promoter in the EBV terminal direct repeat. A third promoter in the LMP1 first intron is activated late in lytic EBV replication and transcribes a 5' truncated D1LMP1 mRNA (115).

LMP1 is a 62 kDa integral membrane protein that is constitutively aggregated in the plasma membrane (Fig.4) (208). It consists of a short cytoplasmic N-terminus (aa 1-24) that is responsible for orienting LMP1 to the cell membrane, six transmembrane domains (aa 25-186) that can induce oligomerisation of LMP1, and a long cytoplasmic C-terminus (aa 187-386) which contains two essential activating domains (C-Terminal-Activating Regions (CTAR1 and 2) (133,171). CTAR1 and CTAR2 have been shown to be involved in B cell transformation. Therefore they are also referred to as Transformation Effector Sites (TES1 and 2) (184,186,203).
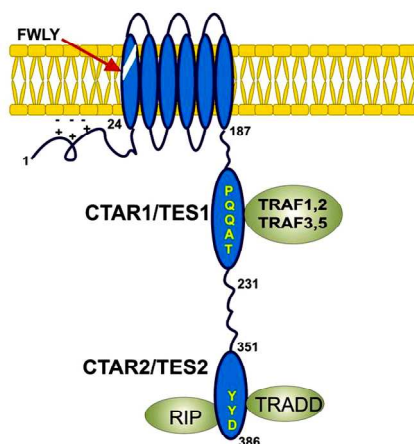
Figure 4. Structure of LMP1 and its associated factors (Kieff E, Cahir McFarland ED, 2005)

Biochemical and reverse genetic analyses indicate that LMP1 is found in plasma- as well as cytoplasmic membranes (233), localizes in lipid rafts (11), and is significantly associated with the cytoskeleton (208).

At its C-terminus, LMP1 interacts with several of the tumor necrosis factor receptor (TNFR)-associated factors (TRAFs) (262), the TNFR-associated death domain protein (TRADD) (186), and the receptor interacting protein (RIP) (184). These interactions at both TES1 and TES2 domains result in activation of several signaling pathways, e.g. nuclear factor (NF)-κB (171,260), p38/mitogen-activated protein kinase (MAPK) activation of activator transcription factor (ATF)-2 (210), Janus kinase (JAK) activation of signal transducer activators of transcription (STAT) (= the JNK pathway) (134) and interferon regulatory factor (IRF) 7 (332).

LMP1 shares many functional similarities with tumor necrosis factor receptor family members (134,262,364). Although LMP1 mimics TNFRs in directly engaging TRAFs and TRADD, LMP1 differs from TNFRs in: (a) a large number of LMP1 molecules form a signaling complex, whereas TNFRs form trimers; (b) LMP1 acts as a constitutively activated receptor-like molecule independent of ligand binding or regulation, whereas TNFRs require ligand for trimerization and signaling; (c) LMP1 has two separate C-terminal domains, TES1 and TES2, which engage TRAFs and TRADD, respectively, whereas TNFR1 engages only TRADD and TNFR2 engages only TRAFs; (d) LMP1 TES2 uses only the 11 amino acids at its C-terminus to activate NF-κB while TNFR1 requires about 70 amino acids; (e) LMP1 engages TRADD without propagating a death signal, whereas TNFR1 can propagate survival or death signals through TRADD; and (h) LMP1 activation of NF-κB is largely IL-1 receptor-associated kinase (IRAK1) and TRAF6 dependent, whereas TNFR activation of NF-κB is largely IRAK1 and TRAF6 independent (13,90,91,108,134, 156,179,202,205,238,259,262,343,366).

The discovery, that LMP1 TES1 induces and associates with TRAF1 and TRAF3, which also associate with CD40 and lymphotoxin β receptor (LTβR) cytoplasmic domains, led to the proposal that LMP1 is a constitutively activated TNFR, similar to CD40 (a critical receptor for B lymphocyte development) (39,262,364). When expressed in B cells, LMP1 induces the production of antibody (Ab) and cytokines, up-regulation of adhesion and costimulatory molecules, and protection from apoptosis (50). LMP1 can substitute for CD40 to induce a T-dependent humoral response in transgenic mice (364), and only the LMP1 C-terminal domain is necessary to replace CD40 in mediating an Ab response that includes isotype switching and affinity maturation (334). Both LMP1 and CD40 activate NF-κB, p38, and JNK (134,155). LMP1 mimics CD40 in engaging TRAF3 trough a $P_{204}QQATDD_{210}$ motif (262). In a recombinant EBV infected LCL, where LMP1 expression can be conditionally regulated, CD40 ligand can maintain LCL proliferation in the absence of LMP1 expression (211). Furthermore, an LMP1 N-terminal and transmembrane domain fusion to the CD40 C-terminal domain (CTD) results in constitutive CD40 C-terminal cytoplasmic domain signaling (155), and can replace LMP1 in LCL outgrowth assays (94). The C-terminal domain of LMP1 is both necessary and sufficient to mediate B cell activation (262,364). In contrast to CD40, however, LMP1 signaling in B cells is amplified and sustained, leading to enhanced B cell activation (49). Consistent with this finding, transgenic expression of a chimeric CD40-LMP1 molecule in mice leads to B cell hyperactivation, autoreactivity, and abnormal lymphoid architecture in secondary lymphoid organs (334). Thus, LMP1's exaggerated signaling properties give it the ability to promote B-cell mediated disorders.

Most of the functions of LMP1 are derived from the C-terminus. The same study that identified TRAF1 and TRAF3 as LMP1 interacting proteins (262) showed that TES1 (aa187-231) was sufficient to interact with TRAF3. Subsequently, TRAF2 and TRAF5 were also found to bind to LMP1 in the same region (90,91,202). Utilizing a LMP1 TES1 mutant, the TRAF binding motif within TES1 was identified as $_{204}PQQAT_{208}$ (Fig.5 lower) (91,262).

TRAFs were initially discovered as adaptor proteins that couple the TNFR family to signaling pathways. More recently they have also been shown to be signal transducers of Toll/ interleukin-1 family members. Seven members of the TRAF family have been identified. All TRAF proteins, with the exception of TRAF1, contain a RING finger at their N-terminal region, followed by a variable number of ZF motifs that may be involved in binding of polyubiquitin chains (38,46). At their C-terminus, all TRAFs, including TRAF1, contain a domain that mediates binding to adapter proteins, such as TRADD, or direct binding to the cytoplasmic segments of those TNFR family members that do not rely on adapter proteins, such as CD40 or BAFF-R (38,46). Consistent with this notion, the C-terminal regions of TRAF1 and TRAF2 are responsible for interacting with LMP1 (262). In EBV-transformed

B cells, significant amounts of TRAF1, TRAF2, TRAF3, and TRAF5 are complexed with LMP1. In contrast, in epithelial cells having no TRAF1, LMP1 complexes only with TRAF2, TRAF3, and TRAF5 (90).

Furthermore, TRAF6 has been shown to be essential for LMP1 mediated NF-κB and JNK activation in mouse embryonic fibroblasts (MEF) (238,317,374). Initially TRAF6 was identified as a signal transducer involved in the activation of NF-κB by CD40 (179) and interleukin 1 (57). Overexpression of TRAF6 activates NF-κB, and a dominant negative mutant of TRAF6 inhibits NF-κB activation by IL-1 but not TNF. TRAF6 also activates p38 and JNK when overexpressed (330). TRAF6 is an E3 ubiquitin-ligase that promotes lysine (K)63-polyubiquitination of many proteins, including itself (65), and creates a number of docking sites that are in a yet unknown mechanism are important for IKK activation (1.3 NF-κB signaling).
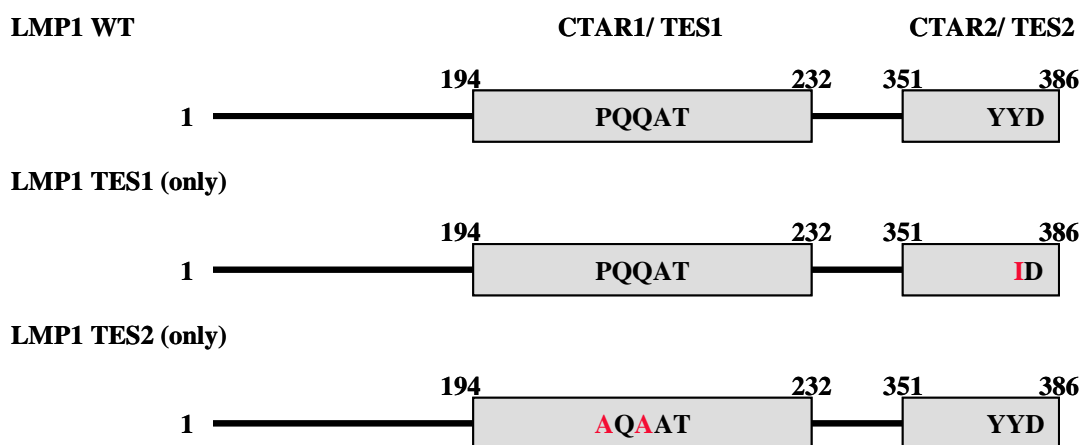
Figure 5. LMP1 WT, LMP1 TES1 only as a consequence of TES2 $Y_{384}YD$ to ID mutation **and LMP1 TES2 only** as a consequence of TES1 PQQAT to $AQAAT_{208}$ mutation (91,186)

Other LMP1-interacting proteins are TRADD and RIP. The N-terminus of TRADD (aa 1-194) specifically interacts with the C-terminal TES2 domain of LMP1 (aa 355-386), but not with an LMP1 mutant with the last three amino acids changed from $_{384}YYD_{386}$ to $_{384}ID_{385}$ (56) (Fig. 5 middle).

RIP is a TNFR1-associated protein. Similar to TRADD, RIP contains a C-terminal death domain that mediates protein-protein interactions with TNFR1 and TRADD (166). Although the RIP-binding region on LMP1 TES2 overlaps with the TRADD-binding region (aa355-386), RIP requires a broader protein sequence for interaction (184). LMP1 interacts directly with RIP, stably associates with RIP in LCLs, but does not require RIP for NF-κB activation (185). RIP has been thought to be is essential for TNFR mediated NF-κB activation (356), however, a recent publication describing survival and NF-κB activation after TNFα treatment in RIPK1-/- MEFs challenges this belief (388). Despite constitutive association with TRADD or RIP, LMP1 does not induce apoptosis in EBV-negative Burkitt lymphoma or human embryonic kidney 293 cells (185).

Beyond its role in NF-κB, p38, and JNK signaling, LMP1 also activates IFN regulatory factor (IRF) 7 (176, 412,413). Furthermore, LMP1 has the ability to upregulate anti-apoptotic factors like A20, Bcl-2, Bfl-1 (158,219, 302), cytokines (IL-6, IL-8, IL-18) (107,401,407), cell surface receptors (CD23, CD40, EGFR) (171,211,259,379), the adhesion molecule ICAM1 (254), the transcription factor Ets-1 (212), Cyclin D2 (18), the Tpl-2/Cot serin-threonin kinase (106) and many others. Moreover there are some LMP1 downregulated genes like the adhesion molecule E-cadherin (361) and the surface molecule CD99 (213).

1.3 Nuclear Factor-κB-Signaling

Nuclear factor-κB (NF-κB) was identified about 20 years ago as a transcription factor that binds to the intronic enhancer of the kappa light chain gene (κB-site) in B cells (322,323) and emerged as important regulator of inflammation, innate and adaptive immunity, cell proliferation, and apoptosis (43,196,228,304).

Mammalian cells express five NF-κB proteins: NF-κB1 (p50 and its precursor p105), NF-κB2 (p52 and its precursor p100), RelA (p65), c-Rel, and RelB, encoded by *NFKB1, NFKB2, RELA, REL,* and *RELB* respectively, which share a N-terminal Rel homology domain (RHD) responsible for sequence specific DNA binding and dimerization. NF-κB proteins form a variety of homo- and heterodimers which bind to κB sites within the promoters/ enhancers of target genes and regulate transcription through the recruitment of coactivators and corepressors. In its inactive state, NF-κB dimers are associated with inhibitory proteins, the IκB proteins. IκBs retain NF-κB dimers in the cytoplasm of nonstimulated cells, thereby preventing their nuclear translocation and subsequent DNA binding (156).

Various inflammatory stimuli such as tumor necrosis factor (TNF)-α, or lipopolysaccharide (LPS) activate the NF-κB dimers by triggering a signaling pathway that leads to the phosphorylation by an IκB kinase (IKK), ubiquitylation, and degradation of IκB. The degradation of IκB exposes a nuclear localization signal on the NF-κB proteins, which now move into the nucleus and stimulate the transcription of specific genes (156).

NF-κB plays an important role in lymphocyte and myeloid differentiation, in T cell differentiation, and in natural killer (NK) cell and B cell development. Physiological activation of NF-κB during lymphocyte maturation and activation mediates expression of genes involved in proliferation, and survival as well as genes involved in immunity to infection (228). However, dysregulated NF-κB activation results in aberrant expression of its target genes that regulate cell proliferation or survival, including cyclin D1, cyclin D2, BCL-2, BCL-XL, c-Myc, c-Myb (99,132,164, 358), as well as cytokines such as IL-2, IL-6, and CD40L that regulate growth and proliferation of lymphocytes (197). Therefore, constitutively active NF-κB has been implicated in various lymphoid malignancies, including acute lymphocyte leukaemia, chronic myelogenous leukaemia, several forms of Hodgkin's lymphoma, T cell lymphoma, activated B cell-like diffuse large B cell lymphoma (ABC-DLBCL), MALT lymphoma, the plasma cell cancer multiple myeloma (MM), and more (197).

1.3.1 NF-κB-activating Pathways

Many different stimuli activate NF-κB via different receptors, including the TNF receptor superfamily, IL-1 receptor/Toll-like receptor (TLR) superfamily, the T cell receptor, and the B cell receptor (315). The major and most well studied activation pathway used by most stimuli is the canonical (or classical) NF-κB signaling pathway, which mainly results in activation and translocation of RelA/p50 and c-Rel/p50 heterodimers. This pathway centers around the IκB kinase (IKK) complex consisting of the catalytic subunits IKKα and IKKβ, and the regulatory subunit NEMO (for NF-κB essential modulator; also called IKKγ, FIP-3) (195).

Receptor engagement results in activation of the IKK complex (92). Activated IKK, mainly IKKβ (168, 231), phosphorylates IκBα on Ser32 and Ser36, leading to its lysine (K) 48-polyubiquitination at lysine 19 and subsequent degradation via the S26 proteasome pathway, thereby exposing a nuclear localisation signal (NLS) and inducing nuclear translocation of RelA/p50 heterodimers. Canonical NF-κB activation depends on IKKβ and NEMO, but can be independent of IKKα. The mechanism by which the IKK complex is activated is different from one receptor to another.

Canonical NF-κB signaling by the TNF receptor family member TNFR1 is the most well studied pathway which gives the clearest evidence of the activation of IKK (Fig.6 right). Binding of TNFα to TNFR1 induces receptor trimerization and recruitment of the adapter protein TNFR1-associated death domain protein (TRADD). TRADD is thought to recruit TRAF2, TRAF5, and RIP1 to ligated TNFR1 (64,167,257,288). Although RIP1 is a member of a small family of related protein kinases, in NF-κB signaling, RIP1 evidently does not function as a kinase (356). It rather acts as an adapter that enhances IKK recruitment to the activated receptor. IKK activation by multiple receptor signaling pathways has been shown to depend on K63-linked nondegradative polyubiquitination (65). For the TNFα signaling pathway, TRAF2 causes K63-linked polyubiquitination of RIP1 (101,390) and also recruits IKK to the receptor complex, where binding of NEMO to polyubiquitinated RIP1 is thought to stabilize IKK interaction with the receptor complex (101,390). How the binding of NEMO to K63-linked polyubiquitin chains of RIP1 triggers IKK activation is unknown. Autophosphorylation of IKK (301) or activation by upstream kinases such as MEKK3 and TAK1/ TAB2/ TAB3 have been proposed (40,180,375).
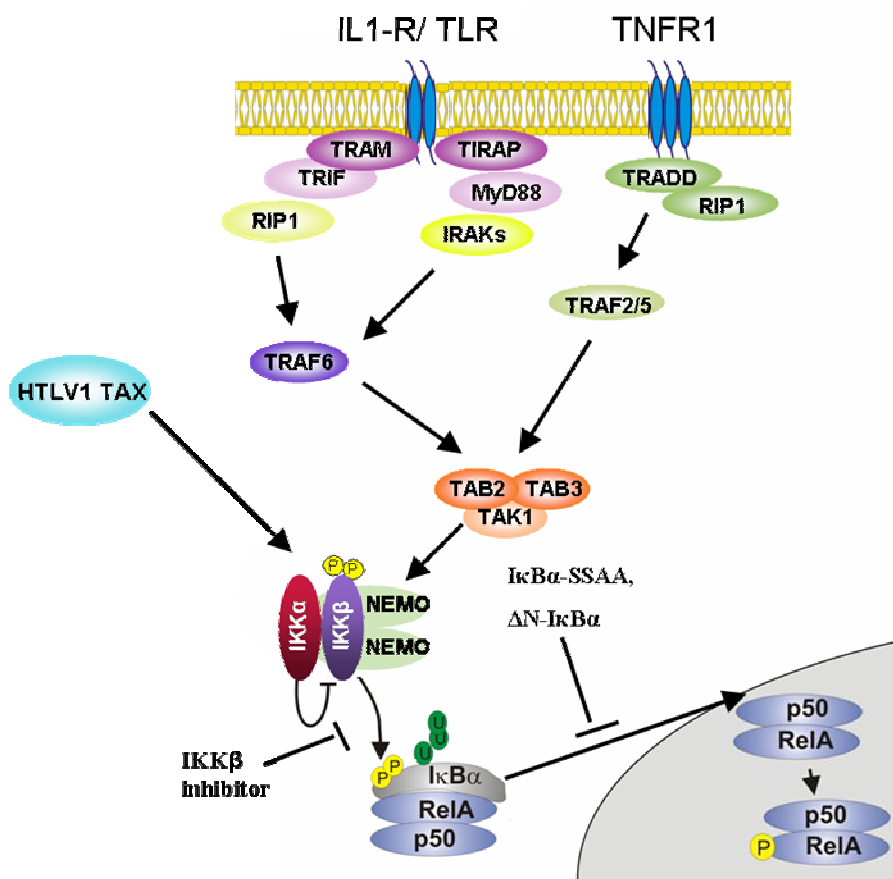
Figure 6. Canonical NF-κB signaling by IL-1/ Toll like recepors and TNFR1 (156,197).

Members of the IL-1R/ TLR family are also potent activators of classical NF-κB signaling (Fig.6 left). In IL-1R/ TLR receptor signaling, ligand binding results in recruitment of receptor-specific adapters. The cytoplasmic regions of IL-1R/ TLR family members share a common motif called TIR domain. Two major TIR domain containing adapters – MyD88 (myeloid differentiation primary response gene 88), and TRIF (TIR domain containing adapter-inducing IFN-β) – are either directly recruited to TLRs (for example TLR3 and TLR9), or bind to TLRs (for example TLR2 and TLR4) via intermediary adapters such as TIRAP (Toll/ interleukin-1 receptor adapter protein) or TRAM. The MyD88 dependent pathway leads to IKK activation via TRAF6 (57,200,347). The RING domain ubiquitin ligase

(E3) TRAF6, in conjunction with the specific dimeric ubiquitin-conjugating enzyme Ubc13/Uev1A complex (E2), is responsible for K63-linked polyubiquitination of itself and downstream proteins such as IRAK-1 (74). Following recruitment by IRAKs, TRAF6 likely binds to the TAK1/ TAB2/ TAB3 complex, leading to TAK1-mediaded IKK activation (180,272,292,346,375). Independent of MyD88, TRIF can recruit TRAF6 directly, leading to activation of TAK1 and IKK, similar to the MyD88 dependent pathway. In addition to TRAF6, TRIF also recruits RIP1, which might cooperate with TRAF6 to facilitate TAK1 and IKK activation (Fig. 6).

Antigen receptors also activate NF-κB via the canonical pathway. Engagement of antigen receptors on B and T lymphocytes results in activation of protein kinase C isoenzymes PKCθ in T cells (339) and PKCβ in B cells (336), which play central roles in recruiting additional factors. In T cell receptor (TCR) signaling, stimulation of the receptor likely results in sequential recruitment of a number of proteins including the Src (Lck and Fyn) and Syk (ZAP70) family kinases and the adapter proteins LAT and SLP-76, which then activate intracellular signaling components like phospholipase C (PLC) γ1, Vav1, and 3-phosphoinositide-dependent kinase 1 (PDK1) (325). Activation of PLCγ1 results in generation of inositol-1,4,5-triphosphat (IP_3) and Ca^{2+}, as well as diacylglycerol (DAG), which in turn stimulates PKCθ. Signals from TCR and CD28 costimulation result in activation of phosphoinositide-3-kinase (PI3K), which facilitates recruitment of PKCθ to the immunological synapse (IS) (160,325,369,383). Activation of PKCθ leads to the formation of a complex between CARMA1 [caspase recruitment domain (CARD) membrane-associated guanylate kinase (MAGUK) protein 1]), BCL10, and MALT1 (mucosa-associated lymphoid tissue 1) (325,383). This complex called CBM, promotes the K63-linked polyubiquitination of NEMO and subsequent IKK activation (418).

Besides the canonical pathway, a second pathway – the alternative or noncanonical pathway – is well established for NF-κB activation. This pathway has been described for lymphotoxin α and β (LTαβ), CD40L, BAFF (B-cell activating factor), RANKL (receptor activator of NF-κB ligand), TWEAK (TNF-related weak inducer of apoptosis) and for viruses such as human T-cell leukaemia virus (HTLV) and EBV (73,75,87,273,309,321,393,394, 403). The noncanonical NF-κB pathway is characterized by processing of p100 to p52 and by its independence from IKKβ and NEMO. Instead the alternative pathway relies on the activation of IKKα by the NF-κB-inducing kinase (NIK) (393,394).

A well studied receptor utilizing the noncanonical pathway for NF-κB activation is CD40 (Fig. 7). In resting cells, p100, via its C-terminal ankyrin repeats, binds and keeps RelB in the cytosol. NIK is maintained at very low levels owing to rapid proteasome-dependent degradation (232). TRAF3 links NIK to an E3 complex containing TRAF2 and cellular inhibitor of apoptosis (cIAP) 1/2, thereby promoting cIAP1/2-mediated K48-linked NIK polyubiquitination and proteasomal degradation (206,368,370). Activation of CD40 by CD40L leads to recruitment of the cIAP1/2 - TRAF2 - TRAF3 complex to the receptor, where cIAP1/2 undergoes TRAF2- dependent K63-linked polyubiquitination (365). K63-linked ubiquitination of cIAP1/2 enhances their K48-specific E3 ubiquitin ligase activity toward TRAF3, leading to proteasomal degradation of the latter (368,370). As a result, TRAF3 levels in the cell drop, and NIK can no longer be recruited to the cIAP1/2-TRAF2 complex. This leads to stabilization and accumulation of newly synthesized NIK and its activation presumably via autophosphorylation, resulting in activation of IKKα (232). Once phosphorylated by IKKα on specific serine residues located in both the N- and C-terminal regions (395), p100 is ubiquitinated and cleaved to generate p52, which migrates as heterodimer with RelB to the nucleus and regulates transcription of its target genes.
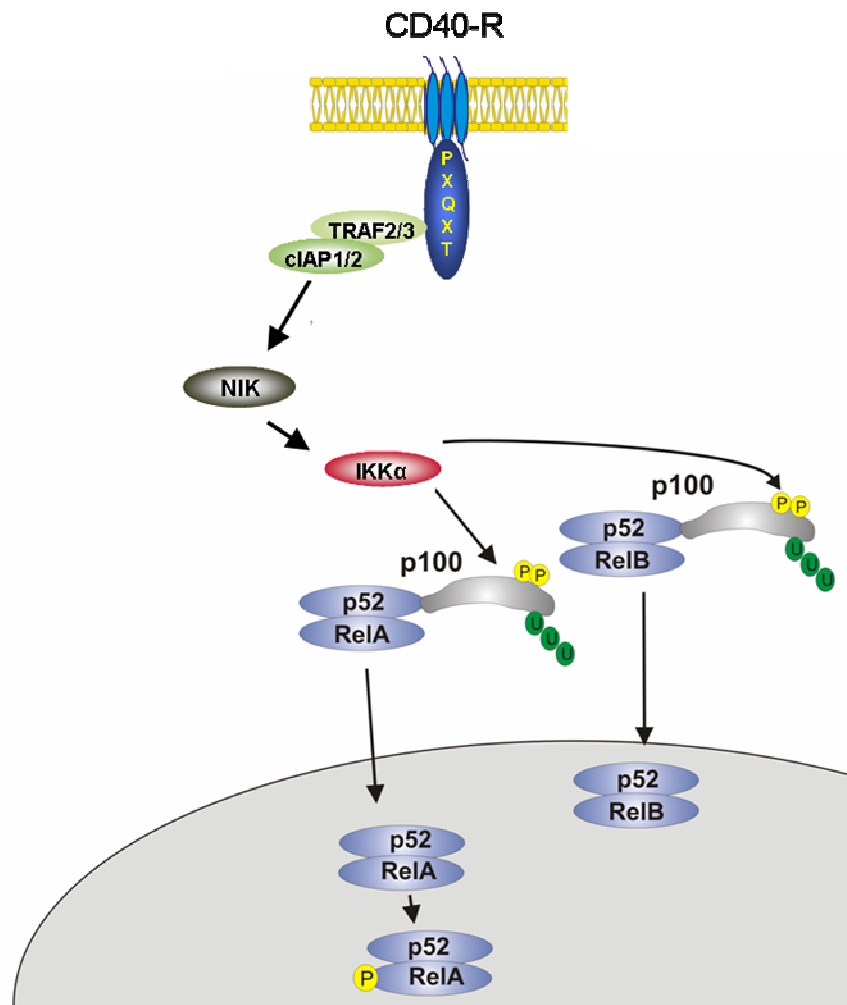
Figure 7. Noncanonical NF-κB signaling by CD40 (156,197).

Importantly, the canonical NF-κB pathway feeds into the noncanonical pathway through upregulation of NF-κB2 expression, but processing of p100 is stricktly dependent on its phosphorylation by IKKα and activation of IKKα by NIK (321,394). Moreover, stabilization of NIK also induces canonical signaling by activating IKKβ (14, 410). Beyond that, p100 processing regulates nuclear localization of RelA in addition to RelB (32).

Another NF-κB signaling pathway – the atypical pathway – which is triggered by DNA damage such as UV (198), relies on sequential p38 and Casin kinase 2 (CK2) activations (198), and involves phosphorylation and subsequent IκB degradation via an IKK-independent pathway.

Prompt activation of NF-κB is essential for a successful immune response, but it needs to be terminated to avoid tissue damage. Beyond that, uncontrolled NF-κB signaling can increase the risk of cancer and autoimmune disease (196). A number of mechanisms are involved at different steps of the pathway to terminate NF-κB signaling. Major regulators are IκB proteins that are involved in feedback inhibition of NF-κB. Newly synthesized IκBα enters the nucleus as a monomer, where it associates with DNA-bound p50:RelA dimers, leading to their inactivation and export into the cytoplasm (266). Furthermore, IKKα, involved in degradation of RelA (224), NIK (197), A20, and CYLD have been described as negative regulators. A20 was proposed to act in a two-step mechanism by first removing K-63-linked polyubiquitin chains from RIP1 (385). In the second step, the E3 ligase domain of A20 promotes K48-linked polyubiquitination of RIP1, leading to its proteasomal degradation (385). In contrast, the tumor suppressor CYLD (cylindromatosis) has been shown to remove K63-linked polyubiquitin chains from NEMO as well as from TRAF2 (217,360), leading to termination of the signaling.

15

1.3.2 NF-κB Essential Modulator (NEMO)

NEMO [for NF-κB essential modulator (also IKBKG, IKKγ, FIP3)] is the regulatory subunit of the IKK complex, which is responsible for the activation of NF-κB. NEMO is encoded by a gene called "inhibitor of kappa light polypeptide gene enhancer in B-cells, kinase gamma (*IKBKG*)". *IKBKG,* which is located at the X-chromosome, is a 23-kb gene structured in nine exons and four alternative noncoding first exons (Fig.8/9) (124,328). It encodes for multiple gene products. A non-functional partial second copy of the *IKBKG* gene (*IKBKG* pseudogene, IKBKGP/delta NEMO) is located 31,6kb distal to exon 10 (Fig.8).

Figure 8. Schematic representation of the genomic organization of the *IKBKG* gene (left) and the *IKBKG* pseudogene (right) at the Xp28 chromosome (adapted from 126).

NEMO is a 48kDa protein that is highly conserved and not related to IKKα or IKKβ. Although devoid of catalytic activity, NEMO is required for signaling in all canonical NF-κB pathways (122). Furthermore, NEMO deficient mice die embryonically of massive hepatocyte apoptosis (243,303).
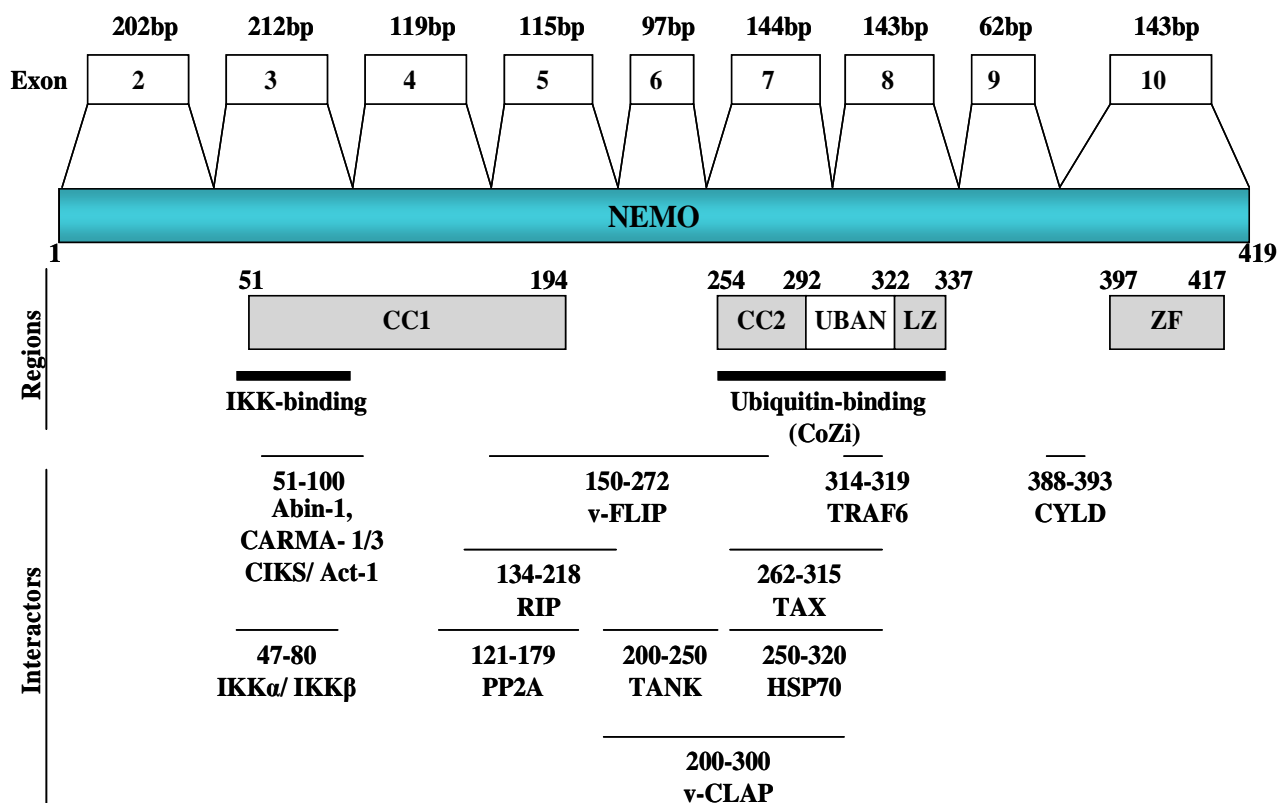
Figure 9. Schematic structure of the NEMO coding exons 2-10, functional regions of NEMO and interaction domains. CC(coiled-coil- domain), LZ (leucine zipper), ZF (zink finger), UBAN (Ubiquitin binding in Abin and NEMO), CoZi (ubiquitin binding domain; encompassing CC2, UBAN, and LZ) ABIN (A20-binding inhibitor of NF-κB activation), CARMA (CARD-containing MAGUK protein), CIKS (Connection to IKK and SAPK/JNK), Act-1 (NF-κB activator 1), v-CLAP (viral-CARD-like apoptotic protein), FLIP (FLICE-like inhibitory protein), Hsp70 (heat shock protein (70 kDa)), PP2A (protein phosphatase 2A), TANK (TRAF family member associated NF-κB activator).

A large proportion of the protein is predicted to form coiled coils. Sequence analysis of NEMO indicate that it consists of two coiled coil (CC1, CC2) domains that are separated by α-helices, a leucine zipper (LZ) domain, and a zink finger (ZF) domain (101)(Fig.9). The recently described UBAN motif (**U**biquitin **b**inding in **A**bin and **N**EMO) is located between CC2 and LZ. These domains are required for the correct assembly of the IKK complex (122,127) and for the recognition and recruitment of signaling molecules, whose interaction with NEMO is thought to be essential for the IKK-mediated NF-κB activation.

The C-terminal region of NEMO mediates activation of IKK and interaction with upstream signaling adapters, whereas the N-terminus is responsible for interaction with IKKs (244,300). IKKα and IKKβ bind NEMO through their C-terminal hexapeptide NEMO-binding domain (NBD) (Leu-Asp-Trp-Ser-Trp-Leu) (252,253). Binding to IKKs requires NEMO residues aa47-80, located within the first coiled-coil motiv (100,245,253). Competition experiments and biophysical analyses using a NBD peptide indicate that NEMO binds IKKβ with considerably higher affinity than IKKα (253).

Despite great efforts, the oligomeric state of NEMO and the exact mechanism of IKK activation by NEMO remains a matter of controversy. NEMO has variously been described to form monomers, dimers, trimers, or tetramers (4,122,351). A number of recent studies describing partial crystal structures such as the second coiled-coil region, together with the LZ (referred to as CoZi), demonstrate that NEMO forms a parallel, dimeric coiled-coil, in accordance with other studies that reported a dimeric assembly (41,235,293,351). The full-length protein has been recently shown to form a dimer that exists in a relatively weak equilibrium with tetramers (182).

A key step towards a better understanding of the regulatory role of NEMO in IKK activation was the observation that NEMO interacts specifically with polyubiquitin chains (390). Protein ubiquitination is a post-translational modification involved in the regulation of diverse cellular processes such as protein degradation, cell signaling, DNA damage response and transport processes. At least eight types of differently linked ubiquitin chains exist, including K6-, K11-, K27-, K29-, K33-, K48-, and K63-linked, and linear ubiquitin chains. Ubiquitination involves the formation of an isopeptide linkage between the amino group of a substrate lysine side chain and the carboxy terminus of ubiquitin, mediated through a cascade of reactions catalysed by three enzymes—E1, E2 and E3. E3 ligases such as TRAFs and IAPs (89,368) recognize substrate proteins and facilitate the transfer of ubiquitin from an E2 donor (Ubc13-Uev1a) (283). Ubiquitin itself has seven lysine residues, all of which can act as acceptors for further ubiquitination, generating polyubiquitin chains (178). Most non-proteolytic functions of ubiquitin chains are currently associated with K63-linked ubiquitin polymers (178,284), whereas K48-linked polyubiquitin targets substrate proteins for proteasomal degradation (162) (Fig.10a). K6-, K11-, K27-, K29-, and K33-linkages are not well characterized.

In addition to the lysine-mediated polyubiquitin chain formation, the amino terminus of ubiquitin can be used to form polyubiquitin. In this head-to-tail linkage (referred to as a linear ubiquitin chain) a peptide bond is formed between Ub1 glycine 76 and Ub2 methionine 1 (Fig.10b). Linear linkages can be assembled by an E3 ligase complex known as the linear ubiquitin chain assembly complex (LUBAC), which is composed of two RING–IBR–RING proteins—HOIL-1L and HOIP (214) (RING = really interesting new gene; IBR = in-between RING; HOIL-1L = long isoform of haem-oxidized iron-regulatory protein ubiquitin ligase 1; HOIP = HOIL-1L interacting protein). However, the role of linear ubiquitin linkages is at present poorly understood.

Ubiquitin chains are recognized by specific protein domains or motifs such as the zink finger and the ubiquitin-binding domain (UBD), which have been described in a large number of proteins (143,163,174).
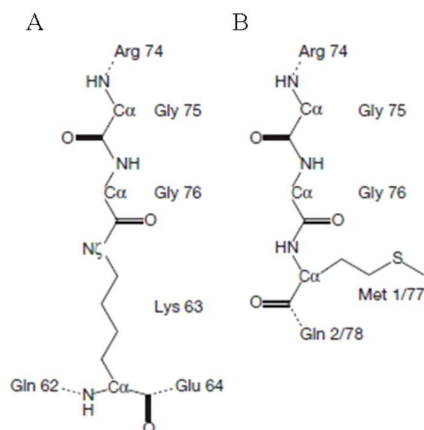
Figure 10. Structure of K63 and linear ubiquitin chains. (A) Chemical representation of the K63 linkage. Other isopeptide linkages, such as K48, differ only in the type of neighbouring residues. (B) Representation of the peptide linkage in a linear ubiquitin chain between Gly 76 and Met 1 of the second molecule (Gly= glycine; Met= methionine) (adapted from 216).

The recently published crystal structures of linear and K63-linked diubiquitin molecules demonstrate that both adopt highly similar open conformations (216). In contrast, the K63-linked and linear ubiquitin structures have been shown to be markedly different from K48-linked ubiquitin dimers and ubiquitin tetramers (102). The same study demonstrated that, despite the similar structures of linear and K63-linked ubiquitin chains, many deubiquitinating enzymes (DUBs), which recognize the linkage between ubiquitin molecules (or ubiquitin and substrates), and UBDs, which interact with a hydrophobic ubiquitin surface centred on isoleucin 44 (174), can discriminate between these two types of chains, emphasizing a remarkable specificity within the ubiquitin system. All analysed DUBs, except CYLD, cleaved linear chains less efficiently compared with other chain types, or not at all. Likewise, most analysed UBDs showed chain specificity, and were able to select distinct linkages from an ubiquitin chain mixture (216).

Nemo binds to polyubiquitin through a region encompassing the second coiled coil and the leucine zipper (termed CoZi, aa 254–337; 101,181,390). The CoZi domain contains a small conserved 30 amino-acid region which has also been identified in the NEMO-like proteins Optineurin and Abin-1,2,3 (319,372,416). This region was named NUB (NEMO ubiquitin binding), UBAN (Ubiquitin binding in Abin and NEMO) or NOA (Nemo Optineurin Abin) (hereafter referred to as UBAN). A few years ago it was demonstrated that direct binding of NEMO to K63-linked polyubiquitin chains is crucial for IKK recruitment and NF-κB activation, and that NEMO specifically binds K63-linked polyubiquitin chains within the CoZi domain (101,390). However, a recent determination of the structure of the UBAN region complexed with K63 or linear diubiquitin indicates that the UBAN motif binds to both types of chains, but exhibits a 100 fold higher affinity for linear diubiquitin while the contact points between UBAN and either linear or K63-linked ubiquitin chains are almost identical (235). A different recent report presents the crystal structure of the UBAN motif bound to linear diubiquitin and proposes that NEMO binds two linear ubiquitin chains that would run 'parallel' to the NEMO dimeric coiled-coil (293).

Besides the UBAN motif, it was shown that the C-terminal ZF of NEMO represents a second UBD (77). The same group recently demonstrated that neither the UBAN domain nor the ZF shows any specificity for K63-linked ubiquitin chains, and that their affinity for polyubiquitin chains is relatively low. However, a 170-aa fragment of NEMO containing the two UBDs (encompassing CC2-LZ-ZF) (called bipartite UBD or NOAZ) exhibits high affinity and high specificity for K63-linked polyubiquitin chains, indicating that the presence of both UBAN motif and ZF is required for the specific high-affinity binding of NEMO to K63-linked chains. Further, this study showed by affinity measurements and mutagenesis, that binding to linear chains was only dependent on the UBAN motif and did not

require the presence of the C-terminal ZF. In addition, they observed that the affinity of full-length NEMO for K63-linked ubiquitin chains was stronger than for linear chains (222).

Beyond its ability to recognize ubiquitin chains, it has been shown that NEMO itself becomes modified with ubiquitin following NF-κB activation (101,390), and that the particular lysine residue that accepts ubiquitin depends on the stimulus. It has been demonstrated that T-cell receptor signaling triggers K63-linked ubiquitination of NEMO at K399 (337,418), while MDP-induced Nod2–RICK stimulation triggers K63-linked polyubiquitination of NEMO at K285. Stimulation of TLR leads to ubiquitination of K285 and K399 (1,2). Further, the *Shigella* bacteria protein IpaH9.8 has recently been identified as an ubiquitin E3 ligase that targets NEMO residues K309 and K321 for K27-linked polyubiquitination (19). Moreover, recently it was demonstrated that NEMO becomes modified with linear polyubiquitin chains that are attached by the HOIP/HOIL-1 dimeric E3 ligase complex LUBAC (357). LUBAC has been shown to bind to NEMO in the IKK complex after stimulation with TNFα, and to conjugate linear chains onto K285 and/or K309 *in vitro*. Wild-type NEMO—but not a NEMO mutant with arginine substitutions at K285 and K309—was linearly ubiquitinated in cells in a signal-dependent manner (357). Importantly, the involvement of LUBAC in NF-κB activation was confirmed in genetically modified mice lacking its subunit HOIL-1L; TNFα-mediated activation of NF-κB was severely impaired in primary hepatocytes and MEFs from HOIL-1L-null mice (357).

While there are numerous reports demonstrating K63 and/ or linear ubiquitination of NEMO, and the ability of NEMO to recognize polyubiquitinated signaling intermediates, what continues to be lacking is an understanding of how regulatory ubiquitination functions during activation of the IKK complex. Furthermore, the linker region of NEMO, that separates the UBAN motif from the ZF, includes a number of predicted or identified phosphorylation sites (61) whose function is also currently unknown. However, despite a number of question marks, various models by which NEMO induces activation of NF-κB have been proposed. The ability of NEMO to recognize polyubiquitinated signaling proteins seems to be required for NF-κB activation in many signaling pathways, such as TNFR, TCR, or IL-1R/TLR. Upon stimulation, K63-linked polyubiquitination of downstream molecules such as RIP (226,390), IRAK1 (74), MALT1 (274), and Bcl10 (391), was thought to promote the binding of NEMO to these molecules, thus determining the recruitment and activation of the IKK complex. Recently, LUBAC was identified as a component of the TNFR1 signaling complex (TNF-RSC) (144). This study showed that NEMO is not required for LUBAC recruitment to the TNF-RSC (144), even though it can bind LUBAC (357). Based on their findings and other recent reports they suggest a model whereby NEMO recruitment to the TNF-RSC is significantly enhanced by LUBAC-mediated assembly of linear polyubiquitin chains. LUBAC attaches linear chains to NEMO and possibly other TNF-RSC components (such as Abins via their UBAN domain (216,293) and cIAPs via their UBA domain (143)), thereby stabilizing the entire complex and increasing the retention times of NEMO and other signaling components.

For the activation of the IKK complex, a number of models including trans-autophosphorylation and IKK kinase-mediated phosphorylation have been suggested (146). It is known that the N-terminal region of NEMO binds to IKKα/IKKβ (414), and that the CoZi region contains the oligomerisation domain required for IKK assembly (5,289,351). In addition, it has been shown that NEMO is recruited to activated TNF receptor complexes by interaction with polyubiquitin chains via its UBAN domain (101,181,390). One model suggests that interaction with linear ubiquitin chains may induce clustering of NEMO, which could lead to multimerization of the IKK complex, and, possibly followed by trans-autophosphorylation, results in activation of IKK (183). Alternatively, NEMO might act as a carrier or platform that is responsible for bringing IKKα and IKKβ in close proximity to activators such as TAK1 to

promote phosphorylation and activation (390). A different model assumes that the CoZi domain undergoes stimulus-dependent conformational changes that in turn might induce activation of the kinases (41).

Beyond its role in canonical NF-κB activation, NEMO was found to have IKK-independent functions. It is required for activation of the MAP kinases (MAPK) p38 and JNK (398). This function is mediated through the participation of NEMO in formation of a large signaling complex required for recruitment of the MAPK kinase kinases (MAP3K) MEKK1 and TAK1 to activated TNFR family members (249). Furthermore, NEMO also has a role in activation of the interferon (IFN) response, where it acts through a poorly defined mechanism to promote activation of the IFN response factors (IRFs) following viral infection (415).

In addition to its interaction with ubiquitin chains and to being the target of multiple post-translational modifications including phosphorylation, small ubiquitin-like modification (SUMOylation), and ubiquitination (61,170,319), NEMO also acts as an assembly platform that facilitates the incorporation of various viral proteins into the IKK signalosome, such as the Kaposi sarcoma-associated herpesvirus (KSHV) encoded protein vFLIP (viral FLICE [FADD (Fas-associated death domain)-like interleukin 1β-converting enzyme]-inhibitory protein) and the human T lymphotropic virus (HTLV)-1 encoded protein Tax (116,338). HTLV-1 Tax is the causative agent of adult T cell lymphoma (ATL). It activates the IKK complex by direct binding to NEMO at aa262-315 (190), resulting in constitutive activation of NF-κB (60,285). Similar to Tax, the KSHV viral protein v-FLIP induces a constitutively activated IKK complex by direct interaction with NEMO (62,234). KSHV causes the B cell malignancy primary effusion lymphoma (PEL).

Mutations affecting the gene encoding NEMO, which is located on the X chromosome, cause severe human pathologies including IP (familial incontinentia pigmenti), ID (immunodeficiency), and EDA-ID (anhidrotic ectodermal dysplasia with immunodeficiency) (78,79,126,328). These mutations have been found to be distributed throughout the entire molecule, and have been demonstrated to more or less severely affect the NF-κB response.

IP is a rare dominant disorder that is embryonic lethal in affected males (125,221). In females it affects ectodermal tissues and causes severe skin defects. In addition, IP female patients can also suffer from severe defects such as mental retardation, microcephaly, or seizueres (123,124,328). The most frequent IP causing mutation results from a recurrent exon 4_10 genomic rearrangement in the *IKBKG* gene, leading in most cases to the complete loss of NF-κB activation. However, there are also a number of reports describing IP causing point mutations in the *IKBKG* gene (78,117,316,320).

IP is allelic with EDA-ID, a rare X-linked recessive immunodeficiency syndrome which exclusively affects males (188). It combines the severe sensitivity to infection (as presented in ID) with abnormal development of skin adnexa (hair follicles, sweat glands, and teeth). EDA-ID patients suffer from skin inflammation and impaired NF-κB activation in response to numerous stimuli such as TNFα, IL-1, and LPS. This disease is due to *IKBKG* hypomorphic mutations, often missense or small deletions/insertions, which mainly affect the zinc finger domain of NEMO. These mutations reduce but do not eliminate NF-κB activation, explaining why affected male patients survive (15,95,420). Female patients carrying the same *IKBKG* mutations exhibit very mild signs of IP (15).

1.4 Mechanism of EBV LMP1 mediated NF-κB activation

Epstein-Barr virus (EBV)-encoded latent membrane protein 1 (LMP1) is oncogenic and indispensable for EBV-mediated B cell transformation. LMP1 acts as a constitutively activated receptor-like molecule independent of ligand binding or regulation (134). LMP1 is capable of activating several intracellular signaling pathways including the NF-κB pathway, which contributes to the EBV-mediated cell transformation. Two regions in the cytoplasmic carboxyl tail of LMP1, namely TES1 and TES2, are responsible for NF-κB activation (184). It is shown that a mutated recombinant EBV lacking the cytoplasmic tail of LMP1 is severely impaired in its ability to activate NF-κB and to immortalize primary B lymphocytes *in vitro* (203).

LMP1 TES1 induces and associates with TRAFs (91,149,184,262). The role of individual TRAFs in LMP1 mediated NF-κB signaling is partially elucidated in knockout MEFs. Although TES1 strongly binds TRAF1, TRAF2, TRAF3, and TRAF5, and TRAF1 and TRAF3 heterodimerize with TRAF2 and TRAF5, respectively, LMP1 does not require TRAF2 or TRAF5 for NF-κB activation in MEFs (239). Furthermore, in murine B cell lymphoma that lack TRAF3, LMP1 TES1 and TES2 failed to activate NF-κB, whereas TRAF2 was dispensable (396,397). TRAF3 overexpression inhibits LMP1 TES1 mediated NF-κB activation in HEK293 cells (91). Moreover, NF-κB activity is hyper basal in TRAF3 KO MEFs (145,275), resulting in the idea that TRAF3 is a negative regulator of NF-κB. TRAF binding to TES1 results in strong activation of NF-κB inducing kinase (NIK) and IKKα phosphorylation of p100 NF-κB2, leading to p52/ RelB nuclear translocation (20,105,239,308).

LMP1 TES2 engages death domain protein such as TRADD and RIP (184,186,260). TRADD binding to TES2 results in IKKβ phosphorylation of IκBα, canonical NF-κB activation, and nuclear translocation of p50/RelA and p52/RelA complexes (105,204,308). LMP1 interacts directly with RIP, stably associates with RIP in LCLs, but does not require RIP for NF-κB activation (185).

Surprisingly, LMP1 activation of NF-κB has been shown to be TRAF6 dependent (238,317). TRAF6 K63-linked polyubiquitination is critical for TAK1 activation downstream of IL-1/ Toll like receptors. However, MyD88 or IRAK4, two other components characteristic of IL-1R/ TLR signaling, are dispensable for LMP1 mediated NF-κB activation (238). The role of TRAF6 in LMP1 signaling is not completely understood. It is know that TRAF6 does not directly interact with LMP1, but can be recruited to TES2 through a direct or indirect interaction with TRADD (317).

IL-1 receptor associated kinase (IRAK1) has also been shown to be essential for LMP1 mediated NF-κB activation (238). The critical role of IRAK1 in LMP1-induced NF-κB activation seems to be in mediating RelA serine 536 phosphorylation through an effect on p38 or other RelA serine 536 kinases (331).

Experiments in TAK1 knockout MEFs, utilizing incorporation of tagged ubiquitin mutants that are specific for K63 and K48 chains, revealed that most but not all LMP1 TES2-mediated NF-κB activation is TAK1 dependent even though it is entirely TRAF6 dependent. It has been proposed that at least one additional unidentified kinase can mediate TES2 activation of NF-κB which could be another TRAF6 dependent kinase. However, a different study utilizing RNAi knockdown experiments suggested a complete dependence on TAK1 in 293 cells (389).

Both TES1 and TES2 activities can be inhibited with a dominantly active IκBα, indicating that IKKβ activation is important for both TES1 and TES2 mediated NF-κB activation (90,259). Furthermore, LMP1 mediated RelA nuclear translocation is independent of IKKα but substantially dependent on IKKβ (238).

Based on these findings, the following model for LMP1 mediated NF-κB activation can be proposed: LMP1 TES1 binds TRAF1 and TRAF3 and induces complex formation of TRAF1/2 and TRAF3/5. These complexes activate NIK, leading to phosphorylation and activation of IKKα which which results in p100 processing to p52. RelB/p52 and RelA/p52 complexes then translocate to the nucleus (Fig11, right). LMP1 TES2 associates with TRADD. TRADD directly or indirectly associates with TRAF6. In a yet unknown mechanism, the TRAF6 E3 ubiquitin-ligase activity is induced, resulting in activation of TAK1 and possibly another TAK1 like kinase. TAK1 activates the IKK complex, resulting in phosphorylation of IκBα on Ser32 and Ser36, leading to its K48-polyubiquitination at lysine 19 and subsequent degradation via the S26 proteasome pathway, thereby exposing a nuclear localisation signal (NLS) and inducing nuclear translocation of RelA/p50 heterodimers (Fig.11 left). Both LMP1 TES1 and TES2, possibly through TRAF3 and TRAF6, respectively, induce IRAK1 activation of p38 and possibly other kinases that phosphorylate RelA in p50/RelA and p52/RelA complexes (Fig.11).
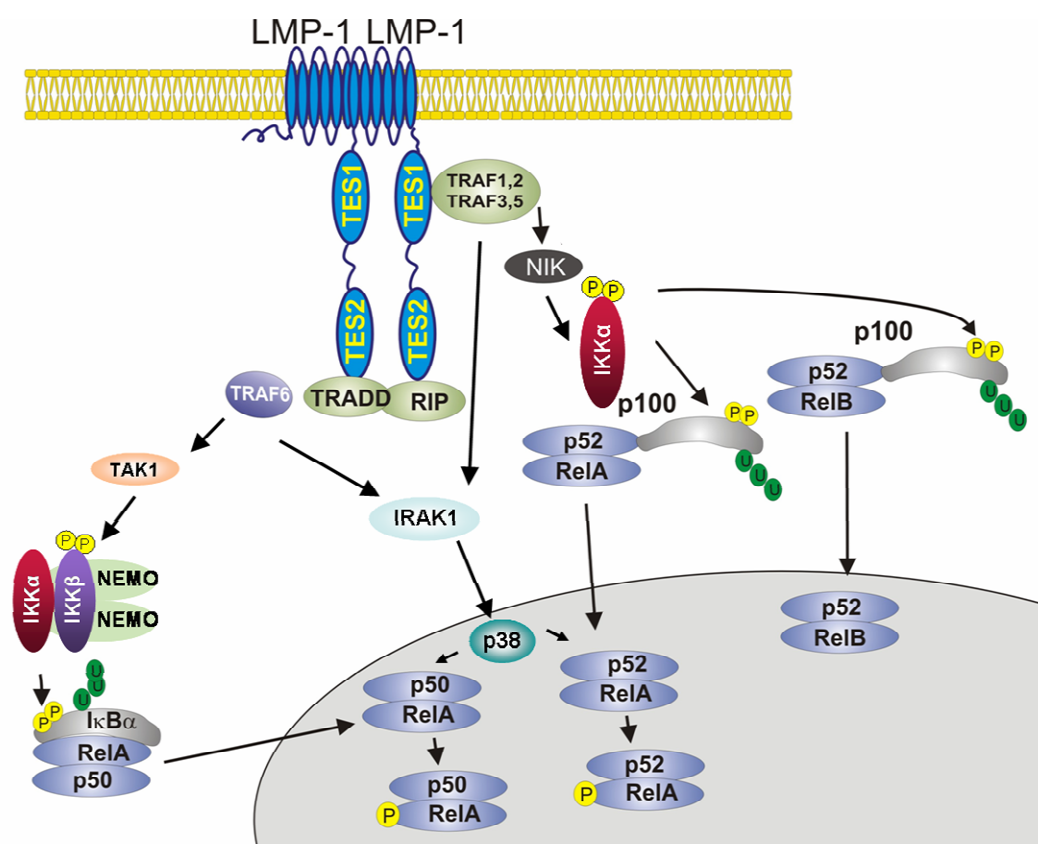
Figure 11. A model of LMP1 mediated NF-κB activation (adapted from: Song YJ, Cahir-McFarland ED, Kieff E 2006/2008). LMP1 utilizes two distinct pathways to activate NF-kappaB: a major one through TES2/ TRAF6/ TAK1/ IKKβ (canonical pathway) and a minor one through TES1/ TRAF3/ NIK/ IKKα (noncanonical pathway).

Taken together, the data indicate that LMP1 mediated NF-κB signaling can not be simply modelled after a TNF- or IL-1/ Toll like receptor. In contrast to LMP1, TNFR1 and CD40 require TRAF2 for signaling. In addition, TNFR1 mediated NF-κB activation may also require RIP. Furthermore, LMP1 activation of NF-κB is largely IRAK1 and TRAF6 dependent, whereas TNFR activation of NF-κB is largely IRAK1 and TRAF6 independent. In contrast to the IL-1R/ TLR-mediated NF-κB pathways, the LMP1 TES2-mediated NF-κB pathway does not require MyD88, or IRAK4 for TRAF6 engagement.

1.5 Reason for my Work

Previously published data from our lab reported that LMP1 mediated NF-κB activation is independent of NEMO/ IKKγ (238,239). Based on data obtained with GFP-RelA nuclear translocation assays, NF-κB reporter assays, and quantitative real-time PCR, M. Luftig *et al.* suggested that LMP1 is able to induce, besides the canonical (IKKβ/ NEMO-dependent) and noncanonical (NIK/IKKα-dependent) NF-κB activation pathway, a third, atypical canonical IKKβ-dependent/ NEMO (IKKγ)-independent NF-κB activation pathway (238,239). First, they demonstrated in NEMO/ IKKγ wildtype and knockout mouse embryonic fibroblast (MEF) experiments that NEMO/ IKKγ is not essential for LMP1-mediated NF-κB activation. NEMO/ IKKγ wildtype and knockout MEFs were transfected with GFP-RelA and IκBα-encoding plasmids in the presence or absence of an LMP1 expression plasmid or TNFα stimulation. When LMP1-mediated NF-κB activation in NEMO/ IKKγ knockout MEFs was compared to wildtype MEFs, GFP-RelA nuclear translocation and NF-κB-dependent reporter activity was similar in both cell lines. In contrast, TNFα induced GFP-RelA nuclear translocation in wildtype, but not in NEMO/ IKKγ knockout MEFs (Fig.12) (238).
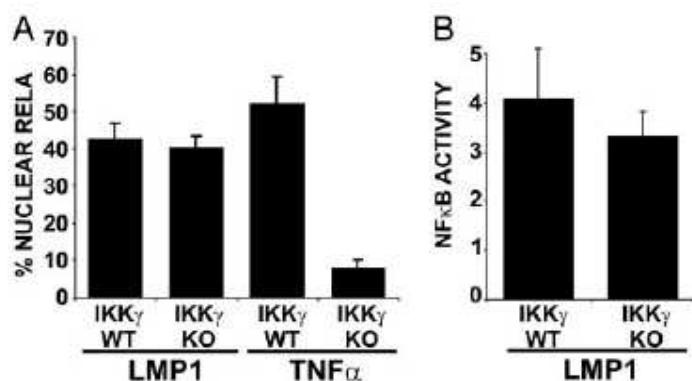
Figure 12. NEMO/ IKKγ is not essential for LMP1-mediated NF-κB activation. (A) NEMO/ IKKγ WT and KO MEFs were transfected with GFP-RelA and IκBα-encoding plasmids in the presence or absence of an LMP1 expression plasmid or TNFα stimulation. The percentage of cells with nuclear translocation of GFP-RelA induced by LMP1 or TNFα is shown. Average values +/- SD are shown from three experiments. (B) NEMO/ IKKγ WT and KO MEFs were transfected with reporter plasmids alone or with LMP1. Mean folds of NF-κB activation SD by LMP1 are shown from four experiments. (graph taken from Luftig *et. al.*, Ref. 238)

In their second experiment Luftig *et al.* tried to identify LMP1 regulated genes that are induced by canonical IKKβ versus noncanonical IKKα NF-κB activation and investigated for this reason the expression of 30 chemokines, cytokines, and receptors by quantitative real-time PCR in wildtype versus IKKα, IKKβ, or NEMO/ IKKγ knockout MEFs. Although all LMP1-induced gene expression tested was IKKβ-dependent, they found that LMP1 is unique in its ability to activate certain genes, such as MIP-2, in an NEMO/ IKKγ -dependent, IKKα-independent manner and others, such as I-TAC, in an NEMO/ IKKγ -independent, IKKα-independent manner (Fig.13) (239).
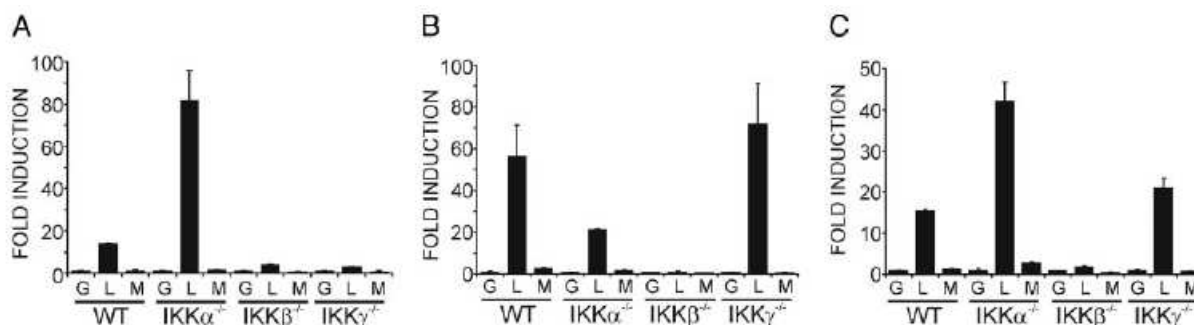
Figure 13. LMP1 induces canonical, noncanonical, and atypical NF-κB-dependent gene expression. WT, IKKα, IKKβ, and IKKγKO MEFs were transduced with GFP(G)-, LMP1 WT (L)-, or LMP1 DM (M)-expressing retrovirus. After 24 h, RNA was harvested, reverse transcribed, and quantitated by using MIP-2-specific(A), MIG-specific(B), or I-TAC-specific(C) primers. cDNA copy number was normalized to β-2 microglobulin cDNA as an internal control and is shown as fold induction relative to GFP-expressing retrovirus for each MEF +/- standard error. QPCR was performed in duplicate for each gene, and experiments were repeated at least twice. (graph taken from Luftig *et. al.*, Ref. 239)

For LMP1 mediated NF-κB activation, both the canonical and the noncanonical pathway are well established. The current thinking is that LMP1 TES2 mainly triggers canonical NF-κB signaling with activation of the IKK/NEMO complex, IκBα phosphorylation, and nuclear translocation of p50/RelA complexes. LMP1 TES1 is thought to mainly activate noncanonical NF-κB signaling via NIK, IKKα, p100 and p52. Further, it has been demonstrated that in cells lacking NEMO, the IKK complex cannot be activated by any of the known inducers of canonical NF-κB signaling.

We started this project because there were conflicting data about LMP1 mediated NF-κB signaling in NEMO knockout cells. One research group thought that in these cells LMP1 is unable to activate the canonical NF-κB pathway and that nuclear translocation of p65 is abolished (105). In contrast, Luftig *et al.* suggested, based on data described above, that LMP1 uniquely might be able to activate NF-κB not only via the canonical (IKKβ/NEMO dependent) and the noncanonical (NIK/IKKα dependent) pathways, but via a third pathway which is NEMO independent but IKKβ dependent. The hypothesis was that because NEMO is critical for IKKα/IKKβ/NEMO complex assembly and LMP1 differs from TNF- and Toll-like receptors in constitutively forming unusually large aggregates in the plasma membrane, LMP1 complexes may induce aggregates of TRAFs, death domain proteins, or other intermediate signaling molecules and thereby substitute for NEMO in assembling IKKα and IKKβ (238,239). Alternatively, LMP1 may preferentially engage an NEMO-like protein such as FIP-2 (229,230), or the cell lines utilized in these experiments may express NEMO mutant proteins that uniquely support LMP1 mediated NF-κB activation.

The experiments reported here were undertaken to investigate the role of NEMO in LMP1 mediated NF-κB activation. Understanding the molecular basis for LMP1's abberant NF-κB signaling is of great interest, both for understanding how this signaling pathway is regulated, and for potential application of this information to design therapies that target LMP1 function.

2. MATERIAL AND METHODS

2.1 Material

2.1.1 Equipment

Equipment	Model/ Company
Agarose gel equipment	Model B1A, Owl-Separation System, Inc., Portsmouth, USA
Autoclaves	Amsco Scientific, Inc., Wescodyne, VT, USA
Balance	PJ 400 and AB54-S, Mettler Toledo, Bedford, MA, USA
Centrifuge	IEC Centra GP8R, Thermo Electron Corp., Waltham, MA, USA IEC Centra CL 2 Centrifuge, Thermo Electron Corp., Waltham, MA, USA Model J2-21 Centrifuge, Beckman Coulter, Fullerton, CA, USA Sorvall® MC 12V, Thermo Fisher Scientific Inc., Waltham, MA, USA Sorvall® RC 5C Plus, Thermo Fisher Scientific Inc., Waltham, MA, USA Sorvall® Discovery 90SE, Thermo Fisher Scientific Inc., Waltham, MA, USA accuSpin™ Micro, Model 235C, Thermo Fisher Scientific, Waltham, MA, USA Micro-Centrifuge, Thermo Fisher Scientific Inc., Waltham, MA, USA Micro14, Thermo Fisher Scientific Inc., Waltham, MA, USA.
Cell counter	Hemacytometer (Bright Line), Hausser Scientific, Horsham, PA, USA
Distillation	102S All-Glass Water Still, Ultrascience, Inc., Evanston, IL, USA
FACS	FACS calibur, Becton Dickinson and Company, Franklin Lakes, NJ, USA
Freezer	-20ºC, Summit, GE Healthcare, Piscataway, NJ, USA -80ºC, Harris, Thermo Fisher Scientific Inc., Waltham, MA, USA -135ºC, Cryogenic Preservation System, Queue Cryostar , USA
Geiger counter	Model 3, Survey Counter LUDLUM Measurements, Inc., Boston, MA
Gel Dryer	Model 583, Bio-Rad Laboratories, Hercules, CA, USA
Gel electrophoresis equipment	Bio-Rad Mini PROTEAN® 3 System, Bio-Rad Laboratories, Hercules, CA, USA
Gel Shift Assay equipment	Bio-Rad Protean™ Dual Vertical Slab gel electrophoresis cell, Bio-Rad Laboratories, Hercules, CA, USA Laboratories, USA
Hoods	SterilGARD Hood, Class II, Type A/ B3, Baker Company, Buffalo, NY, USA
Ice Machine	Hoshizaki F-300 BAF, Hoshizaki America Inc., USA
Image Eraser	SF, Molecular Dynamics Inc., Sunnyvale, CA, USA
Imaging system for agarose gels (UV-transilluminator)	BioDoc-It™ Imaging System (camera, lens kit, 50mm UV blocking ethidium bromide filter, transilluminator, darkroom cabinet, LCD monitor, Compact Flasch Memory card and reader, thermal printer (Mitsubishi, Part-No. 89-0069-02), thermal paper (4 rolls, Part-No. 89-0038-01), UVP, Inc., USA
Incubator	CO2 Incubator, Model 6300, NAPCO, Inc., Waltham, MA, USA
Kodak Image Station 4000 R	Eastman Kodak Company, Rochester, NY, USA
Luminometer	OPTOCOMP 1, MGM Instruments, Hamden, CT, USA
Magnet Stirrer	Bell-Stir, Bellco Glass, Inc., USA
Microplate Reader	Model 3550, Bio-Rad Laboratories, Hercules, CA, USA Laboratories, USA
Microscope	1. Fluorescence microscope Axiovert 200, 2. Confocal microscope PCM 2000 (Nikon) coupled to Axioscop, Laser AttoArc HBO 100 W, (Red HeNe, Melles Griot; Green HeNe) 3. Microscope No. 4760438 4. Axiovert 25 (1-4 Carl Zeiss, Inc., Jena, Germany)
Nucleofector Device	Cat.-No. AAD-1001, Amaxa/ Lonza, Inc., Köln, Germany
pH-Meter	Φ44 pH Meter, Beckman Coulter, Fullerton, CA, USA
Pipettes	Pipetman P20 (2-20µl), Pipetman P200 (50-200µl), Pipetman P1000 (200-1000µl), all Gilson, Inc., Middleton, WI, USA
Phosphoimager	SI, Molecular Dynamics Inc., Sunnyvale, CA, USA

Equipment	Model/ Company
Powersupply	EC250-90, E-C Apparatus Corporation, Hayward, CA, USA
Refrigerator	ISOTEMP, Thermo Fisher Scientific Inc., Waltham, MA, USA
Scintillation counter	LS 5000TD, Beckman Coulter, Fullerton, CA, USA
Shaker/ Mixer	Hematology/ Chemistry Mixer 346 Lab-Line Instruments, Maharashtra, India Junior Orbit Shaker, Lab-Line Instruments, Inc., Maharashtra, India GIO Gurotory® Shaker, New Brunswick Sci. Corp., New Brunswick, NJ, USA
Spectrophotometer	U-2000, with 5-cell changer, Hitachi, Inc., Tarrytown, NY
Stirrer/ Hotplate	Model PC-320, Corning, Inc., Corning, NY, USA, Corning, NY, USA
Stroage Phosphor Screen	20x25cm, Molecular Dynamics, Inc., Sunnyvale, CA, USA
Thermal Cycler	GeneAmp PCR System 9600, Perkin Elmer Corp., Wellesley, MA, USA
Thermostat	Thermolyne Type 17600 Dry-Bath Dry Bath Incubator, Thermo Fisher Scientific Inc., Waltham, MA, USA Temp-Blok Heater, S/P® American Scientific Products, Columbus, OH, USA
Vortex Mixer	S/ P®, Cat.-No. S8223-1, American Scientific Products, Columbus, OH, USA
Water bath	16ºC Precision 280 Series, Thermo Fisher Scientific Inc., Waltham, MA, USA 32ºC Model 182, Precision Scientific, Inc., Chicago, IL, USA 37ºC Model 182, Precision Scientific, Inc., Chicago, IL, USA 37ºC Model 1245, VWR Scientific Products, West Chester, PA, USA, Inc. 42ºC Model 181, Precision Scientific, Inc., Chicago, IL, USA 55-60ºC Thelco 184, Precision Scientific Corporation, Inc. 65ºC Model 184, Precision Scientific, Inc., Chicago, IL, USA
Western blot equipment	Bio-Rad Mini PROTEAN® 3 System, Bio-Rad Laboratories, Hercules, CA, USA

2.1.2 Kits and Consumables

Kits	Company	Catalognumber
BCA* Protein Assay Reagent	Pierce, Rockford, MA, USA	23225
Cell Line Nucleofector Kit V	Amaxa/ Lonza, Inc., Köln, Germany	VCA-1003
DharmaFECT™ 1 Transfection Reagent	Thermo Fisher Scientific, Waltham, MA, USA	T-200(01-07)-03
Effectene® Transfection Reagent	QIAGEN Inc., Valencia, CA, USA	301427
EndoFree Plasmid Maxi Kit	QIAGEN Inc., Valencia, CA, USA	12362
Galacto-Light Plus™ System	Applied Biosystems, Foster City, CA, USA	BL 300
Genejuice® Transfection Reagent	Novagen, Madison, WI, USA	70967-M00005945
Luciferase Assay System	Promega Corp., Madison, WI, USA	E4030; E4530
MEF Nucleofector™ Kit 2	Amaxa/ Lonza, Inc., Köln, Germany	VPD-1005
MycoAlert™ Kit	Cambrex Bio Science Rockland, Inc., Rockland, ME, USA	LT27-237; LT27-238
Oligotex mRNA Midi Kit	QIAGEN Inc., Valencia, CA, USA	70042
Prime-It II Random Primer Labeling Kit	Stratagene, La Jolla, CA, USA	300385
ProLong® Antifade Kit	Invitrogen, Inc., Carlsbad, CA, USA,	P7481
ProLong® Antifade Reagent	Invitrogen, Inc., Carlsbad, CA, USA,	P36930
QIAEX II Gel Extraction Kit	QIAGEN Inc., Valencia, CA, USA	20051
QIAprep 96 Turbo Miniprep Kit	QIAGEN Inc., Valencia, CA, USA	27104
QIAprep Spin Miniprep Kit	QIAGEN Inc., Valencia, CA, USA	27104
QIAquick Gel Extraction Kit	QIAGEN Inc., Valencia, CA, USA	28704
QuikChange® II Site-Directed Mutagenesis Kit	Stratagene, La Jolla, CA, USA	200523
SilverQuest™ Silver Staining Kit	Invitrogen, Inc., Carlsbad, CA, USA,	LC6070
SuperScript™ III First-Strand Synthesis System for RT-PCR	Invitrogen, Inc., Carlsbad, CA, USA	18080-051

Kits	Company	Catalognumber
TOPO TA Cloning® Kit for Sequencing	Invitrogen, Inc., Carlsbad, CA, USA	K4575-J10
*Trans*IT®-Jurkat Transfection Reagent	Mirus Bio Corp., Madison, WI, USA	MIR 2120
*Trans*IT®-LT1 Transfection Reagent	Mirus Bio Corp., Madison, WI, USA	MIR 2300
UltraClean™ Endotoxin Removal Kit	MO Bio Laboratories, Inc., Carlsbad, CA, USA	12615
Western Lightning™ Chemiluminescence Reagent	Perkin Elmer Corp., Wellesley, MA, USA	NEL104

The kits were used according the manufacturer's instructions.

Consumables	Company	Catalognumber
Aluminiun foil	Thermo Fisher Scientific, Waltham, MA, USA	01-213-105
Blades	GARVEY Products, San Dimas, CA, USA	335
Centrifuge Tubes	Beckmann Coulter, Fullerton, CA, USA Corning, Inc., Corning, NY, USA,	362181; 362183 430791; 430829
Dialysis-membrane	Spectrum Lab., Rancho Dominguez, CA, USA	132 678
Electroporation Cuvette 0,2cm	USA Scientific, Ocala, FL, USA	82911
FACS tubes	BD Falcon, Franklin Lakes, NJ	REF 352235; REF 352052
Fiber Pads	Bio-Rad Laboratories, Hercules, CA, USA	170-3933
Film footage	Eastman Kodak Company, Rochester, NY, USA	178 8207
Filter paper	Thermo Fisher Scientific, Waltham, MA, USA	05-714-4
Glass plates	Electron Microscopy Sciences, Hatfield, USA	63424-06
Luminometer Tubes	Sarstedt Inc., Newton, NC, USA	55.476
Lens Paper	VWR Scientific Prod., West Chester, PA, USA	52846-001
Microcentrifuge Tubes	Corning, Inc., Corning, NY, USA Thermo Fisher Scientific, Waltham, MA, USA	3620; 3622 02-681-375
Microscope Slides	Thermo Fisher Scientific, Waltham, MA, USA	12-550-34
Microscope cover glass	Thermo Fisher Scientific, Waltham, MA, USA	12-542-B; 12-545-M; 12-545-C
Nitrocellulose Membran	Bio-Rad Laboratories, Hercules, CA, USA	162-0115 162-0159
Nylon Membrane Genescreen™	Perkin Elmer Corp., Wellesley, MA, USA.	NEF 988
PCR Tubes	Corning, Inc., Corning, NY, USA	6542
Pipette Tips	Corning, Inc., Corning, NY, USA USA Scientific, Ocala, FL, USA	4853; 4867 1111-1210
Pipette Tips (Aerosol-Barrier)	Thermo Fisher Scientific, Waltham, MA, USA	02-707-33; 02-707-116
PVC foil	Thermo Fisher Scientific, Waltham, MA, USA	15-610
Round-bottom tube	Becton Dickinson and Co., Franklin Lakes, NJ	352059
Spincolumns MicroSpin™ S-200 HR	Pharmacia Biotech, San Francisco, CA, USA	27-5120
Transfer Pipettes	Thermo Fisher Scientific, Waltham, MA, USA	13-711-7

2.1.3 Chemicals

Chemicals	Company	Catalognumber
Aceton	Thermo Fisher Scientific, Waltham, MA, USA	A16S-4
Acetic Acid	Thermo Fisher Scientific, Waltham, MA, USA	A38-212
Acrylamide	National Diagnostics, Charlotte, NC, USA	EC-890
Agarose GPG/LE	American Bioanalytical, Natick, MA, USA	AB00972-0500
Ampicillin	Sigma-Aldrich, St. Louis, MO, USA	A1593-25g
Ammoniumperoxodisulfat APS	Sigma-Aldrich, St. Louis, MO, USA,	A-6761

Chemicals	Company	Catalognumber
BCA* Protein Assay Reagent	Pierce, Rockford, MA, USA	23225
Blasticidin S hydrochloride	Sigma-Aldrich, St. Louis, MO, USA	15205
Boric acid	American Bioanalytical, Natick, MA, USA	AB250
Brilliant Blue	Sigma-Aldrich, St. Louis, MO, USA	B-7920
Bromphenyl Blue	Sigma-Aldrich, St. Louis, MO, USA	B-7021
1-Butanol	Thermo Fisher Scientific, Waltham, MA, USA	A383-4
Cesiumchlorid	American Bioanalytical, Natick, MA, USA	AB00300-01000
Chloroform	Thermo Fisher Scientific, Waltham, MA, USA	C-606-1
Coomassie Brilliant Blue	Bio-Rad Laboratories, Hercules, CA, USA	161-0400 R-250
Crystal Violet	Sigma-Aldrich, St. Louis, MO, USA	C-0775
dIdC poly(deoxyinosinic-deoxycytidylic) acid, sodium salt,	Sigma-Aldrich, St. Louis, MO, USA	P4929
N,N-Dimethylformamide	Sigma-Aldrich, St. Louis, MO, USA	D-8654
DMSO Dimethylsulfoxid	Fisher Chemicals, Loughborough, UK,	BP 231-1
DRAQ5	Alexis Corporation, Plymouth Meeting, PA, USA	BOS-889-001-R200
DRAQ5	Biostatus Limited, Shepshed, UK	SKU:DR50050
DTT Dithiotreitol	Sigma-Aldrich, St. Louis, MO, USA	43817
Ethyl Alcohol	Pharmaco Products, Inc., Brookfield, CT, USA	111ACS200 111USP200 111000190 111USP190
N-Ethylmaleimide	Sigma-Aldrich, St. Louis, MO, USA	E3876-5G
Ethidium bromide	Sigma-Aldrich, St. Louis, MO, USA	E-8751-5G
EDTA	American Bioanalytical, Natick, MA, USA	AB00500-01000
Formaldehyde Solution 37%	Thermo Fisher Scientific, Waltham, MA, USA	F79-500
G418/ Neomycin	GEMINI Bio-Products, Woodland, CA, USA	400-111P 400-113
X-Gal (BCIG)	5Prime, 3Prime, Inc., Boulder, CO, USA	554511
Glucose	American Bioanalytical, Natick, MA, USA	AB 00715-00500
L-Glutamine	Invitrogen, Inc., Carlsbad, CA, USA	25030-081
Glycerol	American Bioanalytical, Natick, MA, USA	AB0075-04000
Glycine	American Bioanalytical, Natick, MA, USA	AB00730-5000
Guanidine Hydrochloride	Sigma-Aldrich, St. Louis, MO, USA	G-4505-1KG
Hepes Buffer Solution	Gibco, Invitrogen, Inc., Carlsbad, CA, USA	15630-080
Hepes Free Acid	Sigma-Aldrich, St. Louis, MO, USA	H-0891
Hepes Sodium Salt	Sigma-Aldrich, St. Louis, MO, USA	H-3784
Hydrochloric Acid	Fisher Chemicals, Loughborough, UK	A144-500
Hygromycin	EMD Biosciences, Inc., La Jolla, CA, USA	400052
IL-1β/ IL-1F2 recombinant human	R&D Systems, Inc., Minneapolis, MN, USA	201-LB-005
Imidazole	Sigma-Aldrich, St. Louis, MO, USA	I-0125-500G
IPTG Isopropyl-β-D-thiogalacto-pyranoside	Sigma-Aldrich, St. Louis, MO, USA	434582-1G
Kanamycin	Sigma-Aldrich, St. Louis, MO, USA	K-0129
Kanamycin sulfate	Boehringer Mannheim GMBH, Germany	83897422-46
LB Broth, Miller (Luria Bertani)	Fisher Chemicals, Loughborough, UK	BP1426-500
LB Agar	Becton Dickinson and Co., Franklin Lakes, NJ	244510
Magnesiumchloride x 6 H_2O	Sigma-Aldrich, St. Louis, MO, USA	M-0250
Maltose	Sigma-Aldrich, St. Louis, MO, USA	M-5885
D-Mannitol	Sigma-Aldrich, St. Louis, MO, USA	M-4125
2-Mercaptoethanol	Sigma-Aldrich, St. Louis, MO, USA	M-250
2-Mercaptoethanol	Gibco, Invitrogen, Inc., Carlsbad, CA, USA	21985-023
Methanol	Thermo Fisher Scientific, Waltham, MA, USA	A452-4
Methylene Blue	Sigma-Aldrich, St. Louis, MO, USA	M-4159

Chemicals	Company	Catalognumber
MG-132	EMD Biosciences, Inc., La Jolla, CA, USA	474790
Milkpowder 34,8% Protein, Nonfat	Shaws Supermarket, USA	
MOPS 3-(N-morpholino)-propanesulfonic acid	American Bioanalytical, Natick, MA, USA	AB1270
NP40 (Igepal CA-630)	Sigma-Aldrich, St. Louis, MO, USA	13021-500ML
Orange G	Sigma-Aldrich, St. Louis, MO, USA	O-3756
Paraformaldehyd	Polysciences, Inc., Warrington, PA, USA	0380
1,10-Phenanthroline	Sigma-Aldrich, St. Louis, MO, USA	P9375-5G
PBS Phosphate-Buffered Saline	Invitrogen, Inc., Carlsbad, CA, USA	14190-144
Penicillin-Streptomycin	Invitrogen, Inc., Carlsbad, CA, USA,	15070-063
Phenol : Chloroform 5:1	Sigma-Aldrich, St. Louis, MO, USA	P-1944
PMSF (phenylmethylsulfonyl fluoride)	Sigma-Aldrich, St. Louis, MO, USA	P-7626
Plasmocin™:	Invivogen, San Diego, CA, USA,	ant-mpt
Ponceau S	Sigma-Aldrich, St. Louis, MO, USA	P-3504
Potassium Acetate	Thermo Fisher Scientific, Waltham, MA, USA	BP364-500
Potassium Chloride	Sigma-Aldrich, St. Louis, MO, USA	P-4504
Potassium Phosphate KH_2PO_4	Thermo Fisher Scientific, Waltham, MA, USA	BP362-1
Potassium Phosphate K_2HPO_4	Thermo Fisher Scientific, Waltham, MA, USA	BP363-1
2-Propanol	Thermo Fisher Scientific, Waltham, MA, USA	A416-4
Propidium Iodide	Molecular Probes, Eugene, OR, USA	P-3566
Propylene Glycol	Sigma-Aldrich, St. Louis, MO, USA	P2263-1KG
Puromycin	Invivogen, San Diego, CA, USA	ant-pr-1
Puromycin dihydrochloride	Sigma-Aldrich, St. Louis, MO, USA	P7255
SDS Sodium Dodecyl Sulfate	Sigma-Aldrich, St. Louis, MO, USA	L-5750
S.O.C. medium,	Invitrogen, Inc., Carlsbad, CA, USA,	15544-034
Sodium Acetate	American Bioanalytical, Natick, MA, USA	AB1909
Sodium Azide	Sigma-Aldrich, St. Louis, MO, USA	S-2002
Sodium Chloride	American Bioanalytical, Natick, MA, USA	AB01915-10000
Sodium Fluoride	Sigma-Aldrich, St. Louis, MO, USA	S-1504
Sodium Hydroxide	Fisher Chemicals, Loughborough, UK	S318-1
Sodium Orthovanadate Na_3VO_4	Sigma-Aldrich, St. Louis, MO, USA	S-6508
Sodium Phosphate Na_2HPO_4 x $7H_2O$	Sigma-Aldrich, St. Louis, MO, USA	S-9390
Sodium Phosphate Na_2HPO_4	Sigma-Aldrich, St. Louis, MO, USA	S-0876-500G
Sodium Phosphate NaH_2PO_4	Sigma-Aldrich, St. Louis, MO, USA	S-9638
Succinic Acid	Sigma-Aldrich, St. Louis, MO, USA	S9512
TEMED N,N,N`,N`-Tetramethylendiamin	Sigma-Aldrich, St. Louis, MO, USA	T9281
TNFα, recombinant human	R&D Systems, Inc., Minneapolis, MN, USA	210-TA/CF
TPA 25mg/ml, 1000x	Invitrogen, Inc., Carlsbad, CA, USA,	T6882
Tris	American Bioanalytical, Natick, MA, USA	AB02000-05000
Tris-HCl	American Bioanalytical, Natick, MA, USA	AB02005-05000
Triton®X-100	Sigma-Aldrich, St. Louis, MO, USA	T8787
Trizma Base	Sigma-Aldrich, St. Louis, MO, USA	T-8524
Trizol® Reagent	Invitrogen, Inc., Carlsbad, CA, USA,	15596-026
Trypsin	Invitrogen, Inc., Carlsbad, CA, USA,	25200-114
Tryptone	Fisher Chemicals, Loughborough, UK	BP1421-500
Tween 20	Sigma-Aldrich, St. Louis, MO, USA	P7949
Urea	Mallinckrodt, Inc., Hazelwood, MO, USA	8648
Yeast Extrakt	Fisher Chemicals, Loughborough, UK	BP1422-500

2.1.3.1 Inhibitors

Aprotinin, Sigma-Aldrich, St. Louis, MO, USA, Cat.-No. A-6279, Protease inhibitor, from bovine lung, inhibits Serinproteases and human leukozytäre Elastase

Phosphatase Inhibitor Cocktail 1, Sigma-Aldrich, St. Louis, MO, USA, Cat.-No. P2850, contains Cantharidin, Bromotetramisole and Microcystin LR; for Serine/ Threonine Protein Phosphatases and L-Isozymes of Alkaline Phosphatases

Phosphatase Inhibitor Cocktail 2, Sigma-Aldrich, St. Louis, MO, USA, Cat.-No. P5726, contains Sodium orthovanadate, Sodium molybdate, Sodium tartrate, and Imidazole; for Tyrosine Protein Phosphatases, Acid and Alkaline Phosphatases

Protease Inhibitor Cocktail, Sigma-Aldrich, St. Louis, MO, USA, Cat.-No. P8340, contains [4-(2-Aminoethyl) benzenesulfonyl fluoride hydrochloride], Aprotinin, Bestatin hydrochloride, E-64-[N(trans-Epoxysuccinyl)-L-leucine 4-guanidinbutylamide], Leupeptin hemisulfate salt, Pepstatin A

Tpl2 Kinase Inhibitor, Calbiochem, EMD Biosciences, Inc., La Jolla, CA, USA, Cat.-No. 616373, 4-(3-Chloro-4-fluorophenylamino)-6-(pyridine-3-yl-methylamino)-3-cyano-[1,7]-naphthyridine

Casein Kinase II Inhibitor II, DMAT, Calbiochem, EMD Biosciences, Inc., La Jolla, CA, USA, Cat.-No. 218699, 2-Dimethylamino-4,5,6,7-tetrabromo-1H-benzimidazole

Calmodulin Kinase II Inhibitor, Sigma-Aldrich, St. Louis, MO, USA, Cat.-No. C1360, rat, recombinant

IKKβ Inhibitor IV, Calbiochem, EMD Biosciences, Inc., La Jolla, CA, USA, Cat.-No. 401481, [5-(*p*-Fluorophenyl)-2-ureido]thiophene-3-carboxamide]

IKKβ Inhibitor III, BMS-345541 Calbiochem, EMD Biosciences, Inc., La Jolla, CA, USA, Cat.-No. 401480, 4-(2'-Aminoethyl)amino-1,8-dimethylimidazo[1,2-a]quinoxaline

IKKβ Inhibitor, SC-514, Calbiochem, EMD Biosciences, Inc., La Jolla, CA, USA, Cat.-No. 401479, $C_9H_8N_2OS_2$

p38 Inhibitor SB 203580, Calbiochem, EMD Biosciences, Inc., La Jolla, CA, USA, Cat.-No. 559389, 4-(4-Fluorophenyl)-2-(4-methylsulfinylphenyl)-5-(4-pyridyl)1H-imidazole

Caspase Inhibitor Q-VD-OPh, Calbiochem, EMD Biosciences, Inc., La Jolla, CA, USA, Cat.-No. 551476, non –O– methylated, N-(2-Quinolyl)valyl-aspartyl-(2,6-difluorophenoxy)methyl ketone

2.1.4 Buffer and Solutions

Buffer and Solution	Composition
BCA Protein Assay Reagent	
BCA Reagent A	contains sodium carbonate, sodium bicarbonate, BCA detection reagent and tartrate in 0,1 N sodium hydroxide
BCA Reagent B	contains 4% cupric sulfate
Cesiumchlorid-Purification DNA	
Buffer A	50mM EDTA, 25mM Tris, pH 8,0; 1% Glucose
Buffer B	0,2N NaOH, 1% SDS
Buffer C	3M KOAc, 115ml Acetic Acid
Nuclear-Cytoplasmic Fractionation	
Buffer A	10mM Hepes, pH 7,9; 10mM KCl; 1,5mM $MgCl_2$ 1mM PMSF, 1mM Sodium orthovanadate, 50mM NaF, 1:100 Protease inhibitor cocktail, (5mM DTT)
Buffer B	20mM Hepes, pH 7,9; 420mM NaCl; 1,5mM $MgCl_2$ 0,2mM EDTA, 20%Glycerol, 1mM PMSF, 1mM Sodium orthovanadate, 50mM NaF, 1:100 Protease inhibitor cocktail, (5mM DTT)

Buffer and Solution	Composition
Buffer for Mass-spectrometry	8M GnHCl, 5% n-Propanol, 100mM NH_4HCO_3; pH 8,6
Blockbuffer for Western blots	5% non-fat dry milk in 1x TBST buffer
Colony Hybridization/ Northernblot Buffer 1 Buffer 2 Buffer 3 Prehybridization Solution Hybridization Solution 50x Denhardt's solution 20x SSC	 0,1% SDS 0,5M NaOH; 1,5M NaCl 0,5M Tris, pH 8,0; 1,5M NaCl 6x SSC, 5x Denhardt's Solution, 0,2% SDS 50ml/l 20x SSC, 100ml/l 50x Denhardt's solution, 50ml/l 10% SDS, 100ml/l HT-DNA (10mg/ml stock) 10g/l Ficoll, 10g/l Polyvinylpyridione, 10g/ BSA 3M NaCl, 300m Trisodium Citrate; pH 7,0
Coomassie Blue staining Staining solution Destaining solution	 30% Methanol, 10% Acetic Acid, 60% ddH_2O, 0,025% Coomassie Brilliant Blue R250 30% Methanol, 10% Acetic acid, 60% ddH_2O
Dephosphorylation buffer (10x) for alkaline Phosphatase	0,5M Tris-HCl, 1mM EDTA; pH 8,5
DNA sample loading buffer (10x)	0,21% Bromophenol Blue, 0,21% Xylene Cyanol, 0,2M EDTA pH 8,0, 50% Glycerol
DNA sample loading buffer, orange	50% Glycerol, 50% ddH_2O, Orange G to taste
DEPC-water	0,1% v/v DEPC
EMSA buffer EMSA buffer 1 (1x Totex) EMSA buffer 2 (1x Lysis EMSA buffer 3 (5x Binding)	 1% Nonidet P-40, 20mM Hepes, pH 7,9; 350mM NaCl, 1mM $MgCl_2$, 0,5mM EDTA, 0,1mM EGTA, 20% Glycerol 100µl Totex-buffer (10x), 5mM DTT, 5mM PMSF, 1% Aprotinin 0,5% Triton X-100; 2,5% Glycerol, 4mM DTT, 10mM Hepes, pH 7,5; 80µg/ml poly (dI-dC)
Ethidiumbromid Solution	10g/l Ethidium bromide in ddH_2O
Fixing sol. for Immunfluorescence	50% Aceton, 50% Methanol
Galacto-Light Plus™ System Galacto Lysis Solution Galacto Reaction Buffer Diluent	 100mM potassium phosphate, pH 7,8; 0,2% Triton X-100 100mM sodium phosphate, pH 8,0; 1mM $MgCl_2$
His-IP buffer His-IP buffer A (pH 6,3 or 8,0) His-IP buffer G His-IP elution buffer	 8M Urea, 0,1M Na_2HPO_4/ NaH_2PO_4, 10mM Tris 8,0, 10mM β-mercaptoethanol 6M Guanidine hydrochloride, 0,1M Na_2HPO_4/ NaH_2PO_4, 10mM Tris 8,0, 10mM β-mercaptoethanol 150mM Tris pH 6,8; 250mM Imidazol
Immunoprecipitation (IP)-buffer	0,5% NP40, 100mM NaCl, 20mM Tris pH 7,5; 0,5mM EDTA, 1:100 Protease inhibitor cocktail; 0,5mM PMSF
In-vitro kinase assay Buffer PD Kinase buffer	 20mM Tris pH 8,0; 250mM NaCl; 0.05% NP40, 3mM EDTA, 3mM EGTA 20mM Hepes pH7.6; 20mM β-glycerophosphate; 0,1mM Na_3VO, 10mM $MgCl_2$, 50mM NaCl, 1mM DTT
IKK in- vitro kinase assay (IVK) buffers (Nick Shinners) IVK buffer A IVK buffer 2 (1x ELB) IVK buffer 3 (kinase buffer)	 10mM Hepes, pH 7,4; 10mM KCl; 0,1mM EDTA, 0,1mM EGTA, 1,5mM $MgCl_2$, 300mM Sucrose, 0,4% NP40, 1mM DTT (fresh), 0,5mM PMSF (fresh) 50mM Hepes (sodium salt), 250mM NaCl, 5mM EDTA, 0,1% NP40 10mM Hepes, 5mM $MgCl_2$, 1mM $MnCl_2$, 12,5mM β-glycerophosphate, 2mM NaF, 250µM Na_3VO_4, 1mM DTT

Buffer and Solution	Composition
IKKα-IP buffer (Bayon et al.)	50mM Tris, pH 8,0; 1mM EDTA, 0,1% NP40, 250mM NaCl, 10% Glycerol, 1mM Na_3VO_4, 20mM β-glycerophosphate, 0,5mM PMSF
Kodak GBX developer & replenisher	contains Hydroquinone, Diethylene glycol, Potassium sulfite, Sodium sulfite, 4-hydroxymethyl-4-methyl-1-phenyl-3-pyrazolidinone
Kodak GBX fixer & replenisher	contains Sodium bisulfite, Ammonium bisulfite, Ammonium thiosulfate, Aluminium sulphate, Sodium tetraborate-pentahydrate
LB Broth, Miller Luria Bertani (LB)	10g/l Tryptone, 10g/ NaCl, 5g/l Yeast Extrakt
LB Agar	10g Tryptone, 10g NaCl, 5g Yeast Extract, 15g Agar, 40g LB Agar
MCLB buffer for TAP purification *(Mat Sowa)*	50mM Tris pH 7,5; 150mM NaCl, 0,5% NP40, 10mM NaF; 0,5mM PMSF, 1:100 Phosphatase inhibitor cocktail I & II, 1:100 Protease inhibitor cocktail, 4mM N-Ethylmaleimide, 4mM 1,10-Phenanthroline
10x MOPS	0,4M MOPS, 0,1M Sodiumacetate, 0,01M EDTA
NEBuffer 1	10mM Bis Tris Propane-HCl, 10mM $MgCl_2$, 1mM DTT; pH 7,0
NEBuffer 2	10mM Tris-HCl, 10mM $MgCl_2$, 50mM NaCl, 1mM DTT; pH 7,9
NEBuffer 3	50mM Tris-HCl, 10mM $MgCl_2$, 100mM NaCl, 1mM DTT; pH 7,9
NEBuffer 4	20mM Tris-acetate, 10mM Magnesium acetate, 50mM Potassium acetate, 1mM DTT; pH 7,9
NETN buffer (GST)	1mM EDTA, 150mM NaCl, 20mM Tris pH8,0; 0,5% NP40,
PBS (10x)	137mM NaCl, 2,7mM KCl, 4,3mM Na_2HPO_4, 1,47mM KH_2PO_4; pH 7,4
10x PCR Buffer (*Taq* DNA Polymerase)	200mM Tris-HCl pH 8,4; 500mM KCl
QIAGEN Buffer and Solutions Buffer EB	10mM Tris-HCl, pH 8,5
Buffer P1 (resuspension buffer)	50mM Tris-Cl, pH 8,0; 10mM EDTA, 100µg/ml RNase A
Buffer P2 (lysis buffer)	200mM NaOH, 1% SDS (w/v)
Buffer P3 (neutralization buffer)	3M Potassium acetate, pH 5,0
Buffer QBT (equilibration buffer)	750mM NaCl, 50mM MOPS, pH 7,0; 15% Isopropanol (v/v), 0,15% Triton® X-100 (v/v)
Buffer QC (wash buffer)	1M NaCl, 50mM MOPS, pH 7,0; 15% Isopropanol (v/v)
Buffer QN (elution buffer)	1,6M NaCl, 50mM MOPS, pH 7,0; 15% Isopropanol
RIPA lysis buffer	50mM Tris, pH 8,0; 2mM EDTA, 1,0% NP40, 150mM NaCl, 0,1% SDS, 0,25% NaDOC, 1:100 Proteaseinhibitor cocktail, 5mM NaF, 1mM Na_3VO_4, 0,5mM PMSF, 12,5mM β-glycerophosphate, 2mM Sodiumpyrophosphate
SDS PAGE Sample Buffer	10ml Glycerol, 10ml SDS (20%), 23,75ml ddH2O, 6,25ml Tris (1M, pH 6,8), Bromphenol Blue to taste; fresh: 8µl β-Mercaptoethanol/ 1ml Sample Buffer
SDS Running buffer (5x)	72g/l Glycine, 15g/l Tris, 5g/l SDS
S.O.C. medium	2% Tryptone, 0,5% Yeast Extract, 10mM NaCl, 2,5mM KCl, 10mM MgCl2, 10mM MgSO4, 20mM Glucose
SuperScript™ III First-Strand Synthesis System for RT-PCR, Invitrogen, Inc., Carlsbad, CA, USA Superscript 10x RT buffer	200mM Tris-HCl pH 8,4; 500mM KCl
T4 DNA Ligase Buffer (1x)	50mM Tris-HCl pH 7,5; 10mM $MgCl_2$, 10mM DTT, 1mM ATP, 25µl/ml BSA
Tandem Flag-HA IP Buffer (Guillaume Adelmant 2008) Lysis/ Flag IP buffer	150mM NaCl, 50mM Tris pH 7,5; 1mM EDTA, 0,5% NP40, 10% Glycerol, 1:100 Protease inhibitor cocktail
HA – IP buffer	150mM NaCl, 50mM Tris pH 7,5, 1mM EDTA, 0,05% NP40, 10% Glycerol, 1:100 Protease inhibitor cocktail
TBE (10x)	890mM Tris, 890mM Boric acid, 20mM EDTA; pH 8,3
TBE (0,5x)	45mM Tris, 45mM Boric acid, 1mM EDTA; pH 8,0
TBST (1x)	10mM Tris-HCl, pH 7,5; 150 mM NaCl, 0,1% Tween-20
TE (1x)	10mM Tris-HCl, 1mM EDTA

Buffer and Solution	Composition
TOPO TA Cloning ® Kit for Sequencing, Invitrogen, Inc.,	
10x PCR buffer	100mM Tris-HCl pH8,3; 500mM KCl, 25mM MgCl$_2$, 0,01% Gelatin
Salt solution	1,2M NaCl, 0,06M MgCl$_2$
Transferbuffer for Western blots	14,25g/l Glycine, 3g/l Tris, 200ml/l Methanol
Tryphan blue (stock)	10g Phenol, 10ml Glycerol, 10ml Lactic Acid, 10ml ddH$_2$O, 0,02g Tryphan Blue
Tryphan Blue (working solution)	Stock + Ethanol (96 % ; 1:2 v/v)

2.1.5 Antibiotics

Antibiotic	Stock conc. mg/ml	Final conc. µg/ml	Mode of action	Mode of resistance
Ampicillin	100	100-1000	bacteriocidal; only kills growing *E.coli*; inhibits cell wall synthesis by peptidoglycan cross-link	β-lactamase hydrolyzes ampicillin before it enters the cell
Blasticidin S	100	3-50	inhibits protein synthesis in both prokaryotes and eukaryotes through inhibition of peptide-bond formation in the ribosomal machinery	three Blasticidin S resistance genes: 1. acetyl transferase gene, *bls*, from *Streptoverticillum sp.* 2. two deaminase genes, *bsr*, from *Bacillus cereus*, and *bsd* from *Aspergillus terreus*
Hygromycin B	50	200	aminoglycoside that kills bacteria, fungi and eukaryotic cells by inducing misreading of amino-acyl-tRNA by distorting the ribosomal A-site (decoding center)	Hygromycin B phosphotransferase (Hph) catalyzes the phosphorylation of the 4-hydroxyl group of the cyclitol ring (hyosamine)
Kanamycin	10	30	bacteriocidal; inhibits protein synthesis; inhibits translocation, elicits miscoding, affects 30S ribosomal subunit, causes frameshift mutation	aminoglycoside phosphotransferase, also known as neomycin phosphotransferase, aminoglycoside acetyltransferase, and aminoglycoside nucleotidyltransferase; inactivates kanamycin
Neomycin G418 (Geneticin)	50	500 1000	is an aminonucleoside antibiotic prod. by _Streptomyces fradiae_, inhibits protein synthesis; Neomycin for prokaryotes, G418 (Geneticin) for eukaryotes	resistance is conferred by either one of two aminoglycoside phosphotransferase genes (*neo*)
Plasmocin	25	12-38	contains two bactericidal components: one interferes with ribosome translation, the other acts on DNA replication by interfering with the replication fork	no resistance in liquid cultures has ever been identified
Puromycin	10	1-10	is an aminonucleoside antibiotic prod. by *Streptomyces alboniger*, inhibits peptidyl transfer on both prokaryotic and eukaryotic ribosomes	Fungi and Gram negative bacteria are resistant due to low permeability; the expression of *pac* gene encoding puromycin N-acetyl-trasferase (PAC) confers resistance to transfected mammalian cells expressing it

2.1.6 Bacteria Strains

Bacteria Strain	Genotyp	Company	Catalog-number
DH5α™	F- Φ80*lac*ZΔ(*lac*ZYA-*arg*F)U169 *rec*A1 *end*A1 *hsd*R17(r$_k^-$,m$_k^+$) *pho*A *sup*E44 *thi*-1 *gyr*A96 *rel*A1 λ$^-$	Invitrogen, Inc., Carlsbad, CA, USA New England Biolabs, Ipswich, MA, New England Biolabs, Ipswich, MA,	18265017 C2988 C2987
One Shot® TOP10	F- *mcr*A Δ(*mrr-hsd*RMS-*mcr*BC)Φ80*lac*ZΔM15 Δ*lac*X74 *rec*A1 *ara*D139 Δ(*ara-leu*)7697 *gal*U *gal*K *rps*L (Str^R) *end*A1 *nup*G	Invitrogen, Inc., Carlsbad, CA, USA	C4040-10
XL1- Blue	*rec*A1 *end*A1 *gyr*A96 *thi*-1 *hsd*R17 *sup*E44 *rel*A *lac* [F' *pro*AB *lac*l^{q}ZΔM15 Tn10 (Tet^r)]	Stratagene, La Jolla, CA, USA	200519
BL21(DE3)	B F- *dcm ompT hsd*S (r$_k^-$,m$_k^+$) *gal* λ (DE3)	Stratagene, La Jolla, CA, USA,	200131

2.1.7 Tissue Culture Material and Solutions

Tissue Culture Material	Company	Catalognumber
Material		
Cell Lifter	Corning, Inc., Corning, NY, USA	3008
Cryogenic Vials	Corning, Inc., Corning, NY, USA	7166
Cryospin vials	Marsh Bio Products, Rochester, NY, USA	V9015-W
Filter	Nalgene Nunc Thermo Fisher, Rochester, NY Whatman Inc., Piscataway, NJ, USA	125-0020 6722-5000
Flasks	Becton Dickinson and Co., Franklin Lakes, NJ	353136; 353112
Glass Plates for Acrylamid-gels	Bio-Rad Laboratories, Hercules, CA, USA	1653312, 1653308
Pipettes	Becton Dickinson and Co., Franklin Lakes, NJ	357521; 357507; 357543 357551; 357535; 357550
Pipette Tips	Corning, Inc., Corning, NY, USA	4864; 4809
Plates	Becton Dickinson and Co., Franklin Lakes, NJ	353046; 353043; 353072 353025; 353003
Reservoir	Corning, Inc., Corning, NY, USA	4870
Storage Bottle	Corning, Inc., Corning, NY, USA	8393; 8396
Syringes and Needles	Becton Dickinson and Co., Franklin Lakes, NJ	309603; 309604; 305190
Tubes	Becton Dickinson and Co., Franklin Lakes, NJ	352098, 352097
Solutions		
DMEM medium	Invitrogen, Inc., Carlsbad, CA, USA	11995-040
RPMI 1640	Invitrogen, Inc., Carlsbad, CA, USA	11875-085
Trypsin (with 0.5% EDTA)	Invitrogen, Inc., Carlsbad, CA, USA	25300-054
Neugem Serum (replaced by Fetalplex)	GEMINI Bio-Products, Woodland, CA, USA	100602
Fetalplex™ Animal Serum Complex	GEMINI Bio-Products, Woodland, CA, USA	100602
Newborn Calf Serum (NCS)	HyClone/ Peribo, Logan, Utah	ALM15201
Tet System approved fetal bovine serum (FBS)	Clontech Lab., Inc.Mountain View, CA, USA	631106
Blasticidine S hydrochloride	Sigma-Aldrich, St. Louis, MO, USA	15205
G418	GEMINI Bio-Products, Woodland, CA, USA	400-111P
L-Glutamine	Invitrogen, Inc., Carlsbad, CA, USA	25030-081
Hygromycin	EMD Biosciences, Inc., La Jolla, CA, USA	400052
Penicillin-Streptomycin	Invitrogen, Inc., Carlsbad, CA, USA	15070-063
Plasmocin™	Invivogen, San Diego, CA, USA	ant-mpt
Puromycin	Invivogen, San Diego, CA, USA	ant-pr-1

2.1.8 Cell Lines and Media

Cell Line	Organism/ Disease	Properties	Morphology	Media
HEK 293	*Homo Sapiens* embryonic kidney	adherent, transformed with adenovirus 5 DNA	epithelial	DMEM, 10% Fetalplex serum, 2mM glutamin
HEK 293 (Tet-system)	*Homo Sapiens* embryonic kidney	adherent, transformed with adenovirus 5 DNA, contains stably integrated GFP-LMP1-TES2 under the control of a Tet-system	epithelial	DMEM, 10% Tet-free FBS, 2mM glutamin
HEK 293T	*Homo Sapiens* embryonic kidney	adherent, cells contain Adeno- and SV-40 viral DNA sequences, express SV40 T antigen	epithelial	DMEM, 10% Fetalplex serum, 2mM glutamin
Hela	*Homo Sapiens* cervix, adenocarcinoma	adherent, produces keratin, cells contain human papilloma virus 18 (HPV-18) sequences	epithelial	DMEM, 10% Fetalplex serum, 2mM glutamin
Jurkat WT	*Homo Sapiens* T lymphocyte, acute T cell leukemia	suspension, produces interleukin-2	lymphoblast	RPMI 10% Fetalplex serum, 2mM glutamin
Jurkat A45 (NEMO/ IKKγ mutant) *Nils Jacobsen, (B. Seed Laboratory)*	*Homo Sapiens* T lymphocyte, acute T-cell-leukemia	suspension, chemically mutagenized with ICR 191, cells contain NF-κB-CD14, NF-κB-GFP, NF-κB-Puromycin, Bcl-2, CrmA; selected for defect in TNF-α-signaling (CD14-)	lymphoblast	RPMI 10% Fetalplex serum, 2mM glutamin
Jurkat 2Cγ	*Homo Sapiens* T lymphocyte, acute T-cell-leukemia	suspension, produces interleukin-2; = 2C reconstituted with NEMO	lymphoblast	RPMI 10% Fetalplex serum, 2mM glutamin
Jurkat 2C (NEMO/ IKKγ mutant) *(Harhaj, Sun, 2000, Ref. 153)*	*Homo Sapiens* T lymphocyte, acute T-cell-leukemia	suspension, chemically mutagenized with ICR 191, cells contain NF-κB-CD14; selected for defect in HTLV-I-Tax (CD14-) signaling and a defect in NF-κB activation by PMA/ CD28	lymphoblast	RPMI 10% Fetalplex serum, 2mM glutamin
MEF	*Mus musculus*	adherent	fibroblast	DMEM, 10% Fetalplex serum, 2mM glutamin 50µm β-ME
MEF (NEMO/ IKKγ ko) *(Makris C, 2000, Ref. 243)*	*Mus musculus*	adherent, knockout of NEMO by homologous recombination; defective in activation of NF-κB	fibroblast	DMEM, 10% Fetalplex serum, 2mM glutamin 50µm β-ME

Cell Line	Organism/ Disease	Properties	Morphology	Media
Rat-1	*Rattus norvegicus*	adherent, parental cell line of 5R	fibroblast	DMEM, 10% Fetalplex, 2mM glutamin + 10% old medium
5R (NEMO/ IKKγ mutant) *(Yamaoka S, 1998, Ref. 400)*	*Rattus norvegicus*	adherent, transformed with HTLV-Tax; defective in activation of NF-κB by LPS, PMA, IL-1, and HTLV-I-Tax	fibroblast	DMEM, 10% Fetalplex, 2mM glutamin + 10% old medium
U-2 OS	*Homo Sapiens* bone, osteosarcoma	adherent, produces osteosarcoma derived growth factor (ODGF)	epithelial	DMEM, 10% Fetalplex serum, 2mM Glutamin
70Z.3	*Mus musculus* B-cell lymphoma	suspension, parental cell line of 1.3E2	lymphoblast	RPMI 10% NCS, 2mM glutamin 50μm β-ME
1.3E2 (NEMO/ IKKγ mutant) *(Rooney JW, 1990)*	*Mus musculus* B-cell lymphoma	suspension, isolated by immunoselection from 70Z.3 cells (LPS$^-$/ IFN$^+$); defective in activation of NF-κB by LPS, PMA	lymphoblast	RPMI 10% NCS, 2mM glutamin 50μm β-ME

Freeze medium for all cells (exept 293 with Tet system) was growth medium containing 10% DMSO.
293 cells containing the Tet system were frozen in Tet free fetal bovine serum containing 10% DMSO.

2.1.9 Antibodies

Antibody	Company	Catalognumber
Anti-A20	BD Biosciences, Palo Alto, CA, USA	550859
Anti-Bax, NT	upstate cell signalling solutions, NY, USA	06-499
Anti-Bcl 3 (C-14)	Santa Cruz Biotech. Inc.,Santa Cruz, CA, USA	sc-185
Anti-Bcl 10 (331.3)	Santa Cruz Biotech. Inc.,Santa Cruz, CA, USA	sc-5273
Anti-DBC1	Center for Advanced Biotechnology and Medicine (CABM), Eileen White	Ref. 340
Anti-FIP3 (NEMO)	M. Horwitz	Ref. 229,230
Anti-FLAG® M2	Stratagene, La Jolla, CA, USA	200470-21
Anti-GAPDH	Chemicon International, Temecula, CA, USA	LV 1366182
Anti-GAPDH (FL-335)	Santa Cruz Biotech. Inc.,Santa Cruz, CA, USA	sc-25778
Anti-HA-Probe (F-7)	Santa Cruz Biotech. Inc.,Santa Cruz, CA, USA	sc-7392
Anti-HA-Probe (Y-11)	Santa Cruz Biotech. Inc.,Santa Cruz, CA, USA	sc-805
Anti-IκBα	Cell Signaling Tech.®, Inc., Danvers, MA,USA	9242
Anti-IκB-α (C-21)	Santa Cruz Biotech. Inc.,Santa Cruz, CA, USA	sc-371
Anti-IκB-α (C-21)-G	Santa Cruz Biotech. Inc.,Santa Cruz, CA, USA	sc-371-G
Anti-IκBε	Cell Signaling Tech.®, Inc., Danvers, MA,USA	9249
Anti-IKKα	BD Biosciences, Palo Alto, CA, USA	556532
Anti-IKKα (M-110)	Santa Cruz Biotech. Inc.,Santa Cruz, CA, USA	sc-7183
Anti-IKKβ (H-4)	Santa Cruz Biotech. Inc.,Santa Cruz, CA, USA	sc-8014
Anti-IKKβ (H-470)	Santa Cruz Biotech. Inc.,Santa Cruz, CA, USA	sc-7607
Anti-IKKγ (FL-419)	Santa Cruz Biotech. Inc.,Santa Cruz, CA, USA	sc-8330
Anti-IKKγ (NEMO, FIP3)	BD Biosciences, Palo Alto, CA, USA	559675
Anti-IKKγ/ NRP (NEMO, FIP3)	eBioscience, Inc., USA	14-6335-63
Anti-IKKγ (NEMO, FIP3)	Imgenex, San Diego, CA, USA	IMG-4044
Anti-IKKγ (NEMO, FIP3)	Imgenex, San Diego, CA, USA	IMG-4045
Anti-IKKε	Cell Signaling Tech.®, Inc., Danvers, MA,USA	2686

Antibody	Company	Catalognumber
Anti-IRAK-1 (F-4)	Santa Cruz Biotech. Inc.,Santa Cruz, CA, USA	sc-5288
Anti-IRAK-1 (H-273)	Santa Cruz Biotech. Inc.,Santa Cruz, CA, USA	sc-7883
Anti-JNK1 (FL)	Santa Cruz Biotech. Inc.,Santa Cruz, CA, USA	sc-571
Anti-LMP1 S12C10	Ref. 155	
Anti-mouse CD16/ CD23 (Fc γ III/ II Receptor)	BD Biosciences, Palo Alto, CA, USA	553142
Anti-NFκB p50 (H-119)	Santa Cruz Biotech. Inc.,Santa Cruz, CA, USA	sc-7178
Anti-NFκB p50 (NLS)	Santa Cruz Biotech. Inc.,Santa Cruz, CA, USA	sc-114
Anti-NFκB p52	Abcam, Cambridge, MA, USA	ab 7972-1
Anti-NFκB p52	upstate cell signalling solutions, NY, USA	05-361
Anti-NFκB p65 (A)	Santa Cruz Biotech. Inc.,Santa Cruz, CA, USA	sc-109
Anti-NFκB p65 (C-20)	Santa Cruz Biotech. Inc.,Santa Cruz, CA, USA	sc-372
Anti-NFκB p65 (F-6)	Santa Cruz Biotech. Inc.,Santa Cruz, CA, USA	sc-8008
Anti-NIK (A-12)	Santa Cruz Biotech. Inc.,Santa Cruz, CA, USA	sc-8417
Anti-p38 MAPK	Cell Signaling Tech.®, Inc., Danvers, MA,USA	921
Anti-p38 MAPK (C-20)-G	Santa Cruz Biotech. Inc.,Santa Cruz, CA, USA	sc-535-G
Anti-p-300 (N-15)	Santa Cruz Biotech. Inc.,Santa Cruz, CA, USA	sc-584
Anti-PAK1/2/3	Cell Signaling Tech.®, Inc., Danvers, MA,USA	2604
Anti-γ-PAK (N-19)	Santa Cruz Biotech. Inc.,Santa Cruz, CA, USA	sc-1872
Anti-Rel B (C-19)	Santa Cruz Biotech. Inc.,Santa Cruz, CA, USA	sc-226
Anti-c-Rel (C) X	Santa Cruz Biotech. Inc.,Santa Cruz, CA, USA	sc-71
Anti-RIP	BD Biosciences, Palo Alto, CA, USA	51-6559-GR
Anti-RIP (K-20)	Santa Cruz Biotech. Inc.,Santa Cruz, CA, USA	sc-1169
Anti-Sp1 (PEP 2)	Santa Cruz Biotech. Inc.,Santa Cruz, CA, USA	sc-59
Anti-TANK (C-20)	Santa Cruz Biotech. Inc.,Santa Cruz, CA, USA	sc-1997
Anti-TRADD (N-19)	Santa Cruz Biotech. Inc.,Santa Cruz, CA, USA	sc-1165
Anti-TRAF2 (H-10)	Santa Cruz Biotech. Inc.,Santa Cruz, CA, USA	sc-7346
Anti-TRAF6	Cell Signaling Tech.®, Inc., Danvers, MA,USA	4743S
Anti-TRAF6 (C-20)	Santa Cruz Biotech. Inc.,Santa Cruz, CA, USA	sc-6223
Anti-TRAF6 (H-274)	Santa Cruz Biotech. Inc.,Santa Cruz, CA, USA	sc-7221
Anti-TRAF6 (D-10)	Santa Cruz Biotech. Inc.,Santa Cruz, CA, USA	sc-8409
Anti-α-Tubulin (aN-18)	Santa Cruz Biotech. Inc.,Santa Cruz, CA, USA	sc-12836
Anti-α-Tubulin, clone B-5-1-2	Sigma-Aldrich, St. Louis, MO, USA-Aldrich	T 5168
Anti-Ub (P4D1)	Santa Cruz Biotech. Inc.,Santa Cruz, CA, USA	sc-8017
Anti-Phospho-IKKα (Ser180)/ IKKβ (Ser181)	Cell Signaling Tech.®, Inc., Danvers, MA,USA	2681S
Anti-Phospho-IKKα (Ser176)/ IKKβ (Ser180)	Cell Signaling Tech.®, Inc., Danvers, MA,USA	2697S
Anti-Phospho- IκBε (Ser 18/ 22)	Cell Signaling Tech.®, Inc., Danvers, MA,USA	4924S
Anti-Phospho-NFκB p65 (Ser 276)	Cell Signaling Tech.®, Inc., Danvers, MA,USA	3037S
Anti-Phospho-NFκB p65 (Ser 468)	Cell Signaling Tech.®, Inc., Danvers, MA,USA	3039S
Anti-Phospho-NFκB p65 (Ser 536)	Cell Signaling Tech.®, Inc., Danvers, MA,USA	3036S
Anti-Phospho-p38 MAPK (Thr180/Tyr182)	Cell Signaling Tech.®, Inc., Danvers, MA,USA	9215S
Anti-Phospho-p38 MAPK (Thr180/Tyr182)	New England Biolabs, Ipswich, MA, USA	9211S
Anti-Phospho-PAK1 (Ser-144)/ PAK2 (Ser141)	Cell Signaling Tech.®, Inc., Danvers, MA,USA	sc-2606
Anti-Phospho-γ-PAK (Ser-141)	Santa Cruz Biotech. Inc.,Santa Cruz, CA, USA	sc-16775
Anti-Phospho-SAPK/ JNK (Thr183/Tyr185)	Cell Signaling Tech.®, Inc., Danvers, MA,USA	9255S
Anti-Mouse IgG Peroxidase-conjugated	Jackson Immuno Research Lab., Inc., West Grove, PA, USA	715-035-151
Anti-Rabbit IgG Peroxidase-conjugated	Jackson Immuno Research Lab., Inc., West Grove, PA, USA	711-035-152
Streptavidin-Peroxidase Polymer	Sigma-Aldrich, St. Louis, MO, USA	S2438

Antibody	Company	Catalognumber
Anti-Mouse IgG TrueBlot™ HRP	eBioscience Inc., San Diego, CA, USA	18-8817-33
Anti-Rabbit IgG TrueBlot™ HRP	eBioscience Inc., San Diego, CA, USA	18-8816-33
Anti-Mouse IgG (H+L) Alexa Fluor® 488	Molecular Probes, Eugene, OR, USA,	A-11029
Anti-Rabbit IgG (H+L) Alexa Fluor® 488	Molecular Probes, Eugene, OR, USA,	A-11034
Anti-Mouse IgG (H+L) Alexa Fluor® 568	Molecular Probes, Eugene, OR, USA,	A-11031
Anti-Rabbit IgG (H+L) Alexa Fluor® 568	Molecular Probes, Eugene, OR, USA,	A-11011

2.1.10 Beads

Beads	Company	Catalognumber
Anti-FLAG-M2	Sigma-Aldrich, St. Louis, MO, USA	A-2220
GST-IκBα-beads	(Ellen Cahir-McFarland)	
GST-IκBα-SSAA-beads	(Ellen Cahir McFarland)	
HA-probe (F-7) AC	Santa Cruz Biotech. Inc.,Santa Cruz, CA, USA	sc-7392-AC
Protein A Sepharose™ CL-4B	Invitrogen, Inc., Carlsbad, CA, USA,	10-1042
Protein G Sepharose™ 4 Fast Flow	GE Healthcare, Piscataway, NJ, USA	17-0618-02
Ni-NTA Agarose	QIAGEN Inc., Valencia, CA, USA	1018244
Ni-NTA Superflow	QIAGEN Inc., Valencia, CA, USA	1018611

2.1.11 Enzyms

Name	Source	Recognition Site	Reaction Conditions
BamHI	*E. coli* strain that carries the BamHI gene from *Bacillus amyloliquefaciens* H (ATCC 49763)	5`…G/GATCC…3` 3`…CCTAG/G…5`	NEBuffer 3+BSA Incubate at 37°C
EcoRI	*E. coli* strain that carries the cloned EcoRI gene from *E. coli* RY13 (R.N Yoshimori)	5`…G/AATTC…3` 3`…CTTAA/G…5`	NEBuffer 1-4, U Incubate at 37°C
EcoRV	*E. coli* strain that carries the EcoRV gene from plasmid J62 pLG74 (L.l. Glatman).	5`…GAT/ATC…3` 3`…CTA/TAG…5`	NEBuffer 3+BSA Incubate at 37°C
HindIII	*E.coli* strain that carries the Hind III gene from *Haemophilus influenzae* Rd	5`…A/AGCTT…3` 3`…TTCGA/A…5`	NEBuffer 2 Incubate at 37°C
NdeI	*E. coli* strain that carries the NdeI gene from *Neisseria denitrificans* (NRCC 31009)	5`…CA/TATG…3` 3`…GTAT/AC…5`	NEBuffer 2 or 4 Incubate at 37°C
NotI	*E. coli* strain that carries the NotI gene from *Nocardia otitidis-caviarum* (ATCC 14630)	5`…GC/GGCCGC…3` 3`…CGCCGG/CG…5`	NEBuffer 3+BSA Incubate at 37°C
SmaI	*E.coli* strain that carries the Sma I gene from *Serratia marcescens*	5`…CCC/GGG…3` 3`…GGG/CCC…5`	NEBuffer 4 Incubate at 25°C
XhoI	*E. coli* strain that carries the XhoI gene from *Xanthomonas holcicola* (ATCC 13461)	5`…C/TCGAG…3` 3`…GAGCT/C…5`	NEBuffer 2+BSA Incubate at 37°C

Name	Source	Recognition Site	Reaction Conditions
Phosphatase, alkaline (CIAP)	Calf intestine	removal of terminal monoesterified phosphate from both ribo- and deoxyribo-oligonucleotide	50 pmol DNA 1unit Phosphatase 37ºC for 60min
T4 DNA Ligase	*E.coli* C600 pcl857 pPLc28 lig8	catalyzes the formation of a phosphodiester bond between 5´phosphate and 3´hydroxyl termini	1x Ligase buffer 0.1-1µM in 5´termini 16°C, 4hrs
DNA Polymerase (Klenow Fragment, 3'à5' exo-)	*E.coli* strain containing a plasmid with a fragment of the *E.coli* polA (D355A, E357A) gene starting at codon 324	Klenow Fragment (3'à5' exo-)*	1x NEBuffer 2 33µM dNTPs incubated at 37°C
Taq DNA Polymerase, recombinant	*E.coli* expressing a cloned *Thermus aquaticus* DNA polymerase gene	**	1x PCR buffer 1.5mM MgCl2 1-2.5 units *Taq* 0.8mM dNTP mix 1µM Primer mix
Taq DNA Polymerase, native	*Thermus aquaticus* YT1	**	1x PCR buffer 1.5mM MgCl2 1-2.5 units *Taq* 0.8mM dNTP mix 1µM Primer mix

*Klenow Fragment (3'$\rightarrow$5' exo-) is a N-terminal truncation of DNA Polymerase I which retains polymerase activity, but has lost the 5'$\rightarrow$3' exonuclease activity and has a mutation (D355A, E357A) which abolishes the 3'$\rightarrow$5' exonuclease activity .

***Taq* DNA Polymerase has both a 5'$\rightarrow$3' DNA polymerase and a 5'$\rightarrow$3' exonuclease activity but lacks a 3'$\rightarrow$5' exonuclease activity.

Enzym	Company	Catalognumber
BamHI	New England Biolabs, Ipswich, MA, USA	R0136L
EcoRI	New England Biolabs, Ipswich, MA, USA	R0101L
EcoRV	New England Biolabs, Ipswich, MA, USA	R0195L
HindIII	New England Biolabs, Ipswich, MA, USA	R0104L
NdeI	New England Biolabs, Ipswich, MA, USA	R0111L
NotI	New England Biolabs, Ipswich, MA, USA	R0189L
SmaI	New England Biolabs, Ipswich, MA, USA	R0141L
XhoI	New England Biolabs, Ipswich, MA, USA	R0146L
Phosphatase, alkaline (CIAP)	Boehringer Mannheim, Germany	713023
T4 DNA Ligase	New England Biolabs, Ipswich, MA, USA	M0202S
DNA Polymerase (Klenow Fragment, 3'à5' exo-)	New England Biolabs, Ipswich, MA, USA	M0212L
Taq DNA Polymerase, recombinant	Invitrogen, Inc., Carlsbad, CA, USA	10342-020
Taq DNA Polymerase, native	Invitrogen, Inc., Carlsbad, CA, USA	18038-042

2.1.12 Peptides

Peptides/ Sequence	Company	Catalognumber
FLAG-Peptide	Sigma-Aldrich, St. Louis, MO, USA	F3290
Influenza Hemagglutinin (HA) Peptide N-Tyr-Pro-Tyr-Asp-Val-Pro-Asp-Tyr-Ala-C	Sigma-Aldrich, St. Louis, MO, USA	12149-1MG
Inhibitory Peptide to human NEMO, IKKγ DRQIKIWFQNRRMKWKK *TALDWSWLQTE* (underlined = IKKγ/ NEMO binding sequence)	Imgenex, San Diego, CA, USA	IMG-2000 IPG012610
Control Peptide DRQIKIWFQNRRMKWKK	Imgenex, San Diego, CA, USA	IMG-2000 H012913P

2.1.13 Nucleotids

Nucleotides	Company	Catalognumber
dIdC (deoxinosin-deoxycytosin)	Invitrogen, Inc., Carlsbad, CA, USA,	16335-092
dNTP-Mix*	Invitrogen, Inc., Carlsbad, CA, USA,	18427-088
$p^{32}\alpha$-dATP- (2´-desoxyadenosin-5´-triphosphat)	Perkin Elmer Corp., Wellesley, MA, USA	BLU512H
$p^{32}\alpha$-dCTP (2´-desoxycytidine-5´-triphosphat)	Perkin Elmer Corp., Wellesley, MA, USA	BLU513H
$p^{32}\alpha$-dGTP (2´-desoxyguanosine-5´-triphosphat)	Perkin Elmer Corp., Wellesley, MA, USA	BLU514H

*dNTP-Mix = Mix of 2´-deoxynucleoside 5´-triphosphates: dATP, dCTP, dGTP, dTTP, 10mM each

2.1.14 Plasmids

Plasmid	Reference/ Provider/ Company
GFP-RelA (p65)	D. Ballard, Vanderbilt University, Nashville, TN, USA
HA-Ub-K63 only	ZJ. Chen, University of Texas Southwestern Medical Center, TN, USA
His-Ub	Eric Johannson, BWH Boston, MA, USA
pBABE-hygro h-tert	Karl Münger, BWH Boston, MA, USA (obtained from Weinberg laboratory)
pBABE-puro	Karl Münger, BWH Boston, MA, USA
pBluescript II KS/ SK (+)	Invitrogen, Inc., Carlsbad, CA, USA,
pcDNA3 empty	Invitrogen, Inc., Carlsbad, CA, USA,
pcDNA-Flag-h-TRAF6	Washington University
pcDNA3-FIKKβ	91,343
pcDNA3-TAX	Ellen Cahir Mc-Farland, BWH Boston, MA, USA
pCMV-SPORT6	Open Biosystems, Boston, MA, USA
pCMV4-ΔN-IκBα	47
pCMV4-IκBα-SSAA ($S_{32}A/S_{36}A$)	66, D.Ballard, Vanderbilt University, Nashville, TN, USA
pCMV6-XL4/5/6- NEMO/ IKKγ	OriGene Technologies, Inc., Rockville, MD, USA
pCR4-TOPO	Invitrogen, Inc., Carlsbad, CA, USA,
pDsRed-Monomer-C1	BD Biosciences, Palo Alto, CA, USA, Cat.-No. 632466
pGEX-KG	Eric Johannson, BWH Boston, MA, USA
pGK2-LMP1	91,343
pGK2-LMP1-ID (YYD384-386ID)	91,343
pGK2-LMP1-PQ (P204A/ Q206A)	91,343
pGK2-LMP1-CD40CT	155
pGK-β-galactosidase	91
pGK2-3xLuc	260
pmaxGFP	Amaxa/ Lonza, Inc., Köln, Germany
pNFkB-d2EGFP	BD Biosciences, Palo Alto, CA, USA, Cat.-No. 6054-1
pRK5-Flag-RIP	166, David Goeddel (Tularik)
pSG5	Invitrogen, Inc., Carlsbad, CA, USA,

The pGK2 vector was constructed from pcDNA3. The modifications are: the pCMV promoter of pcDNA3-plasmid is sensitive to NF-κB inhibition. Therefore this promoter was replaced with the NF-κB-insensitive pGK promoter (phosphoglucokinase) using the restriction enzymes BglII and HindIII (Ref: Cahir McFarland ED). The pCMV and T7 promoter was cut out (Fig.14).
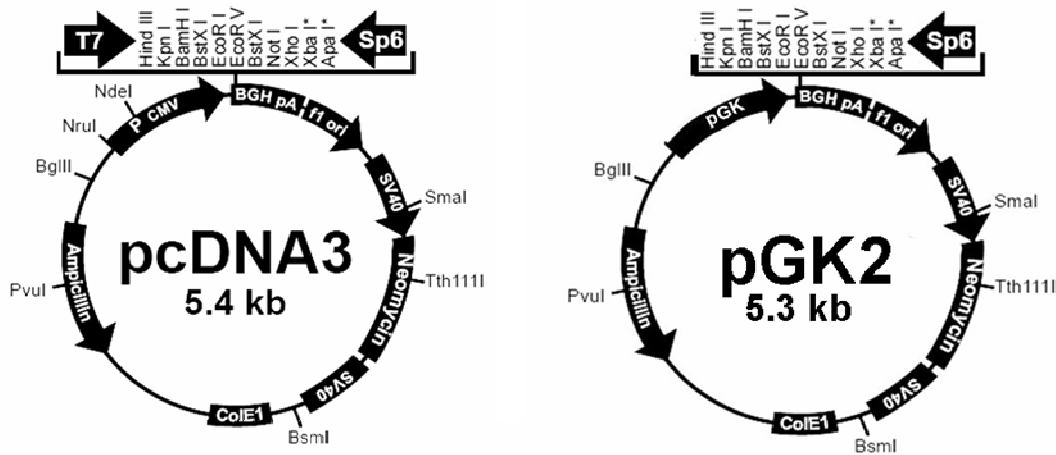

Figure 14. pcDNA3 and pGK2 plasmids

2.1.15 Primer and Constructs

Primer	Sequence
Abin1_HAforw_HindIII	5'-TGACCCAAGCTTACCACCATGTATCCATATGACGTCCC AGACTATGCCGAAGGGAGAGGACCGTACCGGATC-3'
Abin1_HArev_EcoRV	5'-ACTCGGGATATCTCACTGAGGCCCCTCACGGTCATTTTTTGG-3'
pGK2_forw1	5'-TGTTCTCCTCTTCCTCATCTCCGGGCCTTTCGACCT-3'
pGK2_forw2	5'-GCACGCTTCAAAAGCGCACGTCTGCCGCGCTGTTCT-3'
pGK2_forw3	5'-GCAATGGAAGCGGGTAGGCCTTTGGGGCAGCGGCCAATAGC-3'
Nemo 1 forward	5'-TATAGTTTGGCAGCTAGCCCTTGCC -3'
Nemo 2 forward	5'-GGAGTTCCTCATGTGCAAGTTCCA -3'
Nemo 3 forward	5'-GCTGCAGCAGCAGCACAGCGTGCA -3'
Nemo 4 forward	5'-GCACAAGATTGTGATGGAGACCGT -3'
Nemo 5 forward	5'-GGAGCCACCTGACTTCTGCTGTCC -3'
Nemo 6 reverse	5'-GGGCACGTCCTCGGCAGGCAG -3'
Nemo 7 reverse	5'-GCTCCAGCTGCTCCTGCAGGAGCT -3'
Nemo 8 reverse	5'-GATAGGCCACCTGCAACTGGGCCA -3'
Nemo 9 reverse	5'-TCTGCTGCTGGCATCTCTTCAGGT -3'
Nemo 10 reverse	5'-TCCCCAGAGGAGACTCTTCGCCCA -3'
GSTprimer	5'-CCTTTGCAGGGCTGGCAAGCC-3'
GSTforwHindIII	5'-GATCAAGCTTACCACCATGTCCCCTATACTAGGTTAT-3'
GSTrevBamHI	5'-CCCGGGGATCCCACGACCTTCGATCAGATCCGATTT-3'
Nemo1GST_forw_aa372_BamHI	5'-GGTCGAGGATCCGCCTACCTCTCCTCTCCCCTGGCCCTG-3'
Nemo2GST_forw_aa394_BamHI	5'-GGTCGAGGATCCTTCTGCTGTCCCAAGTGCCAGTATCAG-3'
Nemo3GST_rev_aa419_NotI	5'-TGAATTGCGGCCGCCTACTCAATGCACTCCATGAC ATGTATCTG-3'
Nemo4GST_forw_aa133_BamHI	5'-GGTCGAGGATCCCAGCAGATGGCTGAGGACAAGGCCTCT-3'
Nemo5GST_rev_aa200_NotI	5'-TGAATTGCGGCCGCCTAGTCCACCTGCACGCTGTGCTGCTGCT-3'
Nemo6GST_rev_aa224_NotI	5'-TGAATTGCGGCCGCCTACCTCTTCTCCTCCGAGGCGGCCTGGC-3'
Nemo7GST_rev_aa250_NotI	5'-TGAATTGCGGCCGCCTACACCACGCTGCTCTTGAT GTGGTTGTCGTA-3'
Nemo8GST_forw_aa1_BamHI	5'-GGTCGAGGATCCATGAATAGGCACCTCTGGAAGAGCCAA-3'
Nemo9GST_rev_aa50_NotI	5'-TGAATTGCGGCCGCCTAGGTCTCAGGAGCGCCCTGT TCTGAAGGCAG-3'

Primer	Sequence
Nemo1_forwHA_BamHI_WT	5'-GATCGGATCCACCACCATGTATCCATATGACGTCC CAGACTATGCCAATAGGCACCTCTGGAAGAGC-3'
Nemo2_rev_NotI	5'-AGAGGCGGCCGCCTAAGGGGCGGGGGGCAAGGGGGC-3'
Nemo3_rev_Stop_aa372	5'-GATAGCGGCCGCCTACTTCAGCACCGGAACGGTCTC-3'
Nemo4_rev_Stop_aa303	5'-GATAGCGGCCGCCTACTTGATGAGGTTGTCGTATTC-3'
Nemo5_rev_Stop_aa245	5'-GATCGGATCCACCACCATGTATCCATATGACGTC CCAGACTATGCCCTCCAGCGCTGCCTGGAGGAG-3'
Nemo6_forwHA_BamHI_aa51	5'-GAGCACCTGAAGAGATGCCAGAGGAAGCTGGCCCAGTTGCAG-3'
Nemo7_forw_del	5'-CTGCAACTGGGCCAGCTTCCTCTGGCATCTCTTCAGGTGCTC-3'
Nemo8_rev_del	5'-GGTCGACTCGAGGCCTACCTCTCCTCTCCCTGGCCCTG-3'
Nemo9_rev_stop_aa394_NotI	5'-GGTCGACTCGAGATGAATAGGCACCTCTGGAAGAGCCAA-3'
Nemo1GST_forw_aa372_XhoI	5'-GGTCGACTCGAGTTCTGCTGTCCCAAGTGCCAGTATCAG-3'
Nemo2GST_forw_aa394_XhoI	5'-TGAATTAAGCTTCTACTCAATGCACTCCATGACATGTATCTG-3'
Nemo3GST_rev_aa419_HindIII	5'-GGTCGACTCGAGCAGCAGATGGCTGAGGACAAGGCCTCT-3'
Nemo4GST_forw_aa133_XhoI	5'-TGAATTAAGCTTCTAGTCCACCTGCACGCTGTGCTGCTG-3'
Nemo5GST_rev_aa200_HindIII	5'-TGAATTAAGCTTCTACCTCTTCTCCTCCGAGGCGGCCTGGCG-3'
Nemo6GST_rev_aa224_HindIII	5'-TGAATTAAGCTTCTACACCACGCTGCTCTTGATGTGGTTGTCG-3'
Nemo7GST_rev_aa250_HindIII	5'-GGGAGCGGCCGCCTAAGGTGGCTCCTCGGGGGGGCTCCTCCT-3'
Nemo8GST_forw_aa1_XhoI	5'-TGAATTAAGCTTCTAGGTCTCAGGAGCGCCCTGTTCTGAAGG-3'
Nemo9GST_rev_aa50_HindIII	5'-ACCGTTCCGGTGCTGAAGGCCTACCTCTCCTCTCCC-3'
DeletionofNemo303-372_forw1	5'-GGGAGAGGAGAGGTAGGCCTTCAGCACCGGAACGGT-3'
DeletionofNemo303-372_rev1	5'-GAGCACCTGAAGAGATGCCAGGCCTACCTCTCCTCTCCC-3'
DeletionofNemo133-372_forw1	5'-GGGAGAGGAGAGGTAGGCCTGGCATCTCTTCAGGTGCTC-3'
DeletionofNemo133-372_rev1	5'-GATAGCGGCCGCCTACTTGATGTGGTTGTCGTATTC-3'
Forw2NemoS31A	5'-GGCTGGCTTCCCTAGGGGAGCCTCTTCGCCCAGTACGTC-3'
Rev2NemoS31A	5'-GCCATGCTGCACCTGCCTGCAGAACAGGGCGCTCCGGAGACC-3'
Forw2NemoS43A	5'-GGTCTCCGGAGCGCCCTGTTCTGCAGGCAGGTGCAGCATGGC-3'
Rev2NemoS43A	5'-GATCGGATCCACCACCATGGATATCCATATGACGT CCCAGACTATGCCAATAGGCACCTCTGGAAGAGC-3'
ForwNemoE315A	5'-GCGGACTTCCAGGCTGCGAGGCAGGCGCGCGAGAAGCTGGCC-3'
RevNemoE315A	5'-GGCCAGCTTCTCGCGCGCCTGCCTCGCAGCCTGGAAGTCCGC-3'
NemoHISforw_HindIII_NdeI	5'-AGCTTACCACCATGCATCATCACCATCACCACTC GGCCGCTGGAGGATATCCA-3'
NemoHISrev_HindIII_NdeI	5'-TATGGATATCCTCCAGCGGCCGAGTGGTGATGGTG ATGATGCATGGTGGTA-3'
HisHAforw_HindIII_EcoRI	5'-ATGCAAGCTTACCACCATGCATCATCACCATCACCAC TCGGCCGCTGGAGGATATCCATATGACGTCCCAGACTAT GCCAGCAGAGAAGGCGGAAGC-3'
NemoFlagHAforw_H3_BamHI	5'-AGCTTACCACCATGGACTACAAGGACGACGATGACAAGTCG GCCGCTGGAGGATATCCATATGACGTCCCAGACTATGCCG-3'
NemoFlagHArev_H3_BamHI	5'-GATCCGGCATAGTCTGGGACGTCATATGGATATCCTCCA GCGGCCGACTTGTCATCGTCGTCCTTGTAGTCCATGGTGGTA-3'
ForwHindIII_Flag_BamHI	5'-GATCAAGCTTACCACCATGGAGACTACAAGGACGACGAT GACAAGGATCGGATCCAC-3'
NemoFLAGforw_HindIII_NdeI	5'-AGCTTACCACCATGGACTACAAGGACGACGATGACAAGT CGGCCGCTGGAGGATATCCA-3'
NemoFLAGrev_5pr	5'-TATGGATATCCTCCAGCGGCCGACTTGTCATCGTCGTCCT TGTAGTCCATGGTGGTA-3'
NemoFLAG_PCRforw	5'-ATGCAAGCTTACCACCATGGACTACAAGGACGACGATGACA AGTCGGCCGCTGGAGGATATCCATATGACGTCCCAGACTATGCC-3'
IKKβ Hind III sense	5´-GTGCAAGCTTCGATGAGCTGGTCACCTTCCCTGACAACGC AGACATGTGGGGCCTGGGAA-3'
IKKβ SmaI antisense	5'-GTACCCCGGGTTATGAGGCCTGCTCCAGGCAGCT-3'

Primer	Sequence
T6HIS_HAforwHindIII	5'-ATGCAAGCTTACCACCATGCATCATCACCATCACCAC TCGGCCGCTGGAGGATATCCATATGACGTCCCAGACTAT GCCAGCAGAGAAGGCGGAAGC-3'
T6revBamHI	5'-ATGCGGATCCCTATACCCCTGCATCAGTACTTCGTGG-3'
TRAF6_HAforw_HindIII	5'-TGACCCAAGCTTACCACCATGTATCCATATGACGTCCCAGA CTATGCCAGTCTGCTAAACTGTGAAAACAGCTGT-3'
TRAF6_HArev_EcoRV	5'-ACTCGGGATATCCTATACCCCTGCATCAGTACTTCGTGGCTG-3'
Oligonucleotide for Electrophoretic Mobility Shift Assay (EMSA) (Ref. 204)	
NF-κB probe oligo 1	5'-CCC GGA ATT CTG GGG ATT CCC CAT GGG GAT TCC CCA TGG GGA TTC CCC AGG ATC CCG -3'
NF-κB probe oligo 2	5'-CCC GGG ATC CTG GGG AAT CCC CAT GGG GAA TCC CCA TGG GGA ATC CCC AGA ATT CCG -3'
SuperScript™ III First-Strand Synthesis System for RT-PCR, Invitrogen, Inc., Carlsbad, CA, USA	
Sense Control Primer	5'-GCTCGTCGTCGACAACGGCTC-3'
Antisense Control Primer	5'-CAAACATGATCTGGGTCATCTTCTC-3'
TOPO TA Cloning® Kit for Sequencing, Invitrogen, Inc., Carlsbad, CA, USA	
M13 Forward primer (-20)	5'-GTAAAACGACGGCCAG-3'
M13 Reverse Primer	5'-CAGGAAACAGCTATGAC-3'
T3 primer	5'-ATTAACCCTCACTAAAGGGA-3'
T7 primer	5'-TAATACGACTCACTATAGGG-3'
QuikChange® II Site-Directed Mutagenesis Kit, Stratagene, La Jolla, USA	
Oligonucleotide control primer 1	5'CCA TGA TTA CGC CAA GCG CGC AAT TAA CCC TCA C 3'
Oligonucleotide control primer 2	5' GTG AGG GTT AAT TGC GCG CTT GGC GTA ATC ATG G 3'

Construct	Primer used	Vector
Flag-HA	NemoFlagHAforw_HindIII_BamHI NemoFlagHArev_HindIII_BamHI	pGK2
Flag-HA-NEMO 1-419	NEMO1_forwHA_BamHI_WT NEMO2_rev_NotI NemoFLAGforw_HindIII_NdeI NemoFLAGrev_5pr	pGK2
Flag-HA-NEMO 51-419	NEMO6_forwHA_BamHI_aa51 NEMO2_rev_NotI NemoFLAGforw_HindIII_NdeI NemoFLAGrev_5pr	pGK2
Flag-HA-NEMO1-372	NEMO1_forwHA_BamHI_WT NEMO3_rev_Stop_aa372 NemoFLAGforw_HindIII_NdeI NemoFLAGrev_5pr	pGK2
Flag-HA-NEMO 1-303	NEMO1_forwHA_BamHI_WT NEMO4_rev_Stop_aa303 NemoFLAGforw_HindIII_NdeI NemoFLAGrev_5pr	pGK2
Flag-HA-NEMO 1-245	NEMO1_forwHA_BamHI_WT NEMO5_rev_Stop_aa245 NemoFLAGforw_HindIII_NdeI NemoFLAGrev_5pr	pGK2
Flag-HA-NEMO Δ133-224	NEMO1_forwHA_BamHI_WT NEMO2_rev_NotI NEMO7_forw_del NEMO8_rev_del NemoFLAGforw_HindIII_NdeI NemoFLAGrev_5pr	pGK2

Construct	Primer used	Vector
Flag-HA-NEMO 1-372/ Δ133-224	NEMO1_forwHA_BamHI_WT NEMO3_rev_Stop_aa372 NEMO7_forw_del NEMO8_rev_del NemoFLAGforw_HindIII_NdeI NemoFLAGrev_5pr	pGK2
HA-Abin1	ABIN1_HAforw_HindIII ABIN1_HArev_EcoRV	pGK2
His-HA-NEMO 1-419	NEMO1_forwHA_BamHI_WT NEMO2_rev_NotI NemoHISforw_HindIII_NdeI NemoHISrev_HindIII_NdeI	pGK2
GST	GSTforwHindIII GSTrevBamHI	pGK2
GST/ NEMO aa1-50	Nemo8GST_forw_aa1_BamHI Nemo9GST_rev_aa50_NotI	pGK2-GST
GST-NEMO aa373-419	Nemo1GST_forw_aa372_XhoI Nemo3GST_rev_aa419_HindIII	pGEX-KG
GST-NEMO aa133-224	Nemo4GST_forw_aa133_XhoI Nemo6GST_rev_aa224_HindIII	pGEX-KG
IKKβ full lenght	IKKβ Hind III sense IKKβ SMA I antisense	pGK2
NEMO S31A	Forw2NemoS31A Rev2NemoS31A	pGK2
NEMO S43A	Forw2NemoS43A Rev2NemoS43A	pGK2
NEMO E315A	ForwNemoE315A RevNemoE315A	pGK2

2.1.16 siRNA

siRNA	Sequence
NEMO	5'-AACAGGAGGUGAUCGAUAA-3'
NEMO	5'-GAAGCGGCAUGUCGAGGUC-3'
NEMO	5'-GAAUGCAGCUGGAAGAUCU-3'
NEMO	5'-GGAAGAGCCAACUGUGUGA-3'
TRAF6	5'- GGAGACAGGUUUCUUGUGA-3'
TRAF6	5'- GAUAUGAUGUAGAGUUUGA-3'
TRAF6	5'- GGCCAUAGGUUCUGCAAAG-3'
TRAF6	5'-GCGCUUGCACCUUCAGUUA-3'
RIPK1	5'-GAAAGAGUAUUCAAACGAA-3'
RIPK1	5'-CCACUAGUCUGACGGAUAA-3'
RIPK1	5'-GAAGCCAACUACCAUCUUU-3'
RIPK1	5'-GCACAAAUACGAACUUCAA-3'
scrambled dsRNA	5'-AUGAACGUGAAUUGCUCAA-3'
scrambled dsRNA	5'-UAAGGCUAUGAAGAGAUAC-3'
scrambled dsRNA	5'-AUGUAUUGGCCUGUAUUAG-3'
scrambled dsRNA	5'-UAGCGACUAAACACAUCAA-3'
GAPDH	5'-UGGUUUACAUGUUCCAAUA-3'
NEMO (Ambion, Inc.)	5'-CCUUACGCUUCAGCUGUUGtt-3' (sense)
NEMO (Ambion, Inc.)	5'-CAACAGCUGAAGCGUAAGGtg-3' (antisense)

(Dharmacon Thermo Fisher Scientific Inc., Chigago, IL, USA)
NEMO: ON-TARGETplus SMART pool L-003767-00-0020, Human IKBKG, NM_003639, 20nmol
TRAF6: ON-TARGETplus SMART pool L-004712-00-0020, Human TRAF6, NM_004620, 20nmol
RIPK1: siGENOME set of 4 Upgrade MU-004445-02-0002, Human RIPK1, NM_003804, 2nmol x 4
Scrambled dsRNA was used as negative control (silences firefly luciferase): ON-TARGETplus Non-targeting pool, Cat.-No. D-001810-10-20
siGLO RISC-free siRNA (non-targeting siRNA with fluorescent label and impaired ability for RISC interaction, a co-transfection marker), Cat.-No. D-001600-01-05, 5nmol (proprietary sequence)
GAPDH (glyceraldehyde-3-phosphat dehydrogenase) siRNA, Cat.-No. D-001140-01-05, 5nmol
OPTN: siGENOME SMART pool reagent M-0016269-00-0005, Human OPTN, NM-021980, 5nmol

Ambion, Inc./ Applied Biosystems, Foster City, CA and Austin, TX, USA
NEMO siRNA targeting 3' untranslated region, ID # 139260, P/N: AM51333, NM_003639, 20nmol

2.1.17 Ladder

Ladder	Company	Catalognumber
1kb-DNA-Ladder	Invitrogen, Inc., Carlsbad, CA, USA	15615-016
HyperLadder I	Bioline USA Inc., Taunton, MA, USA	Lot-No: 105B
BenchMark™ Pre-Stained Protein Ladder	Invitrogen, Inc., Carlsbad, CA, USA	10748-010
Biotinylated Marker	Sigma-Aldrich, St. Louis, MO, USA	SDS-6B

2.2 Methods

### 2.2.1 Cell Culture and Cell Transfections

2.2.1.1 Cell Culture

Suspension cells (Jurkat, 70Z.3, 1.3E2) were grown in T75 flasks (37ºC incubator, 5% CO_2) in RPMI/ Serum/ Glutamin-medium (2.1.8) and split every 2 or 3 days, to keep them in log-growth phase ($2x10^5$-$8x10^5$ cells/ ml). For transfection, suspension cells were always split 2 days before to a concentration of $2x10^5$cells/ml.

Adherent cells (HeLa, MEF, HEK 293, Rat-I, 5R, U2-OS) were grown in T75 or T175 flasks (37ºC incubator, 5% CO_2) in DMEM/ Serum/ Glutamin-medium (2.1.8) and split 1:10 at 80-90% confluency. For amaxa nucleofection and reverse transfection (2.2.1.4.1&2) cells in growth phase were used. For transfection with Effectene® (2.2.1.4.1) adherent cells were plated 1 day before in a 6-well plate at a concentration of $0,9$-$4x10^5$cells per well.

2.2.1.2 Cell Counting

To determine the cell concentration, a counting chamber called Hemacytometer (Neubauer Kammer) was used (Fig.15). Cells were mixed 1:1 with tryphan blue which stains dead or dying cells; viable cells are able to repell the dye and do not stain. The mixture was introduced into one of the V-shaped wells of the Hemacytometer. The cells were count in the four corner squares. To determine the final number of cells/ml the counted cells were multiplied by the dilution factor of trypan blue and multiplied by 10^4 (the number of cells per 1x1x0,1mm area = cells x $1*10^{-4}$ cm^3 ($1*10^{-4}$ ml)).
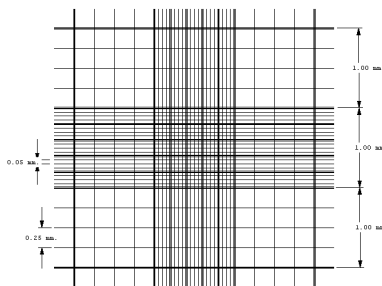
Figure 15. Hemacytometer (Hausser)

2.2.1.3 Freezing/ Thawing of Cell Lines

Freezing

Healthy cultures, in the mid-log phase of growth, were resuspended in the appropriate cold freeze medium (2.1.8) and immediately stored at -135ºC.

Thawing

After retrieving the vials from -135ºC, cells were warmed in a 37ºC water bath and pipetted into fresh medium. To remove the DMSO, cells were pelleted (3min, 1200rpm) and resuspend in fresh, warm medium.

2.2.1.4 Transient Transfection of Eucaryotic Cells

Many research techniques in molecular biology require a foreign gene to be inserted into a host cell. Since the phospholipid bilayer of the plasma membrane has a hydrophobic exterior and a hydrophobic interior, any polar molecule, including DNA, is unable to freely pass through the membrane. Several methods are used to

transfer polar molecules like DNA into host cells, including electroporation and lipofection (24,139). The DNA introduced in the transfection process is usually not integrated into the nuclear genome, it will be diluted through mitosis or degraded within a few days.

2.2.1.4.1 Lipofection

Lipofection is a technique used to inject genetic material into a cell by means of lipids or liposomes which can easily merge with the cell membrane since they are both made of a phospholipid bilayer.

Effectene[®] *Transfection Reagent*

Effectene[®] Transfection Reagent is a non-liposomal lipid formulation. It is used in conjunction with an Enhancer and a DNA-condensation buffer EC. In the first step, the DNA is condensed by interaction with the Enhancer in a defined buffer system. Effectene Reagent is then added to the condensed DNA to produce Effectene-DNA complexes, which are directly added to cells.

The day before transfection, $0,9\text{-}4\text{x}10^5$ adherent cells like MEFs, HeLa or HEK293, were seed in one well of a 6-well cell culture plate. The transfection was performed according the manufacturer's instructions using 0,4µg DNA, 3,2µl Enhancer, 150µl buffer EC, and 10µl Effectene Reagent. After 10min incubation, the DNA-Effectene complex was pipeted to the cells (in 1-2ml media). The cells were stored over night in the incubator at 37°C.

Effectene[®] Transfection Reagent was also used for reverse transfection. For this method Effectene-DNA complexes were prepared (0,4µg DNA, 3,2µl Enhancer, 150µl buffer EC, 10µl Effectene) and added to one well of a 6-well cell culture plate before the cells ($1\text{x}10^5$ HEK293; in growth phase) were split on top.

2.2.1.4.2 Electroporation

Electroporation is a significant increase in the electrical conductivity and permeability of the cell plasma membrane caused by an externally applied electrical field. In this procedure, a large electric pulse temporarily disturbs the phospholipid bilayer, allowing polar molecules like DNA to pass into the cell (270,341). The concept of electroporation is based on the relatively weak nature of the phospholipid bilayer's hydrophobic/ hydrophilic interactions and its ability to spontaneously reassemble after disturbance which leaves the cell intact.

Nucleofection (Amaxa)

The amaxa nucleofector technology is a non-viral method which is based on a combination of electrical parameters and cell-type specific solutions. It delivers DNA directly into the nucleus and does not rely on cell division for the transfer of DNA into the nucleus. Due to the nuclear DNA delivery, the expression of the transfected construct starts very shortly post nucleofection.

Transfection of MEFs

The transfection was performed using amaxa nucleofection according the manufacturer's instructions following the protocol for MEFs. $1\text{x}10^5\text{-}3\text{x}10^5$ cells at a confluency of 70-80% were transfected with 4-5µg DNA using 100µl PBS or 100µl amaxa solution for MEF transfection, and program A23 or T20 at the nucleofector device. The cells were reconstituted in 20ml media in a 10cm^2 tissue culture dish and incubated over night 37°C.

Transfection of Jurkat Cells

The transfection was performed according the manufacturer's instructions following the general protocol for amaxa nucleofection of suspension cell lines. The cells were split two days before transfection. 8×10^6 cells were transfected with 4-5µg DNA using 100µl solution V and program S18 at the nucleofector device. The cells were reconstituted in 5ml media in one well of a 6-well cell culture plate and incubated for 24-72 hrs at 37°C.

2.2.1.4.3 Transfection with siRNA

Small interfering RNA (siRNA) is a class of double-stranded RNA molecules, 20-25 nucleotides in length, that are involved in the RNA interference (RNAi) pathway, where it disturbs the expression of a specific gene. SiRNAs can be exogenously introduced into cells by various transfection methods to knockdown transiently a gene of interest (34,103,104,119,128,147,255).

Transfection of HEK293 Cells with siRNA

For HEK293 cells, DharmaFECT™ siRNA transfection reagent was used. Two days before transfection 4.0×10^5 HEK293 cells were seed in T75 flasks to be 60% confluent the day of transfection. The reverse transfection was performed in 6-, 12-, 48-, or 384-well plates according table 2. 13µl DharmaFECT™ transfection reagent was mixed with 1ml serumfree DMEM medium and incubated for 5 minutes at room temperature. Then appropriate amounts of siRNA (Tab.2), buffer and transfection reagent – medium mixture where combined in one well and incubated for 20 minutes. Meanwhile HEK 293 cells were trypsinized, counted and resuspend in DMEM with 20% serum. After 20 minutes $2,5 \times 10^5$ cells/ml were add to each well. The cells were stored for 48-96 hrs in the incubator at 37°C.

Culture Format (wells/plate)	Surface Area (cm²/well)	siRNA Volume (1µM) (µl)	siRNA Buffer (µl)	Transfection Reagent* (µl)	Serum-free Medium* (µl)	Final Transfection Volume (µl)
384	0,06	2	8	0,13	9,9	40
48	1	16	64	1,04	79	320
12	3,8	64	256	8,32	312	1280
6	9,6	128	512	33,28	607	2560

Table 2. Culture formats and volumes for siRNA transfection of HEK 293 cells with DharmaFECT™
* 13µl DharmaFECT™ transfection reagent in 1ml serumfree DMEM medium

Transfection of Jurkat Cells

Jurkat cells were transfected with siRNA using the amaxa nucleofector technology according the manufacturer's instructions following the general protocol for nucleofection of suspension cell lines. The cells were split two days before transfection. $1-1,5 \times 10^6$ cells were transfected with 1,5-3µl siRNA (20µM stock) using solution V and program S18 at the nucleofector device. The cells were reconstituted in 5ml media in a 6-well culture dish plate and incubated at 37°C.

Cells where either harvested after 72 hrs to perform westernblot analysis.

Or cells where transfected again, 48 hrs after the first transfection, with 1µl siRNA (20µM stock), reporter plasmids and various other plasmids using 100µl solution V and program S18 at the nucleofector device. For this second transfection, all the cells in one well of a 6-well plate were used for one transfection. The cells were reconstituted in 5ml media in a 6-well culture dish plate and incubated at 37°C. 24-48 hrs after the second transfection cells were harvested to perform reporter assays and westernblot analysis.

2.2.1.5 Stable Transfection of Eucaryotic Cells

To accomplish that a transfected gene remains in the genome of the cell and its daughter cells, a stable transfection must occur. For this reason, a marker gene is co-transfected, which gives the cell some selectable advantage, such as resistance towards a certain antbiotic, or expression of a fluorescent protein. Some of the transfected cells have integrated the foreign genetic material, including the marker gene, into their genome and only those were able to proliferate under selection with an antibiotic. Cells containing a fluorescent protein as selection marker can be sorted by fluorescence activated cell sorting (FACS). Only cells with a stable transfection remained and were cultivated further.

For stable transfection linearized DNA was precipitated with NaCl/ isopropanol to remove restriction enzymes and impurities. Then $4x10^5$ MEFs or HEK293 cells were transfected with 0,4µg DNA/ well (9:1 gene of interest : marker gene) in a 6-well plate using Effectene® Transfection Reagent (150µl buffer EC, 3,2µl Enhancer, 10µl Effectene). Two days after transfection, cells were transferred into 100x20mm TC plates under selection with Puromycin, Hygromycin, or G418 (2.1.5). Cells containing dsRed DNA as fluorescence marker were selected 6-8 days after transfection.

2.2.2 Microbiological Methods

2.2.2.1 Transformation of Bacteria

Transformation is the genetic alteration of a cell resulting from the uptake and expression of foreign DNA (22). *E.coli* bacteria were transformed by heat shock.

50µl competent cells (DH5α) were thawed on ice. After addition of 25ng of DNA, the cells were incubated on ice for 30min, transferred to a 42ºC water bad for 45 seconds and then incubated on ice for 2min. The bacteria were resuspend in 1ml of S.O.C medium with no antibiotics and incubated at 37ºC for 1 hour, while shaking at 150rpm. If cells were transformed with pure plasmid, 50µl were taken and plated on a LB/ antibiotic plate and stored over night at 37ºC. If cells were transformed with DNA from a ligation, all bacteria were pelleted, resuspend in 100µl S.O.C medium, plated on a LB/ antibiotic plate, and stored over night at 37ºC.

2.2.2.2 Bacteria Culture

E.coli bacteria were grown in LB medium at 37°C, while shaking at 150-220rpm.

For plasmid DNA expansion a colony of bacteria, harboring the plasmid DNA of interest, was picked, transferred into a 14ml Falcon tube containing 2ml of LB medium supplemented with the appropriate antibiotic, and incubated at 37ºC while shaking. After 24 hours the culture was transferred to an Erlenmeyer flask, containing 500ml of the same media, and incubated for another 24 hours.

For cultivation of *E.coli* BL-21 see 2.2.3.3.2 GST-tagged protein expression and isolation.

Competent cells (DH5α and BL-21) were stored at -80ºC.

2.2.3 Molecularbiological Methods

2.2.3.1 DNA

2.2.3.1.1 DNA Extraction

Extraction of Plasmid-DNA from Bacteria

For small scale plasmid DNA preparations from 2ml *E.coli* DH5α overnight cultures, a QIAprep Spin Miniprep Kit was used according the manufacturer´s instructions. After isolation, the DNA was resuspended in endofree TE buffer, incubated with restriction enzymes and electrophoretically checked for content of the right insert within the plasmid.

To extract plasmid DNA from 500ml *E.coli* DH5α overnight cultures, two different methods were used: the EndoFree Plasmid Maxi Kit or cesiumpreparation.

Cesiumpreparation of DNA

This method used for the isolation of large scale plasmid DNA is a modification of an alkaline lysis procedure followed by equilibrium ultracentrifugation in cesium chloride-ethidium bromide gradients (35,313, 384). Cells were harvested by centrifugation (15min, 5000rpm), lysed 5min in 10ml Buffer A, and treated with alkaline detergent (20ml freshly prepared Buffer B, inverting 3-6 times). After 5-10min incubation at room temperature, the detergent solubilized proteins and membranes were precipitated with potassium acetate (15ml Buffer C) by incubation on ice for 10min. The lysate was cleared first by 10min centrifugation at 7000rpm and filtration through several kimwipes into a new centrifuge bottle. The plasmid DNA was precipitated by addition of 0.6 volumes of isopropanol (27ml, incubation 10min at room temperature) and collected by centrifugation (10min, 7000rpm). After washing with 70% ethanol and 10-15min air drying, the DNA pellet was dissolved in 20ml TE buffer and loaded into a polyallomer centrifuge tube. The tube was filled up with cesium chloride (final concentration 1g/ml). Ethidium bromide was added to a final concentration of 10mg/ml. After ultracentrifugation overnight (45000rpm, 16-20 hours) the ethidium bromide stained plasmid DNA bands, equilibrated within the cesium chloride density gradient, were removed with a 10ml syringe (lower bands). The isolated bands were again subject to ultracentrifugation (65000rpm, 4h). The intercalated ethidium bromide was separated from the DNA first by extraction with butanol (saturated with H_2O) and then by dialyzing against 4l TE buffer for 3 days. The DNA was precipitaded with 1/10 volume of 3M NaOAc and 2 volumes cold 100% ethanol, washed with 70% ethanol and resuspend in sterile TE buffer.

Endofreepreparation of DNA (Maxi-/ Miniprep)

Endotoxins (lipopolysaccharides, LPS) are released during the lysis step of plasmid purification and significantly reduce transfection efficiencies in endotoxin sensitive cell lines. For plasmid DNA preparations with integrated endotoxin removal step, an EndoFree Plasmid Maxi Kit was used. The plasmid DNA purification from a 500ml culture was performed according the manufacturer's instructions. After isolation the DNA was resuspended in endofree TE buffer.

To remove endotoxin from pure plasmid DNA the UltraClean™ Endotoxin Removal Kit was used according the manufacturer´s instructions.

2.2.3.1.2 DNA Precipitation

For restriction digest or transfection, DNA needs to be purified (411). For this reason DNA was precipitated with 1/10 volume NaCl and 0.6 volumes isopropanol. After 30min incubation at -20°C and centrifugation (30min, 7000rpm), a 70% alcohol rinse of the pellet was performed to more efficiently desalt the DNA pellet. DNA was resuspended in endofree TE buffer or sterile ddH$_2$O.

2.2.3.1.3 Polymerase Chain Reaction (PCR)

PCR is a method to enzymatically synthesize defined sequences of DNA (70,264,306). The reaction uses two oligonucleotide primers that hybridize to opposite strands and flank the target DNA sequence that is to be amplified. The elongation of the primers is catalyzed by a heat-stable DNA polymerase, such as Taq DNA Polymerase. A repetitive series of cycles involving template denaturation, primer annealing, and extension of the annealed primers by the polymerase, results in exponential accumulation of a specific DNA fragment. Because the primer extension products synthesized in a given cycle can serve as a template in the next cycle, the number of target DNA copies approximately doubles every cycle; thus, 20 cycles of PCR yield about a million copies of the target DNA. The PCR reaction was performed in volumes from 10µl to 100µl. All compounds were mixed in 0.2ml Thermowell® tubes (Tab.3A) and placed in the thermal cycler. After the PCR reaction (Tab.3B), the correct DNA fragment was determined by agarose gel electrophoresis.

A

PCR-Component	Amount
Template	150ng
25µM Primer 1	25pM
25µM Primer 2	25pM
10mM dNTP mix	100µM
25mM MgCl$_2$	1.5mM
10x PCR Rxn Buffer	10µl
H$_2$O	79µl
Taq DNA Polymerase	1µl

B

Reaction	Temperatur	Time
Denaturation	95°C	10min
Denaturation	95°C	30sec
Annealing	55°C	30sec
Extension	72°C	120sec
Cooling	72°C	15min
Storage	4°C	forever

Table 3. (A) PCR reaction, (B) PCR cycle

2.2.3.1.4 Enzymatic Modification of DNA

Restriction

DNA restriction enzymes recognize short, specific pallindrome sequences of DNA bases and break the backbone of the DNA in the region of the recognized sequence. Some restriction enzymes make staggered cuts in the opposite strands creating complementary, single stranded ends ("sticky" ends); other restriction enzymes make a cut across both strands creating DNA fragments with "blunt" ends.

Restriction digests were performed in 1,5ml tubes. BSA was added to the digest depending on the enzyme used. The samples were mixed according Tab.4 and incubated at 37°C for 2-3 hours or overnight. The restriction enzymes and resulting DNA fragments were separated using agarose gel electrophoresis.

Component	Amount
DNA	5µg
10xNEBuffer	5µl
Enzym 1	20U
Enzym 2	20U
100x BSA	1µl
ddH$_2$O	36µl

Table 4. DNA restriction

Dephosphorylation of Plasmid DNA

The removal of the 5'-terminal phosphates from the dsDNA ends prevents vector self-ligation and improves ligation results (31,265,417). For this reason, 50pM DNA was incubated with 1unit alkaline phosphatase (CIAP) and 5µl 10x CIAP buffer at 37°C for 30min. After heat inactivation of CIAP at 80°C for 10min, the enzyme and plasmid DNA were separated using agarose gel electrophoresis.

Ligation

DNA fragments generated by digestion of a plasmid with two restriction enzymes were ligated (344) by incubation with 1x T4 DNA ligase buffer and T4 DNA Ligase over night at 16°C and then electrophoresed in 1% agarose. For inserting a fragment into 100ng plasmid vector about 0.01 (sticky ends) to 1 (blunt ends) units of ligase were used. Fragment and vector were used at an equimolar ratio.

2.2.3.1.5 Isolation of DNA from Agarose

After PCR or enzymatic modification, DNA was separated by agarose gel electrophoresis and purified using the QIAEX II Gel Extraction Kit or the QIAquick Gel Extraction Kit according the manufacturers instructions. Both kits are based on solubilization of agarose and selective adsorption of nucleic acids onto silica-gel particles in the presence of chaotropic salt.

2.2.3.2 RNA

2.2.3.2.1 Isolation of RNA

Total RNA was isolated from cells using Trizol$^®$ Reagent, which is a monophasic solution of phenol and guanidine isothiocyanate. During sample homogenization or lysis, Trizol$^®$ Reagent maintains the integrity of the RNA, while disrupting cells and dissolving cell components. Addition of chloroform, followed by centrifugation, separates the solution into an aqueous phase and an organic phase. RNA remains exclusively in the aqueous phase. After transfer of the aqueous phase, the RNA is recovered by precipitation with isopropyl alcohol.

5-10 x 10^6 animal cells were lysed for 5min at room temperature in 1ml Trizol$^®$ Reagent. After addition of 0,3ml chloroform, shaking, and incubation for 2-3min at room temperature, the samples were centrifugated at 12.000 x g for 15min at 2-8°C. The RNA in the aqueous phase was precipitated with 0,5ml isopropanol. After incubation at room temperature for 10min, and centrifugation at 12.000 x g at 2-8°, the samples were washed once with 75% ethanol and again centrifugated at 7.500 x g for 5min at 2-8°. The RNA was dissolved in RNase-free water and stored at -80°.

Poly (A)$^+$ RNA was isolated from total RNA using the Oligotex mRNA Midi Kit following the protocol for purification of poly (A)$^+$ RNA from total RNA.

2.2.3.2.2 Reverse Transcription

The process of reverse transcription is the creation of DNA from an RNA template (28,33,352). Using the SuperScript™ III First-Strand Synthesis System for RT-PCR, cDNA synthesis was performed in the first step using either total RNA or poly (A)$^+$ RNA primed with oligo(dT) or random primers. In the second step, PCR was performed in a separate tube using primers specific for the gene of interest.

A

Component	Amount
total RNA	up to 5µg
50µM oligo(dT)$_{20}$ Primer, **or**	1µl
50ng/µl random hexamer primer	1µl
dNTP mix (10mM)	1µl
DEPC-treated water	to 10µl

B

Component	Amount
10x RT Buffer	2µl
25mM MgCl$_2$	4µl
0,1 M DTT	2µl
RNaseOUT™ (40U/µl)	1µl
SuperScript™ III RT (200U/µl)	1µl

Table 5. First-strand cDNA synthesis step A and step B

Reaction	Temperatur	Time
oligo(dT)$_{20}$ primed	50°C	50min
Random hexamer primed	25°C	10min
	50°C	50min
Termination	85°C	5min

Table 6. Incubation times and temperatures for first-strand cDNA synthesis

The RNA/ primer mixture (Tab.5A) was incubated in 0.2ml Thermowell® tubes for 5min at 65°C, placed on ice for 1min, then immediately mixed with 10µl of cDNA synthesis mix (Tab.5B) and incubated according Tab.6. After termination and chilling, samples were incubated with 1µl of RNase H for 20min at 37°C. The cDNA was then used for PCR or stored at -20°C.

2.2.3.3 Protein

2.2.3.3.1 Protein Extraction

Protein extracts were prepared for western blotting, immunoprecipitation, electrophoretic mobility shift assay (EMSA), and luciferase/ β-galactosidase reporter assays. The protein concentration was determined using the BCA assay.

For western blotting cells were washed twice with PBS, mixed with 2x SDS Sample buffer (containing 8µl β-mercaptoethanol/ml buffer), and boiled at 100°C for 5min.

To prepare a cell extract containing only soluble proteins for immunoprecipitation, one million cells were incubated in 100-500µl lysis buffer on ice for 30 min, and peletted by centrifugation to remove debrie.

Lysats for EMSA were prepared using two million cells and 100µl lysisbuffer. After incubation on ice for 10-30min and centrifugation, the supernatant was used for the assay or stored at -80°C.

For luciferase/ β-galactosidase reporter assays cells were lysed on ice in 1x reporter lysis buffer for 10min and spun at 9500rpm for 5min to remove debrie.

2.2.3.3.2 GST-tagged Protein Expression and Isolation

Plasmids, containing the GST-tagged gene or DNA fragment, were transformed in BL21 bacteria. One colony was picked and inoculated over night at 37°C in 2ml LB medium with the appropriate antibiotic (ampicillin or kanamycin). The next morning 50ml LB medium was inoculated with 1ml of the overnight culture at 30°C or 37°C. The optical density (OD) was periodically measured using the spectrophotometer. At an OD of 0,8 the culture was split and one half was induced with 2mM IPTG (500µl of 100mM stock). Both, the uninduced and induced cultures were then grown for 2-5 hrs at 30°C or 37°C. After incubation, 1ml of each culture were taken and processed as soluble and insoluble fractions. The bacteria were pelleted for 2min at 11.000rpm, lysed in 300µl of NETN buffer and sonicated 2 times for 30 seconds or longer till transluscent. After 5min. centrifugation at 13.000rpm, the supernatant

was transferred to a new tube and mixed with 300µl of 2x sample buffer. The pellet (insoluble fraction) was mixed with 300µl sample buffer, sonicated, and then diluted with 300µl PBS. 15µl of each sample were subjected to SDS-PAGE and coomassie blue staining.

The remaining 49ml of culture were harvested (10min centrifugation at 2.500g) and frozen for later use.

2.2.4 Analytical Methods

2.2.4.1 DNA/ RNA

2.2.4.1.1 Agarose Gel Electrophoresis

Gel Electrophoresis

Gel electrophoresis is a technique used to separate, and sometimes purify macromolecules – especially proteins and nucleic acids – that differ in size, charge or conformation (36,215). The term „gel" refers to the matrix used to separate the molecules and the term „electrophoresis" describes the migration of charged particles under the influence of an electric field. Biological molecules such as amino acids, peptides, proteins, nucleotides, and nucleic acids posses ionisable groups and, therefore, at any given pH, exist in solution as electrically charged species either as cations or anions, which will migrate either to the cathode or to the anode. Their rate of migration through the electric field depends on the strength of the field, size and shape of the molecules, relative hydrophobicity of the samples, and on the ionic strength and temperature of the buffer in which the molecules are moving. There are two basic types of materials used for gels: agarose and polyacrylamide (2.2.4.3.5).

Agarose Gel Electrophoresis

Agarose is a polysaccharide extracted from seaweed. It is made up of the basic repeat unit agarobiose, which comprises alternating units of galactose and 3,6-anhydrogalactose. Agarose gel electrophoresis is used to check the progression of a restriction enzyme digestion, to determine the yield and purity of a DNA isolation or PCR reaction, and to size fractionate DNA molecules, which then can be eluted from the gel (215,310).

Agarose was typically used at a concentration of 1% in 0,5x TBE buffer. The fluorescent dye Ethidium bromide (final concentration 0,5µg/ml) was added to the gel to enable visualization of the DNA fragments within the gel. The conditions for the electrophoresis were: 125V, 500mA, 45min. A 1kb marker was co-electrophoresed with DNA samples. After electrophoresis DNA fragments were visualized using an ultraviolet transilluminator (BioDoc-It™ Imaging System).

2.2.4.1.2 UV Spectrophotometric Analysis of DNA and RNA

The concentration of a DNA or RNA or sample can be determined by UV spectrophotometry (136,380). The nitrogenous bases in nucleotides have an absorption maximum at 260 nm. In contrast to nucleic acids, proteins have an UV absorption maximum of 280 nm, due mostly to the tryptophan residues. The absorbance of a DNA sample at 280 nm gives an estimate of the protein contamination of the sample. The ratio of absorbance at 260 nm to absorbance at 280 nm is a measure of the purity of the DNA sample, while the optical density determines the quantity. An OD_{260} of 1 is equal to 50µg/ml dsDNA or 40µg/ml ssRNA.

The quantity and quality of DNA and RNA were determined using the U-2000 Spectrophotometer and 10mm quarz glass cuvettes. A 1:200 dilution of DNA or RNA in TE buffer was measured against TE buffer.

2.2.4.1.3 PCR Screen

To isolate colonies of bacteria, containing the desired cloned insert, a PCR screen, using single colonies as DNA template and insert specific primers, was performed. Single colonies were picked, streaked on a second plate and finally immersed in 20µl of PCR mix in a PCR tube. After the PCR reaction, the correct insert was determined by agarose gel electrophoresis.

2.2.4.1.4 Northernblot

Northern blot is a technique to study gene expression by detection of RNA or isolated mRNA in a sample (10). Northern blotting involves the use of electrophoresis to separate RNA samples by size and detection with a hybridization probe complementary to part of, or the entire target sequence. The term 'northern blot' refers specifically to the capillary transfer of RNA from the electrophoresis gel to the blotting membrane.

Total RNA or poly(A)$^+$RNA was separated by agarose gel electrophoresis. The gel was prepared according Tab.7B by first boiling agarose and water. After cooling to ~60°C, ethidium bromide, MOPS buffer and last formaldehyde were added. The samples were prepared according Tab.7A by mixing all components and heating the mixture to 60°C for 5 minutes. After cooling on ice for 2 minutes, the samples were load immediately and run at 100V, 500mA for 2 hours at 4°C. Runningbuffer was 1x MOPS buffer.

A

Component	Amount
Formamide	2µl
Formaldehyde (37%)	2µl
10x MOPS buffer	2µl
Brilliant blue	to taste
total RNA	5µg
ddH$_2$O	to 20µl

B

Component	Amount
Agarose GP/LE	0,5g
ddH$_2$O	35ml
Ethidium bromide	2,5µl
10x MOPS buffer	5ml
Formaldehyde (37%)	10ml

Table 7. Sample (A) and agarose gel (B) preparation for Northern blot

After electrophoresis the gel was washed for 10 minutes in 2x SSC buffer. Since the gels are fragile and the probes are unable to enter the matrix, the RNA samples, now separated by size, were transferred to a nylon membrane over night at room temperature through a capillary blotting system (Fig.16). After transfer, the membrane was rinsed with 2x SSC buffer and baked for 2 hours at 80°C in a vacuum oven to immobilize the RNA through covalent linkage to the membrane.
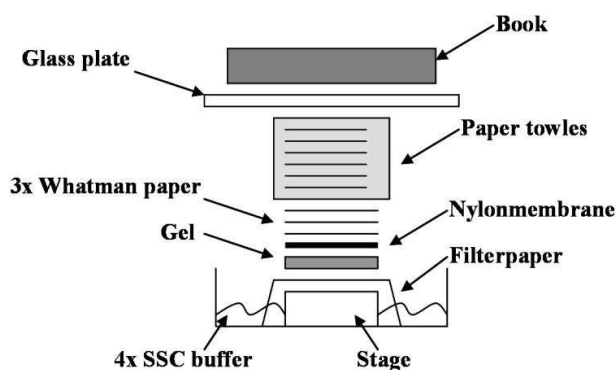
Figure 16. Capillary blotting system for northern blot

For hybridization, the membrane was wet with 2x SSC buffer, placed between two pieces of mesh, rolled-up and placed into a hybridization bottle. After incubation in prehbridization solution for at least 15 minutes at 65°C, the radioactive probe was add and hybridized overnight at 65°C. The radioactive probe was prepared using a Prime-It II Random Primer Labeling Kit. The labelling was performed according the manufacturer's instructions. A NEMO/ IKKγ DNA expression plasmid containing the putative complementary sequence to the RNA of interest was used as DNA template. It was labeled with [α-^{32}P]-dCTP (Tab.8).

Component	Amount	Procedure
DNA	25-50μg	
Primer Random 9-mers	10μl	
(27ODU/ml)		boil @ 95°C 5min
		cool @ RT 30min ; then add:
5x cdCTP buffer	10μl	
(0,1mM of each nt		
except CTP)		
[α-^{32}P]-dCTP	5μl	
Exo(-)-Klenow (5U/μl)	1μl	42°C for 5min

Table 8. Preparation of a radioactive DNA probe.

To remove free radioactive nucleotides, the DNA fragment was spun thru a MicroSpin S-200 HR column. The efficiency of labelling (percent incorporation) was determined by scintillation counting. After 16 hours of incubation with radioactive DNA, the membrane was washed (for 15min at 65°C everytime) once with 2x SSC + 0,1% SDS, once with 0,5x SSC + 0,1% SDS, and once with 0,1x SSC + 0,1% SDS. The membrane was then wraped in cellophane and over night stored in an exposure cassette with phosphor screen. After 24 hours, the phosphor screen was read using the phospho imager.

2.2.4.1.5 Colony – Hybridization

Colony Hybridization is the screening of a library with a labeled probe (radioactive, bioluminescent) to identify a specific sequence of DNA, RNA, enzyme, protein, or antibody (44,85,131,140,299). Hybridization reactions are specific because probes will bind only to sites that have complimentary sequences.

Discrete colonies of bacteria were transferred from an agar plate onto a nitrocellulose membrane by placing the membrane on the agarplate. The membrane was removed as soon as it was completely wet. The cells on the membrane were lysed by incubating the membrane in colony-hybridization buffer 1 for 5 minutes. Then, the DNA was denatured by incubation in colony-hybridization buffer 2 for 5 minutes and incubation in colony-hybridization buffer 3 for 10 minutes. To immobilize the DNA through covalent linkage the membrane was baked in a vacuum oven for 30min at 80°C.

For the hybridization the membrane was wet with ddH$_2$O, placed between two pieces of mesh, rolled-up, and placed into a hybridization bottle. After incubation in prehbridization solution for at least 1h at 65°C, the radioactive probe (making probe: see 2.2.4.2.1 Northernblot) was add and hybridized overnight at 65°C. The next day the membrane was washed twice for 20min with 2x SSC + 1% SDS at 65°C and washed once for 20min with 0,2x SSC + 1% SDS at room temperature. The membrane was then wraped in cellophane and exposed to film at -70°C overnight. The film was observed for black spots that correspond to colonies that hybridized with the probe. These were the colonies that contained the specific sequence that hybridized with the probe. Colonies on the master plate, that have the desired sequence, were then subcultured.

2.2.4.1.6 Electrophoretic Mobility Shift Assay (EMSA)

The gel shift or electrophoretic mobility shift assay (EMSA) is a method to detect DNA-binding proteins (121,127). The assay is based on the observation that complexes of protein and DNA migrate through a nondenaturing polyacrylamide gel more slowly than free DNA fragments or double-stranded oligonucleotides. The gel shift assay is performed by incubating a purified protein, or a complex mixture of proteins (such as nuclear or cell extract preparations), with a ^{32}P end-labeled DNA fragment containing the putative protein binding site. The reaction products are then analyzed on a nondenaturing polyacrylamide gel.

The assay is performed in three steps: first labelling of consensus oligonucleotides, second incubation of cell lysate with antibodies and labeled DNA (DNA binding reactions) and third gel electrophoresis.

The DNA fragment containing the putative protein binding site was labeled with p^{32} according Tab.9A. For the phosphorylation reaction the DNA was incubated at 37ºC for 30min. To remove free radioactive nucleotides, the DNA fragment was spun thru a MicroSpin S-200 HR column. The efficiency of labelling (percent incorporation) was determined by scintillation counting.

A

Component	Amount
DNA-probe (60ng/µl)	180ng
10x NEBuffer 2	1x
100xBSA	2x
dNTP-p^{32} (50mM)	each 5mM
dNTPs (2mM), (except labeled)	0,8mM
DNA Ploymerase (Klenow)	5units
ddH$_2$O	add to 50µl

B

Component	Amount
5x Buffer	6µl
dIdC (2mg/ml)	0,5µg
H$_2$O or Antibody (final 1,5µg)	5µl
Cell lysate	5µl
labeled DNA (diluted 1:10)	2µl
DTT	4mM
ddH$_2$O	11µl

Table 9. (A) Labeling of consensus oligonucleotides, (B) DNA binding reactions

Two million cells were lysed on ice in 100µl lysisbuffer for 10-30min. After centrifugation, the supernatant was used for the assay or stored at -80ºC.

A mastermix was prepared (Tab.9B) with 5xbuffer, dIdC and ddH$_2$O. Then 18µl master mix and cell lysate were first incubated with antibodies or ddH$_2$O as control (15-30min at RT) and then with the labeled DNA fragment (15-30min at RT).

To separate the DNA bound proteins electrophoreticaly continuous polyacrylamid gels were used. The 4.5% polyacrylamid gel was poured according Tab.10 and run empty for at least 1h.

Component	Amount
Acrylamid (30%)	7,5ml
10xTBE	2,5ml
APS	500µl
TEMED	50µl
ddH$_2$O	39,45ml

Table 10. Polyacrylamid gel for EMSA

The conditions for the electrophoresis were: 150V, 500mA, 2 hours. After the polyacrylamid electrophoresis the gel was transferred to a gel dryer (80°C, 1h) and over night stored in an exposure cassette with phosphor screen. After 24 hours the phosphor screen was read using the phospho imager.

2.2.4.3 Protein

2.2.4.3.1 Nuclear – Cytoplasmic – Fractionation

The fractionation method is based on differential lysis of plasma and nuclear membranes by buffers containing different salt levels. After selective lysis of the plasma membrane in 4 volumes buffer A, and incubation on ice for 1 hour, the cells were dounce homogenized 20 times with a tight pestle and spun at 4°C, 9500rpm, for 20 minutes. The supernatant containing the cytoplasmic proteins was separated and the nuclei were washed in 1ml buffer A and then lysed in 3 volumes buffer B (on ice, 30min). The protein concentration was determined by BCA assay. The efficiency of the fractionation was confirmed by Western blot analysis with an antibody specific for the cytoplasmic protein α-Tubulin and the nuclear protein Sp1.

2.2.4.3.2 Immunoprecipitation (IP)

Immunoprecipitation is a method to isolate a protein antigen out of solution using an antibody that specifically binds to that particular protein (245). Antibody-antigen complexes are removed from solution by addition of an insoluble form of an antibody-binding protein such as Protein A- or Protein G-Sepharose™. Because antibodies, that specifically target a certain protein are not always available, proteins of interest can be tagged at the N- or C-terminus and immunoprecipitated using tag-specific antibodies that are coupled to beads, such as FLAG, HA, or GST.

One million cells were lysed in 100µl NP40 lysis buffer, incubated on ice for 30 min and pelleted by centrifugation at 9500rpm to remove debrie; 10% lysate was transferred to another tube and kept as whole cell extract (WCE). To lower the amount of non-specific contaminants, the lysate was precleared by incubation with 10µl Protein G beads at 4°C while shaking. Before IP, all beads were washed three times with PBS and twice with lysis buffer. After 30min, the Protein G beads were collected by centrifugation and the supernatant was incubated with FLAG beads for 3h at 4°C or with HA-beads for 45 minutes to two hours while rotating. Some IPs were performed by first incubating the lysate with 0,5-2µg antibody for 30 minutes at 4°C while rotation. Immune complexes were then precipitated with protein A/G Sepharose, collected by centrifugation at 5000rpm for 1min and washed four times with lysis buffer. To analyse the immunoprecipitates, beads were mixed with SDS-PAGE sample buffer (with or without β-mercaptoethanol). A SDS-PAGE and Western blot was performed, to detect the desired proteins.

His-tagged Pull-Down Assay

Five million cells were washed once with PBS (10%WCE taken), and lysed in 1ml lysis buffer (buffer G containing 5mM imidazole). Following sonication for 30 seconds, His-tagged proteins were immunoprecipitated with Ni-NTA beads, rotating at room temperature for 2 hours. The beads were collected by centrifugation at 6000rpm for 2 minutes, washed once with 1ml buffer G, once with 1ml buffer A (pH 8,0), once with 1ml buffer A (pH 6,3 + 0,2% Triton X-100), once with 1ml buffer A (pH 6,3), and once with buffer A (pH 6,3 + 0,1% Triton X-100. The beads were eluted with 20µl elution buffer moderately shaking for two hours at room temperature. The proteins were subjected to SDS-PAGE analysis.

Tandem FLAG-HA IP (TAP)

Tandem FLAG-HA IP is the consecutive immunoprecipitation of double tagged proteins to gain a higher purification (protocol from Guillaume Adelmant, 2008).

Five 15cm plates (178,8cm^2) with HEK 293 cells were harvested at a confluency of ~ 75%, with or without trypsinisation. After washing with cold PBS, cells were lysed in 3ml MCLB buffer, rotating at 4°C. After one hour of lysis, cells were spun at maximum speed for 20 minutes at 4°C. Two ml of cleared lysate were incubated with 20µl α-FLAG beads at 4°C while gently rotating. After 4 hours, precipitates were collected by centrifugation. The beads were eluted with 200µl 3x FLAG peptide at 250µl/ml. Then equilibrated 15µl α-HA-beads (30µl slurry) were add to the elution and incubated over night with gentle rotating at 4°C. Ones the binding was complete, the beads were collected by centrifugation at 2000rpm at 4°C, and washed five times with 1ml cold MCLB buffer and three times with 1ml PBS. The HA beads were eluted once or twice with 50µl HA-peptide (250µg/ml) for 30 minutes at room temperature. The samples were subjected to westen blot analysis or SDS-PAGE followed by silver staining of proteins (SilverQuest™ Silver Staining Kit) and mass spectrometry analysis.

2.2.4.3.3 In-vitro Kinase Assay

24h after transfection, WT and A45 Jurkat cells were lysed in PD buffer, sonicated and the supernatant incubated with 0,4µg IKKβ antibody and Protein G Sepharose™ for 16h at 4°C. The immunoprecipitates were washed twice with PD buffer and 1x with Kinase buffer. 20µl substrate mix [xµM γ-^{32}P ATP, 5µM ATP, 16µl Kinase buffer, and 20µl GST- IκBα-beads or GST-IκBα-SSAA-beads] were incubated with 20µl Kinase IP at 30°C for 15min. The reactions were terminated by adding 2x SDS sample buffer. The samples were subjected to SDS/PAGE, Western blotting, and autoradiography.

2.2.4.3.4 Bicinchoninic Acid Assay (BCA Assay)

The BCA assay is a biochemical method for determining the total level of protein in a solution (329). The protein concentration is exhibited by a color change of the sample solution from green to purple in proportion to protein concentration, which is based on two chemical reactions. Peptide bonds in protein (amino acids cysteine, tyrosine, tryptophan) reduce Cu^{2+} ions from the cupric sulfate to Cu^{1+}. The amount of Cu^{2+} reduced is proportional to the amount of protein present in the solution. Then two molecules of bicinchoninic acid chelate with each Cu^{1+} ion, forming a purple-colored product that strongly absorbs light at a wavelength of 562 nm. The assay was performed using the BCA Protein Assay Kit according manufacturers instructions. The amount of protein present in a solution was quantified by measuring the absorption spectra at the microplate reader and comparing with protein solutions with known concentrations.

2.2.4.3.5 SDS-Polyacrylamid Gel Electrophoresis (SDS PAGE)

The polyacrylamide gel matrix is formed by the co-polymerization of acrylamide and bis-acrylamide (36,215). Two types of systems- continuous and discontinuous- are used. A continuous system has only a single separating gel and uses the same buffer in the tanks and the gel. In a discontinuous system, a non-restrictive large pore gel, called stacking gel, is layered on top of a separating gel. Each gel is made with a different buffer, and the tank buffer is different from the gel buffers. The resolution obtained in a discontinuous system is much greater than that obtained with a continuous system.

Sodium dodecyl sulfate (SDS) is used in gels and for sample preparation (84,215,220,294,324,382). It is an amphipathic molecule that coats the protein, disrupting the secondary, tertiary, and quarternary structure. Another consequence of treatment with SDS is that it confers a negative charge to the polypeptide in proportion to its length. Since the proteins are denatured and because the negative charge on the protein is exceedingly large, the primary factor determining the rate of migration of the protein through the gel is the size of the protein.

To separate proteins electrophoretically under denaturing conditions, discontinuous polyacrylamid gels were used and poured according Tab.11. For electrophoretic mobility shift assay continous gels were used (2.2.4.2.3 EMSA).

Component		Seperating Gel			Stacking Gel
	6%	8%	10%	12%	
Tris (1,5M, pH 8.8)	5,0ml	5,0ml	5,0ml	5,0ml	1,25ml
Acrylamid	4,0ml	5,34ml	6,66ml	8,0ml	1,66ml
dd H$_2$O	10,8ml	9,44ml	8,14ml	6,8ml	7,0ml
SDS (10%)	200µl	200µl	200µl	200µl	100µl
APS	200µl	200µl	200µl	200µl	100µl
TEMED	20µl	20µl	20µl	20µl	10µl

Table 11. Separating and Stacking Gel

Protein samples were mixed with 2x SDS-PAGE sample buffer, boiled for 5min, and load onto the gel. The conditions for electrophoresis were: 200V, 500mA, 45min, using the Bio-Rad Mini PROTEAN® 3 System. A pre-stained protein ladder was co-electrophoresed with protein samples. After electrophoresis the gels were subjected to coomassie blue staining or western blot.

2.2.4.3.6 Western Blot

Western blot is a method to detect and examine the amount of protein in a given sample of tissue homogenate or cell lysate. It uses first gel electrophoresis to separate denatured proteins. The proteins are then transferred out of the gel and onto a membrane, while maintaining the organization they had within the gel. At the membrane proteins are detected using antibodies specific to the protein (51,359,295).

After SDS-PAGE, proteins were transferred from the gel onto a nitrocellulose membrane using the Bio-Rad Mini PROTEAN® 3 System (100V, 500mA, 1h). To prevent non-specific protein interactions, the membrane was incubated at room temperature in 5% non-fat dry milk/ TBST buffer for at least 30min. Then the membrane was incubated with primary antibody (0.5 - 5µg/ml, diluted in 5% non-fat dry milk/ TBST buffer) under gentle agitation, at 4°C, over night. After rinsing the membrane 3 times in TBST buffer for 10min, it was incubated with secondary antibody (1:5000, in 5% non-fat dry milk/ TBST buffer) for 45min at room temperature. The membrane was washed 3 times with TBST buffer and incubated with chemiluminescence reagent for 1 min. In this chemiluminescence reaction the enzyme horseradish peroxidase catalyzes light emission at 428nm from the oxidation of luminol (production of fluorescence in proportion to the amount of protein). This light was captured on the KODAK Image Station or on Kodak Biomax Light Film. Size approximations were taken by comparing the stained bands to that of the ladder. This process was usually repeated for a structural protein, such as α-tubulin.

2.2.4.3.7 Coomassie Blue Staining

Protein bands seperated by SDS-PAGE were visualized by Coomassie Blue staining (256). Coomassie dyes bind to arginine, histidine and aromatic amino acids of proteins.

After SDS-PAGE, gels were soaked in coomassie blue staining solution for 4h or overnight at room temperature, while shaking. Excess stain was then eluted with destaining solution till distinct protein bands were visible. The molecular weight of the proteins was estimated by comparisson with a molecular weight marker.

2.2.4.3.8 Silver Staining

Protein bands seperated by SDS-PAGE were visualized by silverstaining (318). Silver nitrate forms insoluble silver phosphate with phosphate ions. When subjected to a reducing agent (hydroquinone), it forms black elementary silver. Samples from Tandem Flag-HA IP (TAP) were subjected to SDS-PAGE followed by silver staining of proteins using the SilverQuest™ Silver Staining Kit according the manufacturer´s instructions.

2.2.4.3.9 Reporter Gene Assays

Reporter gene assays are used in studies of gene regulatory elements. In these assays, the reporter gene acts as a surrogate for the coding region of the gene under study. The reporter gene construct contains one or more gene regulatory elements being analyzed, the structural sequence of the reporter gene, and the sequences required for the formation of functional mRNA. Upon introduction of the reporter construct into cells, expression levels of the reporter gene are monitored through a direct assay of the reporter protein's enzymatic activity. The sensitivity of each reporter gene assay is a function of several factors including detection method, reporter mRNA and protein turnover, and endogenous (background) levels of the reporter activity. Both protein turnover and levels of endogenous background vary with each reporter protein and the cell line used.

β-Galactosidase Enzyme Assay

The β-Galactosidase Enzyme Assay System is a method for assaying β-galactosidase activity in lysates prepared from cells transfected with β-galactosidase reporter vectors. It was used as a reporter gene for measuring transfection efficiency. The assay was performed using the Galacto-Light Plus™ System. Cells were lysed on ice in 50-200µl 1x reporter lysis buffer for 10min. After centrifugation at 13000rpm, at 4°C, for 5min, 5-20µl supernatant was transfered to luminometer tubes and incubated with reaction buffer (Galacton Substrate: Reaction Buffer Diluent, 1:100) for 15min. The tubes were placed in a luminometer. After injection of 300µl Light Emission Accelerator and a time delay of 1-2seconds, the absorbance was read at 420nm for 5 seconds.

Luciferase Assay

The luciferase protein is used as a reporter gene for measuring promoter activity or transfection efficiency. The Luciferase Assay is a reagent for quantitation of firefly luciferase.

The assay was performed using the Promega Luciferase Assay System. Cells were lysed on ice in 50-200µl 1x reporter lysis buffer for 10min. After centrifugation at 13000rpm, at 4°C, for 5min, 5-20µl supernatant was transfered to luminometer tubes, which were placed in a luminometer. After injection of 100µl Luciferase Assay Reagent and a time delay of 1-2 seconds, the absorbance was read at 420nm for 10 seconds. Luciferase reporter assays were normalized for transfection efficiency by cotransfecting a β-galactosidase (β-gal) expression plasmid and dividing luciferase by β-gal activity.

2.2.4.3.10 Immunofluorescence (IF)

Immunfluorescence is a method to detect the location and relative abundance of a protein in tissue or single cells by using a primary antibody against the antigen of interest and a secondary, fluorescent dye-coupled antibody that recognizes the primary antibody.

For immunofluorescence cells were grown or placed on glass slides. After removing carefully all medium and washing once with PBS, the cells were fixed onto the glass with aceton/ methanol (1:1) for 1min. The glass slides were air dried and incubated with serum for 30min to prevent unspecific binding of the antibody. Then primary antibodies, diluted in serum, were applied to the slides and incubated for 1 hr at room temperature. After 3 times washing with PBS, the slides were incubated with the fluorochrome conjugated secondary antibody for 30-45 minutes at room temperature, then washed again 3 times with PBS and incubated with Draq5 or propidium iodide (1µl/ 500µl PBS, 1min) to stain the DNA. After the immunostainings, the slides were coverslipped using the Prolong® Atifade Kit. Immunofluorescent labeling was viewed by confocal microscopy or fluorescence microscopy using the green, red and ultraviolet filters.

2.2.4.3.11 GFP-RelA Nuclear Translocation Assay

For this assay, Jurkat cells were split to a concentration of $2x10^5$/ml. Two days later, 2 million cells were cotransfected with 2µg GFP-RelA, 1-1.5µg IκBα and 2µg LMP1. After 18-24 h, cells were fixed on microscope slides with acetone/ methanol (1:1), covered with Prolong Antifade Kit and observed under a fluorescence microscope.

2.2.4.3.12 Flow Cytometry

Flow cytometry is a technique for examining and counting microscopic particles, such as cells and chromosomes, by suspending them in a stream of fluid and passing them by an electronic detection apparatus (86, 192,236). It allows simultaneous multiparametric analysis of the physical and/or chemical characteristics of particles. The principle of flow cytometry is that a beam of light (usually laser light) of a single wavelength is directed onto a hydrodynamically-focused stream of fluid. A number of detectors are aimed at the point where the stream passes through the light beam: several perpendicular to the light beam (Side Scatter (SSC), one in line with it (Forward Scatter or FSC), and one or more fluorescent detectors. SSC depends on the inner complexity of the particle (membrane roughness, the amount and type of cytoplasmic granules, shape of the nucleus) and FSC correlates with the cell volume. Depending on the lamp or laser used to excite the fluorochromes and on the detector available, several fluorescence labels can be used (i.e. green (usually labled FL1): FITC, GFP, Alexa Fluor 488; orange (FL2): PE, PI; red channel (FL3): PerCP, PE-Alexa Fluor 700, PE-Cy5.5).

For my thesis I used flow cytometry to measure cell viability and protein expression, particularly proteins tagged with GFP (green fluorescent protein), or expression of GFP by itself (used as marker for transfection efficiency). To measure GFP expression, HEK 293 cells were trypsinized and washed once with medium before acquisition. Suspension cells were used unwashed. The data generated were plotted in a single dimension (histogram) or in two-dimensional dot plots. For analysis the regions on these plots were sequentially separated, based on fluorescence intensity, by creating a series of subset extractions (gates).

2.2.4.3.13 Mycoplasma Test

Mycoplasma is a type of small bacteria, which lack the rigid cell walls common to most bacteria. Various mycoplasma species are troublesome contaminants of animal and human cell cultures which cannot be detected by visual inspection and may not noticeably affect cell culture growth rates. However, mycoplasma infection has been shown to alter DNA, RNA and protein synthesis, introduce chromosomal aberrations and cause alterations or modifications of host cell plasma membrane antigens.

Mycoplasma was detected using the MycoAlert® Assay according the manufacturer's instructions following the protocol for cuvette/ tube luminometer. This assay is a biochemical test that exploits the activity of mycoplasmal enzymes. The viable mycoplasma is lysed and its enzymes react with the MycoAlert Substrate catalyzing the conversion of ADP to ATP. By measuring the level of ATP in a sample both before (A) and after (B) the addition of the MycoAlert Substrate, a ratio can be obtained which is indicative of the presence or absence of mycoplasma. Ratios B/A of less than 1 means the culture is uninfected

2.2.5 Software

CellQuest Pro (Flow cytometry)

Kodak Molecular Imaging Software 4.0.1, Eastman Kodak Company

Image Quant TL v2003.03 (Phospor imager)

Scanner Control, Molecular Dynamics Version 4.0 (Phosphor imager)

Simple 32 (confocal microscopy)

3. RESULTS

3.1 LMP1 TES2 mediated NF-κB activation requires NEMO.

NEMO is essential for NF-κB activation by TNFα, IL-1β, LPS, or HTLV-I Tax (79,95,243,303,316,420). To explore the role of NEMO in LMP1 mediated NF-κB activation, I assessed the expression of a reporter gene placed under the control of a κB enhancer element and compared LMP1 induced NF-κB activation in wildtype (WT) and NEMO knockout (KO) cell lines. In mouse embryonic fibroblasts (MEF, 243), LMP1 WT and LMP1 TES2 induced robust luciferase reporter activity in WT cells (Fig.17A, lane 4 and 5). However, in NEMO KO MEFs (243) I observed only minimal luciferase activity for LMP1 and no activity for LMP1 TES2 (Fig.17A, lane 4 and 5). Likewise, TNFα, IL-1β, and Tax activated NF-κB in WT but not NEMO KO MEFs (Fig.17A, lane 2, 3 and 5). The assay, repeated in a rat cell line (400), confirmed the result I obtained in MEFs. In WT Rat-I cells, LMP1 activated NF-κB, while it was substantially reduced in the NEMO KO cell line 5R (Fig. 17B, lane 2). The residual NF-κB activation in the KO cell line was mediated by LMP1 TES1 in a NEMO independent manner (Fig. 17B, lane 2 and 4). Furthermore, in HEK293 cells, small interfering RNA (siRNA) targeting NEMO diminished substantially LMP1 TES2 mediated NF-κB activation of an integrated κB-GFP reporter (Fig. 17C and D). These data indicate that NEMO is essential for LMP1 TES2 mediated NF-κB activation.
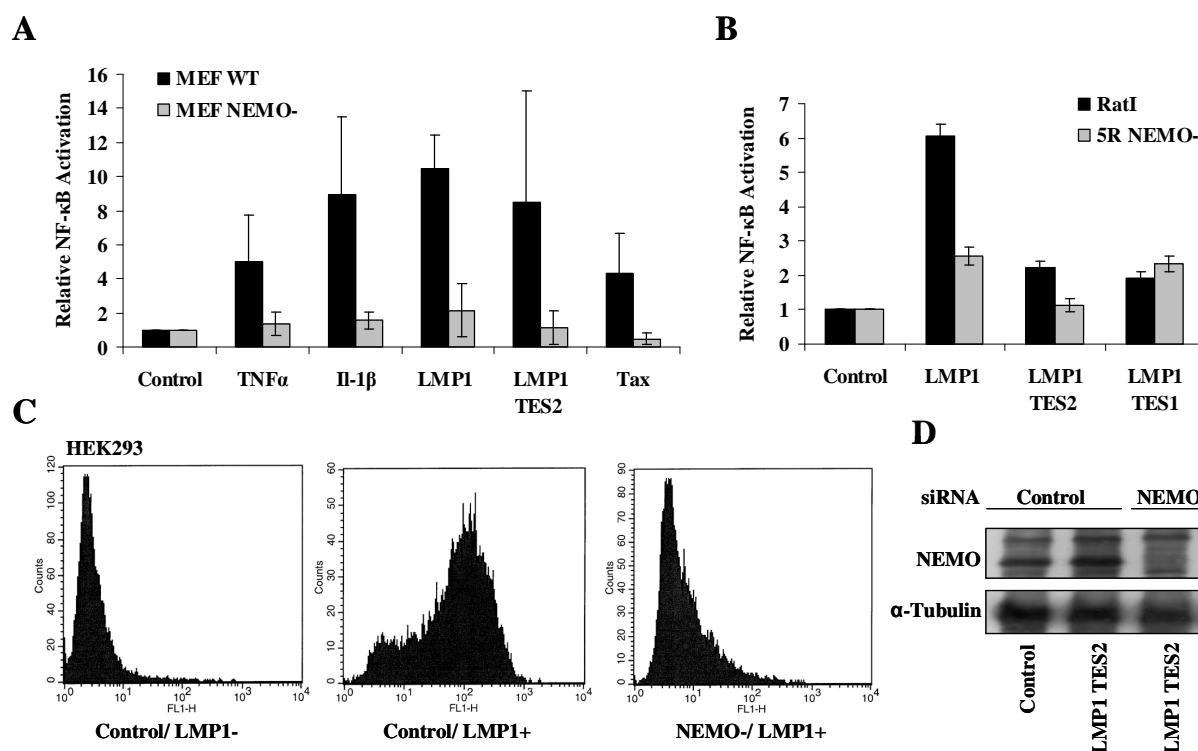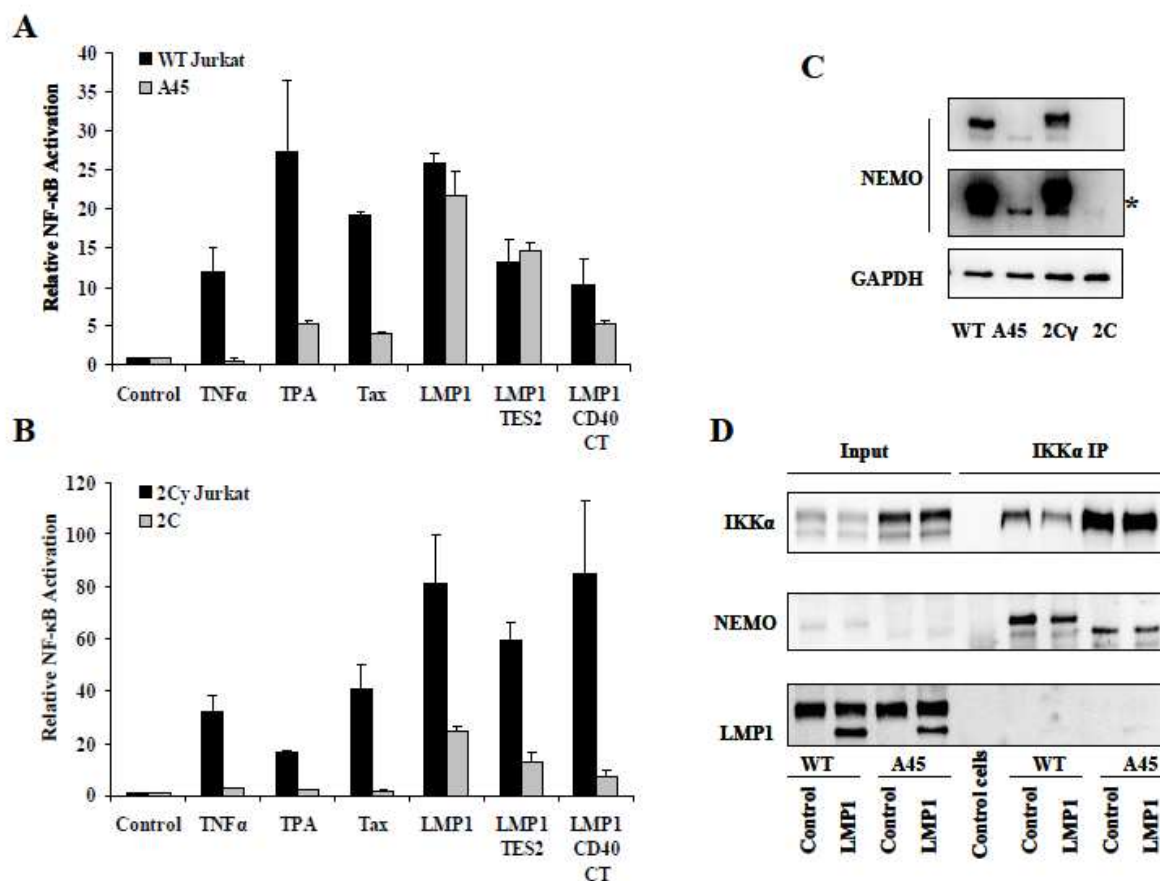

Figure 17. NEMO is required for LMP1-mediated NF-κB activation. (A) NEMO WT and KO MEFs were transfected with both a κB-luciferase reporter construct and a control β-galactosidase plasmid, and empty vector, LMP1 WT, LMP1 TES2 only or HTLV-1 Tax plasmids. Empty vector transfected cells were treated with either 10ng/ml TNFα (lane 2) or 10ng/ml IL-1β (lane 3) for 18h. (B) NEMO WT RatI and NEMO KO 5R cells were transfected with reporter plasmids and empty vector, LMP1 WT, LMP1 TES1 only or LMP1 TES2 only plasmids. (A,B) 24h after transfection, cells were lysed, and the amount of luciferase activity was detected. The mean +/- standard deviation (SD) of folds of NF-κB activation from three experiments is shown. (C) FACS histograms demonstrate GFP levels in HEK293 cells in the absence of LMP1 induction (left), with nontargeting siRNA and LMP1 induction (middle), or with NEMO knockdown and LMP1 induction (right). (D) A total of 45μg of HEK293 lysates prepared from whole cell extracts were immunoblotted with anti-NEMO, and anti-α-Tubulin.

3.2 LMP1 activates NF-κB in mutant Jurkat cells while TNFα and Tax do not activate.

To assess the role of NEMO in LMP1 mediated NF-κB activation in lymphocytes, I performed the same reporter assay in 2 different Jurkat cell lines, A45 and 2C, in which NEMO knockout was generated by somatic cell mutagenesis using ICR191. The A45 cell line (provided by Nils Jacobsen, Seed Laboratory) was selected for a deficiency in TNFα-mediated NF-κB activation, while the 2C cell line (153, provided by Shao-Cong Sun) was incapable to support TPA- (phorbol 12-myristic 13-acetate (PMA)) or Tax- mediated NF-κB activation. In neither cell line, NEMO expression was detected by western blot analysis. In 2C, TPA-and Tax-mediated NF-κB activation was rescued by expression of exogenous NEMO (2Cγ cell line) (153).

Figure 18A shows LMP1 WT and LMP1 TES2 activated NF-κB in NEMO mutant A45 Jurkat cells as well as in WT (Fig. 18A, lanes 5 and 6), whereas TNFα, Tax, TPA and CD40 induced NF-κB activity only in the parental NEMO+ WT cell line (Fig. 18A, lanes 2,3,4 and 7). In 2C cells, LMP1 and LMP1 TES2 activated NF-κB 20-30 fold compared to 60-80 fold in the 2C reconstituted cell line 2Cγ (Fig. 18B, lanes 5 and 6). Again, this contrasted with TNFα, TPA, Tax and CD40 which failed to induce any NF-κB activity in 2C (Fig. 18B, lanes 2,3,4 and 7).



Figure 18. LMP1 activates NF-κB in lymphocytes. (A) NEMO WT and A45 NEMO mutant Jurkat cells or (B) 2Cγ and 2C NEMO mutant Jurkat cells were transfected with both a κB-luciferase reporter construct and a control β-galactosidase plasmid, and empty vector, LMP1 WT, LMP1 TES1 only, LMP1 TES2 only, LMP1 CD40CT or HTLV-1 Tax plasmids. (A/B) Some empty vector transfected cells were treated with either 10ng/ml TNFα or 2,5ng/ml TPA for 18h. 48h after transfection, cells were lysed, and the amount of luciferase activity was detected. The mean +/- SD of folds of NF-κB activation by LMP1, LMP1 TES2, LMP1 CD40 CT, or three other NF-κB stimuli from three experiments is shown. (C) **Jurkat cell lines A45 and 2C express mutant NEMO proteins.** A total of 30μg of Jurkat cell lysates were immunoblotted with anti-NEMO, and anti-GAPDH. Asterix indicates overexposure of blot shown above. (D) **Characterization of the association between endogenes IKKα and endogenes NEMO by Co-IP** in A45 Jurkat cells, transfected with either empty vector or LMP1. 24h after transfection, whole cell extracts were subjected to IP with mouse monoclonal IKKα antibody, followed by IB with rabbit polyclonal anti-IKKα, rabbit polyclonal anti-NEMO, and mouse monoclonal LMP1 antibodies.

Since NEMO is essential for LMP1 mediated NF-κB activation, as shown in Fig. 17, but activated NF-κB in the A45 and 2C cell lines, the results of the reporter assay in Fig. 18 suggested that LMP1 mediated activation in lymphocytes is NEMO independent or A45 and 2C may express NEMO mutant proteins that uniquely support LMP1 mediated NF-κB activation. To investigate these possibilities, I first performed western blot analysis of whole cell extracts (WCE) using a polyclonal antibody raised to full length NEMO which detected the full length protein in the WT and 2Cγ cell lines, and at very low levels a 46kDa and 39kDa protein in A45 and 2C respectively (Fig. 18C). The mutant NEMO protein expressed in 2C was only faintly visible after overexposure of the western blot (Fig. 18C lane 4). To examine whether mutant NEMO can still physically interact with the IKK complex, I performed immuno-precipitations (IP) of endogens IKKα and western blotting (IB) with NEMO antibody. The NEMO mutant expressed in A45 Jurkat cells was incorporated into the IKK complex (Fig. 18d, lanes 3 and 8); the association did not change in the presence of LMP1 (Fig. 18D, lanes 4 and 9). I did not detect a similar association of IKKα and NEMO in the 2C mutant Jurkat cell line, likely due to extremely low levels of expression.

3.3 Jurkat cell lines A45 and 2C express mutant NEMO proteins.

Using Northern blot analysis, I was able to detect NEMO mRNA in the A45 Jurkat cell line, but not in the 2C cell line (data not shown). However, the use of more sensitive reverse transcription-PCR analysis allowed the detection of NEMO transcripts in both cell lines. To define the mutation in NEMO I isolated RNA, performed reverse transcription PCR, amplified the NEMO cDNA in three pieces (using primer pairs 1/7, 3/8, and 5/6, Fig. 19B), cloned, and sequenced the cDNA (Fig. 19A-C).
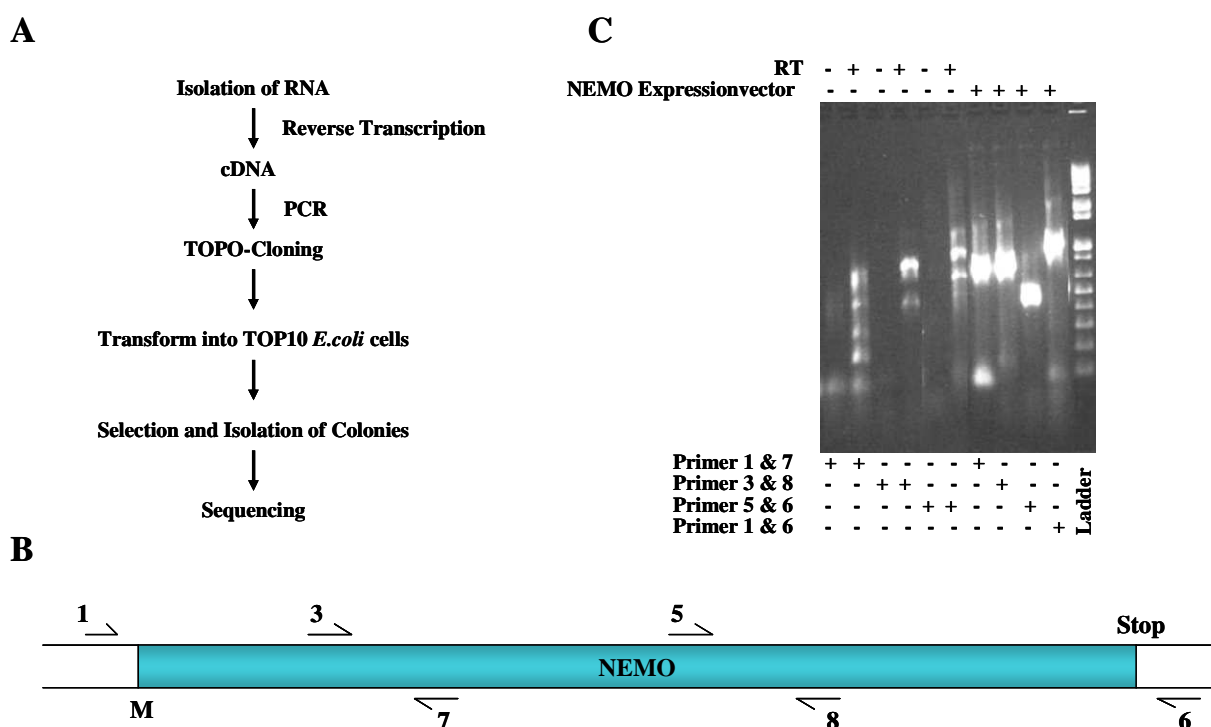
Figure 19. Cloning of NEMO mutants from A45 and 2C cell lines. (A) Schematic of the cloning steps. Total RNA was extracted from A45 and 2C Jurkat cells using Trizol® Reagent. 1μg of total RNA was used as template for reverse transcription with oligo(dT)$_{20}$ (SuperScript™ III First-Strand Synthesis System for RT-PCR). After treatment with 1μl RNase H, the RNA was used for RT-PCR. From the sequence for NEMO (*IKBKG*) cDNA (according to GenBank Accession number NM_003639.3.), gene-specific primers were designed (B) and used to amplify the cDNA by PCR. The PCR product (C) was used for TOPO® Cloning (TOPO TA Cloning® Kit for Sequencing). The product was transformed into DH5α bacteria, isolated and sequenced.

Sequencing of the PCR products, derived from the A45 and 2C Jurkat cell lines, revealed two different mutations in NEMO. The cDNA expressed in A45 results from aberrant splicing of exon 9 into exon 10 and deletion of bases 1376-1491 (the mutation is based on the *IKBKG* cDNA sequence according to GenBank Accession number NM_003639.3). The resulting protein is deleted for amino acids 373-419 encompassing the zink finger with residue 372 fused to the sequence DTCHGVH (Fig. 20A/C). The cDNA from 2C differs from the wildtype with an internal deletion of basepairs 655-930 caused by exon 3 spliced to exon 6 (In-frame deletion). The resulting protein has an internal deletion of residues 133-224 (Fig. 20B/C). Both proteins have intact the IKK binding domain at the amino terminus of NEMO as well as the ubiquitin binding domain encompassing coiled coil 2 (CC2), the UBAN motif and the leucine zipper (LZ).
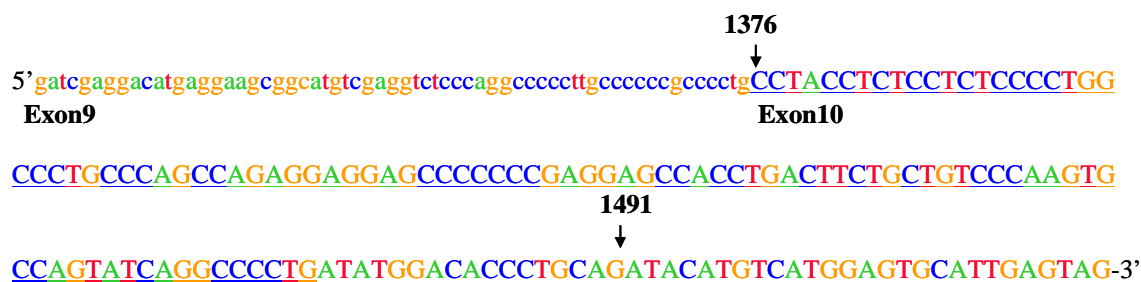
1376

5'gatcgaggacatgaggaagcggcatgtcgaggtctcccaggcccccttgcccccgcccctgCCTACCTCTCCTCTCCCTGG

Exon9   **Exon10**

CCCTGCCCAGCCAGAGGAGGAGCCCCCCCGAGGAGCCACCTGACTTCTGCTGTCCCAAGTG

1491

CCAGTATCAGGCCCCTGATATGGACACCCTGCAGATACATGTCATGGAGTGCATTGAGTAG-3'

Figure 20. (A) Mutation (c.1376C_1491Gdel) in NEMO cDNA in A45 Jurkat cell line.

5'atgccatccggcagagcaaccagattctgcgggagcgctgcgaggagcttctgcatttccaagccagccagagggaggagaaggagttc

Exon3

ctcatgtgcaagttccaggaggccaggaaactggtggagagactcggcctggagaagctcgatctgaagaggcagaaggagcaggctctgc

655

GggaggtggagcacctgaagagatgccagcagCAGATGGCTGAGGACAAGGCCTCTGTGAAAGCCCAG

Exon4

GTGACGTCCTTGCTCGGGGAGCTGCAGGAGAGCCAGAGTCGCTTGGAGGCTGCCACTA
AGGAATGCCAGGCTCTGGAGGGTCGggcccgggcggccagcgagcaggcgcggcagctggagagtgagcgcga

Exon5

ggcgctgcagcagcagcacagcgtgcaggtggaccagctgcgcatgcagggccagagcgtggaggccgcgctccgcatggagcgccag

930

gccgcctcggaggagaaGAGGAAGCTGGCCCAGTTGCAGGTGGCCTATCACCAGCTCTTCCAAG

Exon6

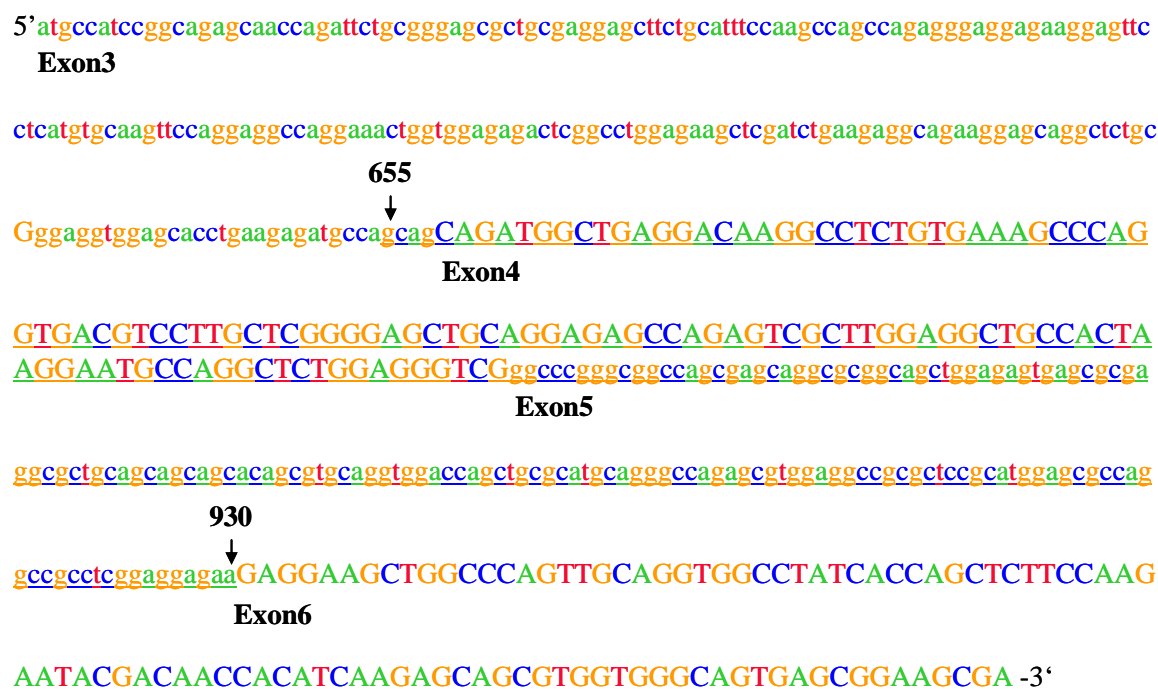AATACGACAACCACATCAAGAGCAGCGTGGTGGGCAGTGAGCGGAAGCGA -3'

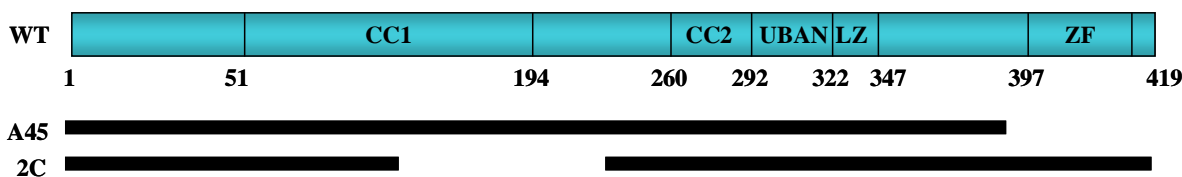**Figure 20.** (B) Mutation (c.655G_930Adel) in NEMO cDNA in 2C Jurkat cell line.

Figure 20. (C) **NEMO stick diagram** with domains as indicated, and schematic representations of WT NEMO, and mutants aa1-372 and Δ133-224 expressed in the A45 and 2C Jurkat cell lines, respectively. (Codon numbering starts from the translation codon 1 according to the GenBank Accession number NP_003630.1)

3.4 Mutant NEMO is required for LMP1 TES2-mediated NF-κB activation.

To demonstrate that the mutant NEMO proteins in the A45 (aa1-372) and 2C (Δ133-224) cell lines were functional for LMP1 mediated NF-κB activation, four siRNAs targeting NEMO were utilized. LMP1 or LMP1 TES2 and a NF-κB luciferase reporter were co-transfected with siRNA. Reporter assays done 3 days post transfection showed substantially reduced LMP1 and no LMP1 TES2 mediated NF-κB activation in both A45 and 2C NEMO mutant Jurkat cell lines (Fig. 21A/B, lanes 2 and 3). Immunoblot analysis for the efficiency of the knockdown showed an approximately 85% reduction of NEMO (Fig. 21C). Thus, LMP1 TES2 mediated NF-κB activation is NEMO dependent in A45 and 2C Jurkat cells.
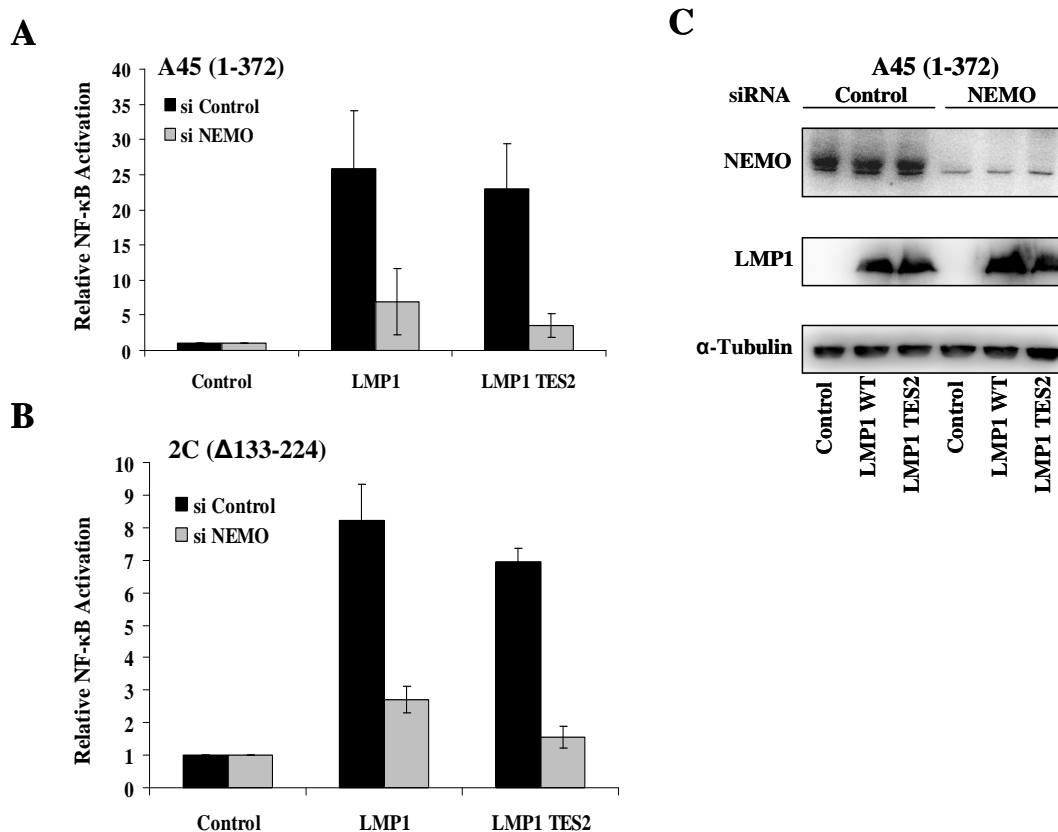
Figure 21. NEMO is required for LMP1-mediated NF-κB activation. (A) A45 [aa1-372] and (B) 2C [Δ133-224] NEMO mutant Jurkat cells were transfected with non-targeting siRNA or siRNA specific to NEMO, both a κB-luciferase reporter construct and a control β-galactosidase plasmid, and empty vector, LMP1 WT or LMP1 TES2 only plasmids. 72h after transfection, cells were lysed, and the amount of luciferase activity was detected. The mean +/- SD of folds of NF-κB activation from three experiments is shown. (C) A total of 25μg of lysates prepared from whole cell extracts were immunoblotted with anti-NEMO, anti-LMP1, and anti-α-Tubulin.

3.5 LMP1 signal transduction to NF-κB in mutant NEMO Jurkat cell lines is IKKβ dependent.

To further define the essential role of NEMO in LMP1 signaling, I investigated various steps in the NF-κB signaling cascade in NEMO WT and the A45 and 2C mutant NEMO Jurkat cell lines. First I examined if the NEMO mutants expressed in A45 and 2C supported IKKβ dependent NF-κB activation. In WT, as well as both NEMO mutant cell lines, I observed only minimal luciferase activity for LMP1 and no activity for LMP1 TES2 in the presence of an IKKβ inhibitor (Fig. 22A/C, lanes 2 and 3). LMP1 and LMP1 TES1 induced similar levels of IKKα mediated p100 processing to p52 in both control (Fig. 22B/D, lanes 2 and 4) and IKKβ inhibitor treated cells (Fig. 22B/D, lanes 6 and 8), indicating the specificity of the inhibitor for IKKβ. The residual NF-κB activation mediated by LMP1 TES1 was similarly unaffected by the IKKβ inhibitor (Fig. 22A/C lanes 2 and 4).
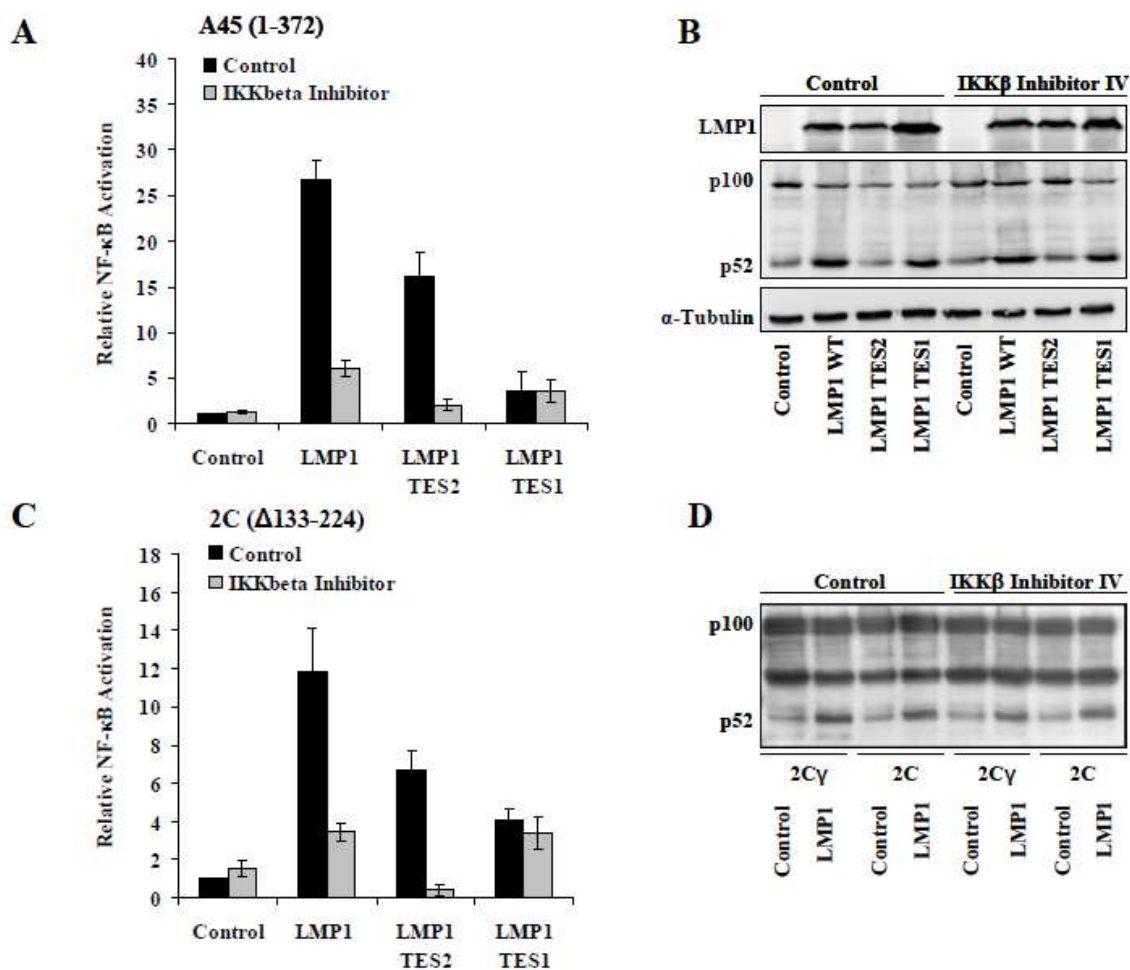
Figure 22. LMP1 signal transduction to NF-κB in mutant NEMO Jurkat cell lines is IKKβ dependent. (A) NEMO WT and A45 mutant Jurkat cells or (C) 2Cγ and 2C mutant Jurkat cells were transfected with both a κB-luciferase reporter construct and a control β-galactosidase plasmid, and empty vector, LMP1 WT, LMP1 TES2 only or LMP1 TES1 only plasmids, and treated with 10μM IKKβ inhibitor IV or DMSO as control for 18h. 24h after transfection, cells were lysed, and the amount of luciferase activity was detected. The mean +/- SD of folds of NF-κB activation by LMP1 from three experiments is shown. (B/D) A total of 25μg of lysates prepared from whole cell extracts from (B) A45 and (D) 2C and 2Cγ, were immunoblotted with anti-p100/ p52, and (B) with anti-LMP1, and anti-α-Tubulin.

To investigate, if other LMP1 mediated NF-κB signaling steps are affected by the NEMO mutation in A45 (aa1-372) and 2C (Δ133-224) Jurkat cells, inducible phosphorylation and degradation of IκBα was examined. In a NF-κB reporter assay, LMP1 and LMP1 TES2 mediated NF-κB activation was inhibited by mutant IκBα proteins, ΔN-IκBα and IκBα-SSAA, that can not be phosphorylated and degraded (Fig. 23A/B, lanes 3-6). In WT, as well as the A45 mutant NEMO cell line, LMP1 TES2 mediated NF-κB induced phosphorylation of IκBα (Fig. 23C, lanes 1 and 2), which was inhibited by an IKKβ chemical inhibitor (Fig. 23C, lanes 3 and 4).

Furthermore, an electrophoretic mobility shift assay (EMSA) showed that both mutant NEMO cell lines induced NF-κB activity like the WT Jurkat cell line. The NF-κB complex activated by LMP1 consists of p50, p52 and RelA (Fig. 24A and B).

These data suggest that in WT as well as both mutant Jurkat cell lines LMP1 functioned normally in promoting the activation of IKKβ and IκBα. Furthermore, NEMO aa1-372 and Δ133-224 uniquely support LMP1 TES2 dependent IKKβ activation, whereas they can not support TNFα, Tax, TPA or CD40-mediated IKKβ activation.

A

B

C

A45 (1-372)
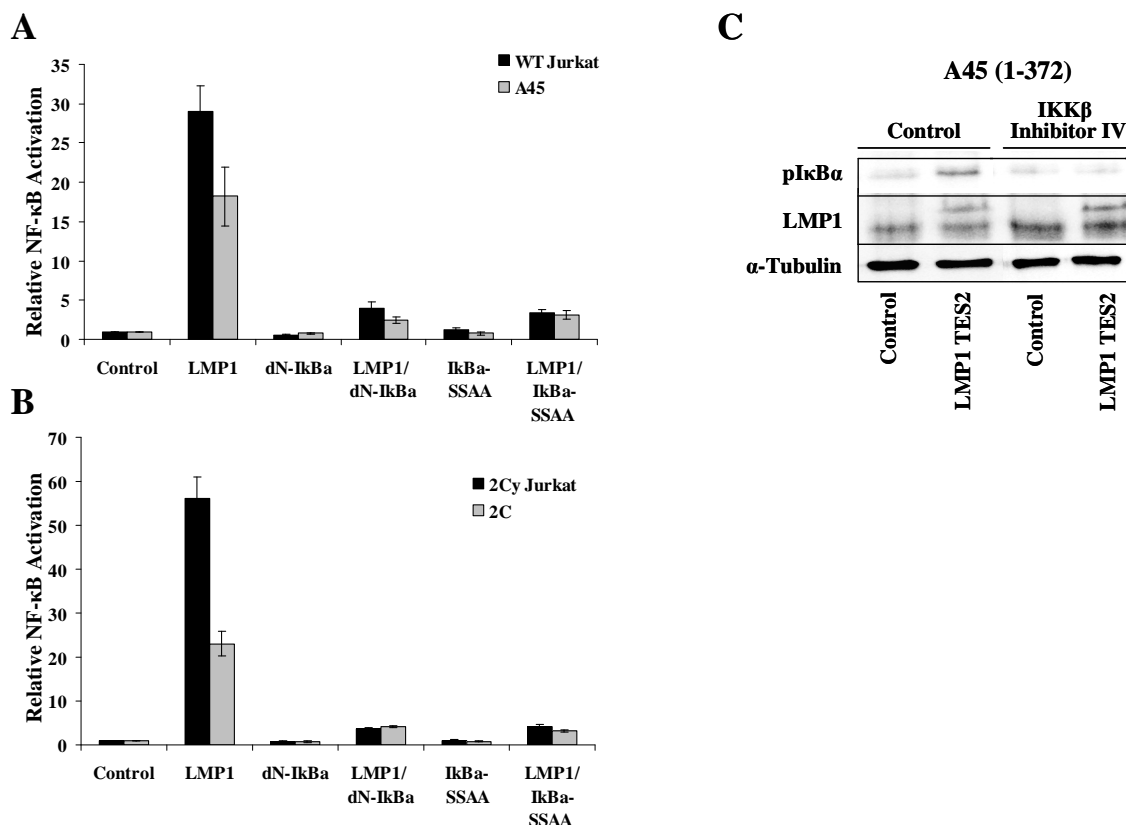
**Figure 23. LMP1 mediated NF-κB activation was inhibited by mutant IκBa proteins ΔN-IκBα and IκBα-SSAA.** (A) NEMO WT and A45 mutant Jurkat cells or (B) 2Cγ and 2C mutant Jurkat cells were transfected with both a κB-luciferase reporter construct and a control β-galactosidase plasmid, or/and empty vector, LMP1 WT, ΔN-IκBα, or IκBα-SSAA plasmids. 24h after transfection, cells were lysed, and the amount of luciferase activity was detected. The mean +/- SD of folds of NF-κB activation is shown. (C) **An IKKβ inhibitor prevents LMP1 TES2 mediated phosphorylation of IκBα.** Lysates prepared from whole cell extracts of A45 NEMO mutant Jurkat cells (transfected with empty vector or LMP1 and treated with DMSO as control or 10μM IKKβ inhibitor IV for 24h) were immunoblotted with anti-phospho-IκBα, anti- LMP1, and anti-α-Tubulin.
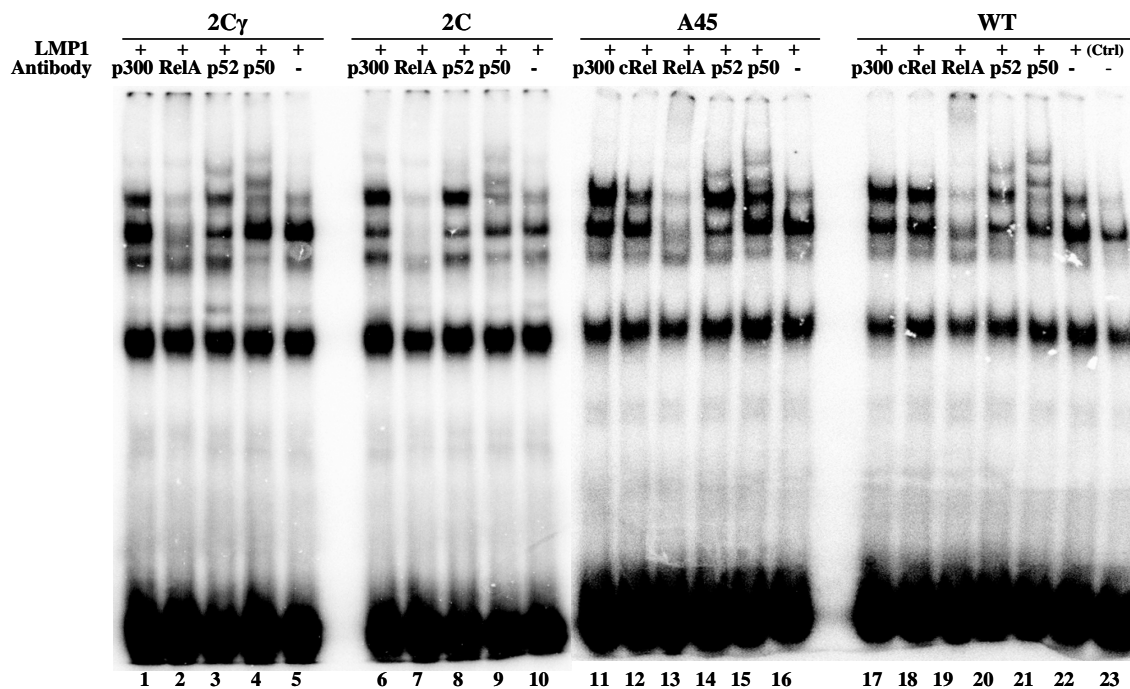
Figure 24A. LMP1 mediated Induction of NF-κB binding activity in 2Cγ, 2C, A45, and WT Jurkat cells. Whole-cell extracts from LMP1- or empty vector (Ctrl) transfected cells were incubated with antibody as indicated and an NF-κB probe. DNA binding was determined by EMSA.

70
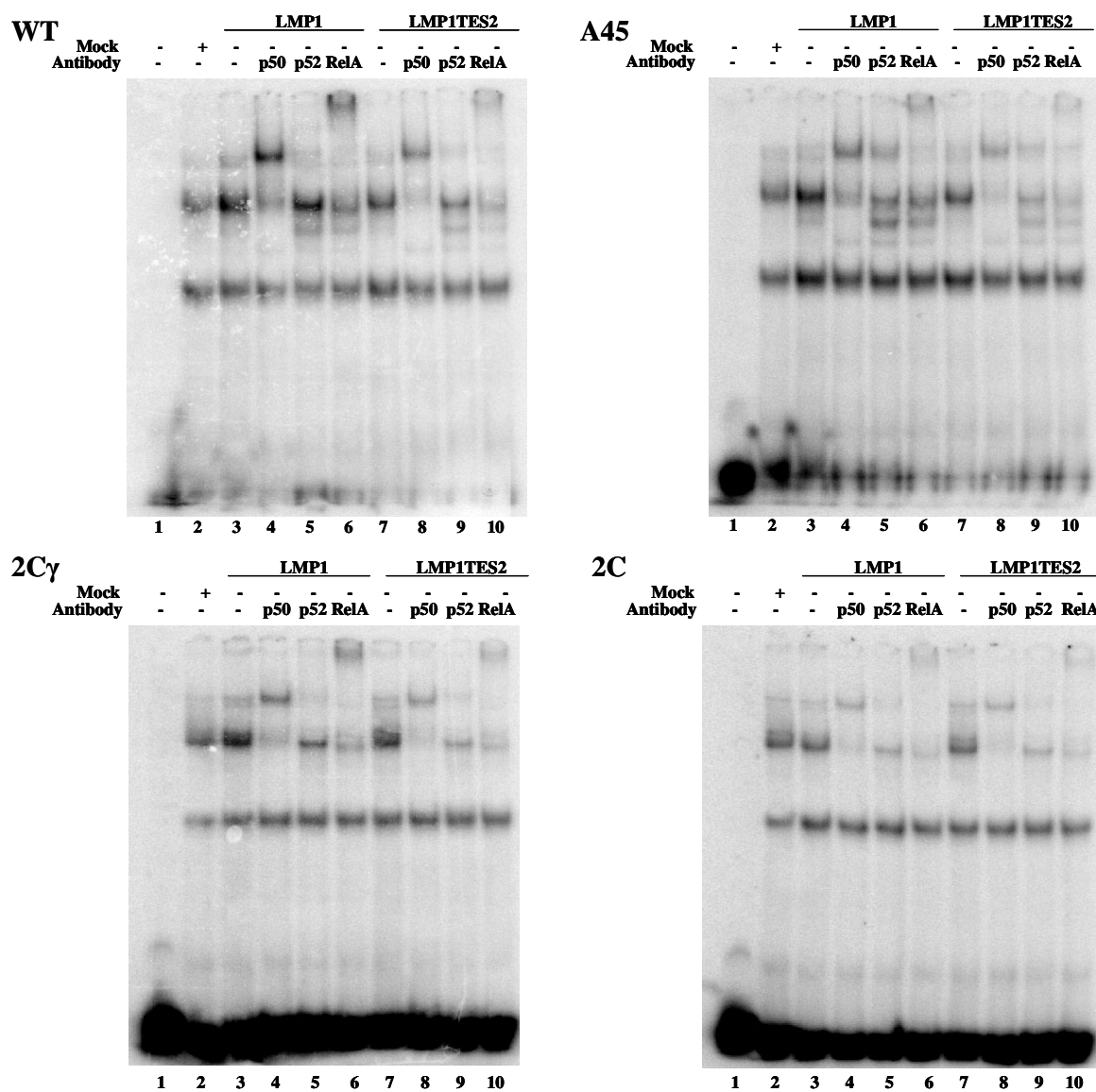
Figure 24B. LMP1 mediated Induction of NF-κB binding activity in 2Cγ, 2C, A45, and WT Jurkat cells. Whole-cell extracts from LMP1, LMP1 TES2, or empty vector (Mock) transfected cells were incubated with antibody as indicated and an NF-κB probe. DNA binding was determined by EMSA.

To verify the findings for LMP1, NEMO, and NF-κB, I generated the WT NEMO and six serial deletion mutants, including the two mutations isolated from the A45 and 2C NEMO mutant Jurkat cell lines. Each were tagged at their N-terminus with a FLAG- and a HA- epitope (Fig. 25A). Human full length NEMO was amplified by PCR from a pCMV6-XL4/5/6-NEMO vector and cloned into a pGK2 vector. All deletion mutants were prepared by conventional PCR and cloned into a pGK2 vector as well. All mutants were confirmed by western blotting with anti-FLAG antibody to express comparably when transfected into human cells (Fig. 25B). Figure 26 shows fluorescent presentations of full-length NEMO and the six truncation mutants stably expressed in MEFs. The subcellular localization of each mutant was comparable and mostly cytoplasmic with a small but reproducible fraction in the nucleus. Full-length NEMO appeared as rounded cytoplasmic speckles. When N- or C-terminal sequences were deleted, the mutant proteins 51-419, 1-245, 1-303 and 1-372 maintained their cytoplasmic speckles; however, they were smaller and more diffuse than speckles from full-length NEMO. The NEMO mutant Δ134-223 coalesced into large cytoplasmic aggregates. The double mutant 1-372/ Δ134-223 showed small cytoplasmic speckles and some larger cytoplamic aggregates (Fig.26).
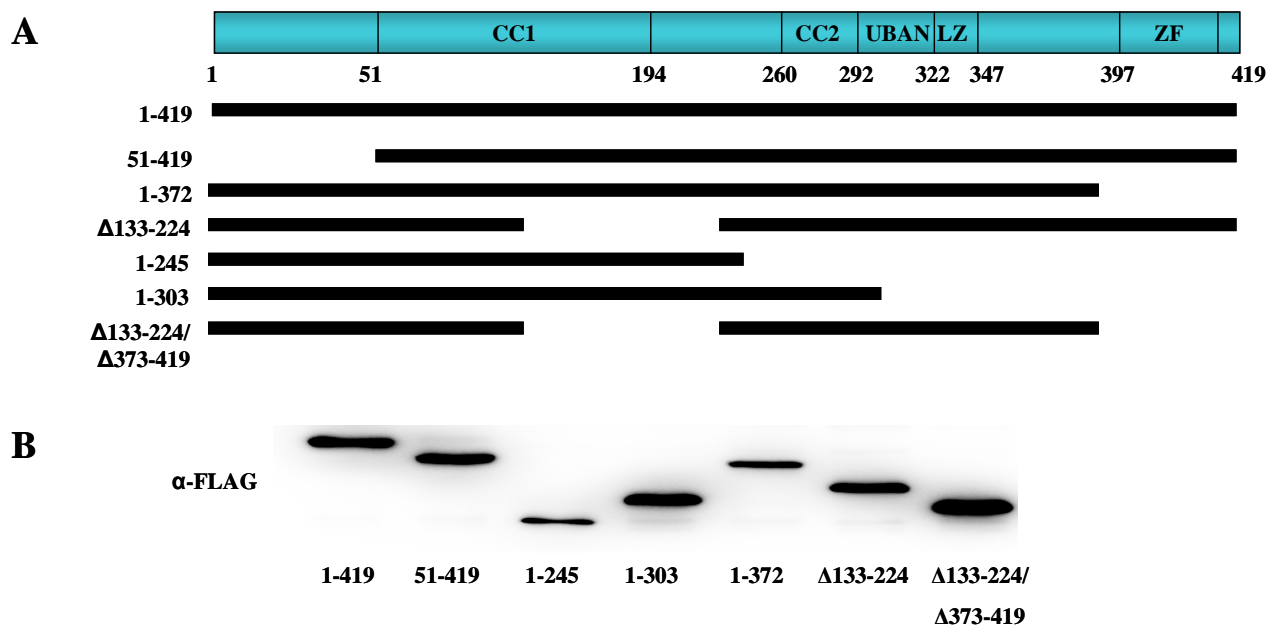
Figure 25. Construction of six NEMO mutants. (A) NEMO stick diagram with domains as indicated, and schematic representations of full-length and six NEMO mutants. (B) Expression of FLAG-HA-NEMO and its truncation mutants in HEK293T cells. HEK293T cells were transfected with FLAG-HA-NEMO vectors expressing full-length NEMO (1-419) and mutants (as indicated). A total of 30μg of lysates prepared from WCE were immunoblotted with anti-FLAG antibody.
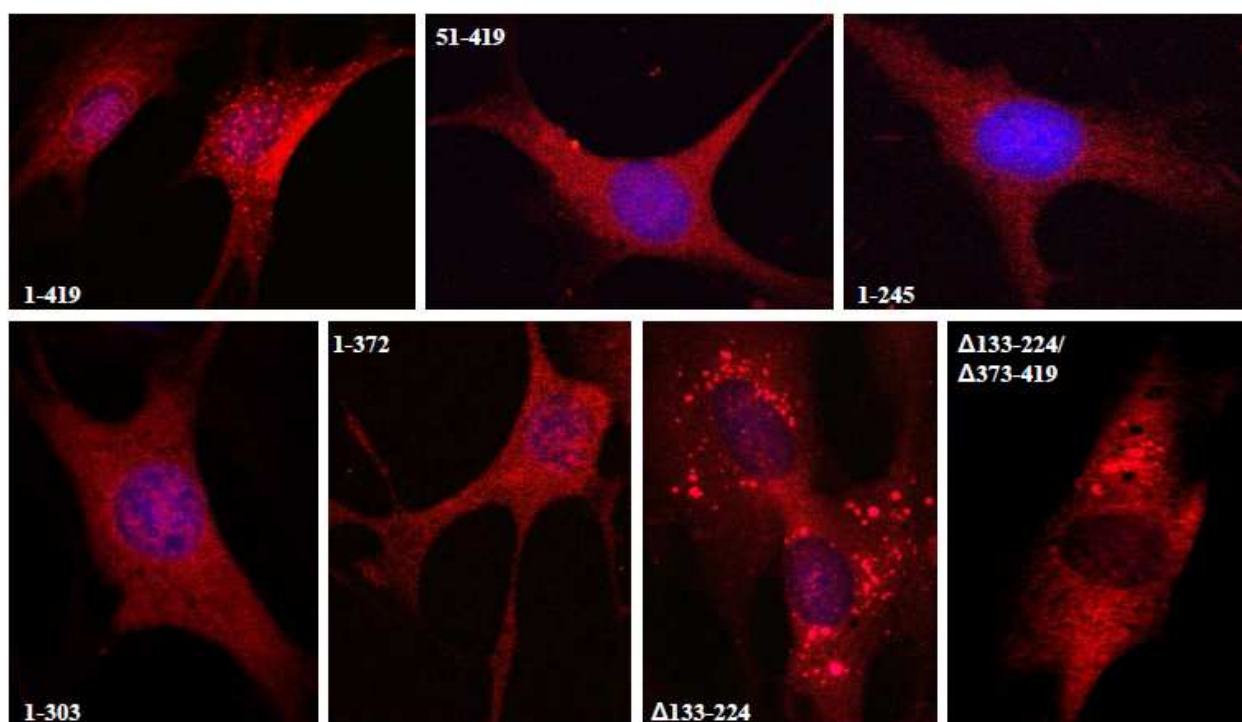
Figure 26. Fluorescent presentations of full-length NEMO and six truncation mutants. NEMO$^{-/-}$ MEFs stably expressing FLAG-HA-tagged full-length or mutant NEMO were fixed onto class slides and stained with antibody specific to human NEMO.

3.6 Reconstitution with NEMO restores LMP1 induced NF-κB activation.

To delineate which domains of NEMO are required for LMP1 TES2 mediated NF-κB activation, NEMO knockout MEFs were stably transfected with FLAG-HA tagged wildtype NEMO and six deletions, including the two mutants isolated from the A45 and 2C Jurkat cell lines. All mutants were expressed at levels similar to endogenous. As expected, in NEMO$^{-/-}$ MEFs, NF-κB could not be activated by any of the tested stimuli, including LMP1 (Fig. 27, lane 3), TNFα, and Tax (Fig. 28, lane 2). Expression of full-length 1-419 NEMO restored LMP1 mediated NF-κB activation (Fig. 27, NEMO 1-419 lane). LMP1 mediated NF-κB activation was similarly reconstituted by expression of NEMO 51-419 (Fig. 27, lane 5). Deletion of residues 373-419 (without the additional DTCHGVH) had no effect on LMP1 TES2 mediated NF-κB activation and confirmed the Zn finger of NEMO is dispensable for LMP1 TES2 mediated NF-κB activation (Fig. 27, NEMO 1-372 lane). Similarly, NEMO Δ133-224 restored LMP1 TES2 mediated NF-κB activation confirming that this region is also dispensable for LMP1 TES2 mediated NF-κB activation (Fig. 27, lane 9). The double mutant 1-372/ Δ133-224 could not reconstitute LMP1 mediated NF-κB activation indicating that the zink finger and the region aa133-224 possibly have a redundant function for LMP1 signaling whereas both are essential for TNFα mediated NF-κB activation (Fig. 27, lane 10). C-terminal truncation of the leucine zipper (LZ) and the Ubiquitin binding domain (UBAN) between amino acids 303 and 372 abrogated the ability of NEMO to restore LMP1 mediated NF-κB activation.
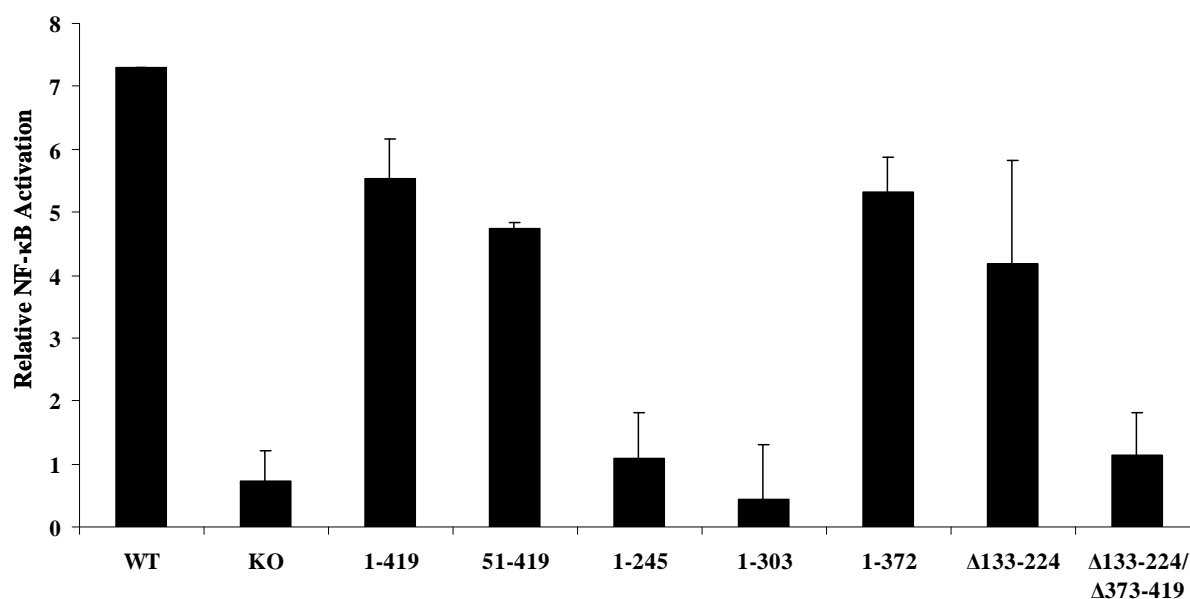
Figure 27. Reconstitution with NEMO restores LMP1 induced NF-κB activation. NEMO$^{-/-}$ MEFs stably expressing FLAG-HA-tagged full-length or mutant NEMO were transfected with a LMP1 TES2 expression plasmid and both a κB-luciferase reporter construct and a control β-galactosidase plasmid. 48h after transfection, cells were lysed, and the amount of luciferase activity was detected. The mean +/- SD of folds of NF-κB activation from three experiments is shown.

As control and to investigate whether different NEMO mutants could distinguish between LMP1 versus other activators of NF-κB, I performed the reconstitution experiment with TNFα and Tax. To this aim, I employed the same NEMO knockout MEFs stably expressing FLAG-HA tagged full lenght NEMO and 6 deletions, including the two mutants isolated from the A45 and 2C Jurkat cell lines. Whereas full-length NEMO was able to completely restore TNFα mediated NF-κB activation, only 65% of Tax induced NF-κB activation could be rescued (Fig. 28, NEMO 1-419 lanes). When different mutants were tested, only one exhibited activity. Mutant 51-419 restored about 50% of TNFα- and Tax mediated NF-κB activity (Fig. 28, lane 4). Mutants 1-245, 1-303, 1-372, Δ133-224, and the double mutant 1-372/ Δ133-224 were completely inactive for TNFα, or Tax mediated NF-κB activation (Fig. 28,

lane 5-9). These results confirm previously published data for TNFα (177). In contrast, Mutant 1-245 has been previously demonstrated to be partially active for Tax mediated NF-κB activation. The same study showed that a mutant NEMO 1-370 fully restored Tax mediated NF-κB activation (177). One explanation for the obvious discrepancy between our and their findings could be the different cell lines and systems used for the experiment. While I performed the experiments in MEFs stably expressing NEMO at levels similar to endogenous, Iha and colleagues utilized E8i cells transiently transfected with NEMO expression plasmids for their reporter assay, possibly resulting in NF-κB activation by overexpression of NEMO.

Taken together, these complementation results suggest that LMP1, TNFα, and Tax signal nonidentically through NEMO.
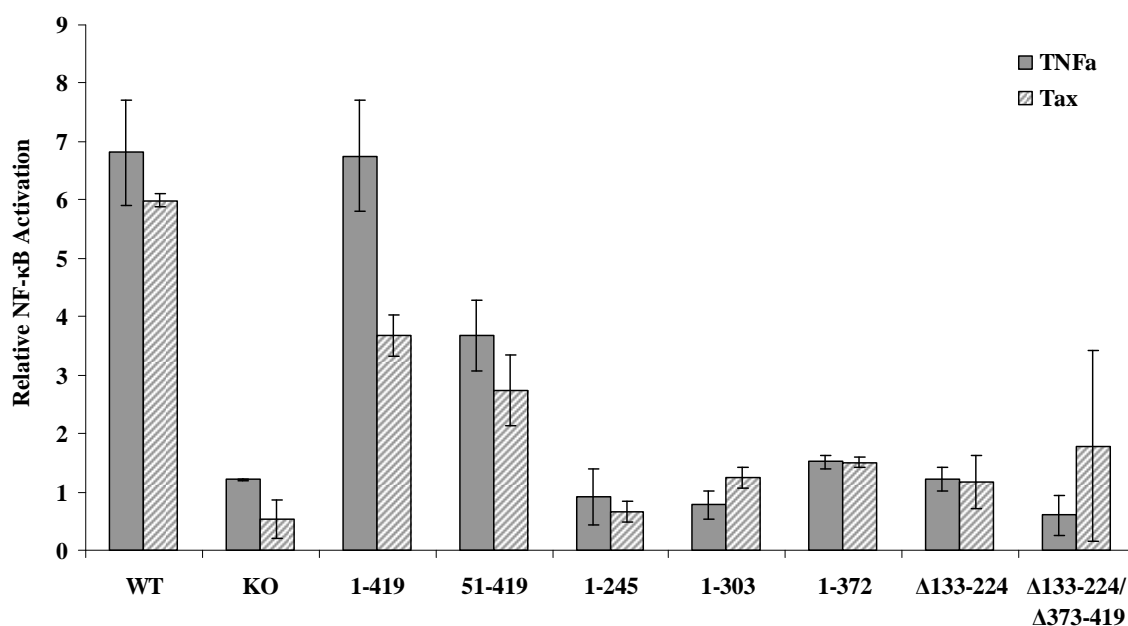
Figure 28. NEMO domains required for functional complementation of TNFα- or Tax-induced NF-κB activation. NEMO$^{-/-}$ MEFs stably expressing FLAG-HA-tagged WT or mutant NEMO were transfected with either Mock or Tax expression plasmids, and both a κB-luciferase reporter construct and a control β-galactosidase plasmid. Mock transfected cells were treated with 10ng TNFα for 18h. 48h after transfection, cells were lysed, and the amount of luciferase activity was detected.

3.7 LMP1 TES2 co-immunoprecipitates with NEMO in HEK239 cells and MEFs.

The known direct interaction of the human T lymphotropic virus (HTLV)-1 encoded protein Tax with NEMO, which results in constitutive activation of NF-κB (60,79,116,285), led us to the hypothesis that LMP1 might also interact directly with NEMO. To examine this possibility and to investigate the mechanism by which the Zn finger and aa133-224 domains function to support LMP1 mediated NF-κB activation, I performed co-immuno-precipitation experiments in two different cell lines.

In mammalian HEK293 cells transiently transfected with plasmids expressing full-length HA-tagged NEMO and FLAG-tagged LMP1, I found that LMP1 TES2 co-immunoprecipitated with WT NEMO (Figure 29A). Furthermore, in MEFs stably expressing full-length and mutant HA-tagged NEMO, LMP1 co-immunoprecipitated with WT NEMO as well as the mutants aa1-372 and Δ133-224 (Figure 29B). These results indicate that LMP1 and NEMO can interact. However, the yield of the immunoprecipitations is very low and since co-IPs do not address whether the observed association between two proteins is direct or indirect, NEMO and LMP1 could be components of a larger multiprotein framework without direct interaction.

A

B
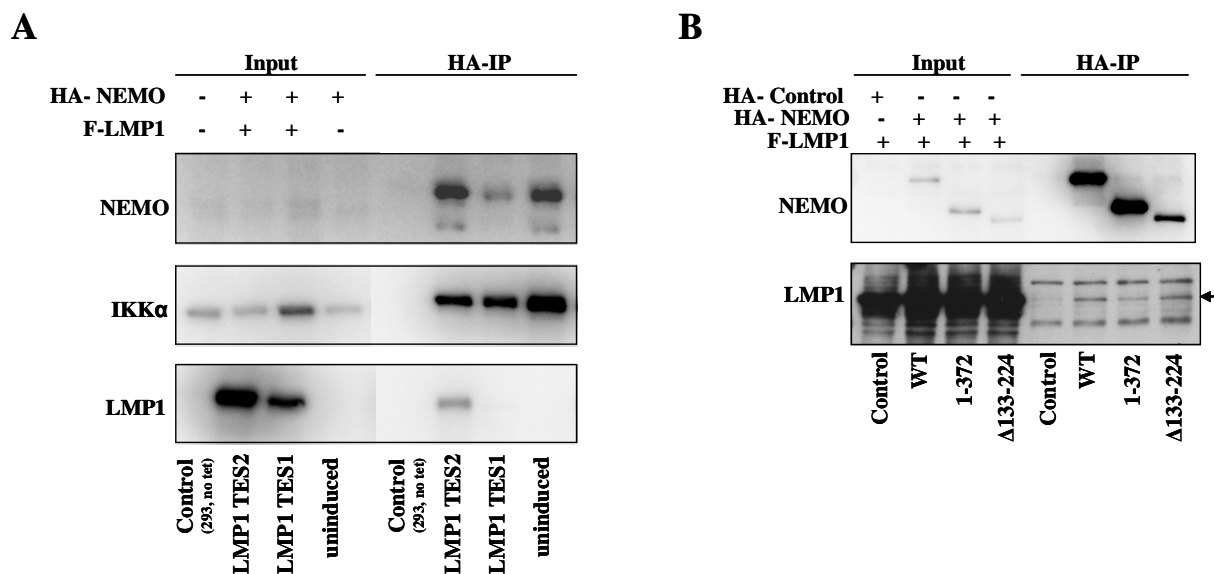
Figure 29. **Characterization of the association between LMP1 and WT and mutant NEMO proteins by Co-IP.** (A) HEK293 cells stably expressing full-length HA-NEMO, and containing a stably integrated LMP1 TES2 locus under the control of a Tet system, were induced with 4-HT and doxycyclin for 16 h (lane 2 and 6). In parallel, the same cell line was transfected with LMP1 TES1 (lane 3 and 7). Uninduced HEK293 cells (lane 4 and 8) and HEK293 cells without Tet-system (lane 1 and 5) were used as controls. 24h after transfection, cell lysates were subjected to IP with HA-probe (F-7) AC, followed by IB with rabbit polyclonal anti-NEMO, mouse monoclonal anti IKKα, and mouse monoclonal anti-LMP1 antibodies. (B) NEMO$^{-/-}$ MEFs stably expressing FLAG-HA-tagged WT or mutant NEMO were transfected with F-LMP1-TES2. 48h after transfection, cell lysates were subjected to IP with HA-probe (F-7) AC, followed by IB with rabbit polyclonal anti-NEMO, and mouse monoclonal anti-LMP1 antibodies. The arrow indicates immunoprecipitated LMP1.

3.8 TRAF6 is required for LMP1-mediated NF-κB activation in mutant Jurkat cell lines.

The E3 ubiquitin-ligase TRAF6 is a well known activator of NF-κB. It promotes K63-polyubiquitination of many proteins, including itself (65), and creates a number of docking sites that are in a yet unknown mechanism are important for IKK activation. It has been demonstrated that, in response to upstream triggers, TRAF6 links polyubiquitin chains to specific NEMO lysine residues (319,320). Furthermore, TRAF6 has been shown to be essential for LMP1 mediated NF-κB activation in mouse embryonic fibroblasts (238,317).

To determine whether TRAF6 is required for LMP1 mediated NF-κB activation in the two Jurkat cell lines expressing mutant NEMO, four siRNAs targeting TRAF6 were utilized. LMP1 or LMP1 TES2 was co-transfected with siRNA and a NF-κB luciferase reporter. SiRNA-mediated silencing of TRAF6 interfered with LMP1 and LMP1 TES2-induced NF-κB activation in both mutant NEMO Jurkat cell lines (Fig. 30A/B, lanes 2 and 3), indicating that TRAF6 is required for LMP1 mediated NF-κB signaling in A45 and 2C NEMO mutant Jurkat cells. Immunoblot analysis for the efficiency of the knockdown showed an approximately 80% reduction of TRAF6.

To confirm the published interaction of TRAF6 with NEMO and to investigate, if the mutant NEMO isolated from A45 and 2C Jurkat cells also interact directly with NEMO, I performed co-immunoprecipitation experiments. In HEK293 cells, transiently transfected with plasmids expressing HA-tagged NEMO and Flag-tagged TRAF6, I found that TRAF6 co-immunoprecipitated with full-length NEMO as well as both NEMO mutants 1-372 and Δ133-224 (Fig. 30D), suggesting that TRAF6 can directly interact with full-length, 1-372, and Δ133-224 mutant NEMO.
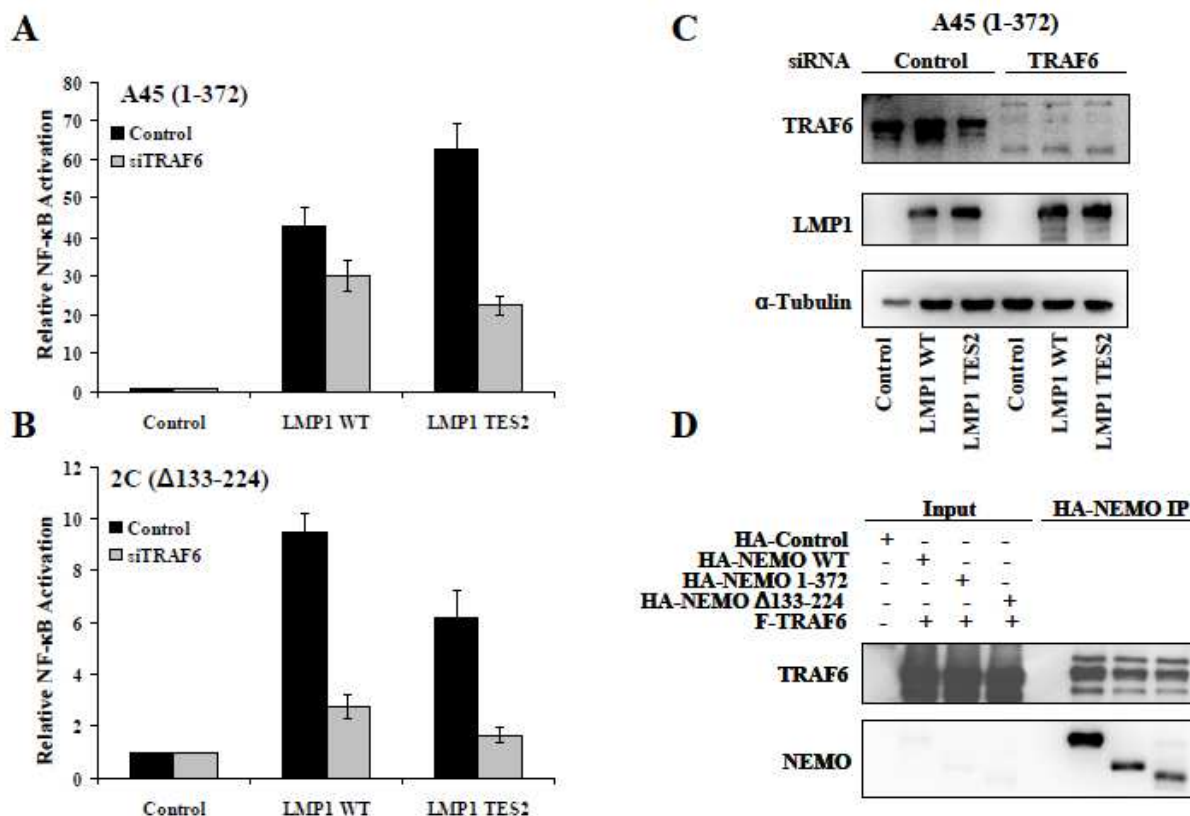
Figure 30. TRAF6 is required for LMP1-mediated NF-κB activation. (A) aa1-372 and (B) Δ133-224 NEMO mutant Jurkat cells were transfected with non-targeting siRNA (control) or siRNA specific to TRAF6, reporter plasmids and empty vector, LMP1 WT or LMP1 TES2 only plasmids. 72h after transfection, cells were lysed, and the amount of luciferase activity was detected. The mean +/- SD of folds of NF-κB activation by LMP1 from three experiments is shown. (C) A total of 25μg of lysates prepared from whole cell extracts were immunoblotted with anti-NEMO, anti-LMP1, and anti-α-Tubulin. (D) **Characterization of the association between TRAF6 and WT and mutant NEMO proteins by Co-IP in MEFs.** NEMO$^{-/-}$ MEFs stably expressing FLAG-HA-tagged full-length or mutant NEMO were transfected with F-hTRAF6. 48h after transfection, cell lysates were subjected to IP with HA-probe (F-7) AC, followed by IB with rabbit polyclonal anti-NEMO, and rabbit polyclonal anti-TRAF6 antibodies.

The reporter assays in A45 and 2C mutant NEMO cell lines and functional complementation assays in MEFs suggested that amino acids 373-419 or a region encompassing amino acids 133-224 are dispensable for LMP1 mediated NF-κB activation. However, the double mutant 1-372/ Δ133-224 could not restore LMP1 mediated NF-κB activation indicating that these two regions likely have a redundant function for LMP1 signaling.

In order to better understand physiological interactions and to identify interacting proteins, I created fusion proteins of glutathione *S*-transferase (GST) and the NEMO regions aa133-224 and aa373-419 (Fig. 31). Unfortunately, because of the limited time I had available to complete this project, I was unable to perform pull-down experiments with these GST fusion proteins. It remains to be seen if these two regions of NEMO after LMP1 induction specifically bind or interact with as yet unknown or not in LMP1 signaling implicated proteins.
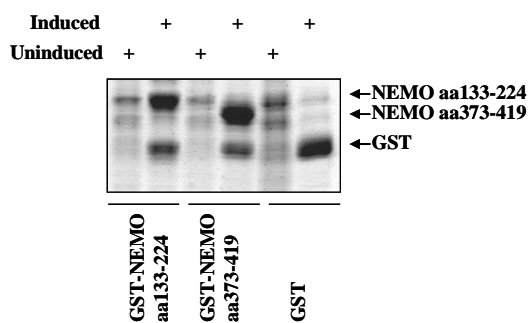
Figure 31. NEMO aa133-224 (lanes 1 and 2) and NEMO aa373-419 (lanes 3 and 4)
were expressed as soluble GST fusions from pGEX-KG in E.coli BL21 (DE3).

In a different approach to identify previously unknown interactions of NEMO involved in LMP1 TES2 mediated NF-κB activation, we employed the HEK293 cell line, containing a stably integrated LMP1 TES2 locus under the control of a Tet system, and stably expressing His-HA-tagged NEMO at levels similar to endogenous. From cells expressing LMP1 TES2 and control cells (without LMP1 induction), NEMO was purified with anti-HA antibody-coupled resin, and trypsinized complexes were subjected directly to mass spectrometry (LC-MS/MS) in duplicate (Experimental procedure: Sowa, Bennet 2007; Ref. 333), to create a database of NEMO-associated proteins in the presence or absence of LMP1 induction. The data sets were analysed using a software platform called Comparative Proteomic Analysis Software Suite (*CompPASS)* (333), which employs a methodology for the identification of high-confidence candidate interacting proteins (HCIPs). To identify bona fide interactors, two scoring metrics were used: the D^N-score and the Z-score. The Z-score is used to analyse proteins that are present in multiple immune complexes but are found at much higher levels in a subset of these, while the D-score incorporates the uniqueness, the abundance of the interactor, and the reproducibility of the interaction within each IP. All raw D-scores are normalized to a global D-score threshold (D^T), producing D^N-scores (333). Interactors in each IP with a D^N-score of ≥ 20 are considered HCIPs.

Out of about 300 identified proteins in our NEMO data set, only 11 were found to be HCIPs. Four of them are know to be NEMO associated proteins, and include NEMO itself, IKKα (*CHUK*), IKKβ (*IKBKB*), and CDC37 (Fig. 32, and Tab. 13). The remaining 7 proteins were identified in either one or the other IP from LMP1 TES2 induced cells, but never in both. It is encouraging to identify proteins that are expected to be HCIPs of NEMO. However, more known interactors are missing, indicating deficiencies in the experimental procedure. With optimized conditions one should be able to obtain a data set containing (in duplicate IPs) all the expected interactors and previously unidentified proteins.
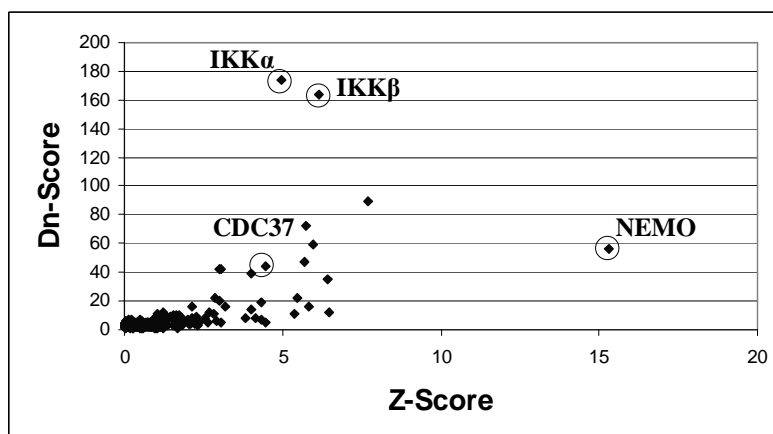
Figure 32. NEMO binding proteins identified using mass spectrometry analysis. Plot of the D^N score versus Z score for proteins identified in the NEMO IP-MS/MS data set. Known associated proteins are marked with a circle.

Z-score	D^n-score	Gene ID	Description
4,97	173,94	CHUK	conserved helix-loop-helix ubiquitous kinase- (Inhibitor of nuclear factor kappa-B kinase subunit alpha)
5,51	155,13	IKBKB	inhibitor of kappa light polypeptide gene enhancer in B-cells, kinase beta- (Inhibitor of nuclear factor kappa-B kinase subunit beta)
10,79	118	NUMA1	nuclear mitotic apparatus protein 1-(Isoform 2 of Nuclear mitotic apparatus protein 1)
10,79	118	MAP4	microtubule-associated protein 4-(Isoform 2 of Microtubule-associated protein 4)
10,79	118	ISOC1	isochorismatase domain containing 1-(Isochorismatase domain-containing protein 1)
4,1	81,75	USP16	ubiquitin specific peptidase 16-(Ubiquitin carboxyl-terminal hydrolase 16)
15,29	56,44	IKBKG	inhibitor of kappa light polypeptide gene enhancer in B-cells, kinase gamma- (NF-kappa-B essential modulator)
6,78	54,46	CDC37	cell division cycle 37 homolog (S. cerevisiae)-(Hsp90 co-chaperone Cdc37)
6,46	47,68	IARS	isoleucyl-tRNA synthetase---(IARS protein)
2,56	19,67	PDXK	pyridoxal (pyridoxine, vitamin B6) kinase-(Isoform 1 of Pyridoxal kinase)
2,48	19,67	KCNH2	potassium voltage-gated channel, subfamily H (eag-related), member 2- (Isoform 1 of Potassium voltage-gated channel subfamily H member 2)

Table 13. NEMO binding proteins identified using mass spectrometry analysis. A total of 11 NEMO binding proteins were identified, with 4 know to have NEMO binding activity from previous work, and the remaining 7 being novel interactors.

3.9 LMP1 induces K63-linked ubiquitination of NEMO.

Beyond our efforts to identify new interactors implicated in LMP1 signaling, we started to investigate if LMP1 is capable to induce specific modification on NEMO that are important in NF-κB signaling. Recent studies have shown that ubiquitination of signaling proteins through K63-linked ubiquitin chains plays an important role in the activation of the NF-κB cascade (65,181). Furthermore, it was demonstrated that NEMO specifically binds K63-linked ubiquitin chains, and that it also becomes ubiquitinated following NF-κB activation (101,319,390). Moreover, the TRAF6 E3 ligase is essential for LMP1 mediated NF-κB activation, which suggests an important role for K63-linked ubiquitin in LMP1 signaling.

To investigate if LMP1 induces K63-linked ubiquitination of NEMO, I employed a HEK293 cell line, containing a stably integrated LMP1 TES2 locus under the control of a Tet system, and stably expressing His-NEMO at levels similar to endogenous. I transfected a HA-tagged K63 only ubiquitin expression plasmid and performed immunopecipitations of NEMO from cells with or without LMP1 induction. I found that expression of LMP1 TES2 induces K63-linked ubiquitination of full-length NEMO (Fig. 33, lane 4).
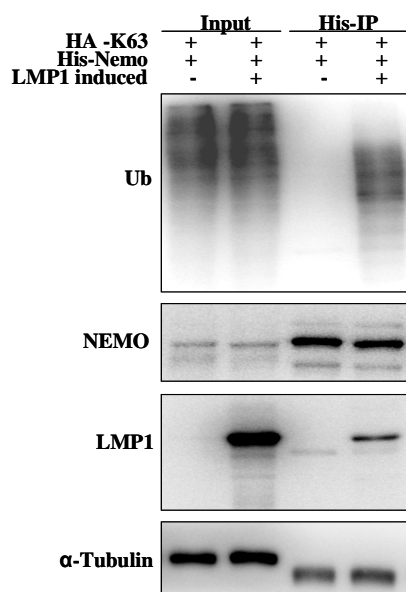
Figure 33. LMP1 induces K63-linked ubiquitination of NEMO. HEK293 cells stably expressing His-NEMO, and containing a stably integrated LMP1 TES2 locus under the control of a Tet system, were transfected with an expression vector containing HA-tagged K63-Ubiquitin (Ub). 8h after transfection, cells were induced with 4-HT and doxycyclin (lane 2 and 4). Uninduced 293 cells (lane 1 and 3) were used as control. 16h after LMP1 TES2 induction, cell lysates were subjected to His-IP with Ni-NTA Agarose. Immunoprecipitated extracts were analyzed for LMP1TES2 mediated K63-linked polyubiquitination of NEMO by western blot with anti-Ub, anti-NEMO, anti-LMP1, and anti-α-Tubulin antibodies.

3.10 Abin-1 inhibits LMP1 mediated NF-κB activation.

In a genomewide siRNA screen for enhancers and suppressors of NF-κB activation by LMP1 TES2 (carried out by Ben Gewurz from our laboratory), Abin-1 was identified as negative regulator. Knockdown of Abin-1 enhances NF-κB activation by LMP1 TES2.

Abin-1 (**A**20 **b**inding **i**nhibitor of **N**F-κB) is a 71kDa protein that physically links A20, a K63-specific deubiquitinase (DUB), which negatively regulates the NF-κB pathway, to NEMO and facilitates A20-mediated de-ubiquitination of NEMO, thus resulting in inhibition of NF-κB (251,277). It is, however, unclear whether Abins act as competitors, or whether they recruit other negative regulators to the IKK complex. Recently published data indicate that the region between amino acids 50-100 of NEMO is required for interaction with Abin-1.

The identification of Abin-1 as negative regulator and the known interaction between Abin-1 and NEMO led us to investigate how Abin-1 was involved in LMP1 mediated signaling. To this aim, I performed NF-κB reporter assays by transfecting HEK293 cells with κB-luciferase and β-galactosidase plasmids in the presence or absence of Abin-1 and various activators of NF-κB. Consistent with previously published data, overexpression of Abin-1 inhibited TNFα- and Tax-mediated activation of NF-κB. Furthermore, Abin-1 also diminished NF-κB activation induced by LMP1 (Fig.34). These results indicate that Abin-1 interferes with activation of NF-κB induced by LMP1 and LMP1 TES2.
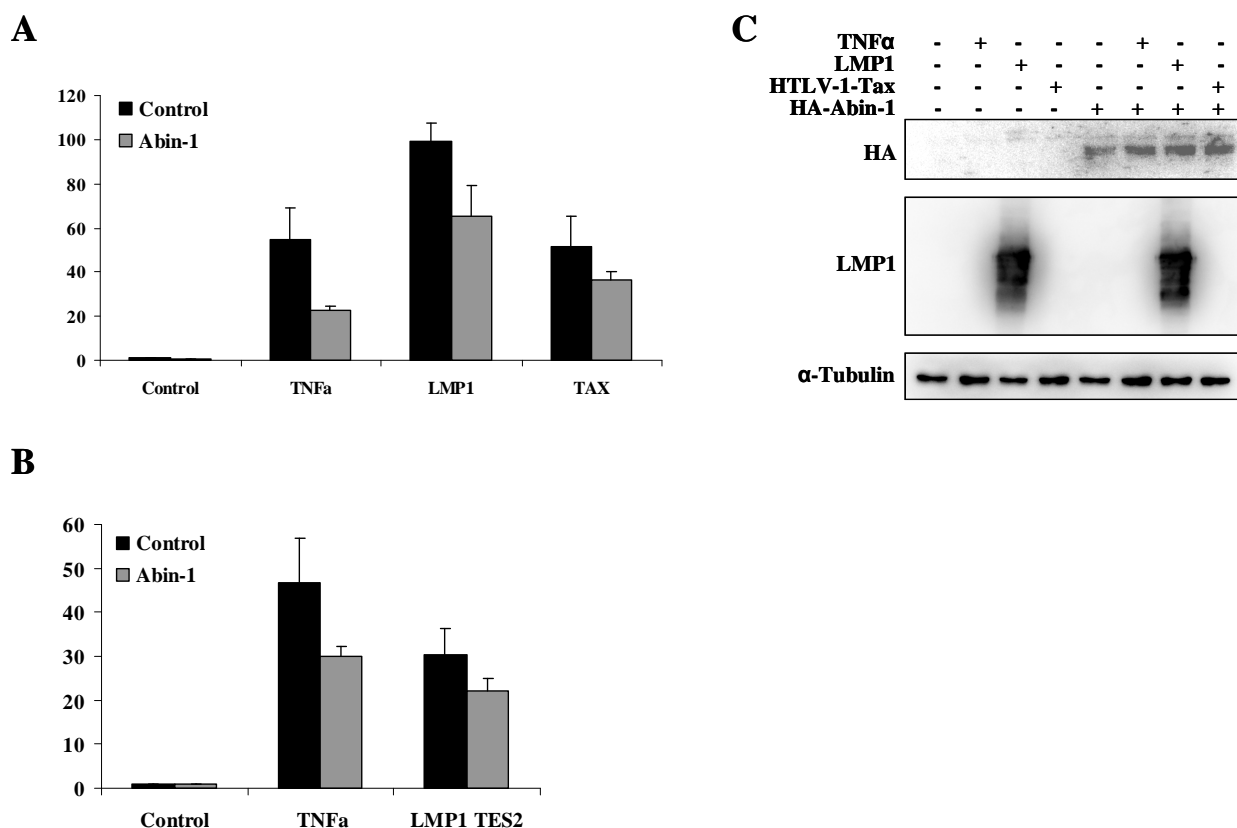
Figure 34. Abin-1 inhibits LMP1 mediated NF-κB activation. HEK293 cells were transfected with both a κB-luciferase reporter construct and a control β-galactosidase plasmid, empty vector and (A) LMP1 and Tax expression plasmids, or (B) a LMP1 TES2 only expression plasmid. Some empty vector transfected cells were treated with 10ng TNFα for 18h. 48h after transfection, cells were lysed and the amount of luciferase activity was detected. The mean +/- SD of folds of NF-κB activation is shown. (C) A total of 25μg of lysates prepared from whole cell extracts were immunoblotted with anti-HA, anti-LMP1, and anti-α-Tubulin

4. DISCUSSION

Various mammalian cell viruses, including EBV, exert their cytotoxic effects by interfering with the function of specific host factors and associated cellular signaling pathways. Therefore, elucidation of the molecular mechanisms by which viral proteins engage specific host factors and modulate cellular signaling pathways is the key to the understanding of virus-associated diseases.

As reviewed in the introduction, EBV is associated with a number of human malignancies, including lymphoproliferative diseases in immune-compromised people (LPD), Burkitt's lymphoma (BL), nasopharyngeal carcinoma (NPC), and Hodgkin's disease (HD) (208). *In vivo*, EBV infects epithelial and B cells. In lymphocytes, EBV establishes a latent infection. The four recognized forms of latency are characterized by the expression of different EBV-encoded proteins. Among these proteins, LMP1 is the only one known to be indispensable for EBV-mediated B cell transformation (201). LMP1 is commonly expressed in above mentioned malignancies. It exerts its functions mainly through two subdomains in its cytoplasmic carboxyl tail: TES1 and TES2. By interaction with specific cellular factors, LMP1 TES1 and TES2 activate various signaling pathways, including JNK, p38, and NF-κB.

The dimeric transcription factor NF-κB plays multiple roles in diverse biological processes, including development, stress responses, cell growth and death, carcinogenesis, and is a major regulator of innate and adaptive immunity and inflammatory responses (197). The IKK complex, which consists of IKKα, IKKβ, and NEMO, has been suggested to be the critical component for canonical NF-κB activation. Although devoid of catalytic activity, the regulatory subunit of the IKK complex, NEMO, plays an important role in activation of NF-κB. The N-terminus of NEMO is required both for the binding of IKKα and IKKβ and their assembly into a complex essential for NF-κB activation (252,300). Current thinking is that NEMO functions as a scaffold protein by adapting various upstream NF-κB-activating signals into the IKK complex. However, how NEMO is contacted by and integrates various signals remains incompletely elucidated.

LMP1 strongly activates NF-κB. Mutations in LMP1, that affect NF-κB activation, are defective for outgrowth of lymphoblastoid cell lines (LCL), and interruption of NF-κB activation causes LCL apoptosis, indicating that LMP1 is critical for NF-κB activation in EBV infected lymphocytes (54,55). Accordingly, the prevention or treatment of EBV associated LPD and HD in immune-compromised people would be greatly benefit from inhibition of LMP1 mediated NF-κB activation. However, global NF-κB inhibitory approaches may be counterproductive, since such treatments could abrogate NF-κB's oncogenic potential but affect other NF-κB activities used for normal cellular proliferation, immunity, or for protecting healthy cells from TNFα induced killing. Therefore, interdiction against one NF-κB activity, while preserving others, would be highly desirable. Such an interruption could be achieved, if structure/ function of components of the NF-κB pathway, such as NEMO, could be dissected in a manner that segregates oncogenic stimuli from proinflammatory cytokine activation.

The experiments reported here investigate the role of NEMO in LMP1 mediated NF-κB activation. Previously published data from our lab reported, that LMP1 mediated NF-κB activation can be NEMO independent while it is dependent of IKKβ (238,239). However, this study demonstrates that this assumption was incorrect. We now find that NEMO is essential for LMP1 TES2 mediated NF-κB activation. Beyond that, we identified two different NEMO mutations that uniquely support LMP1 TES2 dependent NF-κB activation, whereas they can not support TNFα, Tax, TPA or CD40-mediated NF-κB activation.

Using a mouse and a rat cell line deficient for NEMO, I showed that LMP1 mediated NF-κB activation is abolished in the absence of NEMO. These findings were confirmed by a different experiment utilizing siRNA

targeting NEMO in a human cell line. One explanation for the different results obtained by Luftig *et al.* (238,239) lies in the Jurkat cell line A45 they used for their experiments. As I showed in this study, this A45 cell line expresses a mutant NEMO protein that uniquely supports LMP1 mediated NF-κB activation. It does not support TNFα mediated NF-κB activation as tested by Luftig *et al.* (239). Furthermore, the mutant NEMO protein expressed in A45 Jurkat cells was only detectable by one antibody which was only recently made available.

The different results obtained by Luftig *et al.* in mouse embryonic fibroblasts (MEF) are more difficult to explain. The NEMO knockout MEF cell line used by Luftig *et al.* (provided by M. Pasparakis, 316) was made by homologous recombination and has been demonstrated several times to be defective for NF-κB activation by various stimuli, including TPA, LPS, IL-1β, and TNFα. However, when I started working with this cell line, I noticed that these MEFs activated NF-κB in response to TNFα, suggesting that the NEMO KO cell line may have been switched or contaminated with the WT. As mentioned above, at that time it was difficult to detect NEMO by western blot (even the full-length protein) with the available antibodies.

However, utilizing different other NEMO KO cell lines, I was able to show that NEMO is essential for LMP1 mediated NF-κB activation. Beyond that, I identified in two different Jurkat cell lines, A45 and 2C, two different mutations in NEMO that uniquely support LMP1 dependent NF-κB activation.

The first mutation 1-372, identified in A45 Jurkat cells, generates a truncated NEMO protein which lacks the putative zink finger located at the C-terminus. While NF-κB activation by various stimuli including TNFα, TPA, and Tax is significantly decreased or abolished by removal of the zink finger, it is at wild type levels by induction with LMP1. Moreover, NF-κB activation by LMP1 TES2 was slightly hyperactive in A45 cells which could be explained by the missing interaction of NEMO with CYLD. The tumor suppressor CYLD, which has been proposed as a negative regulator of NEMO, is a deubiquitinating enzyme (DUB) capable of cleaving linear and K63-linked ubiquitin chains (216). It contains binding sites for TRAF2 and has been shown to interact with NEMO residues aa388-393 located within the zink finger (307). Suppression of CYLD expression by RNA interference causes an increase in the activity of NF-κB which is attributed to defective removal of K63-linked ubiquitin chains from TRAF2 and NEMO by CYLD (217). In a mechanistically analogous manner, CYLD was found to inhibit signaling from Toll-like receptor 2 by removing K63-linked ubiquitin from TRAF6 (405). The missing interaction of NEMO and CYLD may be a reason why LMP1 is capable to support NF-κB activation in A45 Jurkat cells. However, it cannot explain why other stimuli failed to activate NF-κB. It has been shown that siRNA-mediated silencing of CYLD results in elevated NF-κB activity after TNFα induction (174), suggesting that other or additional interactions, modification, or mechanisms contribute in a stimulus dependent manner to signaling via the NEMO zink finger.

The analysis of the NEMO mutation 1-372 also indicates that the zink finger is neither required for binding to IKKα or IKKβ, nor for activation of the IKK complex after LMP1 induction, as mutant NEMO 1-372 is still incorporated in the IKK complex (Fig.18C) and mediates the activation of IκBα (Fig.23C). However, a number of studies demonstrated that deletions or mutations of the zink finger of NEMO are associated with severe pathologies in humans, and strongly interfere with its ability to activate NF-κB by various stimuli (15,126,150, 188,224,348,353,418). Recently, Cordier *et al.* showed that the M415S mutation, which prevents binding of NEMO to ubiquitin, severely impairs NF-κB activation by TNFα (76). Further, a mutation associated with severe IP pathology, M407V, also interferes with binding of the zink finger to ubiquitin and activation of NF-κB by TNFα. (77,328). These findings and several other studies suggest that binding to ubiquitin is an important function of the zink finger (222,353). Beyond that, Laplantine *et al.* and Cordier *et al.* demonstrated that the NEMO zink finger is capable to bind K48-, K63-linked and linear polyubiquitin chains (with similar affinity). Importantly, they demonstrated that NEMO

specific high-affinity binding to K63-linked polyubiquitin chains requires both the UBAN domain and the C-terminal zink finger, whereas the zink finger is not necessary for binding to linear polyubiquitin chains (77,222). Together, these findings and the data presented here suggest, that for LMP1 mediated NF-κB activation NEMO binding to K63-linked polyubiquitin chains is not required.

The second mutation Δ133-224, identified in 2C Jurkat cells, generates a truncated NEMO protein which has an internal deletion within coiled coil (CC) 1 and the region between CC1 and CC2. The mutated protein lacks, among others, the binding site for RIP. The finding that LMP1 induces NF-κB activation in Δ133-224 mutant NEMO Jurkat cells supports a previous study that showed that RIP is dispensable for LMP1 mediated NF-κB activation (185). However, this mutant is only partially active. The reduction in LMP1 induced NF-κB activation exceeds 50%, suggesting that a part of, or the entire missing region makes an important, although not essential, contribution to LMP1 signaling. On the other hand, the mutant could possibly be misfolded or misdistributed intracellularly. All mutants expressed robustly in HEK293 cells and MEFs when assayed by western blot, indicating that intracellular synthesis was intact. However, when I visualized stably expressed NEMO Δ133-224 in MEFs by immunofluorescence, it more than any other mutant that I surveyed, formed unusual cytoplasmic aggregates (Fig.26). This particular presentation could explain why this mutant is capable to support LMP1 mediated NF-κB activation. Three different recent studies suggested that some amount of NEMO may constitutively exist as oligomers without requiring stimulus induction (177,300,289). By contrast, partially active NEMO mutants such as Δ134-223 may be constitutively oligomerization inefficient, but could be driven to oligomerize by the appropriate stimuli such as LMP1. However, the double mutant 1-372/ Δ133-224 also forms, although to a lesser extend, cytoplasmic aggregates, but failed to reconstitute LMP1 mediated NF-κB activation.

The reconstitution assay further confirmed the findings in the A45 and 2C NEMO mutant Jurkat cell lines. While the mutants 1-372 and Δ133-224 supported LMP1 mediated NF-κB activation, neither 1-372, Δ133-224, nor the double mutant 1-372/ Δ133-224 supported TNFα mediated NF-κB activation. Collectively, these findings suggests that the zink finger and the region aa133-224 likely have a redundant function for LMP1 signaling, whereas both are essential for TNFα mediated NF-κB activation

Several other findings of the present study highlight the importance of the ubiquitin binding domain of NEMO. In the reconstitution assay, I found that C-terminal truncation of the leucine zipper (LZ) and the Ubiquitin binding domain (UBAN) between amino acids 303 and 372 abrogated the ability of NEMO to restore TNFα, Tax, or LMP1 mediated NF-κB activation, indicating that ubiquitin modifications within the ubiquitin binding domain and/ or the ability of NEMO to recognize ubiquitin chains, are essential for activation of NF-κB by all stimuli tested. These results are consistent with those of previous reports describing mutations of NEMO in this region which have been shown to impair NF-κB activation by various stimuli and cause serious X-linked diseases. The mutations L322P, L326P, L329P, and L336P within the leucine zipper have been shown to severely affect NF-κB activation induced by TNFα and IL-1 (244). The E315A and R319Q mutations were identified as immunodeficiency against mycobacterial infections and severely affect IL-12 production (117). The anhidrotic ectodermal dysplasia with immunodeficiency (EDA-ID) causing mutations A288G, D311N, and A323P result in impaired NF-κB activation in response to TNFα, IL-1, LPS, and serum-lysophosphatidic acid (LPA) (78,320).

The molecular analysis of the A323P mutation, which results in impaired polyubiquitination of NEMO and NF-κB activation, has allowed the identification of three lysine residues K314, K318, and K319, which are required for TRAF6 dependent NEMO polyubiquitylation in response to IL-1, LPS, and LPA-induced NF-κB activation (320). Utilizing siRNA, I found that TRAF6 is required for LMP1 mediated NF-κB activation in WT and the two NEMO

mutant Jurkat cell lines. These results support and extend previous studies demonstrating that LMP1 mediated NF-κB activation is defective in TRAF6$^{-/-}$ cells (238,389). Furthermore, I found that TRAF6 co-immunoprecipitated with full-length NEMO as well as and both NEMO mutants 1-372 and Δ133-224 (Fig. 30D), suggesting that TRAF6 can directly interact with full-length, 1-372, and Δ133-224 mutant NEMO. As reviewed in the introduction, TRAF6 is an E3 ubiquitin-ligase that, together with an E2 complex composed of Ubc13 and Uev1A, promotes K63-poly-ubiquitination of many proteins (89). Furthermore, siRNA-mediated silencing of Ubc13 results in defective TNFα mediated NF-κB activation in insect cells and HEK293T cells, indicating the importance of K63-linked polyubiquitin chains in NF-κB activation (12,419). However, the role of K63-linked polyubiquitin chains in NF-κB activation has been questioned in several recent studies. The UBAN motif of NEMO, which was suspected to be a K63-binding motif (101,390), shows a substantially higher affinity for linear chains (235,293). Further, in Ubc13 knockout MEFs, the linear ubiquitin chain assembly complex (LUBAC) can still activate NF-κB after TNFα induction, indicating that K63-linked polyubiquitination has a distinct role from LUBAC-mediated linear ubiquitination in TNFα-induced NF-κB activation (357).

Despite the many studies, the different functions of linear and K63-linked polyubiquitin chains in cell signaling are still poorly understood. Recently, a model for activation of signaling by the TNF-R1-associated protein complex (TNF-RSC) has been proposed, whereby TRADD and TRAF2 recruit cIAPs to the TNF-R1 complex. Then, cIAPs ubiquitylate several components in the complex, leading to recruitment of LUBAC which recognizes cIAP generated polyubiquitin chains. LUBAC is thought to attach linear polyubiquitin chains to NEMO which results in recruitment of more NEMO, thereby stabilizing the entire complex and increasing the retention times of NEMO and other signaling components (144).

However, previous data and the experiments reported here, highlight the differences between TNFα and LMP1 in their respective activation of NF-κB. In contrast to TNFα, LMP1 requires TRAF6 for NF-κB activation. This finding, and the experiment, that showed that LMP1 induces K63-linked polyubiquitination of full-length NEMO (Fig.33), suggest that K63-linked polyubiquitin chains have an important role in LMP1 mediated NF-κB activation. The co-immunoprecipitation experiments further suggest that TRAF6 can mediate K63-linked polyubiquitination of NEMO after LMP1 induction, as TRAF6 directly interacts with NEMO. However, this statement is somewhat speculative, since I have not been able to clearly demonstrate, that LMP1 induces K63-linked polyubiquitination of the NEMO mutants 1-372 and Δ133-224, and that the non-functional NEMO double mutant 1-372/ Δ133-224 does not interact with TRAF6. Therefore, the requirement for TRAF6 may be somewhere else in the LMP1-NF-κB pathway. It has been shown that TAB2 and TAB3 bind to K63-linked polyubiquitin chains which are generated by TRAF6 (89), resulting in recruitment of TAK1 to the receptor. Furthermore, the TAK1–TAB2–TAB3 complex has been shown to be an essential component of NF-κB activation (375). Moreover, TAK1 has been show to be critical for LMP1 mediated NF-κB (389).

Collectively, these experiments suggest that TRAF6 mediated K63-linked polyubiquin chains (possibly attached to NEMO) are required for LMP1 mediated NF-κB activation. In contrast or additionally, the reconstitution assay suggests different models: (1) the lack of requirement of the NEMO zink finger suggests that binding to K63-linked polyubiquitin chains is not required for LMP1 mediated NF-κB activation and that binding to linear polyubiquitin chains may be sufficient, or (2) the region aa133-224 interacts with a protein that co-operates with the UBAN domain to mediate recognition and binding to K63-linked polyubiquitin chains similar to the function of the zink finger. Furthermore, in immunoprecipitation experiments, I found that LMP1 co-immunoprecipitated with WT

NEMO as well as the mutants aa1-372 and Δ133-224. However, the yield of the immunopreciptations is very low suggesting that NEMO and LMP1 are likely components of a larger multiprotein framework without direct interaction.

In a separate study, I found that Abin-1 interferes with activation of NF-κB induced by LMP1 and LMP1 TES2. Abin-1 has recently been shown to links A20, a K63-specific deubiquitinase, to NEMO and facilitates A20-mediated de-ubiquitination of NEMO, thus resulting in inhibition of NF-κB (251,277). A different study demonstrated that Abin-1 is a novel K63-linked and linear ubiquitin-sensing protein that inhibits FADD–caspase 8 association in the death inducing signaling complex, and protects cells against TNFα-induced apoptosis (277).

Taken together, these results indicate, that ubiquitin modifications play a major role in NF-κB signaling. Therefore, understanding the different functions of linear and K63-linked ubiquitin chains in cell signaling remains an outstanding issue. Future experiments, including LUBAC (HOIL-1L and HOIP) knockout, or overexpression studies will provide an insight, if linear polyubiquitin chains are required for LMP1 mediated NF-κB activation. Recently, the A323 mutation has been shown to cause a conformational change of the NEMO protein that inhibits site specific SUMO attachment at residues Lys277 and Lys309 to permit NF-κB activation (170). Therefore, it is likely that other modifications within the ubiquitin binding domain of NEMO play an important role in LMP1 mediated NF-κB signaling. GST-pulldown experiments and immunoprecipitations followed by mass spectrometry will identify new interactors of NEMO that are important for LMP1 signaling. The results, obtained from the experiments reported here, provide some clues to the function of NEMO in LMP1 mediated NF-κB activation. However, a more detailed analysis is still necessary.

5. SUMMARY

Epstein-Barr virus (EBV) is an oncogenic herpes virus that causes human disease including Hodgkin's disease (HD), and Naso-Pharyngeal Carcinoma (NPC). Latent infection integral membrane protein 1 (LMP1), commonly expressed in these malignancies, mimics a constitutively active TNF receptor (TNFR). LMP1 has two C-terminal cytosolic domains, transformation effector sites (TES)1 and -2, that engage TNFR-associated death domain proteins (TRADD and RIP) and TNFR-associated factors (TRAFs), which interact with signaling molecules that mediate activation of several signaling pathways including JNK, p38, and NF-κB.

The transcription factor NF-κB regulates expression of numerous genes controlling immune and stress responses, cellular proliferation, inflammatory reactions, and protection against apoptosis. Dysregulated NF-κB activation results in aberrant expression of its target genes. Therefore, constitutively active NF-κB has been implicated in various lymphoid malignancies. NF-κB activation relies on the IκB kinase (IKK) complex which is composed of IKKα, IKKβ, and the regulatory subunit NEMO. NEMO has been proposed as a universal adaptor of the IKK complex for various stimuli such as TNFα, IL-1, HTLV-1 Tax, and KSHV v-FLIP.

This study demonstrates that NEMO is essential for LMP1 TES2 mediated NF-κB activation. Beyond that, we identified two NEMO mutations that uniquely support LMP1 dependent NF-κB activation, whereas they can not support TNFα, Tax, TPA or CD40-mediated NF-κB activation. The first mutation 1-372, isolated from A45 Jurkat cells, generates a truncated NEMO protein which lacks the putative zink finger located at the C-terminus. The second mutation Δ133-224, isolated from 2C Jurkat cells, generates a truncated NEMO protein which has an internal deletion. Reconstitution experiments in NEMO knockout mouse embryonic fibroblasts, stably expressing full-length or mutant NEMO, indicate that the NEMO zink finger and the region aa133-224 are dispensable for LMP1 mediated NF-κB activation, but are required for TNFα mediated NF-κB activation. The double mutant 1-372/ Δ133-224 failed to reconstitute LMP1 mediated NF-κB activation, suggesting that the zink finger and the region aa133-224 likely have a redundant function for LMP1 signaling, whereas both are essential for TNFα mediated NF-κB activation.

C-terminal truncation of the leucine zipper (LZ) and the Ubiquitin binding domain (UBAN) between amino acids 303 and 372 abrogated the ability of NEMO to restore TNFα, Tax, or LMP1 mediated NF-κB activation, indicating that ubiquitin modifications within the ubiquitin binding domain and/ or the ability of NEMO to recognize ubiquitin chains, are essential for activation of NF-κB by all stimuli tested.

In siRNA experiments, TRAF6 was found to be required for LMP1 mediated NF-κB activation in wildtype, and the two mutant NEMO Jurkat cell lines, A45 and 2C. Furthermore, TRAF6 co-immunoprecipitated with full-length NEMO as well as and both NEMO mutants 1-372 and Δ133-224.

Collectively, these experiments suggest that, in contrast to TNFα, TRAF6 mediated K63-linked polyubiquin chains (possibly attached to NEMO) are required for LMP1 mediated NF-κB activation. Additionally, the reconstitution assay suggests different models: (1) the lack of requirement of the NEMO zink finger indicates that binding to K63-linked polyubiquitin chains is not required for LMP1 mediated NF-κB activation and that binding to linear polyubiquitin chains may be sufficient, or (2) the region aa133-224 interacts with a protein that co-operates with the UBAN domain to mediate recognition and binding to K63-linked polyubiquitin chains similar to the function of the zink finger.

6. ZUSAMMENFASSUNG

Epstein-Barr virus (EBV) ist ein krebserregendes Herpes Virus, daß Krankheiten im Menschen, einschließlich Hodgkin's disease (HD) und Naso-Pharyngeal Carcinoma (NPC), auslöst. Das „latent infection integral membrane protein 1" (LMP1), welches in all diesen Krankheiten exprimiert ist, ahmt einen Tumor Necrose Faktor (TNF)-Rezeptor nach, der permanent aktiv ist. An seinem Carboxylende hat LMP1 zwei wichtige Domänen, TES1 und -2, welche mit verschieden Proteinen, wie zum Beispiel TNFR-assoziierten Todes Domäne Proteinen (TRADD und RIP) und TNFR-assoziierten Faktoren (TRAFs), interagieren und auf diese Weise mehrere intrazelluläre Signalwege aktivieren, einschließlich JNK, p38, und NF-κB.

Der Transkriptions Faktor NF-κB reguliert die Expression zahlreicher Gene die unter anderem wichtige Funktionen in der Regulierung von Immunität, Zellteilung, Entzündungsprozessen und dem Schutz vor programmiertem Zelltod haben. Fehlgesteuerte Aktivierung von NF-κB führt zu übermäßiger Expression von Zielgenen. Übermäßige Aktivierung von NF-κB steht in Zusammenhang mit mehreren Krankheiten des Lymphsystems (Leukemien). Wichtig für die Aktivierung von NF-κB ist der IκB Kinase (IKK) Komplex, der sich aus den zwei Kinasen IKKα und IKKβ, sowie der regulatorischen Untereinheit NEMO zusammensetzt. Nach derzeitigem Model funktioniert NEMO als ein universeller Adapter, der verschiedene NF-κB aktivierende Signale, einschließlich TNFα, IL-1, HTLV-1 Tax und KSHV v-FLIP in den IKK Komplex integriert.

Diese Arbeit demonstriert, dass NEMO für LMP1 TES2 vermittelte Aktivierung von NF-κB notwendig ist. Weiterhin wurden zwei Mutationen in NEMO identifiziert, welche ausschließlich LMP1 vermittelte Aktivierung von NF-κB bewirken, nicht jedoch TNFα, Tax, TPA oder CD40 vermittelte. Die erste Mutation, 1-372, erzeugt ein verkürztes NEMO Protein, dem der vermeintliche Zinkfinger am Carboxylende fehlt. Die zweite Mutation, Δ133-224, führt zu einem verkürzten Protein dem intern 91 Aminosäuren fehlen. Rekonstruktionsexperimente in NEMO$^{-/-}$ Maus Embryo Fibroblast Zellen offenbaren, dass der NEMO Zinkfinger und die Region aa133-224 für LMP1 vermittelte NF-κB Aktivierung entbehrlich sind, jedoch für TNFα vermittelte NF-κB Aktivierung benötigt werden. Der Doppelmutant, 1-372/ Δ133-224, konnte LMP1 vermittelte NF-κB Aktivierung nicht wiederherstellen, was darauf hinweist, dass der Zinkfinger und die Region aa133-224 möglicherweise eine austauschbare Funktion im LMP1 Signalweg haben, während beide Regionen für TNFα unverzichtbar sind. Die Verkürzung des NEMO Proteins um den Leucine zipper und die Ubiquitin bindungs Domäne (UBAN) zwischen den Aminosäuren 303 und 372, hob die Fähigkeit von NEMO auf, TNFα, Tax, oder LMP1 vermittelte NF-κB Aktivierung wiederherzustellen. Dies weist darauf hin, dass Ubiquitin Modifizierungen an der Ubiquitin bindungs domäne und / oder die Fähigkeit von NEMO, Ubiquitin Modifizierungen zu erkennen, unverzichtbar für alle getesteten Stimuli sind, um NF-κB zu aktivieren.

Weiterhin fanden wir in siRNA Experimenten, dass TRAF6 für LMP1 vermittelte Aktivierung von NF-κB in Wildtyp und den beiden Jurkat Zelllinien notwendig ist. Weiterhin stellten wir fest, dass TRAF6 mit Wildtyp NEMO und den beiden Mutanten 1-372 und Δ133-224 co-immunoprezipitiert. Zusammenfassend, diese Experimente demonstrieren, dass im Gegensatz zu TNFα, von TRAF6 hergestellte (möglicherweise an NEMO angebrachte) K63-verbundene Ubiquitin Ketten für LMP1 vermittelte Aktivierung von NF-κB unverzichtbar sind.

Die Rekonstruktionsexperimente legen 2 Modelle nahe: (1) da der NEMO Zinkfinger entbehrlich ist, ist Erkennung und Bindung an K63-verbundene Ubiquitin Ketten für LMP1 vermittelte NF-κB Aktivierung nicht erforderlich, oder (2) die Region aa133-224 interagiert mit einem Protein, daß mit der UBAN domäne kooperiert und Bindung an K63-verbundene Ubiquitin Ketten vermittelt, ähnlich der Funktion des Zinkfingers.

7. REFERENCES

1   **Abbott DW, Wilkins A, Asara J, Cantley LC.** 2004. The Crohn's disease protein, NOD2, requires RIP2 in order to induce ubiquitinylation of a novel site on NEMO. Curr. Biol. **14**, 2217–2227.

2   **Abbott DW, et al.** 2007. Coordinated regulation of Toll-like receptor and NOD2 signaling by K63-linked polyubiquitin chains. Mol. Cell. Biol. **27**, 6012–6025.

3   **Abbot SD et al.** 1990. Epstein-Barr virus nuclear antigen 2 induces expression of the virus-encoded latent membrane protein. J Virol; **64**(5):2126-2134.

4   **Agou F, Ye F, Goffinont S, Courtois G, Yamaoka S, Israel A, Veron M.** 2002. NEMO trimerizes through its coiled-coil C-terminal domain. Mol. Cell **22**, 245–257.

5   **Agou F, Vinolo E, Courtois G, Yamaoka S, Israel A. and Veron M.** 2004. The trimerization domain of NEMO is composed of the interacting C-terminal CC2 and LZ coiled-coil subdomains. J. Biol. Chem.; **279**:27861–27869.

6   **Alberts B, Johnson A, Lewis J, Raff M, Roberts K, Walter P**. 2003. Molecular Biology of the Cell, fourth edition, Garland Science, New York. **5**: 898-899.

7   **Alfieri C, Joncas JH**. 1987. Biomolecular analysis of a defective nontransforming Epstein-Barr virus (EBV) from a patient with chronic active EBV infection. J. Virol. **10**: 3306-9.

8   **Alfieri C, Birkenbach M, Kieff E.** 1991. Early events in Epstein-Barr virus infection of human B lymphocytes. Virology; **181**(2):595-608.

9   **Allday MJ, Crawford DH**. 1988. Role of epithelium in EBV persistence and pathogenesis of B-cell tumours. Lancet **1**:855-857.

10   **Alwine JC, Kemp DJ, Stark GR.** 1977. Method for detection of specific RNAs in agarose gels by transfer to diazobenzyloxymethyl-paper and hybridization with DNA probes. Proc. Natl. Acad. Sci. U.S.A. **74** (12): 5350–4.

11   **Anagnostopoulos I, Hummel M, Kreschel C, Stein H.** 1995. Morphology, immunophenotype, and distribution of latently and/or productively Epstein-Barr virus-infected cells in acute infectious mononucleosis: implications for the interindividual infection route of Epstein-Barr virus. Blood. **85**:744-750.

12   **Andersen PL, Zhou H, Pastushok L, Moraes T, McKenna S, Ziola B, et al.** 2005. Distinct regulation of Ubc13 functions by the two ubiquitin-conjugating enzyme variants Mms2 and Uev1A. J Cell Biol **170**: 745–755

13   **Ansieau SI, Scheffrahn G, Mosialos H, et al.** 1996. Tumor necrosis factor receptor-associated factor (TRAF)-1, TRAF2, and TRAF3 interact in vivo with the CD30 cytoplasmic domain; TRAF-2 mediates CD30-induced nuclear factor kappa B activation. Proc Natl Acad Sci USA; **93**:14053-8.

14   **Annunziata CM, Davis RE, Demchenko Y, Bellamy W, Gabrea A,** et al. 2007. Frequent engagement of the classical and alternative NF-κB pathways by diverse genetic abnormalities in myeloma. Cancer Cell **12**:115–30.

15   **Aradhya S, Courtois G, Rajkovic A, Lewis RA, Levy M, Israel A, Nelson DL.** 2001. Atypical forms of incontinentia pigmenti in male individuals result from mutations of a cytosine tract in exon 10 of NEMO (IKKgamma). Am J Hum Genet **68**:765–771.

16   **ARC Working Group on the Evaluation of Carcinogenic Risk to Humans.** 1997. Epstein-Barr Virus and Kaposi Sarcoma Herpesvirus/ Human Herpesvirus 8. Lyon, France, International Agency for Research on Cancer.

17   **Arch RH, Gedrich RW, Thompson CB.** 1998. Tumor necrosis factor receptor-associated factors (TRAFs)-a family of adapter proteins that regulates life and death. Genes Dev. **12**:2821-30.

18   **Arvanitakis L, Yaseen N, Sharma S.** 1995. LMP1 induces cyclin D2 expression, pRb hyperphosphorylation, and loss of TGF-beta 1-mediated growth inhibition in EBV-positive B cells. J. Immunol. **155**:1047-56.

19   **Ashida H, Kim M, Schmidt-Supprian M, Ma A, Sasakawa C.** 2010. A bacterial E3 ubiquitin ligase IpaH9.8 targets NEMO to dampen the host NF-kB-mediated inflammatory response. Nature Cell Biol; **12**(1)66-74

20   **Atkinson PG, Coope HJ, Rowe M, Ley SC**. 2003. Latent membrane protein 1 of Epstein-Barr virus stimulates processing of NF-kappa B2 p100 to p52. J. Biol. Chem. **278**:51134-42.

21   **Ausubel, F.M., et al.** 1994-2004. Current Protocols in Molecular Biology, John Wiley & Sons, Inc., Brooklyn, New York, 3.10.1-3.10.2.

22   **Avery O, MacLeod C, McCarty M.** 1944. Studies on the chemical nature of the substance inducing transformation of pneumococcal types: induction of transformation by a desoxyribonucleic acid fraction isolated from pneumococcus type III. J Exp Med. ;79(2):137-158.

23   **Aviel S, Winberg G, Massucci M, Ciechanover A.** 2000. Degradation of the EBV LMP1 by the ubiquitin-proteasome pathway. Targeting via Ubiquitination of the N-terminal residue. J. Biol. Chem. 2000. **275**:23491-9.

24   **Bacchetti S, Graham F.** 1977. Transfer of the gene for thymidine kinase to thymidine kinase-deficient human cells by purified herpes simplex viral DNA. Proc Natl Acad Sci USA **74** (4): 1590–4.

25   **Baer R, et al.** 1984. DNA sequence and expression of the B95-8 EBV genome. Nature; **310** (5974):207-211.

26   **Balfour Jr. HH, Holman CJ, Hokanson KM,** et. al. 2005. A prospective clinical study of Epstein-Barr virus and host interactions during acute infectious mononucleosis. J Infect Dis; **192**: 1505-1512.

27   **Ballestas ME, Chatis PA, Kaye KM.** 1999. Efficient persistence of extrachromosomal KSHV DNA mediated by latency-associated nuclear antigen. Science; **284**(5414):641-644.

28   **Baltimore D.** 1970. RNA-dependent DNA polymerase in RNA tumour viruses. Nature; **226**(5252):1209-11.

29   **Bar RS, Clausen KP, et al.** 1974. Fatal infectious mononucleosis in a family. N Engl J Med; **290**:363-367.

30   **Barbera AJ, et al.** 2006. The nucleosomal surface as a docking station for Kaposi's sarcoma herpesvirus LANA. Science; **311**(5762):856-861.

31   **Barford, D.** 1996. Molecular mechanisms of the serine/threonine phosphatases. Trends Bioch Sci,**21**, 11, pp407.

32   **Basak S, Kim H, Kearns JD, Tergaonkar V, O'Dea E, et al.** 2007. A fourth IκB protein within the NF-κB signaling module. Cell **128**:369–81.

33   **Bbenek K, Kunkel AT.** 1993. "The fidelity of retroviral reverse transcriptases". in Skalka, M. A., Goff, P. S.. Reverse transcriptase. New York: Cold Spring Harbor Laboratory Press. pp. p. 85.

34   **Bernstein E, Caudy A, Hammond S, Hannon G.** 2001. Role for a bidentate ribonuclease in the initiation step of RNA interference. Nature **409** (6818): 363–6.

35   **Bick M, Prinz H.** 2002. "Cesium" in Ullmann's Encyclopedia of Industrial Chemistry, Wiley-VCH, Weinheim.

36   **Bier M.** 1959. Electrophoresis. Theory, Methods and Applications. 3rd ed.. Academic Press. pp. 225. LCC 59-7676.

37   **Birkenbach M, Josefsen K, Lenoir G, Kieff E.** 1993. Epstein-Barr Virus-Induced Genes: First Lymphocyte-Specific G Protein-Coupled Peptide Receptors. Journal of Virology. **67**:2209-2220.

38   **Bishop GA**. 2004. The roles of TRAFs in the regulation of B-cell function. Nat. Rev. Immunol. **4**:775–86.

39   **Bishop GA, Hostager BS.** 2001. Signaling by CD40 and its mimics in B cell activation. Immunol Res; **24**:97-109.

40   **Blonska M, You Y, Geleziunas R, Lin X.** 2004. Restoration of NF-κB activation by tumor necrosis factor α receptor complex-targeted MEKK3 in receptor-interacting protein-deficient cells. Mol. Cell. Biol. **24**:10757–65.

41   **Bloor S, Ryzhakov G, Wagner S, Butler PJ, Smith DL, Krumbach R, et al.** 2008. Signal processing by its coil zipper domain activates IKKγ .Proc. Natl. Acad. Sci. U.S.A. **105**:1279–1284.

42   **Blose SH, Feramisco JR.** 1983. Fluorescent methods in the analysis of cell structure. Cold Spring Harbour Laboratory.

43   **Bonizzi G, Karin M.** 2004. The two NF-κB activation pathways and their role in innate and adaptive immunity. Trends Immunol. **25**:280–88.

44   **Born TL, Miyada CG.** Stained colonies facilitate alignment in a nonradioactive colony hybridization. Bio Technigues 10 (4): 480-481.

45   **Bradford MM.** 1976. A rapid and sensitive method for the quantitation of microgram quantitites of protein utilizing the principle of protein-dye binding. Analytical Biochemistry **72**: 248-254.

46   **Bradley JR, Pober JS.** 2001. Tumor necrosis factor receptor-associated factors (TRAFs). Oncogene **20**:6482–91.

47   **Brockman JA, Scherer DC, McKinsey TA, Hall SM, Qi X, Lee WY, Ballard DW.** 1995. Coupling of a signal response domain in I kappa B alpha to multiple pathways for NF-kappa B activation. Mol Cell Biol. **15**:2809-18.

48   **Brooks LA, Lear AL, Young LS, Rickinson AB.** 1993. Transcripts from the Epstein-Barr Virus BamHI A fragment are detectable in all three forms of virus latency. Journal of Virology. **67**:3182-3190.

49   **Brown KD, Hostager BS, Bishop GA.** 2001. Differential signaling and TRAF degradation by CD40 and the EBV oncoprotein LMP1. J. Exp. Med; **193**:943-954.

50   **Busch LK, Bishop GA.** 1999. The EBV transforming protein, LMP1, mimics and cooperates with CD40 signaling in B lymphocytes. J. Immunol; **162**:2555-2561.

51   **Burnette W N.** 1981. 'Western blotting': electrophoretic transfer of proteins from SDS-polyacrylamide gels to unmodified nitrocellulose and radiographic detection with antibody. Analytical Biochemistry **112** (2): 195–203.

52   **Burkitt D, O'Conor GT.** 1961. Malignant lymphoma in African children. A clinical syndrome. Cancer; **14**:258-269.

53   **Cahir-McFarland ED, Izumi KM, Mosialos G.** 1999. Epstein-barr virus transformation: involvement of latent membrane protein 1-mediated activation of NF-kappaB. Oncogene. **18**:6959-64.

54   **Cahir-McFarland ED, Davidson DM, Schauer SL, Duong J, Kieff E.** 2000. NF-kB inhibition causes spontaneous apoptosis in Epstein-Barr virus-transformed lymphoblastoid cells. Proc Natl Acad Sci U S A. **97**:6055-60.

55   **Cahir-McFarland ED, Carter K, Rosenwald A, Giltnane JM, Henrickson SE, Staudt LM, Kieff E.** 2004. Role of NF-kappa B in cell survival and transcription of latent membrane protein 1-expressing or Epstein-Barr virus latency III-infected cells. J. Virol. **78**:4108-19.

56   **Cai X, et al.** 2006. EBV miRNAs are evolutionarily conserved and differentially expressed. PLoS Pathog; **2**(3):e23.

57   **Cao Z, Xiong J, Takeuchi M, et al.** 1996. TRAF6 is a signal transducer for interleukin-1. Nature **383**:443–46.

58   **Capello D, Rossi D, Gaidano G.** 2005. Post-transplant lymphoproliferative disorders: molecular basis of disease histogenesis and pathogenesis. Hematol Oncol; **23**:61-67.

59   **Carbone A.** 2003. Emerging pathways in the development of AIDS-related lymphomas. Lancet Oncol; **4**:22-29.

60   **Carter RS, Geyer BC, Xie M, Acevedo-Suarez CA, Ballard DW.** 2001. Persistent activation of NF-κ B by the tax transforming protein involves chronic phosphorylation of IκB kinase subunits IKKβ and IKKγ. J. Biol. Chem. **276**:24445–48.

61   **Carter RS, Pennington KN, Ungurait BJ, Ballard DW.** 2003. In vivo identification of inducible phosphoacceptors in the IKKg/NEMO subunit of human I{kappa}B Kinase. J Biol Chem **278**: 19642–19648.

62   **Cesarman E, Chang Y, Moore PS, Said JW, Knowles DM.** 1995. Kaposi's sarcoma-associated herpesvirus-like DNA sequences in AIDS-related body-cavity-based lymphomas. N. Engl. J. Med. **332**:1186–91.

63   **Chan CW, Chiang AK, Chan KH, et al.** 2003. Epstein-Barr virus-associated infectious mononucleosis in Chinese children. Pediatr Infect Dis J; **22**:974-978.

64   **Chen G, Goeddel DV.** 2002. TNF-R1 signaling: a beautiful pathway. Science **296**:1634–35.

65   **Chen ZJ.** 2005. Ubiquitin signaling in the NF-kappaB pathway. Nat. Cell. Biol. **7**:758-65.

66   **Chen Z, Hagler J, Palombella VJ, Melandri F, Scherer D, Ballard D, Maniatis T.** 1995. Signal-induced site-specific phosphorylation targets I kappa B alpha to the ubiquitin-proteasome pathway. Genes Dev. **9**:1586– 1597.

67   **Chen ZJ, Bhoj V, Seth RB.** 2006. Ubiquitin, TAK1 and IKK: is there a connection? Cell Death Dif. **13**, 687–692.

68   **Chen ZJ, Sun LJ.** 2009. Nonproteolytic functions of ubiquitin in cell signaling. Mol Cell **33**: 275–286

69   **Cheung A, Kieff E.** 1982. Long internal direct repeat in EBV DNA. J Virol; **44**(1):286-294.

70   **Chien A, Edgar DB, Trela JM.** 1976. Deoxyribonucleic acid polymerase from the extreme thermophile Thermus aquaticus". J. Bacteriol **174**: 1550–1557.

71   **Chiu YH, Zhao M, Chen ZJ.** 2009. Ubiquitin in NF-.B signaling. Chem Rev **109**: 1549–1560.

72   **Chu ZL, Shin YA, Yang JM, DiDonato JA and Ballard DW.** 1999. J. Biol. Chem., **274**, 15297–15300.

73   **Claudio E, Brown K, Park S, Wang H, Siebenlist U.** 2002. BAFF-induced NEMO-independent processing of NF-κB2 in maturing B cells. Nat. Immunol. **3**:958–65.

74   **Conze DB, Wu CJ, Thomas JA, Landstrom A, Ashwell JD.** 2008. Lys63-linked polyubiquitination of IRAK-1 is required for interleukin-1 receptor- and toll-like receptor-mediated NF-kB activation. Mol Cell Biol **28**: 3538-3547.

75   **Coope HJ, Atkinson PG, Huhse B, Belich M, Janzen J, et al.** 2002. CD40 regulates the processing of NF-κB2 p100 to p52. EMBO J. **21**:5375–85.

76   **Cordier F, Vinolo E, Veron M, Delepierre M, Agou F.** 2008. Solution structure of NEMO zinc finger and impact of an anhidrotic ectodermal dysplasia with immunodeficiency-related point mutation. J Mol Biol **377**: 1419–1432.

77   **Cordier F, Grubisha O, Traincard F, Veron M, Delepierre M, Agou F.** 2009. The zinc finger of NEMO is a functional ubiquitin-binding domain. J Biol Chem **284**: 2902–2907.

78   **Courtois G, Gilmore TD.** 2006. Mutations in the NF-kappaB signaling pathway: implications for human disease. Oncogene; **25**: 6831-6843.

79   **Courtois G, Smahi A.** 2006. NF-kappaB-related genetic diseases. Cell Death Differ **13**:843–851.

80   **Crawford DH, Macsween KF, Higgins CD, et al.** 2006. A Cohort Study among University students: identification of risk factors for EBV seroconversion and infectious mononucleosis. Clin Infect Dis; **43**:276-282.

81   **Crowell RE, Du Clos TW, Heaphy E, Mold C.** 1991. C-reactive protein receptors on the human monocytic cell line U-937. Evidence for additional binding to Fc gamma RI. Journal of Immunology **147** (10): 3445–51.

82   **Dambaugh TR, et al.** 1984. U2 region of Epstein-Barr virus DNA may encode Epstein-Barr virus nuclear antigen 2. Proc Natl Acad Sci USA; **81**(23):7632-7666.

83   **Dambaugh TR, Kieff E.** 1982. Identification and nucleotide sequences of two similar tandem direct repeats in Epstein-Barr virus DNA. J Virol; **44**(3):823-833.

84   **Davis BJ, Ornstein L.** 1959. A new high resolution electrophoresis method. Delivered at the society for the study of blood at the New York Academy of Medicine.

85   **Davis G, Duerr B, Jacobs T.** Simultaneous screening of colony blots with radioactive and non-isotopic probes. Bio Techniques 12 (5): 688-689.

86   **DE patent 1815352,** "Flow-through Chamber for Photometers to Measure and Count Particles in a Dispersion Medium", granted 1971-01-14.

87   **Dejardin E, Droin NM, Delhase M, Haas E, Cao Y, Makris C, et al.** 2002. The lymphotoxin-beta receptor induces different patterns of gene expression via two NF-kappaB pathways. Immunity. **17**:525-35.

88   **Delecluse HJ, et al.** 1993. Episomal and integrated copies of Epstein-Barr virus coexist in Burkitt's lymphoma cell lines. J Virol; **67**(3):1292-1299.

89   **Deng L, Wang C, Spencer E, Yang L, Braun A, You J,** 2000. Activation of the IkB kinase complex by TRAF6 requires a dimeric ubiquitin-conjugating enzyme complex and a unique polyubiquitin chain. Cell **103:**351–361.

90   **Devergne O, Cahir McFarland ED, Mosialos G, Izumi KM, Ware CF, Kieff E.** 1998. Role of the TRAF binding site and NF-kB activation in EBV latent membrane protein 1-induced cell gene expression. J Virol. **72**:7900-8.

91   **Devergne O, Hatzivassiliou E, Izumi KM, Kaye KM, Kleijnen MF, Kieff E, Mosialos G.** 1996. Association of TRAF1, TRAF2, and TRAF3 with an Epstein-Barr virus LMP1 domain important for B-lymphocyte transformation: role in NF-kappaB activation. Mol Cell Biol. **16**:7098-108.

92   **Devin A, Cook A, Lin Y, Rodriguez Y, Kelliher M, Liu Z.** 2000. The distinct roles of TRAF2 and RIP in IKK activation by TNF-R1: TRAF2 recruits IKK to TNF-R1 while RIP mediates IKK activation. Immunity. **12:**419-29.

93   **Deyrup AT, Lee VK,** et al. 2006. Epstein-Barr virus-associated smooth muscle tumors are distinctive mesenchymal tumors: a clinicopathologic and molecular analysis of 29 tumors from 19 patients. Am J Surg Pathol; **30**:75-82.

94   **Dirmeier U, Neuhierl B, Kilger E, Reisbach G, Sandberg ML, Hammerschmidt W.** 2003. Latent membrane protein 1 is critical for efficient growth transformation of human B cells by EBV. Cancer Res; **63**:2982-2989.

95   **Doffinger R, Smahi A, Bessia C, Geissmann F, Feinberg J, Durandy A, et al.** 2001. X-linked anhidrotic ectodermal dysplasia with immunodeficiency is caused by impaired NF-kappaB signaling. Nat Genet **27**:277–285.

96   **Dolyniuk M, Pritchett R, Kieff E.** 1976. Proteins of Epstein-Barr virus. I. Analysis of the polypeptides of purified enveloped Epstein-Barr virus. J Virol; **17**(3):935-949.

97   **Dolyniuk M, Wolff E, Kieff E.** 1976. Proteins of EBV. II. Electrophoretic analysis of the polypeptides of the nucleocapsid and glucosamine-and polysaccharide-containing components of enveloped virus. J Virol; **18**(1):289-297.

98   **Douglas MW, et al.** 2004. Herpes simplex virus type 1 capsid protein VP26 interacts with dynein light chains RP3 and Tctex1 and plays a role in retrograde cellular transport. J Biol Chem; **279**(27):28522-28530.

99   **Duyao MP, Kessler DJ, Spicer DB, Bartholomew C, Cleveland JL, et al.** 1992. Transactivation of the c-myc promoter by human T cell leukemia virus type 1 tax is mediated by NF κB. J. Biol. Chem. **267**:16288–91.

100   **Drew D, Shimada E, Huynh K, Bergquist S, Talwar R, Karin M, Ghosh G.** 2007. Inhibitor kappaB kinase beta binding by inhibitor kappaB kinase gamma. Biochemistry **46**:12482-12490.

101   **Ea CK, Deng L, Xia ZP, Pineda G, Chen ZJ.** 2006. Activation of IKK by TNFalpha requires site-specific ubiquitination of RIP1 and polyubiquitin binding by NEMO. Mol. Cell; **22**:245-257.

102   **Eddins MJ, Varadan R, Fushman D, Pickart CM, Wolberger C.** 2007 Crystal structure and solution NMR studies of Lys 48-linked tetraubiquitin at neutral pH. J Mol Biol **367**: 204–211.

103   **Elbashir S, Lendeckel W, Tuschl T.** 2001. RNA interference is mediated by 21- and 22-nucleotide RNAs. Genes Dev **15** (2): 188–200.

104   **Elbashir S, Harborth J, Lendeckel W, Yalcin A, Weber K, Tuschl T.** 2001. Duplexes of 21-nucleotide RNAs mediate RNA interference in cultured mammalian cells. Nature **411** (6836): 494–988.

105   **Eliopoulos AG, Caamano JH, Flavell J, Reynolds GM, Murray PG, Poyet JL, Young LS.** 2003. EBV-encoded LMP1 regulates processing of p100 to p52 via an NEMO-independent signaling pathway. Oncogene. **22**:7557-69.

106   **Eliopoulos AG, Davies C, Blake SS, Murray P, Tsichlis PN, Young LS.** 2002. The oncogenic protein kinase Tpl-2/Cot contributes to EBV-encoded LMP1-induced NF-kB signaling downstream of TRAF2. J. Virol. **76:**4567-79.

107   **Eliopoulos AG, Gallagher NJ, Blake SM, Dawson CW, Young LS.** 1999. Activation of the p38 mitogen-activated protein kinase pathway by EBV-encoded LMP1 coregulates IL-6 and IL-8 production. J. Biol. Chem. **274:**16085-96.

108   **Eliopoulos AG, Dawson CW, Young LS.** 1996. CD40-induced growth inhibition in epithelial cells is mimicked by Epstein-Barr virus-encoded LMP1: involvement of TRAF3 as a common mediator. Oncogene; **13**:2243-54.

109   **Epstein MA, Achong BG, Barr YM.** 1964. Virus particles in cultured lymphoblasts from Burkitt's lymphoma. Lancet. **1:**702-703.

110   **Epstein M, Achong B, Barr Y.** 1965. Morphological and biological studies on a virus in cultured lymphoblasts from Burkitt's lymphoma. J Exp Med; **121**:761-770.

111   **Fafi-Kremer S, Brion JP, et al.** 2005. Long-term shedding of infectious EBV after IM. Infect Dis; **191**:985-989.

112   **Falk K, Ernberg I, Sakthivel R, et al.** 1990. Expression of Epstein-Barr virus-encoded proteins and B-cell markers in fatal infectious mononucleosis. Int J Cancer; **46**:976-984.

113   **Farrell PJ, et al.** 2001. Epstein-Barr virus. The B95-8 strain map. Methods Mol Biol; **174**:3-12.

114   **Faulkner GC, Burrows SR, Khanna R, et al.** 1999. X-Linked agammaglobulinemia patients are not infected with Epstein-Barr virus: Implications for the biology of the virus. J Virol; **73**:1555-1564.

115   **Fennewald S, Van Santen V, Kieff E.** 1984. Nucleotide sequence of an mRNA transcribed in latent growth-transforming virus infection indicates that it may encode a membrane protein. Journal of Virology. **51**:411-419.

116   **Field N, Low W, Daniels M, Howell S, Daviet L, Boshoff C, Collins M.** 2003. Activation of IKK by KSHV vFLIP binds to IKK-. to activate IKK. J. Cell. Sci. **116**, 3721–37.

117   **Filipe-Santos O, Bustamante J, Haverkamp MH, Vindo E, et al.** 2006. X-linked susceptibility to mycobacteria is caused by mutations in NEMO impairing CD40-dependent IL-12 production. J Exp Med. **203**:1745-1759.

118   **Fingeroth JD, et al.** 1984. Epstein-Barr virus receptor of human B lymphocytes is the C3d receptor CR2. Proc Natl Acad Sci USA; **81**(14):4510-4154.

119   **Fire A, Xu S, Montgomery M, Kostas S, Driver S, Mello C.** 1998. Potent and specific genetic interference by double-stranded RNA in Caenorhabditis elegans. Nature **391** (6669): 806–11.

120   **Frangou P, Buettner M, Niedobitek G.** 2005. EBV infection in epithelial cells in vivo: rare detection of EBV replication in tongue mucosa but not in salivary glands. J Infect Dis; **191**:238-242.

121   **Fried M, Crothers DM.** 1981. Equilibria and kinetics of lac repressor-operator interactions by polyacrylamide gel electrophoresis. Nucleic Acids Res. **9** (23): 6505–25.

122   **Fontan E, Traincard F, Levy SG, Yamaoka S, Veron M, Agou F.** 2007. NEMO oligomerization in the dynamic assembly of the IκB kinase core complex. FEBS J. **274**(26):2540–2551.

123   **Fusco F, Bardaro T, Fimiani G, Mercadante V, Miano MG, Falco G, Israel A, et.al.** 2004. Molecular analysis of the genetic defect in a large cohort of IP patients and identification of novel NEMO mutations interfering with NF-kappaB activation. Hum Mol Genet **13**: 1763-1773.

124   **Fusco F, Mercadante V, Miano MG, Ursini MV.** 2006. Multiple regulatory regions and tissue-specific transcription initiation mediate the expression of NEMO/IKKgamma gene. Gene; **383**:99-107.

125   **Fusco F, Fimiani G, Tadini G, Michele D, Ursini MV.** 2007. Clinical diagnosis of incontinentia pigmenti in a cohort of male patients. J Am Acad Dermatol **56**:264–267.

126   **Fusco F, Pescatore A, Bal E, Ghoul A, Paciolla M, Lioi MB, et al.** 2008. Alterations of the IKBKG Locus and Diseases: An Update and a Report of 13 Novel Mutations. Human Mutation; **29**(5):595-601.

127   **Garner MM, Revzin A.** 1981. A gel electrophoresis method for quantifying the binding of proteins to specific DNA regions: application to components of the Escherichia coli lactose operon regulatory system. Nucleic Acids Res. **9** (13): 3047–60.

128   **Gartel AL, Kandel ES.** 2006. RNA interference in cancer. Biomolecular Engineering **23**(1): 17–34.

129   **Gerber P, Lucas S, et al.** 1972. Oral excretion of EBV by healthy subjects and patients with IM. Lancet; **2**:988-989.

130   **Gergeley L, Klein G, Ernberg I.** 1971. Host cell macromolecular synthesis in cells containing EBV-induced early antigens, studied by combined immunofluorescence and radioautography. Virolgy; **45**(1):22-29.

131   **Gergen JP, Stern RH, Wensink PC.** 1979. Filter replicas and permanent collections of recombinant DNA plasmids. Nucleic Acids Res; **7**(8):2115-36.

132   **Ghosh S, Karin M.** 2002. Missing pieces in the NF-κB puzzle. Cell **109**(Suppl.):S81–96.

133   **Gires O, Kohlhuber F, Kilger E, Baumann M, Kieser A, Kaiser C, Zeidler R, et al.** 1999. Latent membrane protein 1 of Epstein-Barr virus interacts with JAK3 and activates STAT proteins. EMBO J. **18**:3064-73.

134   **Gires O, Zimber-Strobl U, Ueffing M, Marschall G, Zeidler R, Pich D, Hammerschmidt W.** 1997. Latent membrane protein 1 of Epstein-Barr virus mimics a constitutively active receptor molecule. EMBO J. **16**:6131-40.

135   **Given D, et al.** 1979. DNA of EBV. Direct repeats of the ends of Epstein-Barr virus DNA. J Virol; **30**(3):852-862.

136   **Glasel J.** 1995. Validity of nucleic acid purities monitored by 260nm/280nm absorbance. BioTechniq. **18**: 62–63.

137   **Glaser SL, Jarrett RF.** 1996. The epidemiology of Hodgkin's disease. In Diehl V, er. Hodgkin's Disease. London: Bailliere Tindall; 401-406.

138   **Gong M, Kieff E.** 1990. Intracellular trafficking of two major Epstein-Barr virus glycoproteins, gp350/220 and gp110. J Virol; **64**(4):1507-1516.

139   **Graham FL, van der Eb AJ.** 1973. A new technique for the assay of infectivity of human adenovirus 5 DNA. Virology **52** (2): 456–67.

140   **Grunstein M, Hogness DS.** 1975. Colony hybridization: a method for the isolation of cloned DNAs that contain a specific gene. Proc Natl Acad Sci U S A; **72**(10):3961-5.

141   **Gulley ML, et al.** 1992. EBV integration in human lymphomas and lymphoid cell lines. Cancer; **70**(1):185-191.

142   **Gulley ML, Chen CL, Raab-Traub N.** 1993. Epstein-Barr virus-related lymphomagenesis in a child with Wiskott-Aldrich syndrome. Hematol Oncol; **11**:139-145.

143   **Gyrd-Hansen M, Darding M, Miasari M, et al.** 2008. IAPs contain an evolutionarily conserved ubiquitin-binding domain that regulates NF-kappaB as well as cell survival and oncogenesis. Nat. Cell Biol. **10**, 1309–1317.

144   **Haas TL, Emmerich CH, Gerlach B, Schmukle AC, Cordier SM, Rieser E, et al.** 2009. Recruitment of the linear ubiquitin chain assembly complex stabilizes the TNF-R1 signaling complex and is required for TNF-mediated gene Induction. Molecular Cell; **36**, 831-844

145   **Hacker H, Redecke V, Blagoev B, Kratchmarova I, Hsu LC, et al.** 2005. Specificity in Toll-like receptor signaling through distinct effector functions of TRAF3 and TRAF6. Nature; **33**:1823-1830.

146   **Hacker H, Karin M.** 2006. Regulation and function of IKK and IKK-related kinases. Sci STKE 2006: re13.

147   **Hamilton A, Baulcombe D.** 1999. A species of small antisense RNA in posttranscriptional gene silencing in plants. Science **286** (5441): 950–2.

148   **Hammerschmidt W, Sugden B.** 1988. Identification and characterization of oriLyt, a origin of DNA replication of Epstein-Barr virus. Cell; **55**(3):427-433.

149   **Hammarskjold ML, Simurda MC.** 1992. Epstein-Barr virus latent membrane protein transactivates the human immunodeficiency virus type 1 long terminal repeat through induction of NF-κB activity. J. Virol. **66**:6469-6501.

150   **Hanson EP, Monaco-Shawver L, Solt LA, Madge LA, et al.** 2008. Hypomorphic NEMO mutation database and reconstitution system identifies phenotypic and immunologic diversity. J Allergy Clin Immunol **122**: 1169–1177.

151   **Harada, S, Kieff E.** 1997. Epstein-Barr virus nuclear protein LP stimulates EBNA-2 acidic domain-mediated transcriptional activation. J Virol; **71**:6611-6618.

152   **Harhaj EW and Sun SC.** 1999. J. Biol. Chem.; **274**:22911–22914.

153   **Harhaj EW, Good L, Xiao G, Uhlik M, Cvijic M, Rivera-Walsh I, Sun SC.** 2000. Somatic mutagenesis studies of NF-κB signaling in human T-cells: evidence for an essential role of IKKγ in NF-κB activation by T-cell costimulatory signals and HTLV-I Tax protein. Oncogene; **19**:1448-1456.

154   **Harris NL, Jaffe ES, Stein H, et al.** 1994. A revised European-American classification of lymphoid neoplasms: a proposal from the International Lymphoma Study Group. Blood; **84**:1361-1392.

155   **Hatzivassiliou E, Miller WE, Raab-Traub N, Kieff E, Mosialos G.** 1998. A fusion of the EBV latent membrane protein-1 (LMP1) transmembrane domains to the CD40 cytoplasmic domain is similar to LMP1 in constitutive activation of EGFR expression, NF-kB, and stress-activated protein kinase. J. Immunol. **160**:1116-21.

156   **Hayden MS, Ghosh S.** 2008. Shared Principles in NF-κB signaling. Cell; **132**: 344-362.

157   **Henderson E, et al.** 1977. Efficiency of transformation of lymphocytes by EBV. Virology; **76**(1):152-163.

158   **Henderson S, Rowe M, Gregory C, Croom-Carter D, Wang F, Longnecker R, Kieff E, Rickinson, A.** 1991. Induction of bcl-2 Expression by protein encoded by Epstein-Barr virus in latent growth-transforming infection. Proc Natl Acad Sci. USA. **81**:7201-11.

159   **Henle W, et al.** 1967. Herpes-type virus and chromosome marker in normal leukocytes after growth with irradiated Burkitt cells. Science; **157**(792):1064-1065.

160   **Herndon TM, Shan XC, Tsokos GC, Wange RL.** 2001. ZAP-70 and SLP-76 regulate protein kinase C-θ and NF-κB activation in response to engagement of CD3 and CD28. J. Immunol. **166**:5654–64.

161   **Herrmann K, Middeldorp J, et al.** 2002. EBV replication in tongue epithelial cells. J Gen Virol; **83**:2995-2998.

162   **Hershko A, Ciechanover A.** 1998. The ubiquitin system. Annu Rev Biochem **67**:425–479.

163   **Hicke L, Schubert HL, Hill CP.** 2005. Ubiquitin-binding domains. Nat Rev Mol Cell Biol **6**: 610–621.

164   **Hinz M, Krappmann D, Eichten A, Heder A, Scheidereit C, Strauss M.** 1999. NF-κB function in growth control: regulation of cyclinD1 expression and G0/G1-toS-phase transition. Mol. Cell. Biol. **19**:2690–98.

165   **Hoshino Y, Morishima T, Kimura H, et al.** 1999. Antigen-driven expansion and contraction of CD8+-activated T cells in primary EBC infection. J Immunol; **163**:5735-5740.

166   **Hsu H, Huang J, Shu HB, Baichwal V, Goeddel DV.** 1996. TNF-dependent recruitment of the protein kinase RIP to the TNF receptor-1 signaling complex.Immunity. **4**:387-96.

167   **Hsu H, Shu HB, Pan MG, Goeddel DV.** 1996. TRADD-TRAF2 and TRADD-FADD interactions define two distinct TNF receptor 1 signal transduction pathways. Cell **84**:299–308.

168   **Hu Y, Baud V, Delhase M, Zhang P, Deerinck T, et al.** 1999. Abnormal morphogenesis but intact IKK activation in mice lacking the IKKα subunit of IκB kinase. Science **284**:316–20.

169   **Huang GJ, Zhang ZQ, Jin DY.** 2002. FEBS Lett., **531**, 494–498.

170   **Huang TT, Wuerzberger-Davis SM, Wu ZH, Miyamoto S.** 2003. Sequential modification of NEMO/IKKgamma by SUMO-1 and ubiquitin mediates NF-kappaB activation by genotoxic stress. Cell **115**:565–576.

171   **Huen DS, Henderson SA, Croom-Carter D, Rowe M.** 1995. The EBV LMP1 mediates activation of NF-kB and cell surface phenotype via two effector regions in its carboxy-terminal cytoplasmic domain. Oncogene. **10**:549-60.

172   **Hurley EA, Thorley-Lawson DA.** 1988. B-cell activation and the establishment of Epstein-Barr virus latency. J Exp Med; **168**(6):2059-2075.

173   **Hurley EA, et al.** 1991. When EBVinfects B-cell lines, it frequently integrates. J Virol; **65**(3):1245-1254.

174   **Hurley JH, Lee S, Prag G.** 2006. Ubiquitin-binding domains. Biochem J **399**: 361–372.

175   **Hurwitz J, Leis JP.** 1972. "RNA-dependent DNA polymerase activity of RNA tumor viruses. Directing influence of DNA in the reaction". J. Virol. **9** (1): 116–29.

176   **Huye LE, Ning S, Kelliher M, Pagano JS.** 2007. Interferon regulatory factor 7 is activated by a viral oncoprotein through RIP-dependent ubiquitination. Mol Cell Biol; **27**:2910-2918.

177   **Iha H, Kibler KV, Yedavalli VRK, Haller K, Jeang KT.** 2003. Segregation of NF-κB activation through NEMO by Tax and TNFα: implications for stimulus-specific interruption of oncogenic signaling. Oncogene; **22**:8912-8923.

178   **Ikeda F, Dikic I.** 2008. Atypical ubiquitin chains: new molecular signals. 'Protein Modifications: Beyond the Usual Suspects' review series. EMBO Rep; **9**:536–542.

179   **Ishida T, Mizushima S, Azuma S, Kobayashi N, Tojo T, Suzuki K, et al.** 1996. Identification of TRAF6, a novel tumor necrosis factor receptor-associated factor protein that mediates signaling from an amino-terminal domain of the CD40 cytoplasmic region. J Biol Chem; **271**:28745-8.

180   **Ishitani T, Takaesu G, Ninomiya-Tsuji J, Shibuya H, Gaynor RB, Matsumoto K.** 2003. Role of the TAB2-related protein TAB3 in IL-1 and TNF signaling. EMBO J. **22**:6277–88.

181   **Israel A.** 2006. NF-kB activation: Nondegradative ubiquitination implicates NEMO. Trends Immunol **27**:395-397.

182   **Ivins FL, Montgomery MG, Smith SMJ, Morris-Davies AC, Taylor IA, Rittinger K.** 2009. Nemo oligomerization and its ubiquitin-binding properties. Biochem J; **421**:243-251.

183   **Iwai K, Tokunaga F.** 2009. Linear polyubiquitination: a regulator of NF-κB activation. EMBO; **10**(7):706-713.

184   **Izumi KM, Cahir McFarland ED, Riley EA, Rizzo D, Chen Y, Kieff E.** 1999. The residues between the two transformation effector sites of EBV LMP1 are not critical for B-cell growth transformation. J. Virol. **73**:9908-16.

185   **Izumi KM, Cahir McFarland ED, Riley EA, Ting AT, Seed B, Kieff E.** 1999. The EBV oncoprotein LMP1 engages the tumor necrosis factor receptor-associated proteins TRADD and receptor-interacting protein (RIP) but does not induce apoptosis or require RIP for NF-kB activation. Molecular and Cellular Biology; **19**(8):5759–5767

186   **Izumi KM, Kieff ED.** 1997. The EBV oncogene LMP1 engages the TNFR-associated death domain protein to mediate B lymphocyte growth transformation and activate NF-kappaB. Proc Natl Acad Sci U S A. **94:**12592-7.

187   **Jaffe ES, Raffeld M.** 2003. Classification of cytotoxic T-cell and NK cell lymphomas. Sem. Hematol; **40**:175-184.

188   **Jain A, Ma CA, Liu S, Brown M, Cohen J, Strober W.** 2001. Specific missense mutations in NEMO result in hyper-IgM syndrome with hypohydrotic ectodermal dysplasia. Nat Immunol **2**: 223–228

189   **Janeway CA, Travers P, Walport M, Shlomchik M.** 2001. Immunobiology: The Immune System in Health and Disease. 5th Edition. New York, Garland Publishing.

190   **Jin DY, Giordano V, Kibler KV, Nakano H, Jeang KT.** 1999. J. Biol. Chem.; **274**:17402–17405.

191   **Johannsen E, et al.** 2004. Proteins of purified Epstein-Barr virus. Proc Natl Acad Sci USA; **101**(46):16286-16291.

192   **Kamentsky.** 1970. Proceedings of the Conference „Cytology Automation" in Edinburgh.

193   **Kanegane H, Kanegane C, Yachie A, et al.** 1997. Infectious mononucleosis as a disease of early childhood in Japan caused by primary Epstein-Barr virus infection. Acta Paediatricia Japan; **39**:166-171.

194   **Kanegane H, Wang F, Tosato G.** 1996.Virus-cell interactions in a natural killer-like cell line from a patient with lymphoblastic lymphoma. Blood; 88(12):4667-4675.

195   **Karin M, Ben-Neriah Y**. 2000. Phosphorylation meets ubiquitination: the control of NF-κB activity. Annu. Rev. Immunol. **18**:621–63.

196   **Karin M, Greten FR. 2005.** NF-κB: linking inflammation and immunity to cancer development and progression. Nat. Rev. Immunol. **5**:749–59.

197   **Karin M. Vallabhapurapu S.** 2009. Regulation and function of NF-κB transcription factors in the immune system. Ann. Rev. Immunol.; **27**:693-733.

198   **Kato T Jr, Delhase M, Hoffmann A, Karin M.** 2003. CK2 is a C-terminal IkappaB kinase responsible for NF-kappaB activation during the UV Response. Mol Cell. **12:**829-39.

199   **Kawanishi M, et al.** 1993. Epstein-Barr virus induces fragmentation of chromosomal DNA during lytic infection.   J Virol; **67**(12):7654-7658.

200   **Kawai T, Akira S.** 2007. Signaling to NF-κB by toll-like receptors. Trends Mol. Med. **13**:460–6.

201   **Kaye KM, Izumi KM, Kieff E.** 1993. Epstein-Barr virus latent membrane protein 1 is essential for B-lymphocyte growth transformation. Proc Natl Acad Sci U S A. **90:**9150-54.

202   **Kaye KM, Devergne O, Harada JN, Izumi KM, Yalamanchili R, Kieff E, Mosialos G.** 1996. TRAF2 is a mediator of NF-kappa B activation by LMP1, the EBV transforming protein. Proc Natl Acad Sci USA. **93:**11085-90.

203   **Kaye KM, Izumi KM, Mosialos G, Kieff E.** 1995. The Epstein-Barr virus LMP1 cytoplasmic carboxy terminus is essential for B-lymphocyte transformation; fibroblast cocultivation complements a critical function within the terminal 155 residues. J Virol. **69:**675-83.

204   **Kaye KM, Izumi KM, Li H, Johannsen E, Davidson D, Longnecker R, Kieff E,** 1999. An Epstein-Barr virus that expresses only the first 231 LMP1 amino acids efficiently initiates primary B-lymphocyte growth transformation. J Virol. **73**:10525-10530.

205   **Kaykas A, Worringer K, Sugden B.** 2002. LMP1's transmembrane domains encode multiple functions required for LMP-1's efficient signaling. J Virol; **76**:11551-60.

206   **Keats JJ, Fonseca R, Chesi M, Schop R, Baker A, et al.** 2007. Promiscuous mutations activate the noncanonical NF-κB pathway in multiple myeloma. Cancer Cell **12**:131–44.

207   **Kieff E, Levine J.** 1974. Homology between Burkitt herpes viral DNA and DNA in continuous lymphoblastoid cells from infectious mononucleosis patients. Proc Natl Acad Sci USA; **71**(2):355-358.

208   **Kieff E, Rickinson AB.** 2007. Epstein-Barr virus and its replication. In: Fields BN, Knipe DM, Howley PM, eds. Fields virology. 4rd ed. Vol. 2. Philadelphia: Lippincott-Raven, pp2603-2700.

209   **Kieff E, Liebowitz D.** 1990. Epstein-Barr Virus and Its Replication. In Virology, 2nd., eds, B. N. Fields & D. M. Knipe, 1889-1920. Raven Press, New York.

210   **Kieser A, Kilger E, Gires O, Ueffing M, Hammerschmidt W.** 1997. EBV latent membrane protein-1 triggers AP-1 activity via the c-Jun N-terminal kinase cascade. EMBO J. **16:**6478-85.

211   **Kilger E, Kieser A, Baumann M, Hammerschmidt W.** 1998. Epstein-Barr virus-mediated B-cell proliferation is dependent upon latent membrane protein 1, which simulates an activated CD40 receptor. EMBO J. **17:**1700-9.

212   **Kim KR, Yoshizaki T, Miyamori H, Hasegawa K, et al.** 2000. Transformation of Madin-Darby canine kidney (MDCK) epithelial cells by EBV LMP1 induces expression of Ets1 and invasive growth. Oncogene. **19:**1764-71.

213   **Kim SH, Shin YK, Lee IS, Bae YM, Sohn HW, Suh YH.** 2001. Viral LMP1-induced CD99 down-regulation in B cells leads to the generation of cells with Hodgkin's and Reed-Sternberg phenotype. Blood. **95:**294-300.

214   **Kirisako T, Kamei K, Murata S, Kato M, Fukumoto H, Kanie M, et al.** 2006 A ubiquitin ligase complex assembles linear polyubiquitin chains. EMBO J **25**:4877–4887.

215   **Kohlrausch F.** 1897. Über Concentrations-Verschiebungen durch Electrolyse im Inneren von Lösungen und Lösungsgemischen. Ann.J.Phys.u.Chem. **62**: 209–239.

216   **Komander D, Reyes-Turcu F, Licchesi1 J.D.F, Odenwaelder P, Wilkinson KD, Barford D.** 2009. Molecular discrimination of structurally equivalent Lys 63-linked and linear polyubiquitin chains. EMBO; **10**(5):466-473.

217   **Kovalenko A, Chable-Bessia C, Cantarella G, Israel A, Wallach D, Courtois G.** 2003. The tumour suppressor CYLD negatively regulates NF-kB signaling by deubiquitination. Nature **424**: 801-805.

218   **Kulwichit W, Edwards RH, Davenport EM, Baskar JF, Raab-Traub N.** 1998. Expression of the EBV latent membrane protein 1 induces B cell lymphoma in transgenic mice. Proc Natl Acad Sci U S A, **95:**11963-11968.

219   **Laherty CD, Hu HM, Opipari AW, Wang F, Dixit VM.** 1992. The Epstein-Barr virus LMP1 gene product induces A20 zinc finger protein expression by activating nuclear factor kappa B. J. Biol. Chem. **267:**24157-60.

220 **Laemmli UK.** 1970. Cleavage of structural proteins during the assembly of the head of bacteriophage T4. Nature **227** (5259): 680–685.

221 **Landy SJ, Donnai D.** 1993. Incontinentia pigmenti (Bloch-Sulzberger syndrome). J Med Genet **30**:53–59.

222 **Laplantine E, Fontan E, Chiaravalli J, Lopez T, Lakisic G, Veron M, et al.** 2009. NEMO specifically recognizes K63-linked poly-ubiquitin chains through a new bipartite ubiquitin-binding domain. EMBO; **28**(19):2885-2894.

223 **Lawrence JB, Singer RH, Marselle LM.** 1989. Highly localized tracks of specific transcripts within interphase nuclei visualized by in situ hybridization. Cell; **57**(3):493-502.

224 **Lawrence T, Bebien M, Liu GY, Nizet V, Karin M.** 2005. IKKα limits macrophage NF-κB activation and contributes to the resolution of inflammation. Nature **434**:1138–43.

225 **Lee ES, Locker J, Nalesnik M, et al.** 1995. The association of Epstein-Barr virus with smooth-muscle tumors occurring after organ transplantation. N Engl J Med; **332**: 19-25.

226 **Li H, Kobayashi M, Blonska M, You Y, Lin X.** 2006. Ubiquitination of RIP is required for tumor necrosis factor alpha-induced NF-kappaB activation. J Biol Chem **281**: 13636-13643.

227 **Li Q, et al.** 1997. EBV uses HLA class II as a cofactor for infection of B lymphocytes. J Virol; **71**(6):4657-4662.

228 **Li Q, Verma IM.** 2002. NF-κB regulation in the immune system. Nat. Rev. Immunol. **2**:725–34.

229 **Li Y, Kang J, Friedman J, Tarassishin L, Ye J, Kovalenko A, Wallach D, Horwitz MS.** 1999. Identification of a cell protein (FIP-3) as a modulator of NF-kappaB activity and as a target of an adenovirus inhibitor of tumor necrosis factor alpha-induced apoptosis. Proc Natl Acad Sci U S A. **96**:1042-7.

230 **Li Y, Kang J, Horwitz MS.** 1998. Interaction of an adenovirus E3 14.7-kilodalton protein with a novel tumor necrosis factor alpha-inducible cellular protein containing leucine zipper domains. Mol Cell Biol. **18**:1601-10.

231 **Li ZW, Chu W, Hu Y, Delhase M, Deerinck T, et al.** 1999. The IKKβ subunit of IκB kinase (IKK) is essential for nuclear factor κB activation and prevention of apoptosis. J. Exp. Med. **189**:1839–45.

232 **Liao G, Zhang M, Harhaj EW, Sun SC.** 2004. Regulation of the NF-κB-inducing kinase by tumor necrosis factor receptor-associated factor 3-induced degradation. J. Biol. Chem. **279**:26243–50.

233 **Liebowitz, D., Wang, D. & Kieff, E.** 1986. Orientation and patching of the latent infection membrane protein encoded by Epstein-Barr Virus. Journal of Virology. **58**:233-237.

234 **Liu L, Eby MT, Rathore N, Sinha SK, Kumar A, Chaudhary PM.** 2002. The human herpes virus 8-encoded viral FLICE inhibitory protein physically associates with and persistently activates the IκB kinase complex. J. Biol. Chem. **277**:13745–51.

235 **Lo YC, Lin SC, Rospigliosi CC, Conze DB, Wu CJ, Ashwell JD, Eliezer D, Wu H.** 2009. Structural basis for recognition of diubiquitins by NEMO. Mol. Cell **33**, 602–615.

236 **Loken MR.** 1990. Immunofluorescence Techniques in Flow Cytometry and Sorting (2nd ed.). Wiley. pp. 341–53.

237 **Luftig MA, Cahir-McFarland E, Mosialos G, Kieff E.** 2001. Effects of the NIK aly mutation on NF-kB activation by the EBV LMP, lymphotoxin beta receptor, and CD40. J Biol Chem. 2001 **276**:14602-6.

238 **Luftig M, Prinarakis E, Yasui T, Tsichritzis T, Cahir-McFarland E, Inoue J, et al.** 2003. Epstein-Barr virus LMP 1 activation of NF-kappaB through IRAK1 and TRAF6. Proc Natl Acad Sci U S A. **100**:15595-600.

239 **Luftig M, Yasui T, Soni V, Kang MS, Jacobson N, Cahir-McFarland E, Seed B, Kieff E.** 2003. Epstein-Barr virus latent infection membrane protein 1 TRAF-binding site induces NIK/IKK alpha-dependent noncanonical NF-kappaB activation. Proc Natl Acad Sci U S A. **101**:141-6.

240 **Magrath I.** 1990. The pathogenesis of Burkitt's lymphoma. Adv Cancer Res; **55**:133-270.

241 **Mauro C, Pacifico F, Lavorgna A, Mellone S, Iannetti A, Acquaviva R, et al.** 2006. ABIN-1 binds to NEMO/IKKgamma and co-operates with A20 in inhibiting NF-kappaB. J Biol Chem **281**: 18482-18488.

242 **McClain KL, Leach CT, Jenson HB, et al.** 1995. Association of Epstein-Barr virus with leiomyosarcomas in Children with AIDS. N Engl J Med; **332**:12-18.

243 **Makris C, Godfrey VL, Krahn-Senftleben G, Takahashi T, Roberts JL, Schwarz T, et al.** 2000. Female mice heterozygote for IKKγ/NEMO deficiencies develop a genodermatosis similar to the human X-linked disorder incontinentia pigmenti. Mol. Cell; **5**:969–979.

244 **Makris C, Roberts JL, and Karin M.** 2002. The carboxyl-terminal region of IkappaB kinase gamma (IKKgamma) is required for full IKK activation. Mol. Cell. Biol. **22**, 6573–6581.

245 **Marienfeld RB, Palkowitsch L, and Ghosh S.** 2006. Dimerization of the I kappa B kinase-binding domain of NEMO is required for tumor necrosis factor alpha-induced NF-kappa B activity. Mol. Cell. Biol. **26**, 9209–9219.

246 **Martin DR, Marlowe RL, Ahearn JM.** 1994. Determination of the role for CD21 during Epstein-Barr virus infection of B-lymphoblastoid cells. J Virol; **68**(8):4716-4726.

247 **Masucci MG, et al.** 1987. Activation of B lymphocytes by Epstein-Barr virus/CR2 receptor interaction. Eur J Immunol; **17**(6):815-820.

248 **Matsuo T, et al.** 1984. Persistence of the entire Epstein-Barr virus genome integrated into human lymphocyte DNA. Science; **226**(4680):1322-1325.

249 **Matsuzawa A, Tseng PH, Vallabhapurapu S, Luo JL, Zhang W, et al.** 2008. Essential cytoplasmic translocation of a cytokine receptor-assembled signaling complex. Science **321**:663–68.

250 **Mattia E, Chichiarelli S, Hickish T, Gaeta A, Mancini C, et al.** 1997. Inhibition of in vitro proliferation of EBV infected B cells by an antisense oligodeoxynucleotide targeted against EBV LMP1. Oncogene. **15(4):**489-93.

251 **Mauro C, Pacifico F, Lavorgna A, Mellone S, Iannetti A, Acquaviva R, et al.** 2006. Abin-1 binds to NEMO/IKKgamma and co-operates with A20 in Inhibiting NF-κB. JBC; **281**(27)18482–18488

252 **May MJ, D'Acquisto F, Madge LA, Glockner J, Pober JS, Ghosh S.** 2000. Selective inhibition of NF-kB activation by a peptide that blocks the interaction of NEMO with the IkB kinase complex. Science **289**, 1550–1554.

253 **May MJ, Marienfeld RB, Ghosh S.** 2002. Characterization of the IκB-kinase NEMO binding domain. J. Biol. Chem. **277**:45992–6000.

254   **Mehl AM, Floettmann JE, Jones M, Brennan P, Rowe M.** 2001. Characterization of intercellular adhesion molecule-1 regulation by Epstein-Barr virus-encoded latent membrane protein-1 identifies pathways that cooperate with NF kappa B to activate transcription. J. Biol. Chem. **276:**984-92.

255   **Menuel S, Fontanay S, Clarot I, Duval R.E, Diez L, Marsura A.** 2008. Synthesis and complexation ability of a novel bis- (guanidinium)-tetrakis-(β-cyclodextrin) dendrimeric tetrapod as a potential gene delivery (DNA and siRNA) system. Study of cellular siRNA transfection. Bioconjugate Chem. **19** (12): 2357–2362.

256   **Merril CR.** 1990. Gel-staining techniques. Methods in Enzymology volume 182. Academic press Inc..

257   **Micheau O, Tschopp J.** 2003. Induction of TNF receptor I-mediated apoptosis via two sequential signaling complexes. Cell **114**:181–90.

258   **Miller N, Hutt-Fletcher LM.** 1992. EBV enters B cells and epithelial cells by different routes. JV. **66:**3409-3414.

259   **Miller WE, Mosialos G, Kieff E, Raab-Traub N.** 1997. EBV LMP1 induction of the epidermal growth factor receptor is mediated through a TRAF signaling pathway distinct from NF-kappaB activation. J.Virol. **71:**586-94.

260   **Mitchell T, Sugden B.** 1995. Stimulation of NF-κB-mediated transcription by mutant derivatives of the latent membrane protein of Epstein-Barr virus. J. Virol. **69:**2968-76.

261   **Moore KW, et al.** 1993. Interleukin-10. Annu Rev Immunol; **11**:165-190.

262   **Mosialos G, Birkenbach M, Yalamanchili R, VanArsdale T, Ware C, Kieff E.** 1995. The EBV transforming protein LMP1 engages signaling proteins of the tumor necrosis factor receptor family. Cell **80:**389-399.

263   **Mullen MM, et al.** 2002. Structure of the Epstein-Barr virus gp42 protein bound to the MHC class II receptor HLA-DR1. Mol Cell; **9**(2):375-385.

264   **Mullis KB, Faloona FA.** 1987. Specific synthesis of DNA in vitro via a polymerase-catalyzed chain reaction. Methods Enzymol. **155**:335-350.

265   **Mumby MC, Walter G.** 1993. Protein serine/threonine phosphatases: structure, regulation, and functions in cell growth. Physiological Reviews,**73**,pp673.

266   **Natoli G, Chiocca S.** 2008. Nuclear ubiquitin ligases, NF-κB degradation, and the control of inflammation. Sci. Signal 1:pe1.

267   **Nemerow GR, Cooper NR.** 1984. Early events in the infection of human B lymphocytes by Epstein-Barr virus: the internalization process. Virology; **132**(1):186-198.

268   **Nemerow GR, et al.** 1985. Identification and characterization of the Epstein-Barr virus receptor on human B lymphocytes and its relationship to the C3d complement receptor (CR2). J Virol 1985; **55**(2):347-351.

269   **Nemerow GR, et al.** 1989. Identification of an epitope in the major envelope protein of Epstein-Barr virus that mediates viral binding to the B lymphocyte EBV receptor (CR2). Cell; **56**(3):369-377.

270   **Neumann E, Schaefer-Ridder M, Wang Y, Hofschneider PH.** 1982. Gene transfer into mouse lymphoma cells by electroporation in high electric fields. Embo J. **1** (7): 841–5.

271   **Ni CY, Wu ZH, Florence WC, Parekh VV, Arrate MP, Pierce S, et al.** 2008. Cutting edge: K63-linked polyubiquitination of NEMO modulates TLR signaling and inflammation in vivo. J Immunol **180**: 7107-7111.

272   **Ninomiya-Tsuji J, Kishimoto K, Hiyama A, Inoue J, Cao Z, Matsumoto K.** 1999. The kinase TAK1 can activate the NIK-I κB as well as the MAP kinase cascade in the IL-1 signalling pathway. Nature **398**:252–56.

273   **Novack DV, Yin L, Hagen-Stapleton A, Schreiber RD, Goeddel DV, et al.** 2003. The IκB function of NF-κB2 p100 controls stimulated osteoclastogenesis. J. Exp. Med. **198**:771–81.

274   **Oeckinghaus A, Wegener E, Welteke V, Ferch U, Arslan SC, Ruland J, Scheidereit C, Krappmann D.** 2007. Malt1 ubiquitination triggers NF-kappaB signaling upon T-cell activation. EMBO J **26**: 4634-4645.

275   **Oganesyan G, Saha SK, Guo B, He JQ, Shahangian A, Zarnegar B et al.** 2005. Critical role of TRAF3 in the Toll-like receptor-dependent and –independent antiviral response. Nature; **41**:1699-1705.

276   **Opelz G, Dohler B.** 2004. Lymphomas after solid organ transplantation: a collaborative transplant study report. Am J Transplant; **4**:222-230.

277   **Oshima S, Turer1 EE, Callahan1 JA, Chai1 S, Advincula1 R, Barrera1 J, et al.** 2009. ABIN-1 is a ubiquitin sensor that restricts cell death and sustains embryonic development. Nature; **457**:906-909.

278   **Papworth MA, et al.** 1997. The processing, transport and heterologous expression of Epstein-Barr virus gp110. J Gen Virol; **78**(Pt9):2179-2189.

279   **Pearson GR, et al.** 1987. Identification of an Epstein-Barr virus early gene encoding a second component of the restricted early antigen complex. Virology; **160**(1):151-161.

280   **Perkins ND.** 2006. Post-translational modifications regulating the activity and function of the nuclear factor kappa B pathway. Oncogene **25**: 6717-6730.

281   **Pfeffer S, et al.** 2005. Identification of microRNAs of the herpesvirus family. Nat Methods; **2**(4):269-276.

282   **Pfeffer S, et al.** 2004. Identification of virus-encoded microRNAs. Science; **304**(5671):734-736.

283   **Pickart CM.** 2001. Mechanisms underlying ubiquitination. Annu Rev Biochem **70**:503–533.

284   **Pickart CM, Fushman D.** 2004. Polyubiquitin chains: polymeric protein signals. Curr Opin Chem Bio **8**:610–616.

285   **Poiesz BJ, Ruscetti FW, Reitz MS, Kalyanaraman VS, Gallo RC.** 1981. Isolation of a new type C retrovirus (HTLV) in primary uncultured cells of a patient with Sezary T-cell leukaemia. Nature **294**:268–71.

286   **Pope J.** 1967. Establishment of cell lines from peripheral leukocytes in IM. Nature; **216**:810-811.

287   **Pope JH. Horne MK, Scott W.** 1968. Transformation of foetal human leukocytes in vitro by filtrates of a human leukaemic cell line containing herpes-like virus. Int J Cancer; **3**(6): 857-866.

288   **Pobezinskaya YL, Kim YS, Choksi S, Morgan MJ, Li T, et al.** 2008. The function of TRADD in signaling through tumor necrosis factor receptor 1 and TRIF-dependent Toll-like receptors. Nat. Immunol. **9**:1047–54.

289   **Poyet JL, Srinivasula SM, Lin JH, Yamaoka S, Tsichlis PN, Alnemri ES.** 2000. Activation of the Ikappa B kinases by RIP via IKKgamma/NEMO-mediated oligomerization. J Biol Chem **275**: 37966-37977.

290   **Pritchett RF, Hayward SD, Kieff ED.** 1975. DNA of Epstein-Barr virus. I. Comparative studies of the DNA of Epstein-Barr virus from HR-1 and B95-8 cells: size, structure, and relatedness. J Virol; **15**(3):556-559.

291   **Purtilo DT, Cassel CK, Yang JP, et al.** 1975. X-linked recessive progressive combined variable immunodeficiency (Duncan's disease). Lancet; **1**:935-940.

292   **Qian Y, Commane M, Ninomiya-Tsuji J, Matsumoto K, Li X.** 2001. IRAK-mediated translocation of TRAF6 and TAB2 in the interleukin-1-induced activation of NFκB. J. Biol. Chem. **276**:41661–67.

293   **Rahighi S, Ikeda F, Kawasaki M, Akutsu M, Suzuki N, Kato R, et al.** 2009. Specific recognition of linear ubiquitin chains by NEMO is important for NF-kB activation. Cell **136**:1098–1109.

294   **Raymond S, Weintraub L.** 1959. Acrylamide gel as supporting medium for electrophoresis. Science **130**: 711.

295   **Renart J, Reiser J, Stark GR.** 1979. Transfer of proteins from gels to paper and detection with antisera: a method for studying antibody specificity and antigen structure. Proc Natl Acad Sci U S A. **76** (7): 3116–3120.

296   **Reschke, M,** 1994-97; www.biografix.de./.../english/images/2/p_2b2a.jpg

297   **Ressing ME, van Leeuwen D, Verreck FA, et al.** 2003. Interference with T cell receptor-HLA-DR interactions by Epstein-Barr virus gp42 results in reduced T helper cell recognition. Proc Natl Acad Sci USA; **100**: 11583-11588.

298   **Rickinson AB, Kieff E.** 1996. Epstein-Barr virus; in Fields BN, Knipe DM, Howley PM (eds): Fields Virology. Philadelphia, Lippinott-Raven, pp 2397-2446.

299   **Riley LK, Caffrey CJ.** Identification of enterotoxigenic E.coli by colony hybridization with nonradioactive digoxigenin-labeled DNA probes. J.Clin. Microbiol. 28(6): 1465-1468.

300   **Rothwarf DM, Zandi E, Natoli G, and Karin M.** 1998. IKK-gamma is an essential regulatory subunit of the IkappaB kinase complex. Nature **395**, 297–300.

301   **Rothwarf DM, Karin M.** 1999. The NF-κB activation pathway: a paradigm in information transfer from membrane to nucleus. Sci. STKE 1999:RE1.

302   **Rowe M, Peng-Pilon M, Huen DS, Hardy R, Croom-Carter D, Lundgren E, Rickinson AB.** 1994. Upregulation of bcl-2 by the Epstein-Barr virus latent membrane protein LMP1: a B-cell-specific response that is delayed relative to NF-kappa B activation and to induction of cell surface markers.J. Virol. **68**:5602-12.

303   **Rudolph D, Yeh WC, Wakeham A, Rudolph B, Nallainathan D, Potter J, Elia AJ and Mak TW.** 2000. Severe liver degeneration and lack of NF-kB activation in NEMO/IKKg-deficient mice.Genes Dev.; **14**:854–862.

304   **Ruland J, Mak TW.** 2003. Transducing signals from antigen receptors to nuclear factor κB. Immunol. Rev. **193**:93–100.

305   **Ryon JJ, et al.** 1993. The lytic origin of herpesvirus papio is highly homologous to Epstein-Barr virus ori-Lyt: evolutionary conseration of transcriptional activation and replication signals. J virol; **67**(7):4006-4016.

306   **Saiki RK, Gelfand DH, Stoffel S, Scharf SJ, Horn GT, Mullis KB, Erlich HA.** 1988. Primer-directed enzymatic amplification of DNA with a thermostable DNA polymerase. Science **239**: 487–91.

307   **Saito, K.** et al. 2004. The CAP-Gly domain of CYLD associates with the proline-rich sequence in NEMO/IKKg. Structure **12**, 1719–1728

308   **Saito N, Courtois G, Chiba A, Yamamoto N, Nitta T, Hironaka N, Rowe M, Yamaoka S.** 2003. Two carboxyl-terminal activation regions of Epstein-Barr virus latent membrane protein 1 activate NF-kappaB through distinct signaling pathways in fibroblast cell lines. J Biol Chem. **278**:46565-75.

309   **Saitoh T, Nakayama M, Nakano H, Yagita H, Yamamoto N, Yamaoka S.** 2003. TWEAK induces NF-κB2 p100 processing and long lasting NF-κB activation. J. Biol. Chem. **278**:36005–12.

310   **Sambrook J, Russel DW.** 2001. Molecular Cloning: A Laboratory Manual 3rd Ed. Cold Spring Harbor Laboratory Press. Cold Spring Harbor, NY.

311   **Sample J, Kieff EF, Kieff ED.** 1994. Epstein-Barr virus types 1 and 2 have nearly identical LMP-1 transforming genes. J Gen Virol; **75**(Pt10):2741-2746.

312   **Sample J, et al.** 1990. Epstein-Barr virus types 1 and 2 differ in their EBNA-3A, EBNA-3B, and EBNA-3C genes. J Virol; **64**(9):4084-4092.

313   **Sartori H. E.** 1984.Cesium therapy in cancer patients. Pharmacol Biochem Behav.;21.1:11-3.

314   **Savard M, et al.** 2000. Infection of primary human monocytes by Epstein-Barr virus. J Virol; **74**(6):2612-2619.

315   **Scheidereit C.** 2006. IkB kinase complexes: gateways to NF-kB activation and transcript. Oncogene; **25**:6685-6705.

316   **Schmidt-Supprian M, Bloch W, Courtois G, Addicks K, Israel A, Rajewsky K, Pasparakis M.** 2000. NEMO/IKK gamma-deficient mice model incontinentia pigmenti. Mol. Cell **5**, 981–992.

317   **Schultheiss U, Puschner S, Kremmer E, Mak TW, Hammerschmidt W, Kieser A.** 2001. TRAF6 is a critical mediator of signal transduction by the viral oncogene latent membrane protein 1.EMBO J. **20**:5678-91.

318   **Schwint OA, Labraga M, Cervino CO, Haffar M, Sequeiros PH,** 2004. A modification of the staining technique of reticular fibres for image analysis of the cardiac collagen network. Cardiovasc. Pathol. **13** (4): 213–20.

319   **Sebban H, Yamaoka S, Courtois G.** 2006. Posttranslational modifications of NEMO and its partners in NF-kappaB signaling. Trends Cell Biol **16**: 569-577.

320   **Sebban-Benin H, Pescatore A, Fusco F, Pascuale V, Gautheron J, Yamaoka S, Ursini MV, Courtois G.** 2007. Identification of TRAF6-dependent NEMO polyubiquitination sites through analysis of a new NEMO mutation causing incontinentia pigmenti. Hum. Mol. Genet.; **16**:2805-2815.

321   **Senftleben U, Cao Y, Xiao G, Greten FR, Krahn G, Chen Y, Hu Y, Fong A, Sun SC, Karin M.** 2001 Activation by IKKalpha of a second, evolutionary conserved, NF-kappa B signaling pathway. Science. **293**:1495-9.

322   **Sen R, Baltimore D.** 1986. Multiple nuclear factors interact with the immunoglobulin enhancer sequences. Cell **46**:705–16.

323   **Sen R, Baltimore D.** 1986. Inducibility of kappa immunoglobulin enhancer-binding protein NF-κB by a posttranslational mechanism. Cell **47**:921–28.

324   **Shapiro AL, Viñuela E, Maizel JV Jr.** 1967. Molecular weight estimation of polypeptide chains by electrophoresis in SDS-polyacrylamide gels. Biochem Biophys Res Commun. **28** (5): 815–820.

325   **Schulze-Luehrmann J, Ghosh S.** 2006. Antigen-receptor signaling to nuclear factor κB. Immunity **25**:701–15.

326   **Sixbey JW, Vesterinen EH, Nedrud JG, Raab-Traub N, Walton LA, Pagano JS.** 1983. Replication of Epstein-Barr virus in human epithelial cells infected in vitro. Nature **306**:480-483.

327   **Sixbey JW, Nedrud JG, Raab-Traub N, er al.** 1984. Epstein-Barr virus replication in oropharyngeal epithelial cells. N Engl J Med. **310**:1225-1230..

328   **Smahi A, Courtois G, Vabres P, Yamaoka S, Heuertz S, Munnich A, Israel A, et al.** 2000. Genomic rearrangement in NEMO impairs NF-kappaB activation and is a cause of incontinentia pigmenti. The International Incontinentia Pigmenti (IP) Consortium. Nature; **405**:466-472.

329   **Smith PK, et al.** 1985. Measurement of protein using bicinchoninic acid. Anal. Biochem. **150**: 76–85.

330   **Song HY, Regnier CH, Kirschning CJ, Goeddel DV, Rothe M.** 1997. Proc Natl Acad Sci USA; 94:9792-9796.

331   **Song YJ, Jen KY, Soni V, Kieff E, Cahir-McFarland E.** 2006. IL-1 receptor-associated kinase 1 is critical for latent membrane protein 1-induced p65/RelA serine 536 phosphorylation and NF-kappaB activation. Proc Natl Acad Sci U S A; **103**(8):2689-94.

332   **Song YJ, Izumi KM, Shinners NP, Gewurz BE, Kieff E.** 2008. IRF7 activation by Epstein-Barr virus latent membrane protein 1 requires localization at activation sites and TRAF6, but not TRAF2 or TRAF3. Proc Natl Acad Sci U S A; **105**(47):18448-53.

333   **Sowa ME, Bennett EJ, Gygi SP, Harper W.** 2007. Defining the Human Deubiquitinating Enzyme Interaction Landscape. Cell; **138**:389-403.

334   **Strunz LL, Busch LK, Munroe ME, Tygrett L, Sigmund C, Waldschmidt TW, Bishop GA.** 2004. Expression of the LMP1 cytoplamic tail in mice induces hyperactivation of B lymphocytes and disordered lymphoid architecture. Immunity; **21**:255-266.

335   **Su IJ, Chen JY.** 1997. The role of EBV in lymphoid malignancies. Crit Rev Oncol Hematol; **26**:25-41.

336   **Su TT, Guo B, Kawakami Y, Sommer K, Chae K, et al.** 2002. PKC-β controls I κB kinase lipid raft recruitment and activation in response to BCR signaling. Nat. Immunol. **3**:780–86.

337   **Sun L, Deng L, Ea CK, Xia ZP, Chen ZJ.** 2004. The TRAF6 ubiquitin ligase and TAK1 kinase mediate IKK activation by BCL10 and MALT1 in T lymphocytes. Mol Cell **14**: 289-301.

338   **Sun SC, Yamaoka S.** 2005. Activation of NF-.B by HTLV-I and implications for Lys 63-linked polyubiquitination by NEMO is a key event in NF-.B activation. Nat. Cell Biol. **8**, 398–406.

339   **Sun Z, Arendt CW, Ellmeier W, Schaeffer EM, Sunshine MJ, et al.** 2000. PKC-theta is required for TCR-induced NF-κB activation in mature but not immature T lymphocytes. Nature **404**:402–7.

340   **Sundararajan R, Chen G, Mukherjee C, White E.** 2005. Caspase-dependent processing activates the proapoptotic activity of deleted in breast cancer-1 during tumor necrosis factor-alpha-mediated death signaling. Oncogene. **24**(31):4908-20.

341   **Sugar IP, Neumann E.** 1984. Stochastic model for electric field-induced membrane pores. Electroporation. Biophys. Chem. **19** (3): 211–25.

342   **Sugden B, Mark W.** 1977. Clonal transformation of adult human leukocytes by EBV. J Virol; **23**(3):503-508.

343   **Sylla BS, Hung SC, Davidson DM, Hatzivassiliou E, Malinin NL, Wallach D, et al.** 1998. EBV-transforming protein LMP1 activates transcription factor NF-kappaB through a pathway that includes the NF-kappaB-inducing kinase and the IkappaB kinases IKKalpha and IKKbeta. Proc Natl Acad Sci. **95**:10106-11.

344   **Tabor, Stanley.** 2001. DNA ligases. Current Protocols in Molecular Biology, Book 1: Wiley Interscience.

345   **Takada K, Ono Y.** 1989. Synchronous and sequential activation of latently infected Epstein-Barr-virus genomes.   J Virol; **63**(1):445-449.

346   **Takaesu G, Kishida S, Hiyama A, Shibuya H, et al.** 2000. TAB2, a novel adaptor protein, mediates activation of TAK1 MAPKKK by linking TAK1 to TRAF6 in the IL-1 signal transduction pathway. Mol. Cell **5**:649–58.

347   **Takatsuna H, Kato H, Gohda J, Akiyama T, Moriya A, et al.** 2003. Identification of TIFA as an adapter protein that links tumor necrosis factor receptor-associated factor 6 (TRAF6) to interleukin-1 (IL-1) receptor-associated kinase-1 (IRAK-1) in IL-1 receptor signaling. J. Biol. Chem. **278**:12144–50.

348   **Tang ED, Wang CY, Xiong Y, Guan KL.** 2003. A role for NEMO/IKKgamma ubiquitination in the activation of the IkappaB kinase complex by tumor necrosis factor-alpha. J Biol Chem **278**: 37297-37305.

349   **Tanner J, et al.** 1987. Epstein-Barr virus gp350/220 binding to the B lymphocyte C3d receptor mediates adsorption, capping, and endocytosis. Cell; **50**(2):202-213.

350   **Tanner J, et al.** 1988. Soluble gp350/220 and deletion mutant glycol-proteins block Epstein-Barr virus adsorption to lymphocytes. J Virol; **62**(12):4452-4464.

351   **Tegethoff S, Behlke J, Scheidereit C.** 2003. Tetrameric oligomerization of IκB and linear polyubiquitin chains. Mol Cell Biol; **23**:2029–2041.

352   **Temin HM, Mizutani S.** 1970 RNA-dependent DNA polymerase in virions of Rous sarcoma virus. Nature; **26**(5252):1211-3.

353   **Temmerman ST, Ma CA, Borges L, Kubin M, Liu S, Derry JM, Jain A.** 2006. Impaired dendritic-cell function in ectodermal dysplasia with immune deficiency is linked to defective NEMO ubiquitination. Blood **108**:2324–2331.

354   **Thorley-Lawson DA.** 2001. Epstein-Barr virus: exploiting the immune system. Nat Rev Immunol **1**:75-82.

355   **Thorley-Lawson DA. and Gross, A.** 2004. Persistence of the Epstein-Barr virus and the origins of associated lymphomas. N. Engl. J. Med. **350:**1328-1337.

356   **Ting AT, Pimentel-Muinos FX, Seed B.** 1996. RIP mediates tumor necrosis factor receptor 1 activation of NF-κB but not Fas/ APO-1-initiated apoptosis. EMBO; **15**(22):6189-6196.

357   **Tokunaga F, Sakata SI, Saeki Y, Satomi Y, Kirisako T, Kamei K, et al.** 2009. Involvement of linear polyubiquitylation of NEMO in NF-kB activation. Nat. Cell Biol. **11**:123–132.

358   **Toth CR, Hostutler RF, Baldwin AS Jr, Bender TP.** 1995. Members of the nuclear factor κB family transactivate the murine c-myb gene. J. Biol. Chem. **270**:7661–71.

359   **Towbin H, Staehelin T, Gordon J.** 1979. Electrophoretic transfer of proteins from polyacrylamide gels to nitrocellulose sheets: procedure and applications. Proc Natl Acad Sci U S A. **76** (9): 4350–4354.

360 **Trompouki E, Hatzivassiliou E, Tsichritzis T, Ashworth A, Mosialos G.** 2003. CYLD is a deubiquitinating enzyme that negatively regulates NF-κB activation by TNFR family members. Nature **424**:793–96.

361 **Tsai CN, Tsai CL, Tse KP, Chang HY, Chang YS.** 2002. The Epstein-Barr virus oncogene product, latent membrane protein 1, induces the downregulation of E-cadherin gene expression via activation of DNA methyltransferases. Proc Natl Acad Sci U S A. **99**:10084-9.

362 **Tsang SF, et al.** 1991. Delineation of the cis-acting element mediating EBNA-2 transactivation of latent infection membrane protein expression. J Virol; **65**(12):6765-6771.

363 **Tugizov SM, Berline JW, Palefsky JM.** 2003. Epstein-Barr virus infection of polarized tongue and nasopharyngeal epithelial cells. Nat Med; **9**(3):307-314.

364 **Uchida J, Yasui T, Takaoka-Shichijo Y.** 1999. Mimicry of CD40 signals by Epstein-Barr virus LMP1 in B lymphocyte responses. Science. **286**:300-303.

365 **Vallabhapurapu S, Matsuzawa A, Zhang W, Tseng PH, Keats JJ, et al.** 2008. Nonredundant and complementary functions of TRAF2 and TRAF3 in a ubiquitination cascade that activates NIK-dependent alternative NF-κB signaling. Nat. Immunol. **9**:1364–70.

366 **VanArsdale TL, VanArsdale SL, Force WR, Mosialos G, Kieff E, et al.** 1997. Lymphotoxin-beta receptor signaling complex: role of tumor necrosis factor receptor-associated factor 3 recruitment in cell death and activation of nuclear factor kappaB. Proc Natl Acad Sci USA; **94**:2460-2465.

367 **Van Hoeven KH, Factor SM, Kress Y, et al.** 1993. Visceral myogenic tumors. A manifestation of HIV infection in children. Am J Surg Pathol; **17**:1176-1181.

368 **Varfolomeev E, Blankenship JW, Wayson SM, Fedorova AV, Kayagaki N, et al.** 2007. IAP antagonists induce autoubiquitination of c-IAPs, NF-κB activation, and TNFα-dependent apoptosis. Cell **131**:669–81.

369 **Villalba M, Bi K, Hu J, Altman Y, Bushway P, et al.** 2002. Translocation of PKCθ in T cells is mediated by a nonconventional, PI3-K- and Vav-dependent pathway, but does not absolutely require phospholipase C. J. Cell Biol. **157**:253–63.

370 **Vince JE, Wong WW, Khan N, Feltham R, Chau D, et al.** 2007. IAP antagonists target cIAP1 to induce TNFα-dependent apoptosis. Cell **131**:682–93.

371 **Vuyisich M, Spanggord RJ, Beal PA.** 2002. The binding site of the RNA-dependent protein kinase (PKR) on the EBER1 RNA from Epstein-Barr virus. EMBO Rep; **3**:622-627.

372 **Wagner S, Carpentier I, Rogov V, Kreike M, Ikeda F, Lohr F, Wu CJ, Ashwell JD, Dotsch V, Dikic I, et al.** 2008. Ubiquitin binding mediates the NF-kappaB inhibitory potential of ABIN proteins. Oncogene; **27**:3739-3745.

373 **Wakiguchi H.** 2002. Overview of EBV-associated diseases in Japan. Crit Rev Oncol Hematol; **44**:193-202.

374 **Wan J, Sun L, Mendoza JW, Chui YL, Huang DP, Chen ZJ, et al.** 2004. Elucidation of the c-Jun N-terminal kinase pathway mediated by Epstein-Barr virus-encoded latent membrane protein 1. Mol Cell Biol; **24**:192-199.

375 **Wang C, Deng L, Hong M, Akkaraju GR, Inoue J, Chen ZJ.** 2001. TAK1 is a ubiquitin-dependent kinase of MKK and IKK. Nature **412**:346–51.

376 **Wang D, Liebowitz D, Kieff E.** 1985. An EBV membrane protein expressed in immortalized lymphocytes transforms established rodent cells. Cell. **43**:831-840.

377 **Wang D, Liebowitz D, Kieff E.** 1988. The truncated form of the EBV latent-infection membrane protein expressed in virus replication does not transform rodent fibroblasts. J Virol. **62**:2337-46.

378 **Wang F, et al.** 1990. EBV latent membrane protein (LMP1) and nuclear proteins 2 and 3C are effectors of phenotypic changes in B lymphocytes: EBNA-2 and LMP1 cooperatively induce CD23. J Virol; **64**(5):2309-2318.

379 **Wang F, Gregory C, Sample C,** 1990. Epstein-Barr virus LMP1 and nuclear proteins 2 and 3C are effectors of phenotypic changes in B lymphocytes: EBNA-2 and LMP1 cooperatively induce CD23. J. Virol **64**:2309-2318.

380 **Warburg O, Christian W.** 1942. Isolierung und Kristallisation des Gärungsferments Enolase. Biochem. Z. **310**: 384–421.

381 **Watry D, et al.** 1991. Infection of human thymocytes by EBV. J Exp Med; **173**(4):971-980.

382 **Weber K, Osborn M.** 1969. The reliability of molecular weight determinations by dodecyl sulfate-polyacrylamide gel electrophoresis. J Biol Chem. **244** (16): 4406–4412.

383 **Weil R, Israel A.** 2004. T-cell-receptor- and B-cell-receptor-mediated activation of NF-κB in lymphocytes. Curr. Opin. Immunol. **16**:374–81.

384 **Wells AF.** 1984. Cesium. Structural Inorganic Chemistry 5th edition Oxford Science Publications.

385 **Wertz IE, O'Rourke KM, Zhou H, Eby M, Aravind L, et al.** 2004. De-ubiquitination and ubiquitin ligase domains of A20 downregulate NF-κB signalling. Nature **430**:694–99.

386 **Wiechelman K, Braun R, Fitzpatrick J.** 1988. Investigation of the bicinchoninic acid protein assay: Identification of the groups responsible for color formation. Anal. Biochem. **175**: 231–7.

387 **Wilson JB, Weinberg W, Johnson R, Yuspa S, Levine AJ.** 1990. Expression of the BNLF-1 oncogene of EBVin the skin of transgenic mice induces hyperplasia and aberrant expression of keratin 6. Cell. **61(7):**1315-27.

388 **Wong WW-L, GentleE, Nachbur U, Anderton H, Vaux DL, Silke J.** 2009. RIPK1 is not essential for TNFR1-induced activation of NF-kB. Cell Death and Differentiation; 1–6.

389 **Wu L, Nakano H, Wu Z.** 2006. The CTAR2 domain of the Epstein-Barr virus-encoded latent membrane protein 1 activates NF-kappa B through TRAF6 and TAK1. J Biol Chem. **281**:2162-9.

390 **Wu CJ, Conze DB, Li T, Srinivasula SM, Ashwell JD.** 2006. Sensing of Lys 63-linked polyubiquitination by NEMO is a key event in NF-kappaB activation. Nat. Cell Biol.; **8**:398-406.

391 **Wu CJ, Ashwell JD.** 2008. NEMO recognition of ubiquitinated Bcl10 is required for T cell receptor-mediated NF-kappaB activation. Proc Natl Acad Sci USA **105**: 3023-3028.

392 www.medicineworld.org/cancer (www.medicineworld.org/images/blogs/ebv-4511290.jpg)

393 **Xiao G, Cvijic ME, Fong A, Harhaj EW, Uhlik MT, Waterfield M, Sun SC.** 2001. Retroviral oncoprotein Tax induces processing of NF-kB2/p100 in T cells: evidence for the involvement of IKKalpha. EMBO J. **20:**6805-15.

394   **Xiao G, Harhaj EW, Sun SC.** 2001. NF-kappaB-inducing kinase regulates the processing of NF-kappaB2 p100. Mol. Cell. **7:**401-9.

395   **Xiao G, Fong A, Sun SC.** 2004. Induction of p100 processing by NF-kappaB-inducing kinase involves docking IkappaB kinase alpha (IKKalpha) to p100 and IKKalpha-mediated phosphorylation. J Biol Chem. **279:**30099-105.

396   **Xie P, Bishop GA.** 2004. Roles of TRAF 3 in signaling to B lymphocytes by carboxy-terminal activating regions 1 and 2 of the EBV-encoded oncoprotein latent membrane protein 1. J Immunol; **173:**5546-55.

397   **Xie P, Hostager BS, Bishop GA.** 2004. Requirement for TRAF3 in signaling by LMP1 but not CD40 in B lymphocytes. J Exp Med; **199:**661-71.

398   **Yamamoto M, Okamoto T, Takeda K, Sato S, Sanjo H, et al.** 2006. Key function for the Ubc13 E2 ubiquitin-conjugating enzyme in immune receptor signaling. Nat. Immunol**. 7:**962–70.

399   **Yamamoto M, Sato S, Saitoh T, Sakurai H, Uematsu S, Kawai T, et al.** 2006. Cutting edge: Pivotal function of Ubc13 in thymocyte TCR signaling. J Immunol **177:** 7520-7524.

400   **Yamaoka S, Courtois G, Bessia C, Whiteside ST, Weil R, Agou F, Kirk HE, Kay RJ, Israel A.** 1998. Complementation cloning of NEMO, a component of the IkappaB kinase complex essential for NF-kappaB activat. Cell. **93:**1231-40.

401   **Yao L, Setsuda J, Sgadari C, Cherney B, Tosato G.** 2001. Interleukin-18 expression induced by Epstein-Barr virus-infected cells. J Leukc. Biol. **69:**779-84.

402   **Yates J, Warren N, Sugden B.** 1985. Stable replication of plasmids derived from Epstein-Barr virus in various mammalian cells. Nature; **313**(6005):812-815.

403   **Yilmaz ZB, Weih DS, Sivakumar V, Weih F.** 2003. RelB is required for Peyer's patch development: differential regulation of p52-RelB by lymphotoxin and TNF. EMBO J. **22:**121–30.

404   **Yoshiama H, et al.** 1997. Epstein-Barr virus infection of human gastric carcinoma cells: implication of the existence of a new virus receptor different from CD21. J Virol; **71**(7): 5688-5691.

405   **Yoshida H, Jono H, Kai H, Li JD.** 2005 . The tumor suppressor CYLD acts as a negative regulator for toll-like receptor 2 signaling via negative cross-talk with TRAF6/TRAF7. J. Biol. Chem. **280** : 41111 – 41121 .

406   **Yoshiyama H, Shimizu N, Takada K.** 1995. Persistent Epstein-Barr virus infection in a human T-cell line: unique program of latent virus expression. EMBO Journal **14:**3706-3711.

407   **Yoshizaki T, Horikawa T, Qing-Chun R, Wakisaka N, Takeshita H, Sheen TS, Lee SY, Sato H, Furukawa M.** 2001. Induction of interleukin-8 by Epstein-Barr virus latent membrane protein-1 and its correlation to angiogenesis in nasopharyngeal carcinoma. Clin. Cancer. Res. **7:**1946-51.

408   **Yuan J, et al.** 2006. Virus and cell RNAs expressed during EBV replication. J Virol; **80**(5):2548-2565.

409   **Zandi E, Rothwarf DM, Delhase M, Karin M.** 1997. The IkappaB kinase complex (IKK) contains two kinase subunits, IKKalpha and IKKbeta, necessary for IkB phosphorylation and NF-kappaB activation. Cell. **91:**243-52.

410   **Zarnegar B, Yamazaki S, He JQ, Cheng G.** 2008. Control of canonical NF-κB activation through the NIK-IKK complex pathway. Proc. Natl. Acad. Sci. USA **105:**3503–8.

411   **Zeugin JA, Hartley JL.** 1985. Ethanol Precipitation of DNA. Focus **7** (4): 1–2.

412   **Zhang L, Wu L, Hong K, Pagano JS.** 2001. Intracellular signaling molecules activated by Epstein-Barr virus for induction of interferon regulatory factor 7. J Virol; **75:**12393-12401.

413   **Zhang L, Pagano JS.** 2001. Interferon regulatory factor 7 mediates activation of Tap-2 by Epstein-Barr virus latent membrane protein 1. J Virol; **75:**341-350.

414   **Zhang SQ, Kovalenko A, Cantarella G, Wallach D.** 2000. Recruitment of the IKK signalosome to the p55 TNF receptor: RIP and A20 bind to NEMO (IKKgamma) upon receptor stimulation. Immunity **12:** 301-311.

415   **Zhao T, Yang L, Sun Q, Arguello M, Ballard DW, et al.** 2007. The NEMO adaptor bridges the nuclear factor-κB and interferon regulatory factor signaling pathways. Nat. Immunol. **8:**592–600.

416   **Zhu G, Wu CJ, Zhao Y, Ashwell JD.** 2007. Optineurin negatively regulates TNFalpha induced NF-kappaB activation by competing with NEMO for ubiquitinated RIP, Curr Biol **17:**1438-1443.

417   **Zhong-Yin Zhang.** 2002. Protein Tyrosine Phosphatases: Structure and Function, Substrate Specificity, and Inhibitor Development. Annual Review of Pharmacology and Toxicology,**42**, pp209.

418   **Zhou H, Wertz I, O'Rourke K, Ultsch M, Seshagiri S, Eby M, Xiao W, Dixit VM.** 2004. Bcl10 activates the NF-kappaB pathway through ubiquitination of NEMO. Nature **427:** 167-171.

419   **Zhou R, Silverman N, Hong M, Liao DS, Chung Y, Chen ZJ, Maniatis T.** 2005. The role of ubiquitination in Drosophila innate immunity. J Biol Chem **280:** 34048–34055

420   **Zonana J, Elder ME, Schneider LC, Orlow SJ, Moss C, Golabi M, et al.** 2000. A novel X-linked disorder of immune deficiency and hypohidrotic ectodermal dysplasia is allelic to incontinentia pigmenti and due to mutations in IKK-gamma (NEMO). Am J Hum Genet **67:**1555–1562.

8. LIST OF ABBREVIATIONS

aa   aminoacid

aminoacids (one letter code)

A	alanine (Ala)
C	cysteine (Cys)
D	aspartic acid (Asp)
E	glutamic acid (Glu)
E	phenylalanine (Phe)
G	glycine (Gly)
H	histidine (His)
I	isoleucine (Ile)
K	lysine (Lys)
L	leucine (Leu)
M	methionine (Met)
N	asparagine (Asn)
P	proline (Pro)
Q	glutamine (Gln)
R	arginine (Arg)
S	serine (Ser)
T	threonine (Thr)
V	valine (Val)
W	tryptophane (Trp)
Y	tyrosine (Tyr)

Ab	antibody
Abin-1	A20 binding inhibitor of NF-κB-1
Amp	ampicilin
AgR	antigen receptor
APS	ammoniumpersulfate
ATL	adult T cell lymphoma
ATP	adenosintriphosphate
approx.	approximately

bp	basepairs
BCIG (x-Gal)	bromo-chloro-indolyl-galactopyranoside
BSA	bovine serum albumin

°C	grad celsius
cc	coiled coil
cIAP	cellular inhibitor of apoptosis
conc.	concentration
CoZi	NEMO (domains CC2 and LZ)
CYLD	cylindromatosis

d	day/ days
ddH$_2$O	double destilled water
Da	Dalton
DEPC	diethylpyrocarbonate, (diethyl dicarbonate, diethyl oxydiformate, ethoxyformic anhydride, or pyrocarbonic acid diethyl ester)
DMEM	Dulbeccos Modified Eagle Medium
DMSO	dimethylsulfoxid
DNA	deoxyribonucleicacid
dIdC	Poly(deoxyinosinic-deoxycytidylic) acid, sodium salt
dNTP	deoxynucleosidtriphosphate
ds	double stranded
DTT	dithiotreitol
DUB	deubiquitinating enzyme

E1	ubiquitin-activating enzyme
E2	ubiquitin-conjugating enzyme
E3	ubiquitin ligase
EBV	Epstein-Barr Virus
E.coli	Escherichia coli
EDA-ID	anhidrotic ectodermal dysplasia with immunodeficiency
EDTA	ethylenediaminetetraacetic acid
EGFP	enhanced green fluorescent protein
FADD	Fas-associated death domain
FBS	fetal bovine serum
Fig.	figure
vFLIP	viral FLICE [FADD (Fas-associated death domain)-like interleukin 1β-converting enzyme]-inhibitory protein
g	gram
g	= rcf (relative centrifugation force) $g = 11{,}18 * r * (rpm/1000)^2$
G	dGMP=deoxyguanosinmonophosphate
GFP	green fluorescent protein
GST	Glutathione *S*-transferase
G418	neomycin
h	hour
HCl	hydrochloric acid
HEK293	human embryonic kidney cells
HeLa	adenocarcinoma cell line (cervix)
HOIL-1L	longer isoform of haem-oxidized iron-regulatory protein ubiquitin ligase 1
HOIP	HOIL-1L interacting protein
HRP	horseradish peroxidase
hrs	hours
HTLV	human T lymphotropic virus
IB	immunoblot
IBR	in-between RING
ID	immunodeficiency
IF	immunofluorescence
Ig	immunoglobulin
IκB	inhibitor of κB
IKK	inhibitor of kappa (κ) B kinase
IL-1 (β)	interleukin-1 (β)
IL-1R	interleukin-1 receptor
IP	immunoprecipitation
IP	incontinentia pigmenti
IPTG	isopropyl *β*-D-thiogalactoside
IRAK	IL-1 receptor associated kinase
JNK	Jun amino-terminal kinase
kbp	kilobasepairs
kD (kDa)	kilodalton
KO	knock out
KSHV	Kaposi sarcoma-associated herpesvirus
l	liter
LMP1	latent membrane protein 1
LUBAC	linear ubiquitin chain assembly complex
LPA	serum-lysophosphatidic acid
LPS	lipopolysaccharide
LZ	leucine zipper

m	milli
M	mol
mA	milliampere
MAPK	mitogen-activated protein kinase
MCLB	mammalian cell lysis buffer
ME (β-ME)	β-mercaptoethanol
MEF	mouse embryonic fibroblasts
MEKK3	MAPK kinase kinase 3
mg	milligramm
min	minute
Mio	million
ml	milliliter
mM	millimol
MOPS	3-(N-morpholino) propanesulfonic acid
mRNA	messenger RNA
µg	microgramm
µl	microliter
µM	micromol
n	nucleotides
NaDOC	Sodiumdeoxycholate
NCS	newborn calf serum
NEM	N-Ethylmaleimide
NEMO	NF-κB essential modulator
NF-κB	nuclear factor-κB
nm	nanometer
nM	nanomol
NOA	NEMO Optineurin Abin (domains CC2 and LZ)
NOAZ	NOA (CC2 and LZ) plus linker and ZF
NP40	Nonidet P-40 or Igepal CA-630
nt	nucleotide
NUB	NEMO ubiquitin binding
NZF	novel zinc finger
OD	optical density
ORF	open reading frame
$p^{32}\alpha$-dATP	2´-desoxyadenosin-5´-triphosphat
$p^{32}\alpha$-dCTP	2´-desoxycytidine-5´-triphosphat
$p^{32}\alpha$-dGTP	2´-desoxyguanosine-5´-triphosphat
PBS	phosphate buffered saline
PEL	primary effusion lymphoma
PKC	protein kinase C
PMA /=TPA	phorbol 12-myristate 13-acetate/ 12-O-Tetradecanoylphorbol-13-acetate
pmol	pikomol
PMSF	phenylmethylsulfonyl fluoride
rcf	relative centrifugation force = g
RING	really interesting new gene
RIPA	radio immunoprecipitation assay buffer
RIP1	receptor interacting protein 1
RNA	ribonucleicacid
RNAse	ribonuclease
rpm	revolutions per minute g = 11,18 * r * (rpm/1000)^2
RT	room temperature
RT	reverse transcriptase
SCFβTrCP	Skp1–cullin–F box (βTrCP)ubiquitin ligase
SD	standard deviation
sec	second
SDS	sodium dodecyl sulphate
ss	single stranded

T	dTMP=deoxythymidinmonophosphat
Tab.	tabelle
TAB	TAK1-binding protein
TAK1	transforming growth factor β-activated kinase 1
TBE	tris-borate-EDTA buffer
TE	tris-EDTA buffer
TEMED	N,N,N`,N`-Tetramethylendiamin
Tet	Tetracycline
TLR	Toll-like receptor
TNFα	tumor necrosis factor α
TNF-R1	TNFα receptor 1
TNF-RSC	TNF-R1 signaling complex
TPA/ =PMA	12-O-Tetradecanoylphorbol-13-acetate/ phorbol 12-myristate 13-acetate
TRAF	TNF receptor-associated factor
tRNA	transfer-RNA
Tris-HCl	tris-(hydroxymethyl)-amminomethane hydrochloride
U	unit
U	dUMP = uridinmonophosphat
UBA	ubiquitin-associated
UBAN	ubiquitin-binding in ABIN and NEMO
UBC	ubiquitin conjugating enzyme
UBD	ubiqitin binding domain
UBL	ubiquitin-like
U-box	UFD2-homology domain
Uev	ubiquitin E2 variant
Vol	volume
WCE	whole cell extract
WT	wild type
x-Gal (BCIG)	bromo-chloro-indolyl-galactopyranoside
XR-MSMD	X-linked recessive Mendelian susceptibility to mycobacterial diseases
ZF	zinc finger

Lebenslauf

Der Lebenslauf ist in der Online-Version aus Gründen des Datenschutzes nicht enthalten.